UNIVERSITY OF BIRMINGHAM

APPENDIX

for

AZOPHOSPHINES: SYNTHESIS, COORDINATION CHEMISTRY AND CATALYSIS

by

EMMA JANE JORDAN-ROSE

A thesis submitted to the University of Birmingham for the degree of

DOCTOR OF PHILOSOPHY

School of Chemistry

College of Engineering and Physical Sciences

University of Birmingham

February 2025

TABLE OF CONTENTS

1.0 Characterisation Spectra

1.1 Azophosphine-Boranes and Azophosphines **1** – **16**

1.1.1 NMR Spectra

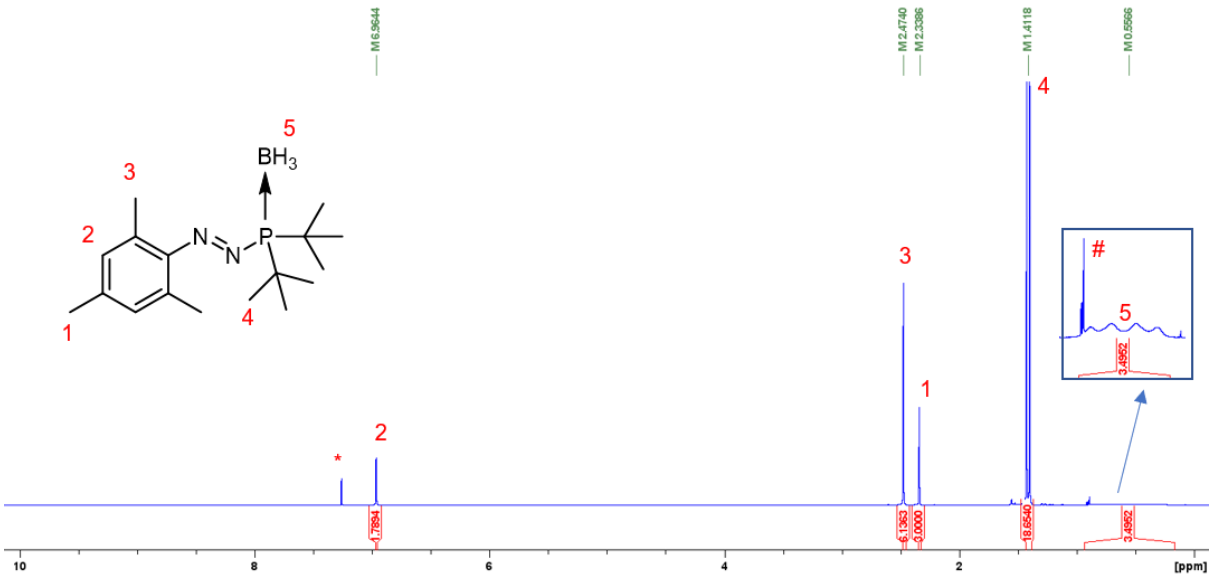

Figure A1. ^{1}H NMR spectrum of **1** in $CDCl_3$. * = residual $CHCl_3$; # = residual hexane.

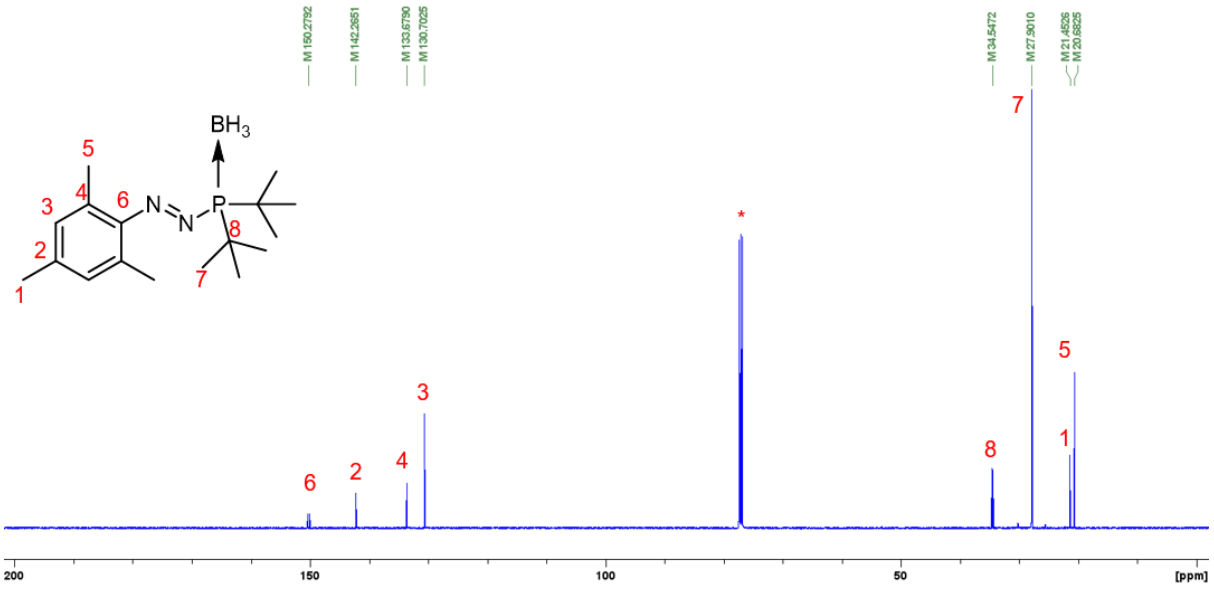

Figure A2. ^{13}C NMR spectrum of **1** in $CDCl_3$. * = $CDCl_3$.

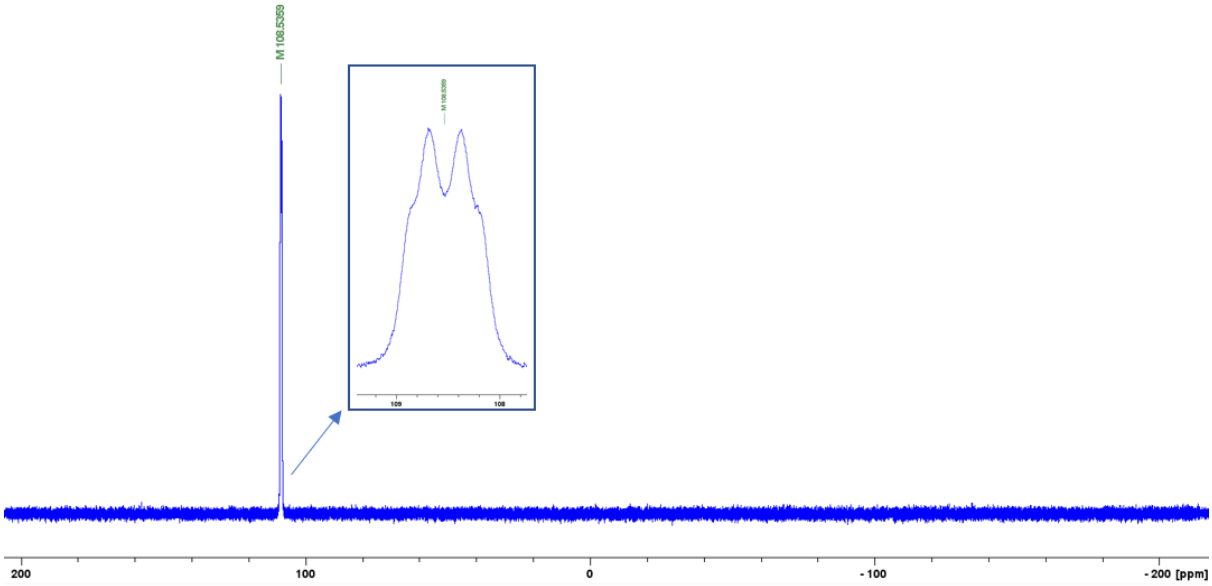

Figure A3. $^{31}P\{^{1}H\}$ NMR spectrum of **1** in $CDCl_3$.

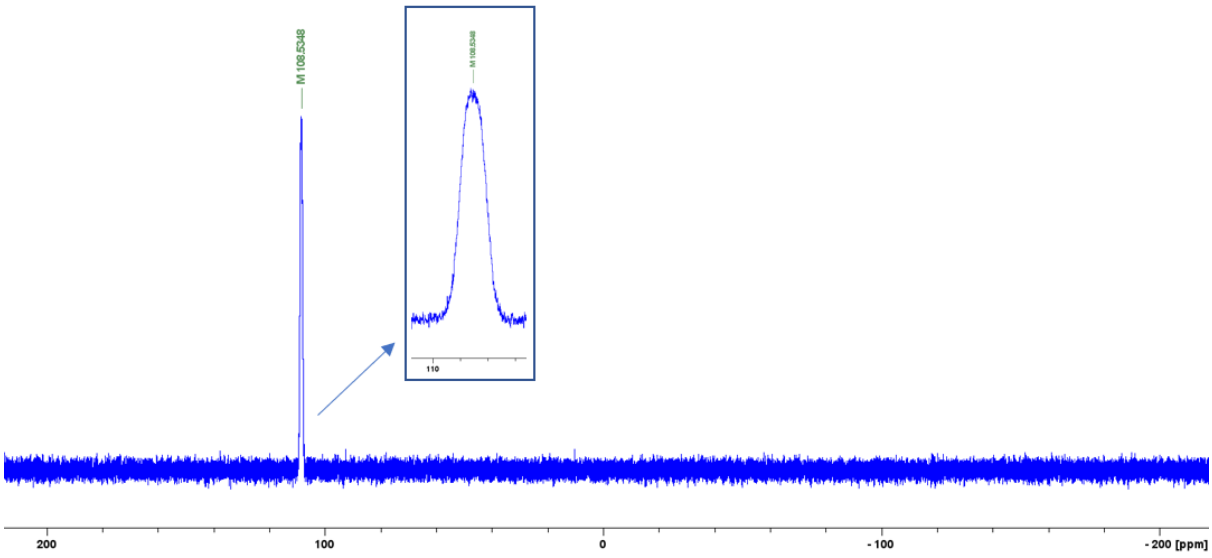

Figure A4. ^{31}P NMR spectrum of **1** in $CDCl_3$.

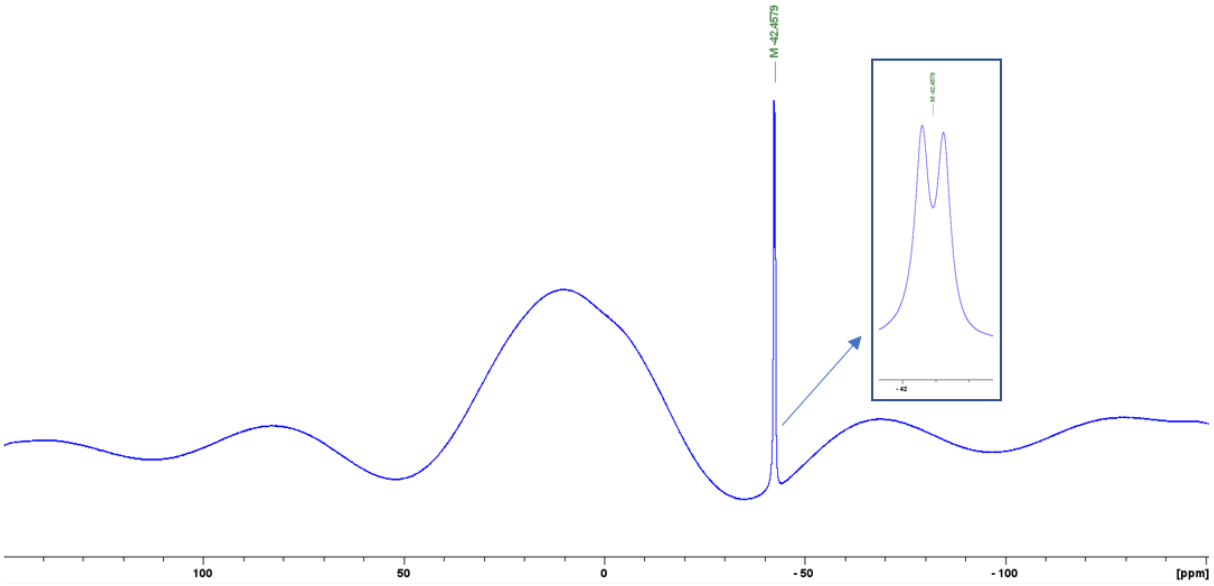

Figure A5. $^{11}B\{^{1}H\}$ NMR spectrum of **1** in $CDCl_3$.

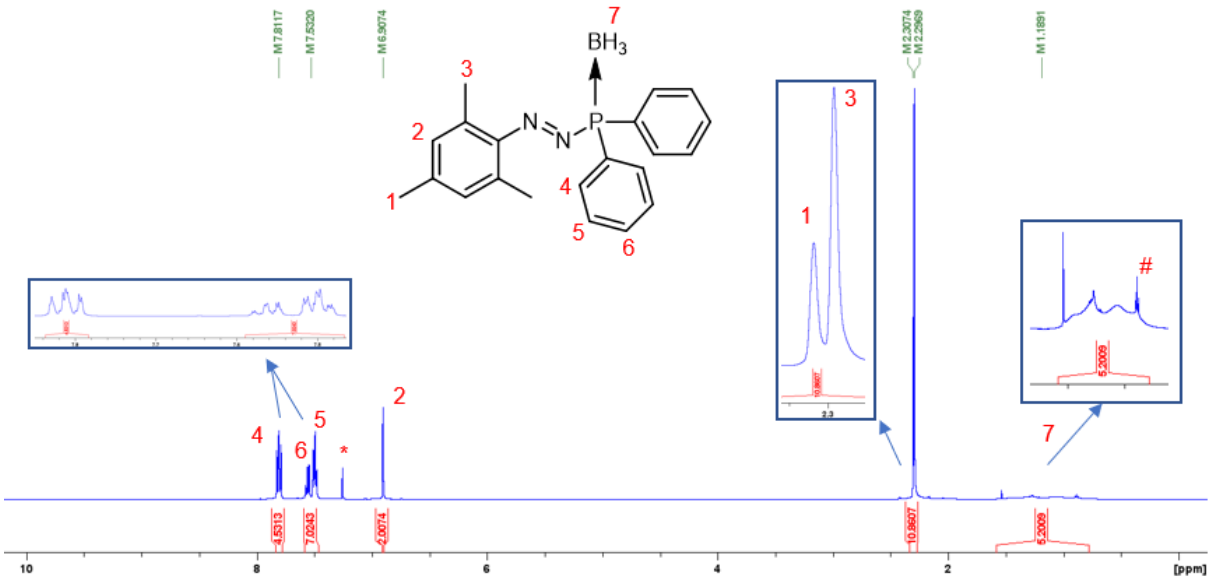

Figure A6. ^{1}H NMR spectrum of **2** in $CDCl_3$. * = residual $CHCl_3$; # = residual hexane.

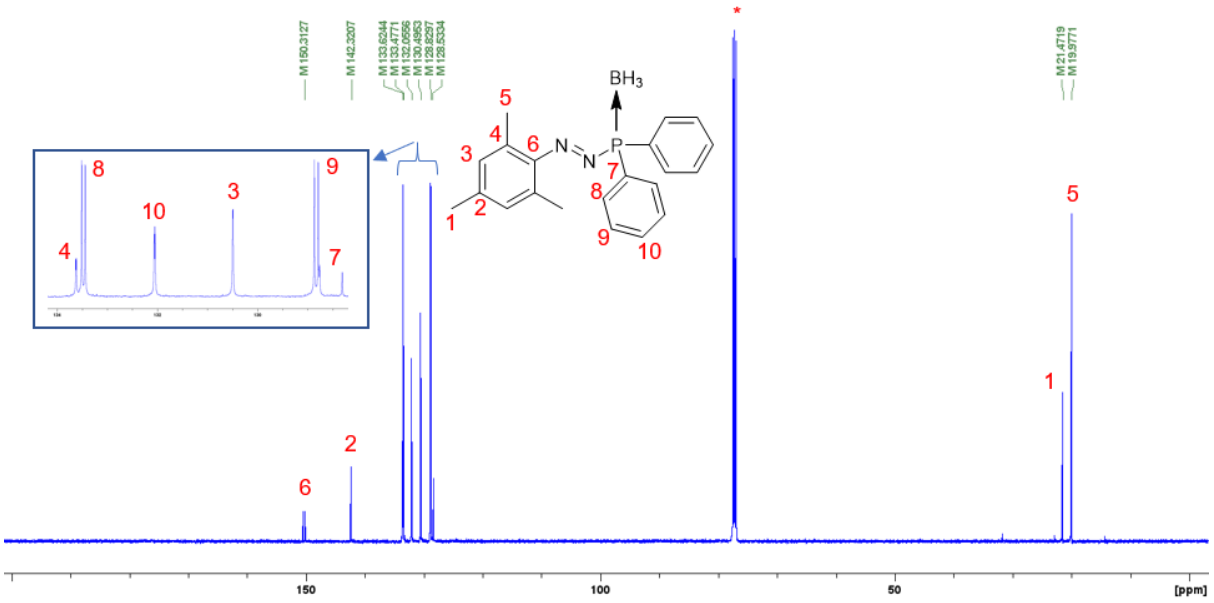

Figure A7. ^{13}C NMR spectrum of **2** in $CDCl_3$. * = $CDCl_3$.

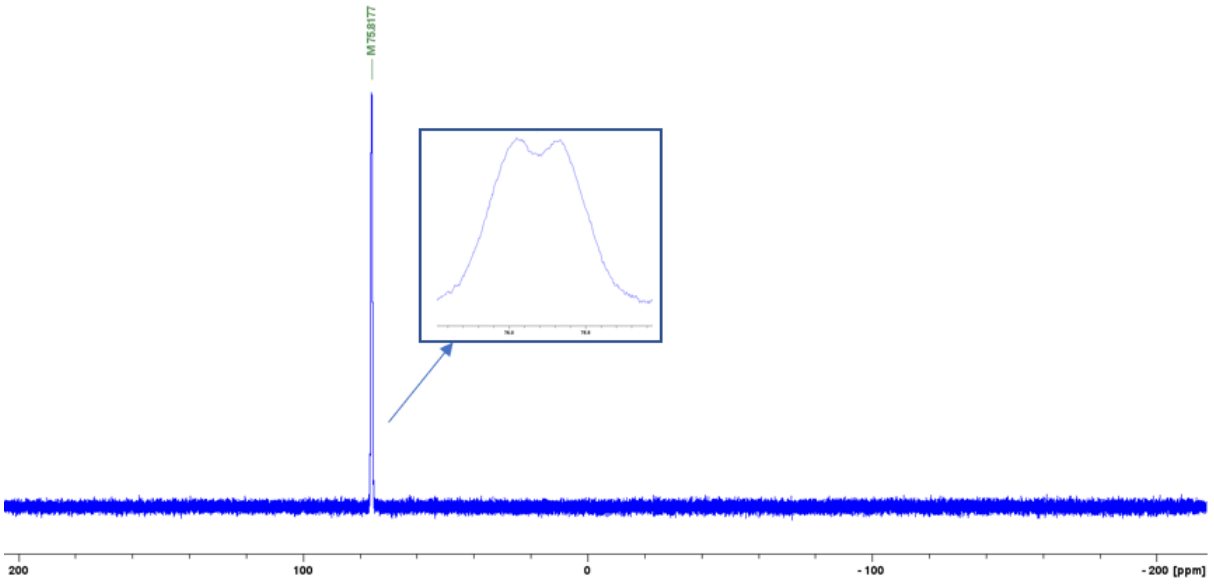

Figure A8. $^{31}P\{^1H\}$ NMR spectrum of **2** in $CDCl_3$.

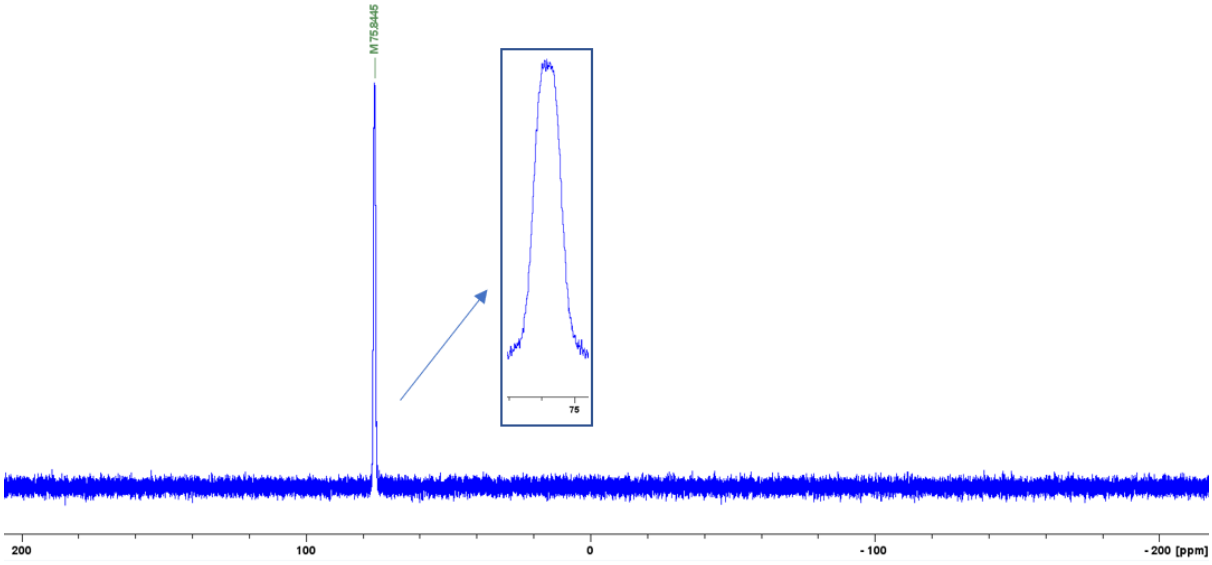

Figure A9. ^{31}P NMR spectrum of **2** in $CDCl_3$.

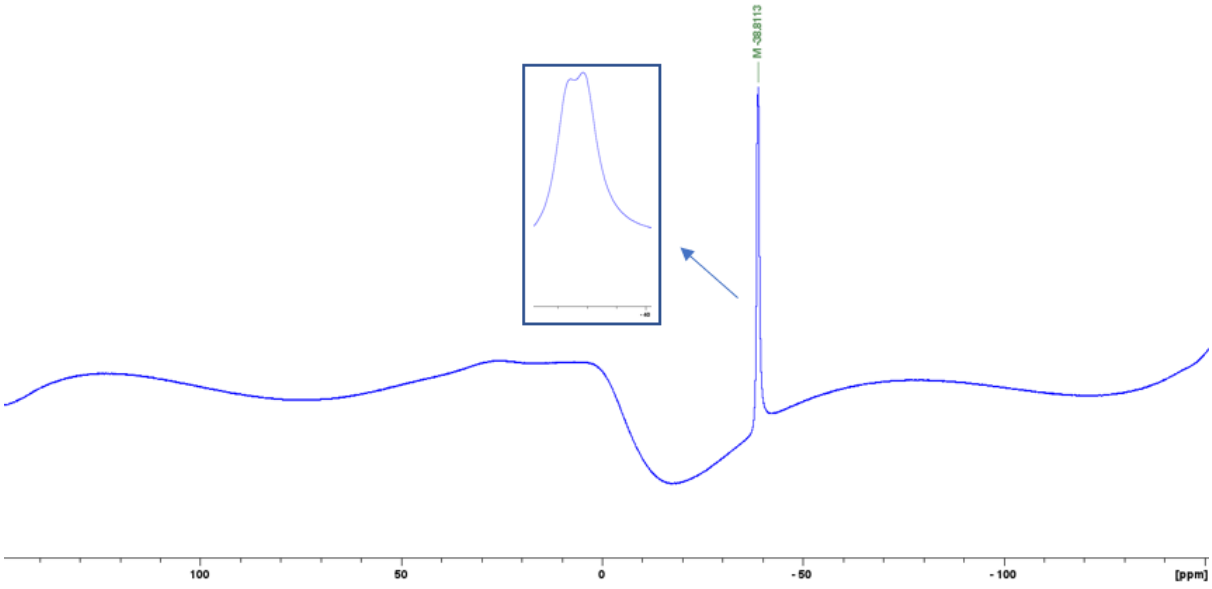

Figure A10. $^{11}B\{^1H\}$ NMR spectrum of **2** in $CDCl_3$.

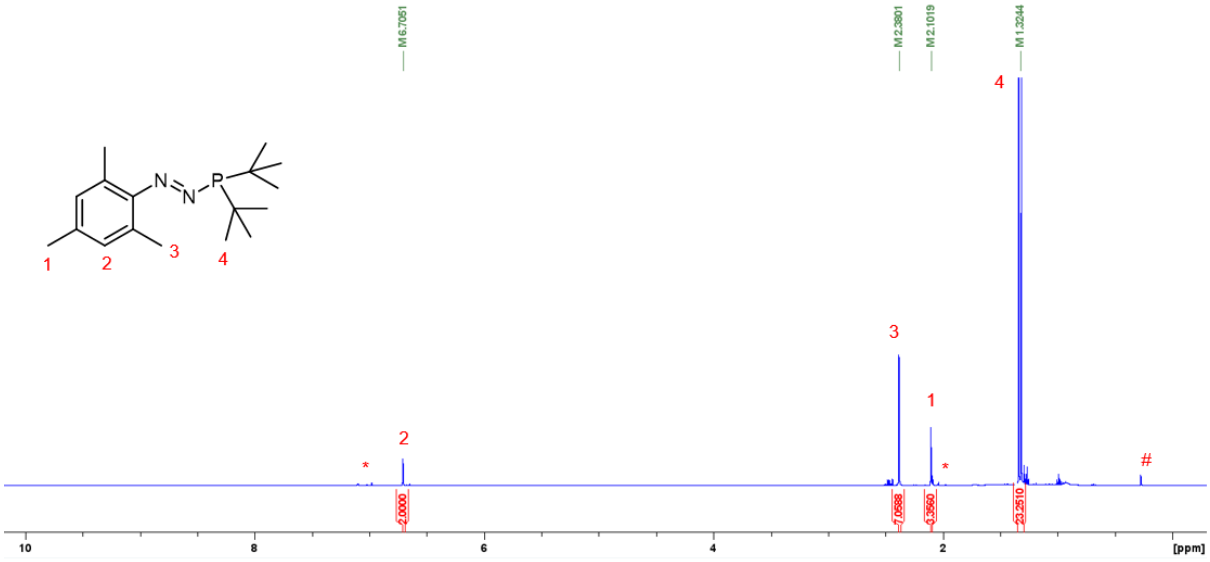

Figure A11. ^{1}H NMR spectrum of **3** in toluene-d_8. * = residual toluene-d_7H; # = silicon grease.

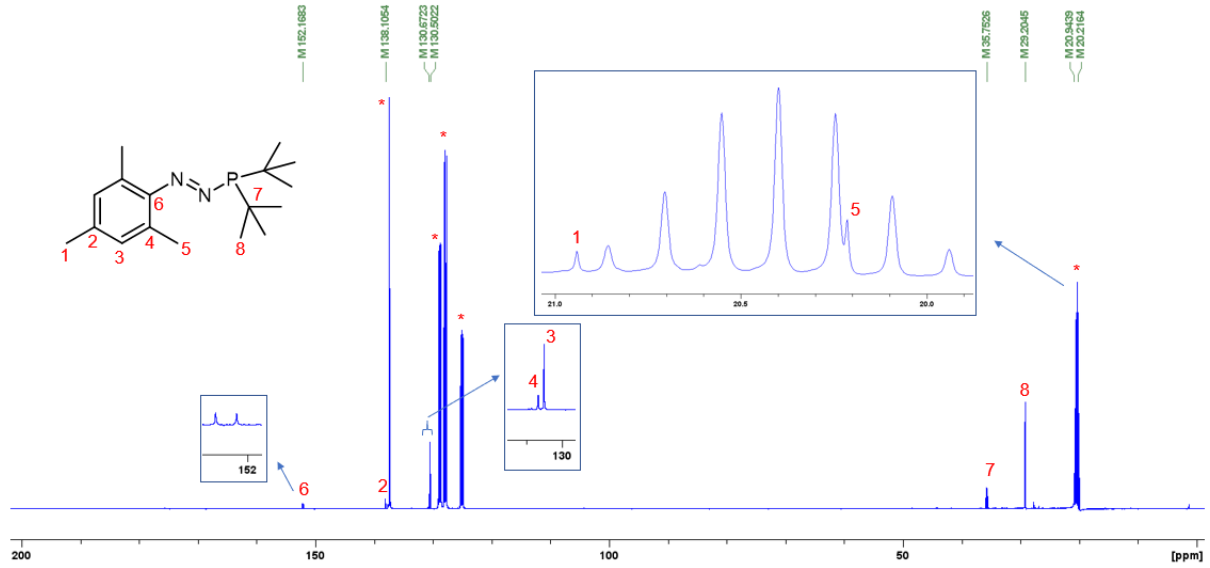

Figure A12. ^{13}C NMR spectrum of **3** in toluene-d_8. * = toluene-d_8.

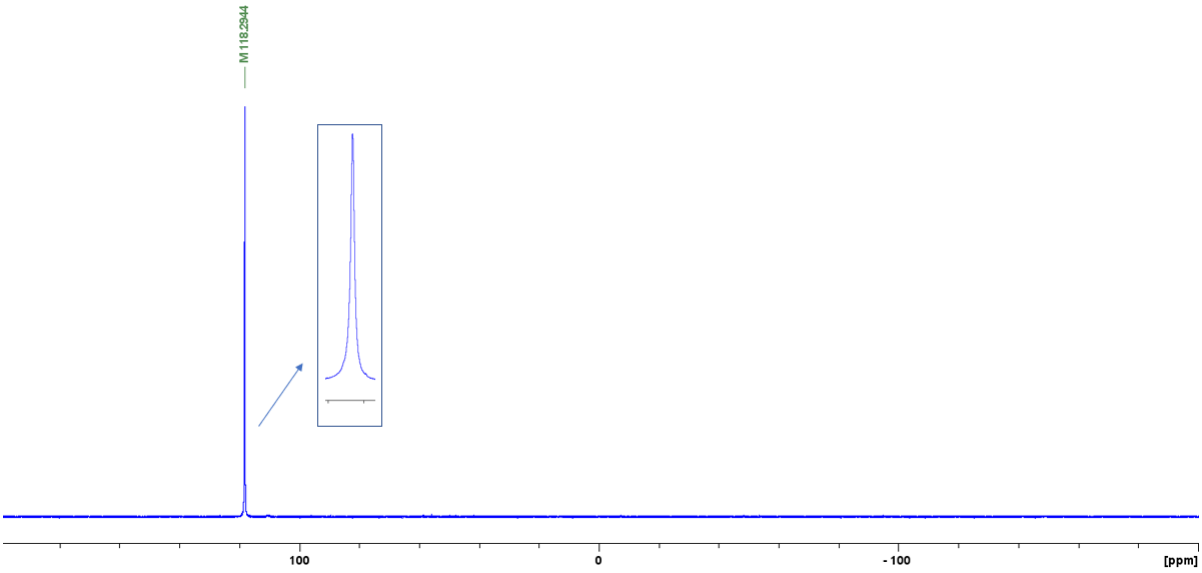

Figure A13. $^{31}P\{^{1}H\}$ NMR spectrum of **3** in toluene-d_8.

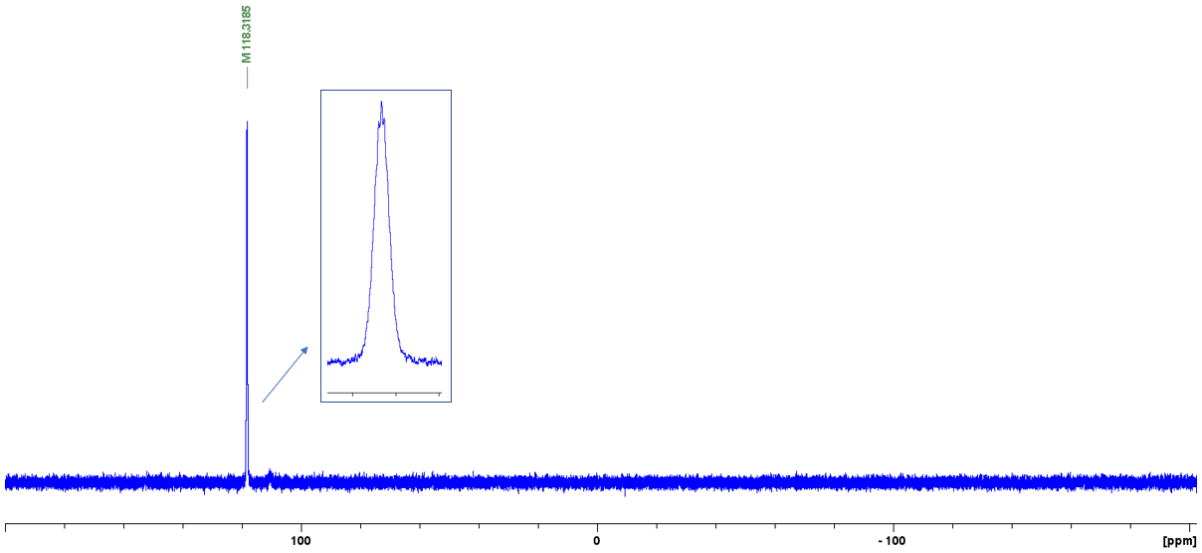

Figure A14. ^{31}P NMR spectrum of **3** in toluene-d_8.

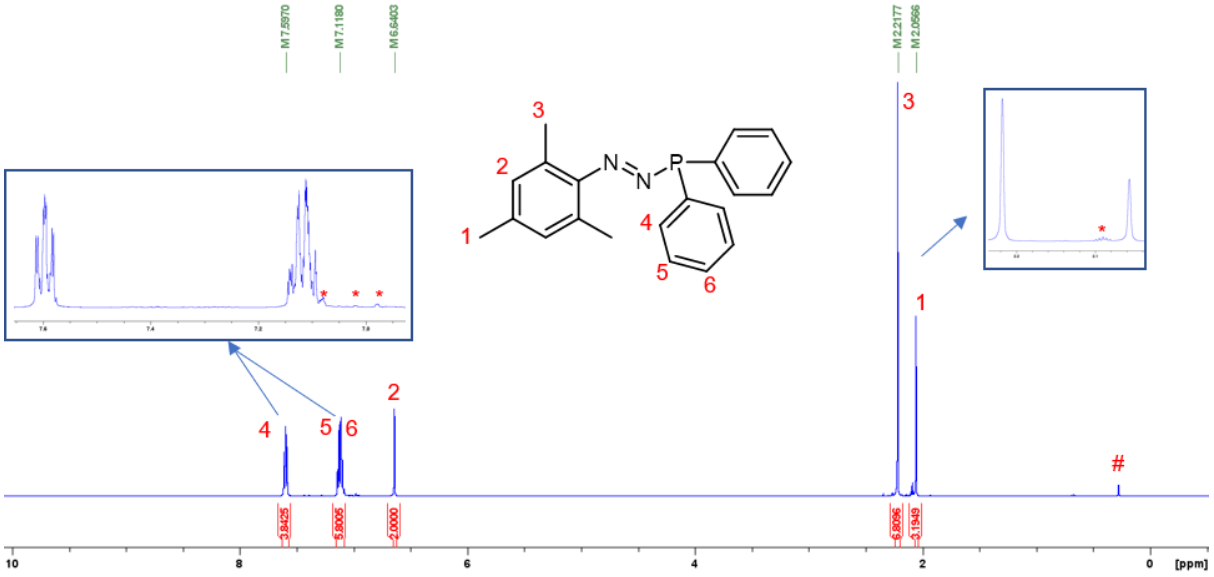

Figure A15. ^{1}H NMR spectrum of **4** in toluene-d_8. * = residual toluene-d_7H; # = silicone grease.

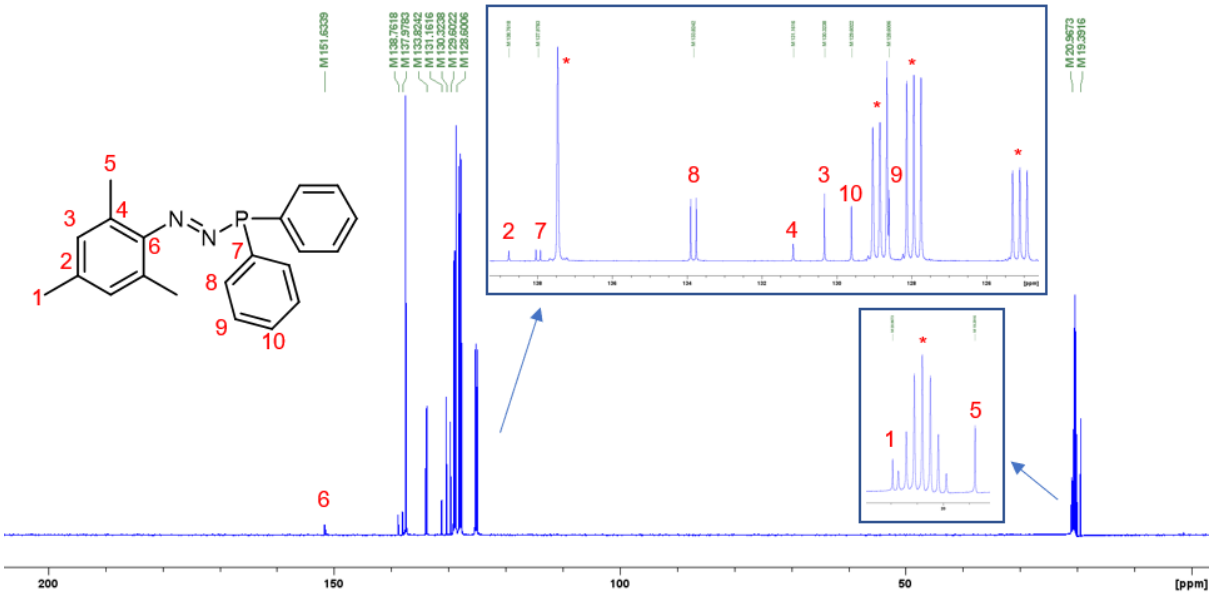

Figure A16. ^{13}C NMR spectrum of **4** in toluene-d_8. * = toluene-d_8

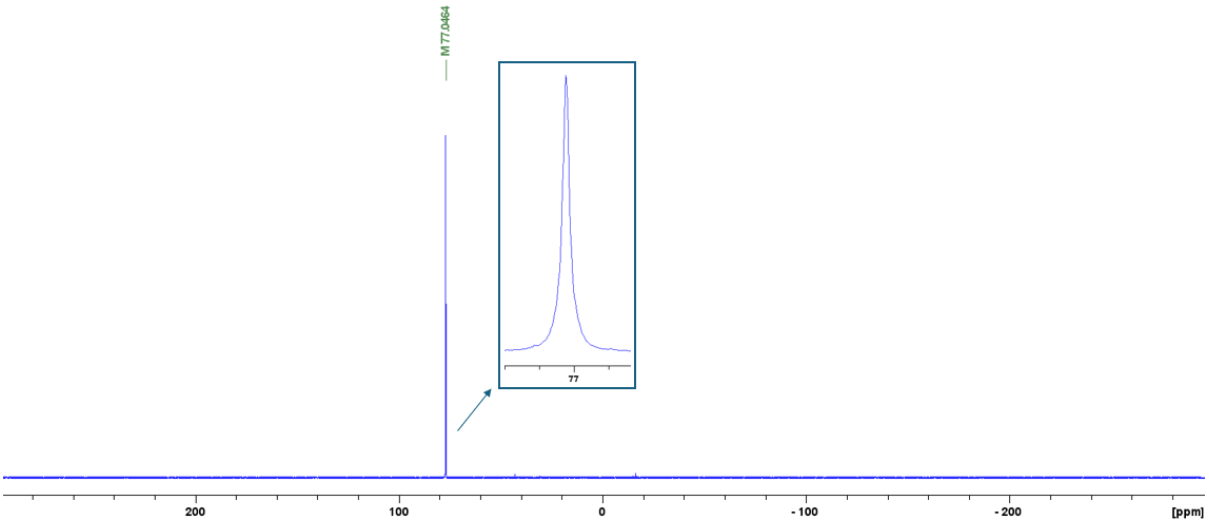

Figure A17. $^{31}P\{^{1}H\}$ NMR spectrum of **4** in toluene-d_8.

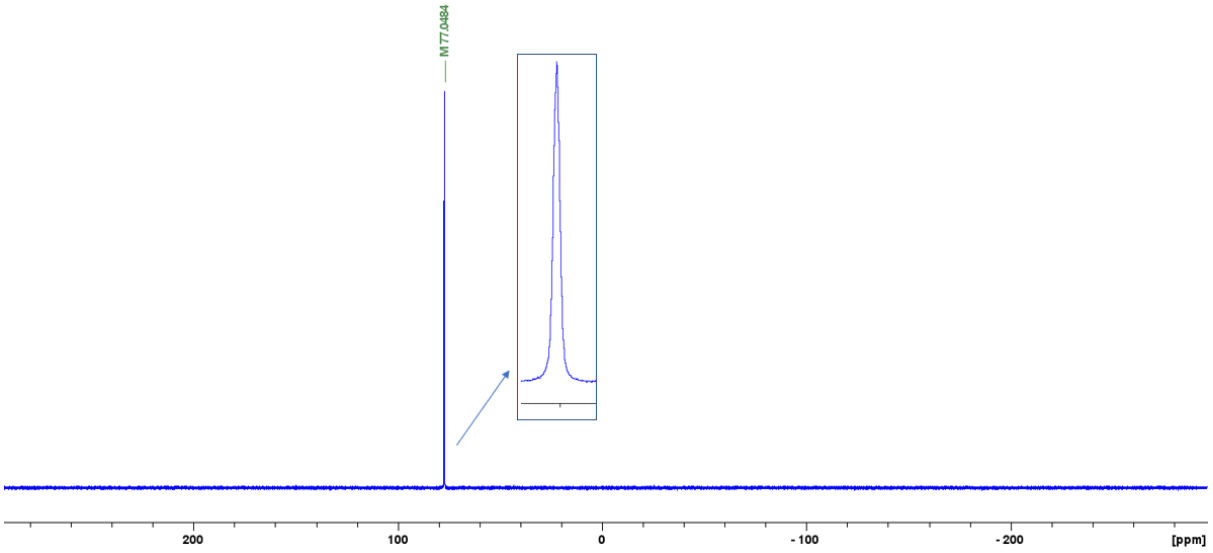

Figure A18. ^{31}P NMR spectrum of **4** in toluene-d_8.

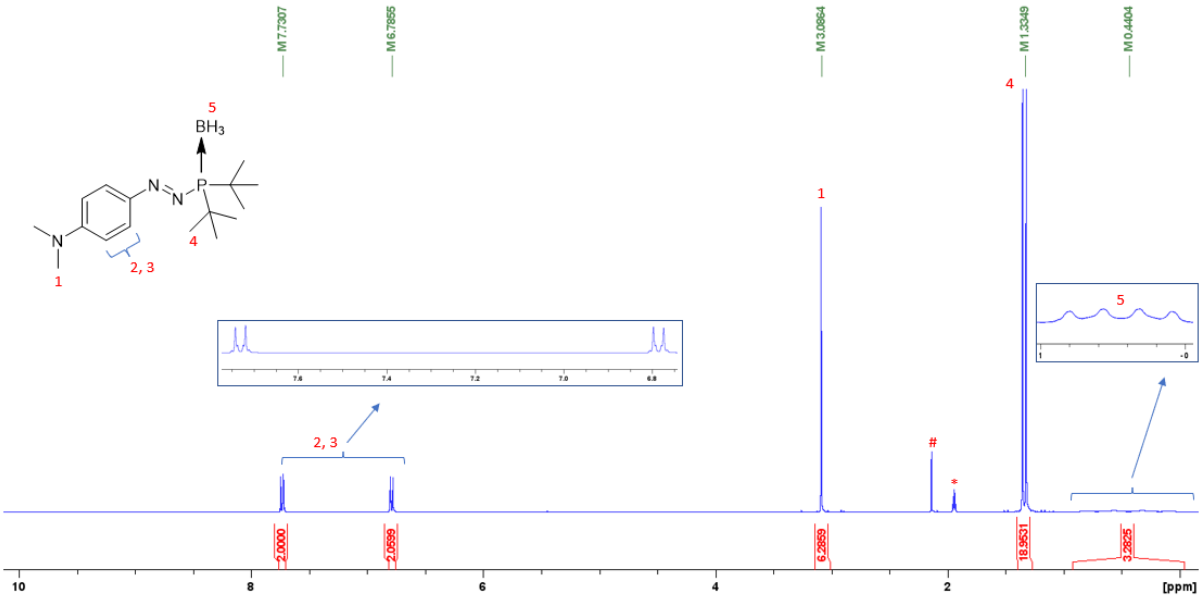

Figure A19. ^{1}H NMR spectrum of **5** in CD_3CN. * = residual CHD_2CN; # = water in CD_3CN.

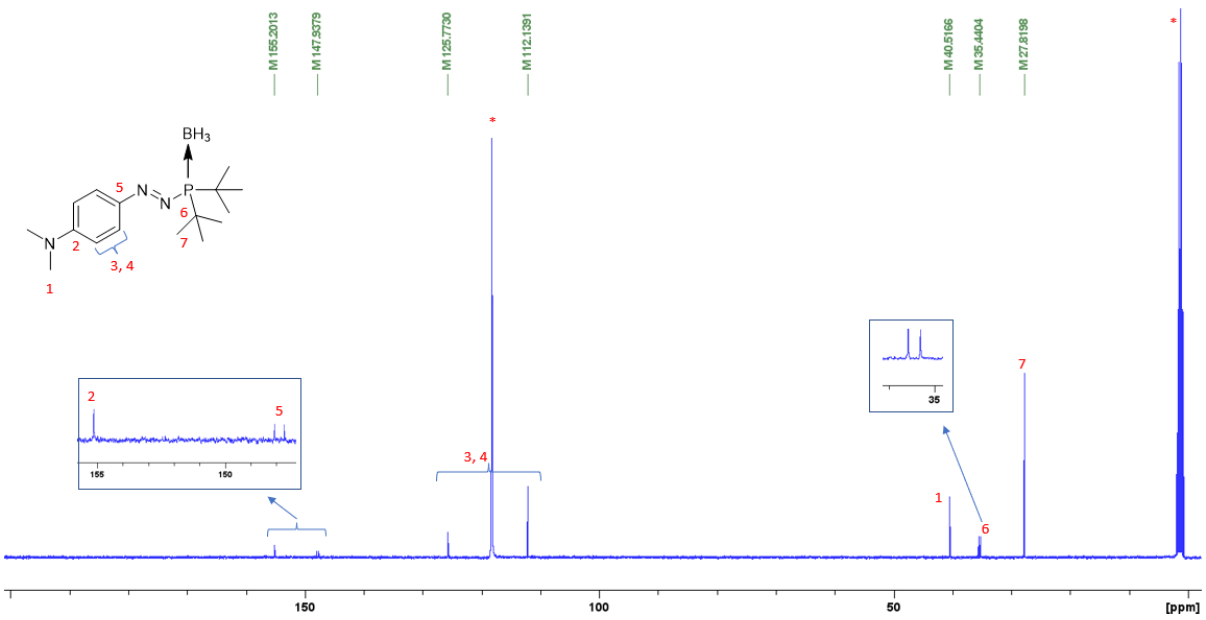

Figure A20. ^{13}C NMR spectrum of **5** in CD_3CN. * = CD_3CN.

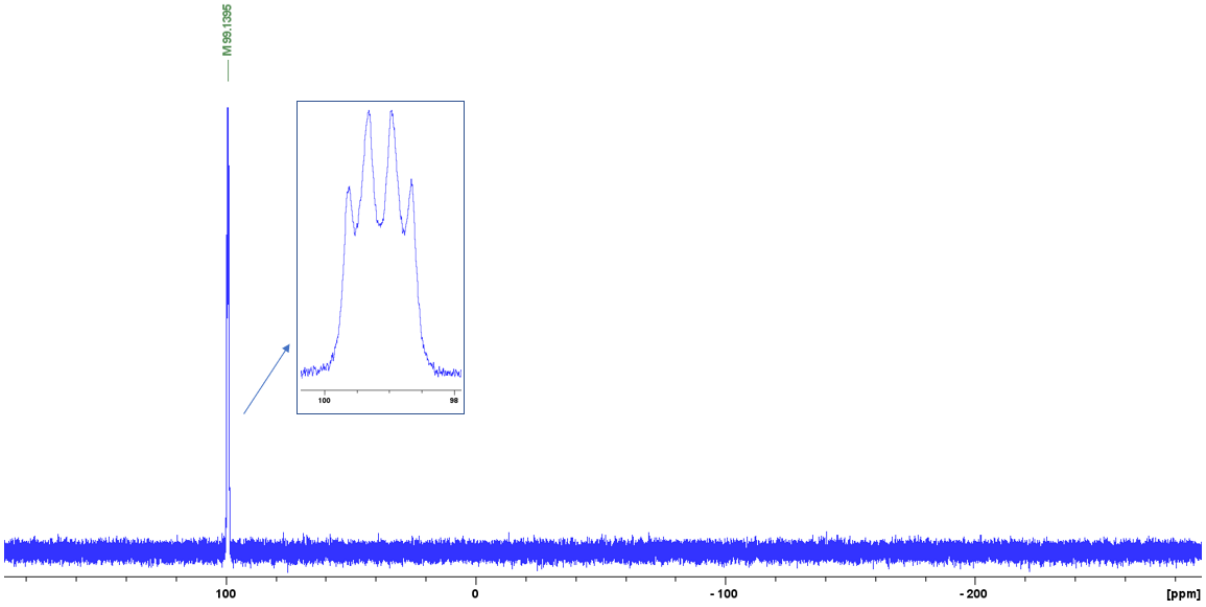

Figure A21. $^{31}P\{^{1}H\}$ NMR spectrum of **5** in CD_3CN.

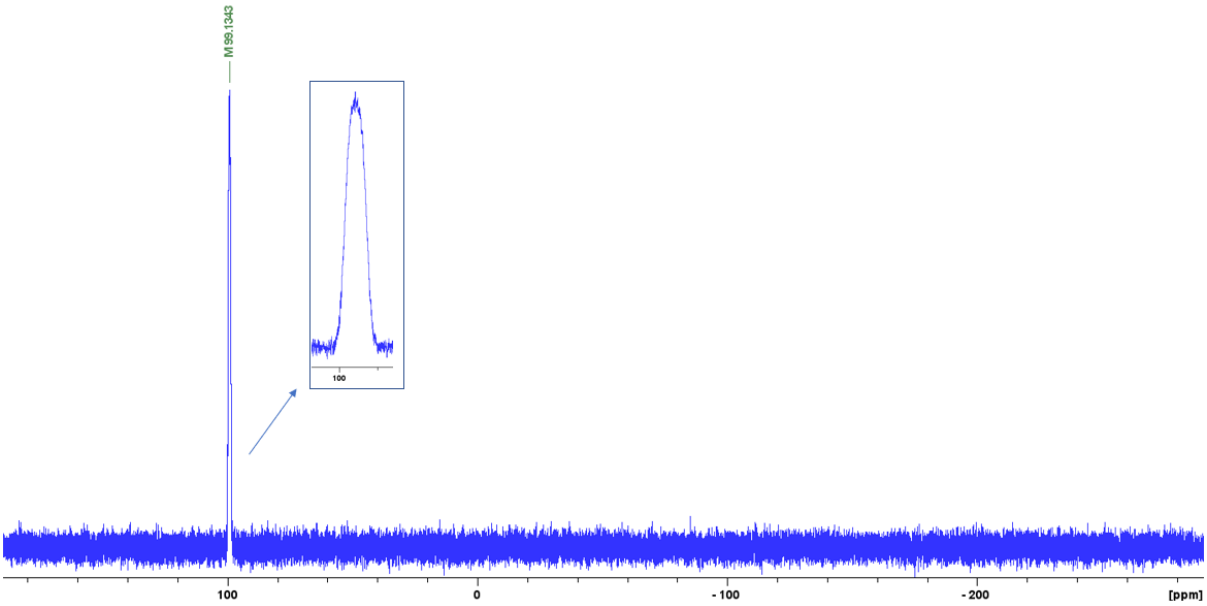

Figure A22. ^{31}P NMR spectrum of **5** in CD_3CN.

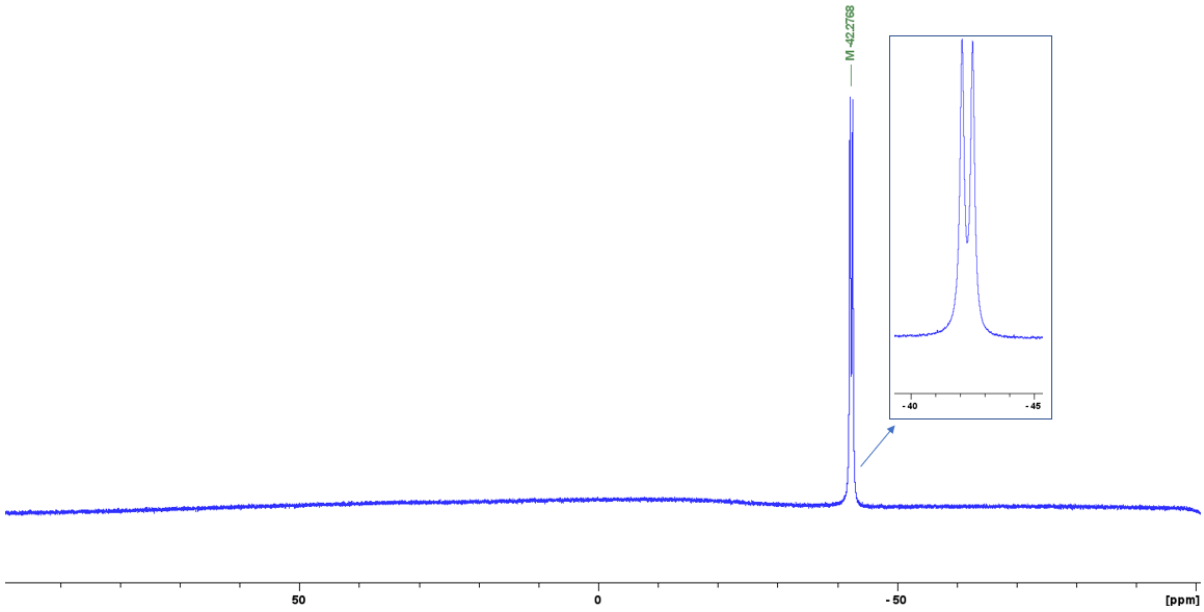

Figure A23. $^{11}B\{^{1}H\}$ NMR spectrum of **5** in CD_3CN.

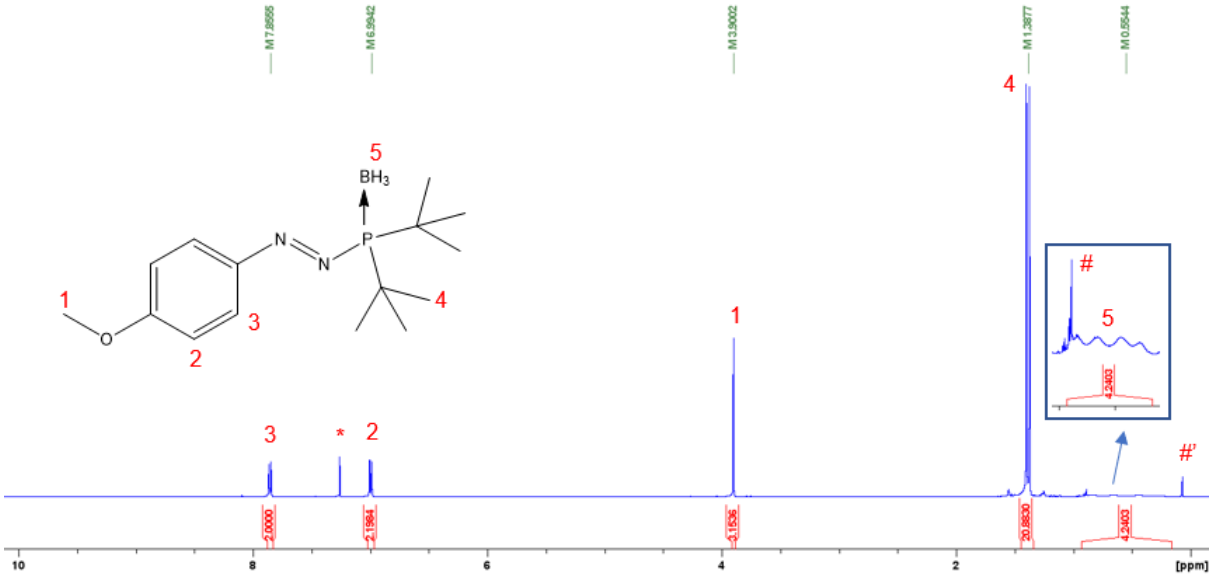

Figure A24. ^{1}H NMR spectrum of **6** in $CDCl_3$. * = residual $CHCl_3$; # = residual hexane; #' = silicon grease.

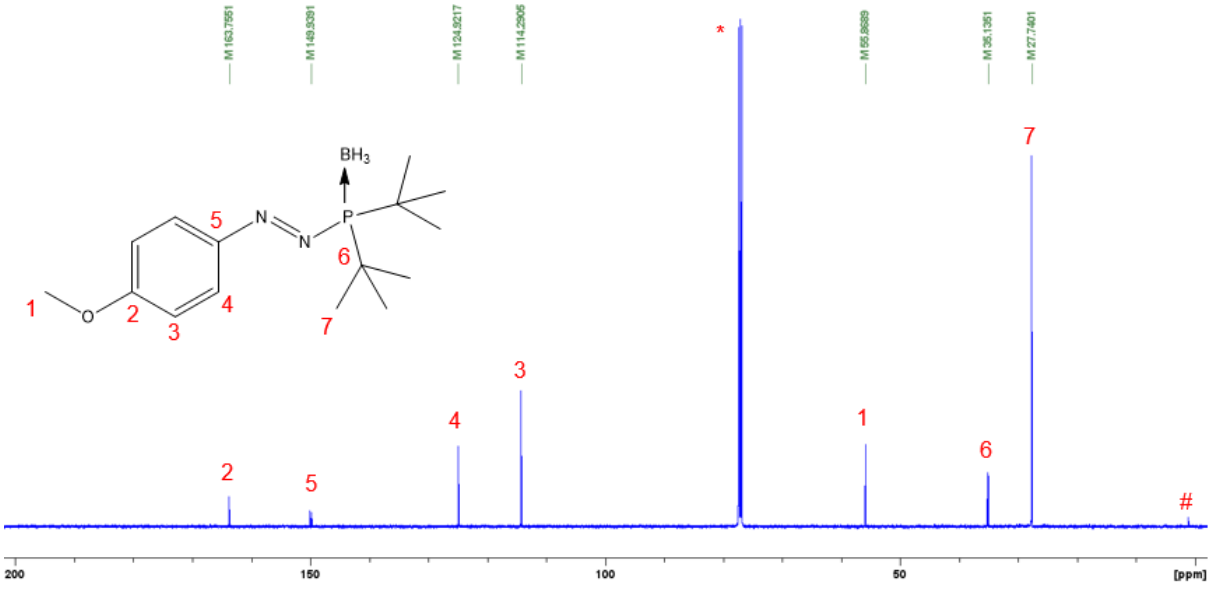

Figure A25. $^{13}C\{^{1}H\}$ spectrum of **6** in $CDCl_3$. * = $CDCl_3$; # = silicon grease.

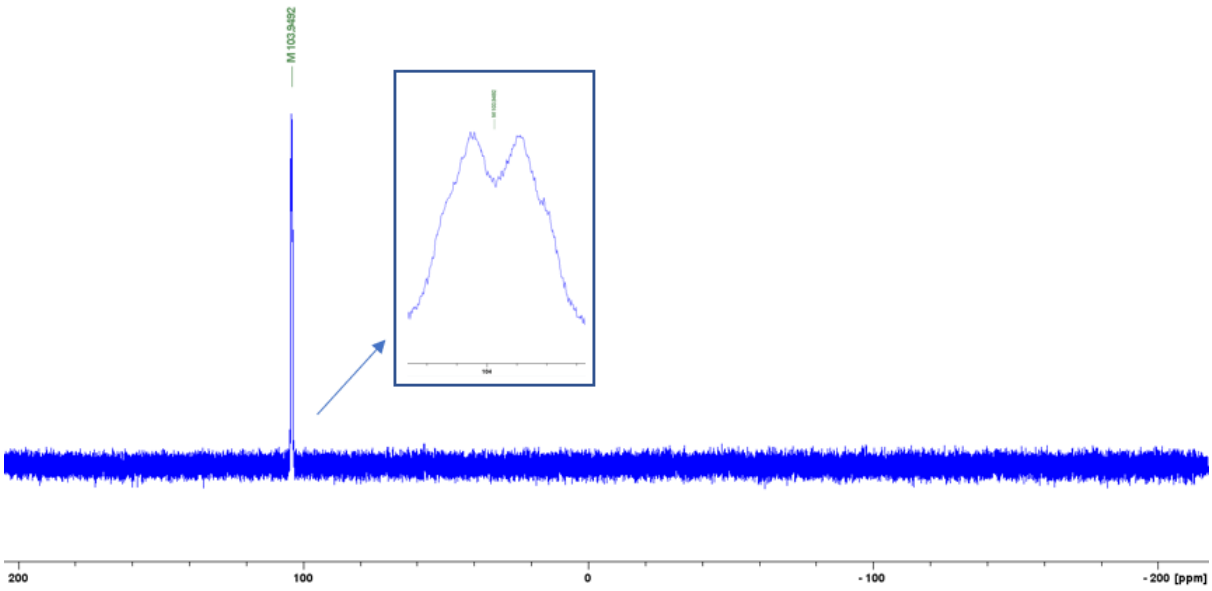

Figure A26. $^{31}P\{^{1}H\}$ spectrum of **6** in $CDCl_3$.

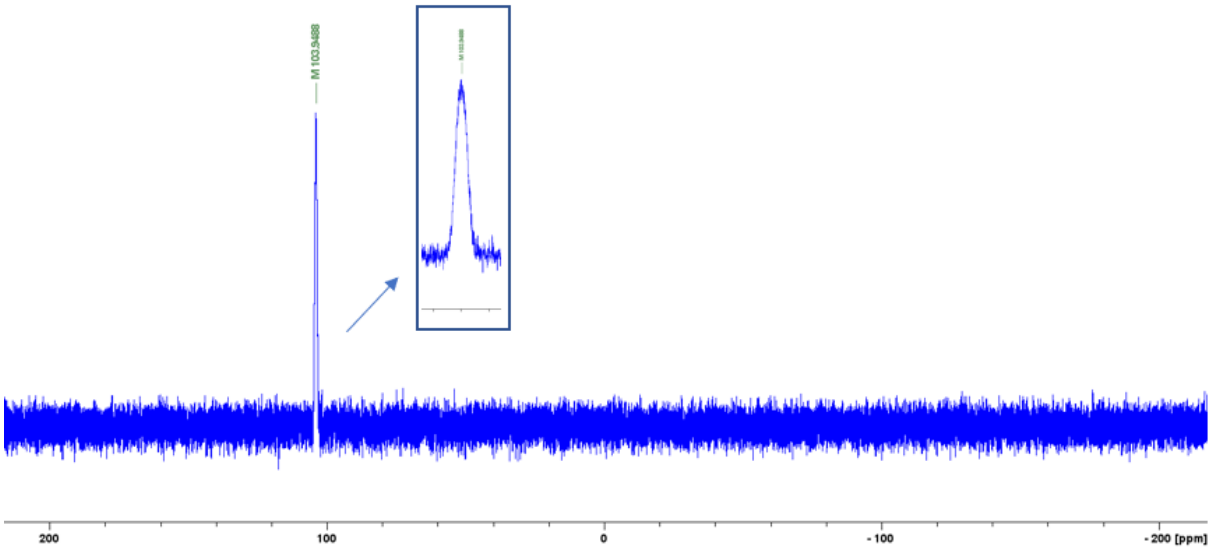

Figure A27. ^{31}P spectrum of **6** in $CDCl_3$.

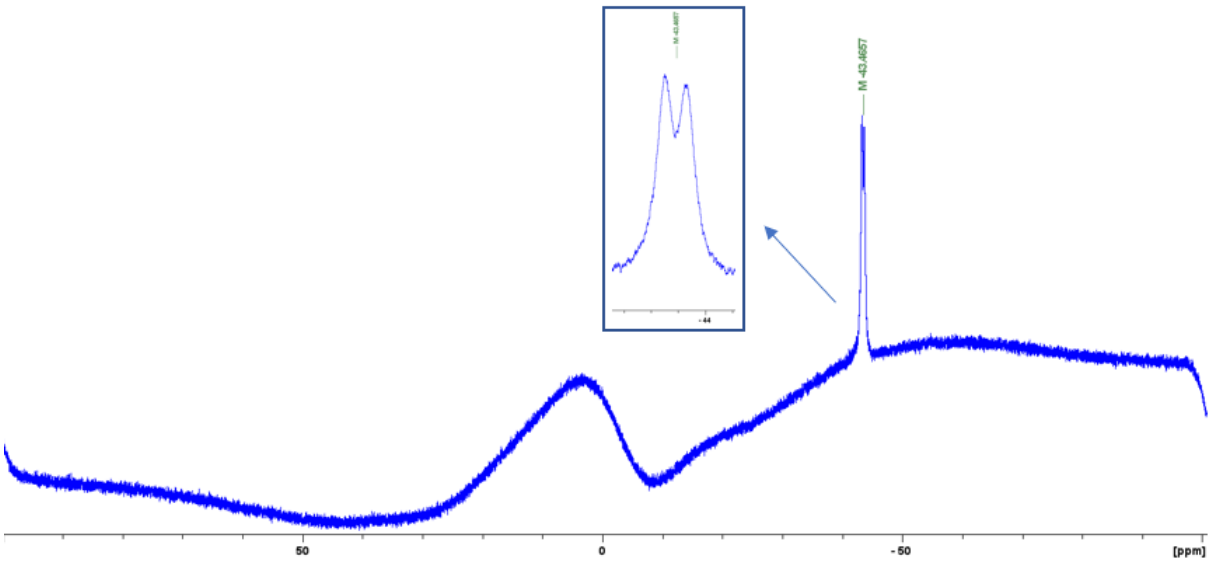

Figure A28. $^{11}B\{^1H\}$ spectrum of **6** in $CDCl_3$.

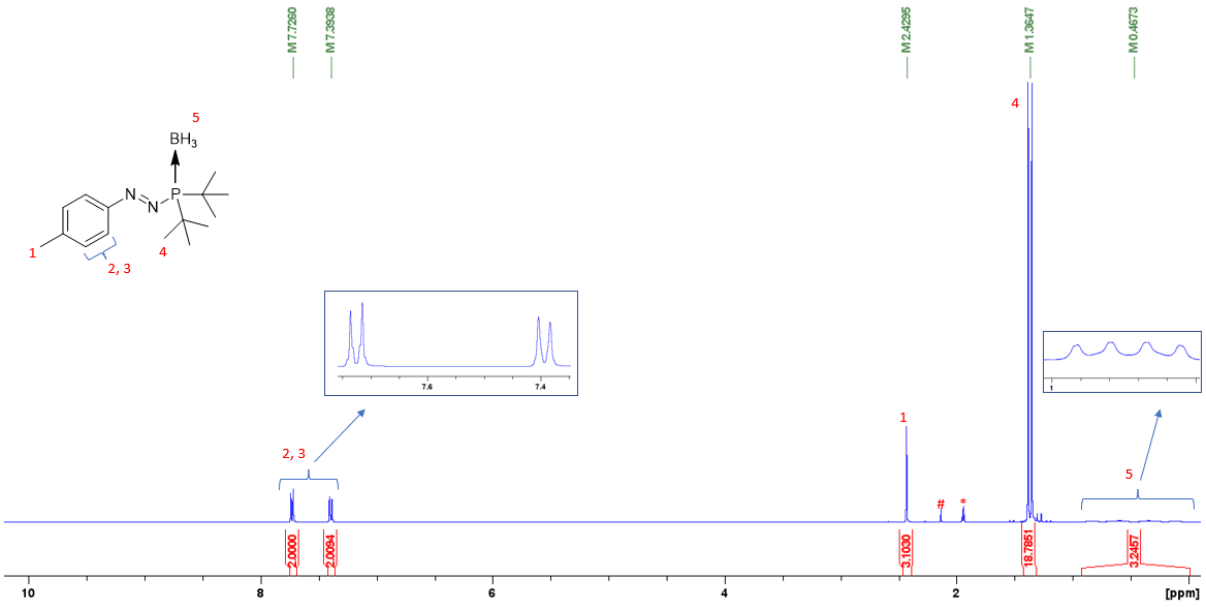

Figure A29. ^{1}H NMR spectrum of **7** in CD_3CN. * = residual CHD_2CN; # = water in CD_3CN.

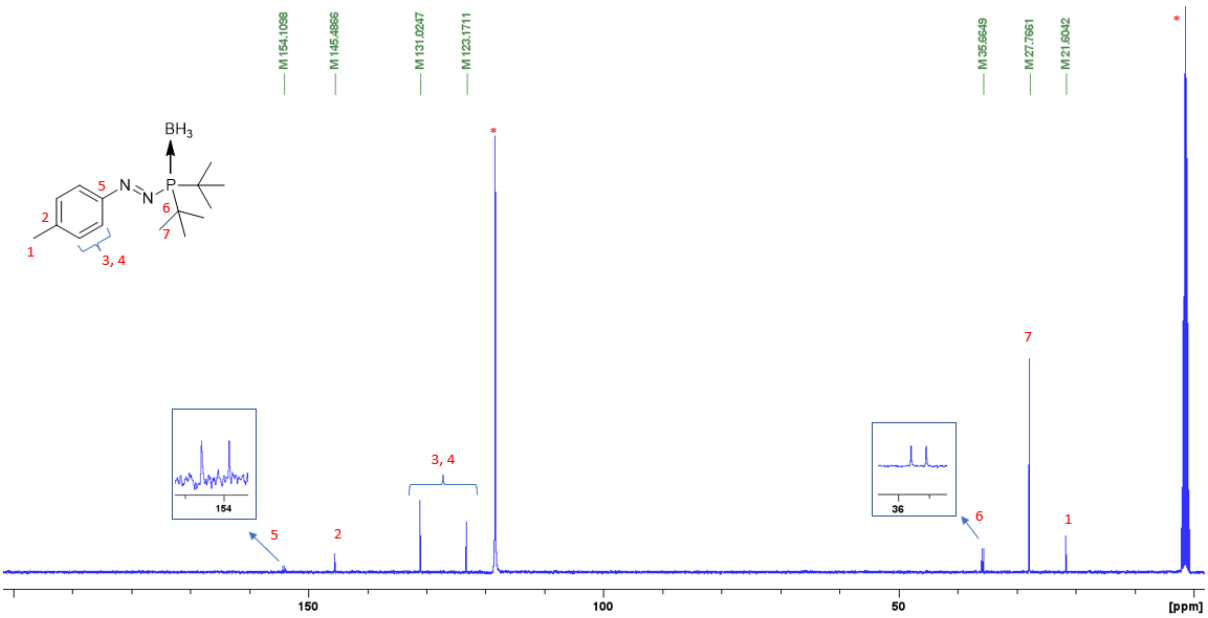

Figure A30. $^{13}C\{^{1}H\}$ spectrum of **7** in CD_3CN. * = CD_3CN.

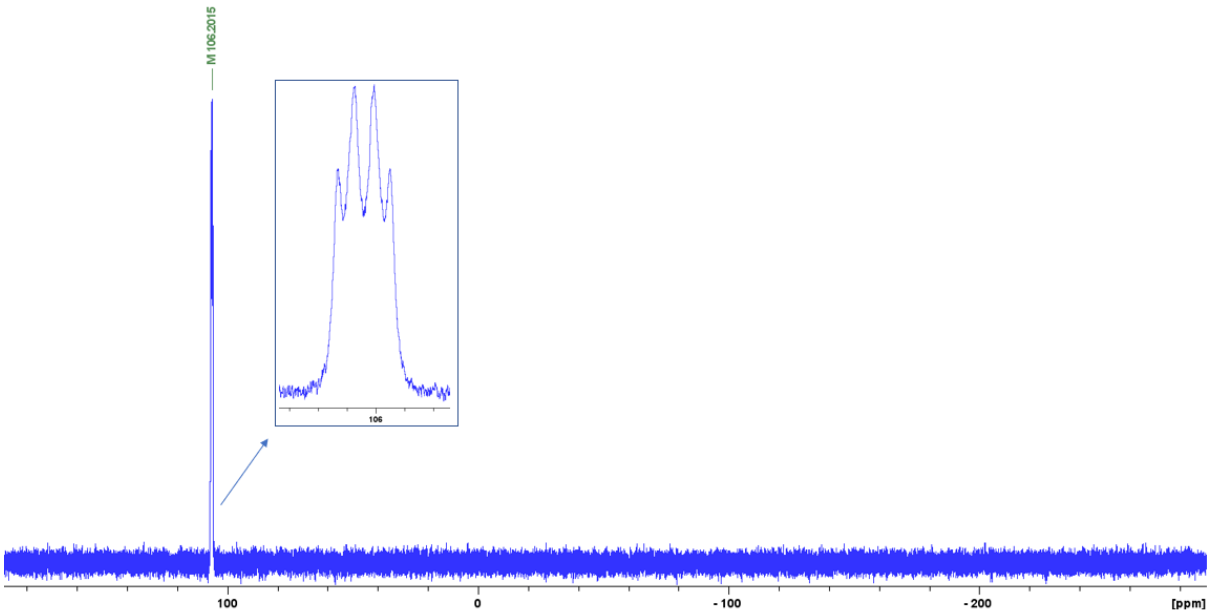

Figure A31. $^{31}P\{^{1}H\}$ spectrum of **7** in CD_3CN.

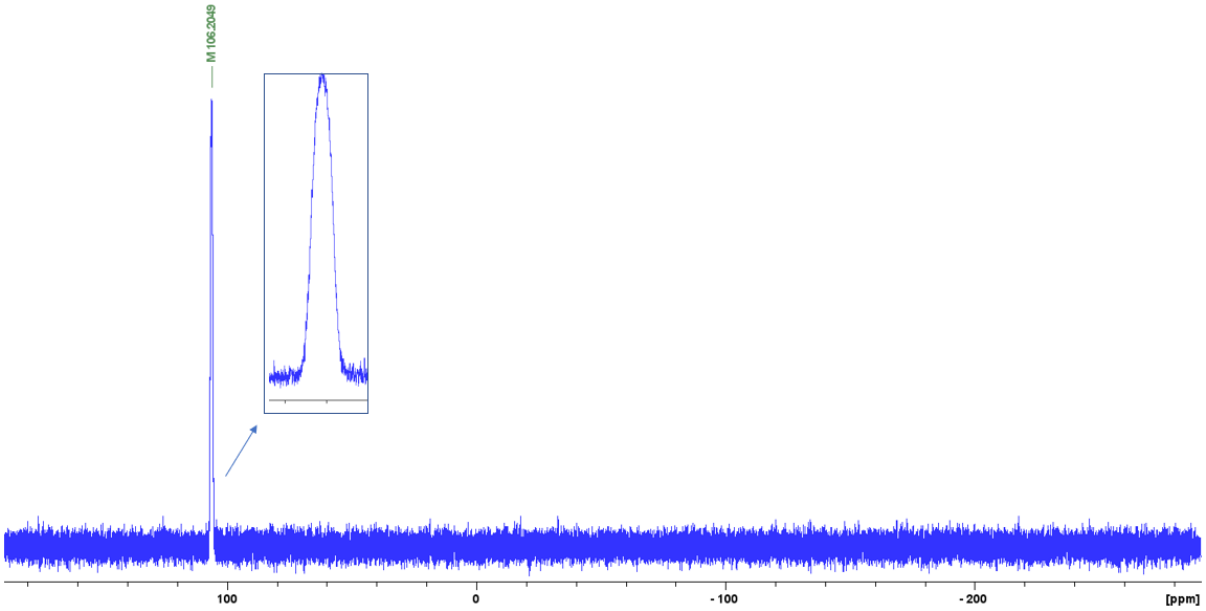

Figure A32. ^{31}P spectrum of **7** in CD_3CN.

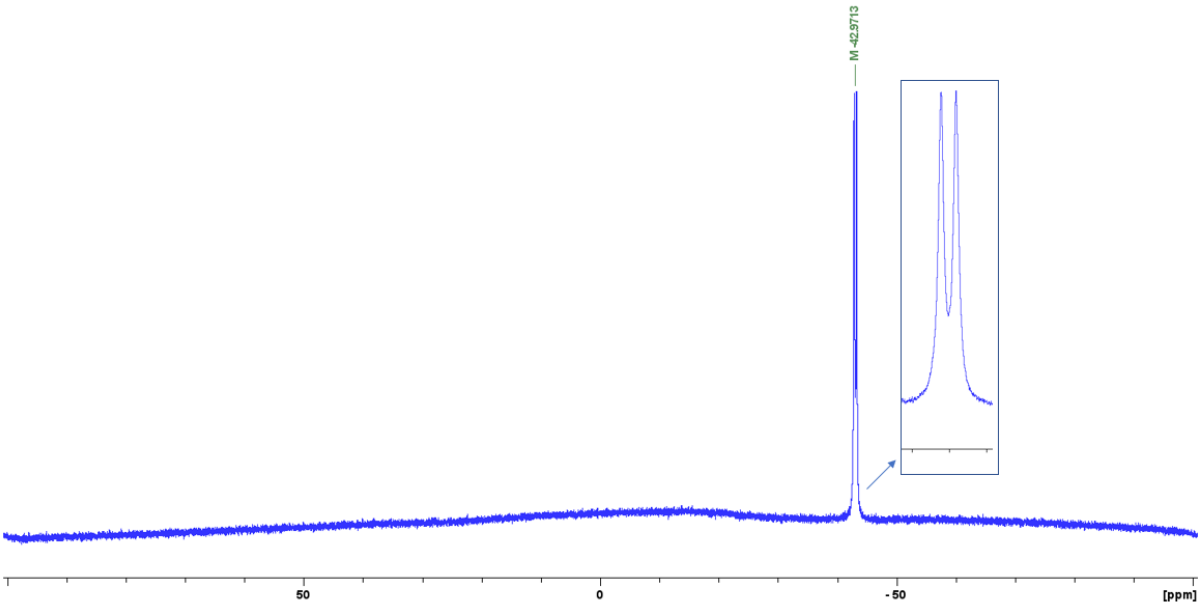

Figure A33. $^{11}B\{^{1}H\}$ spectrum of **7** in CD_3CN.

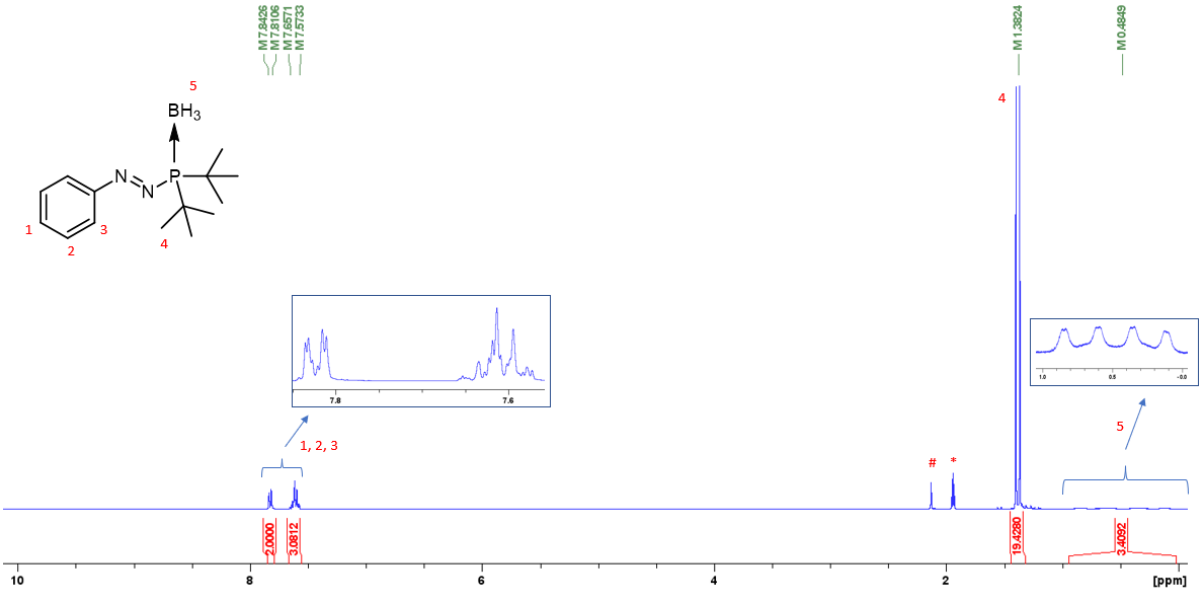

Figure A34. ^{1}H NMR spectrum of **8** in CD_3CN. * = residual CHD_2CN; # = water in CD_3CN.

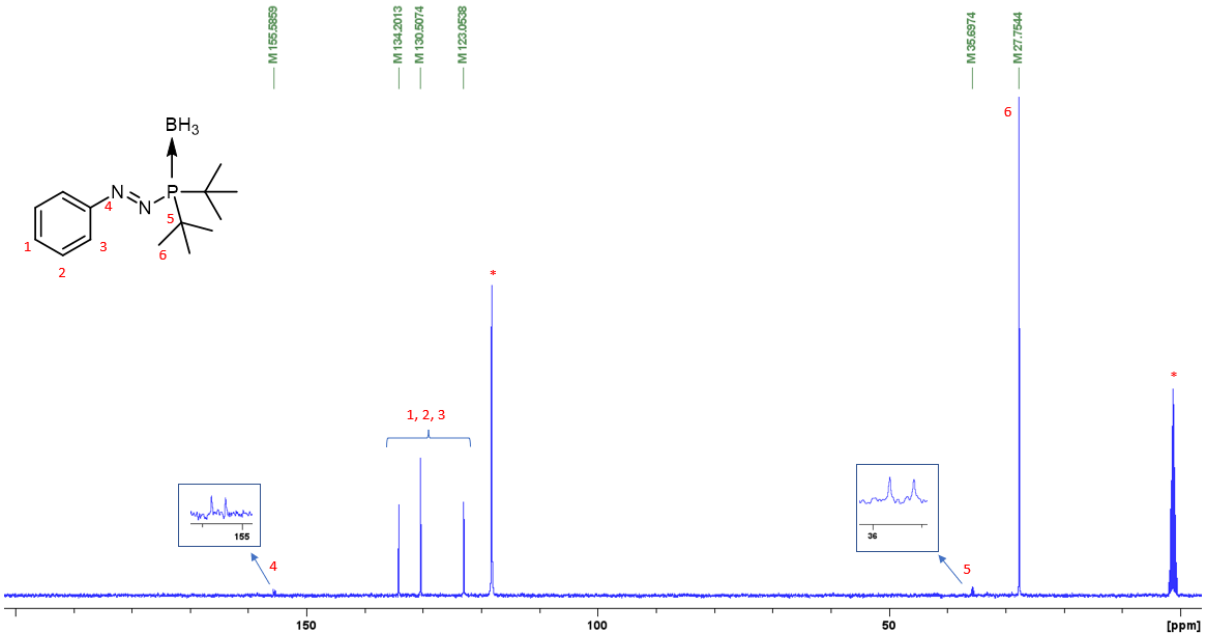

Figure A35. $^{13}C\{^{1}H\}$ spectrum of **8** in CD_3CN. * = CD_3CN.

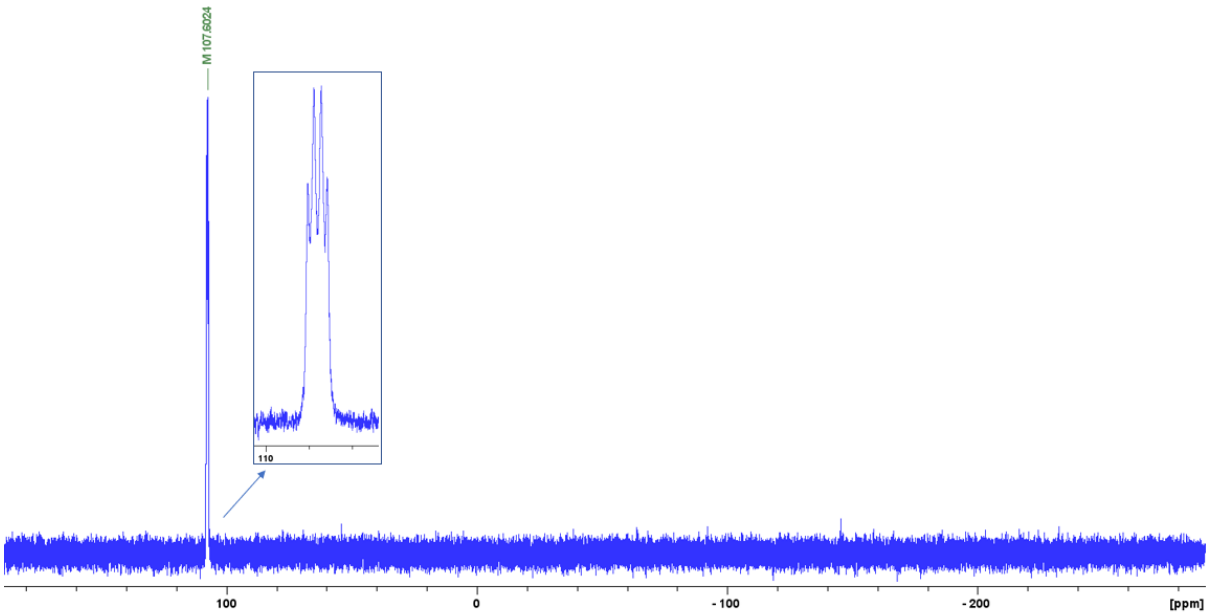

Figure A36. $^{31}P\{^{1}H\}$ spectrum of **8** in CD_3CN.

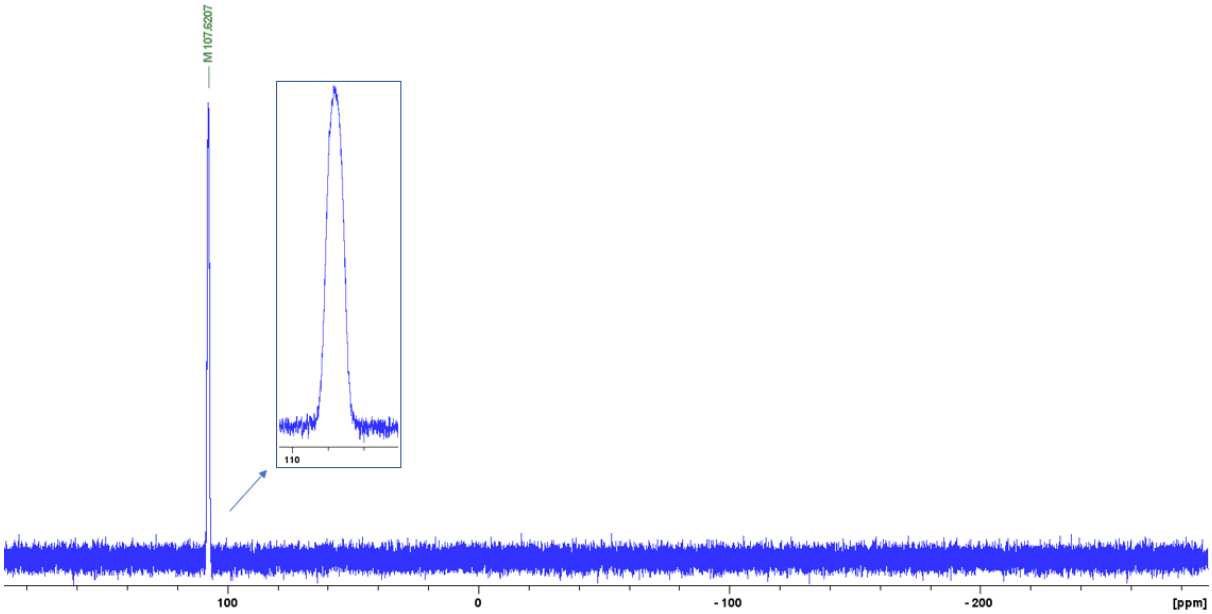

Figure A37. ^{31}P spectrum of **8** in CD_3CN.

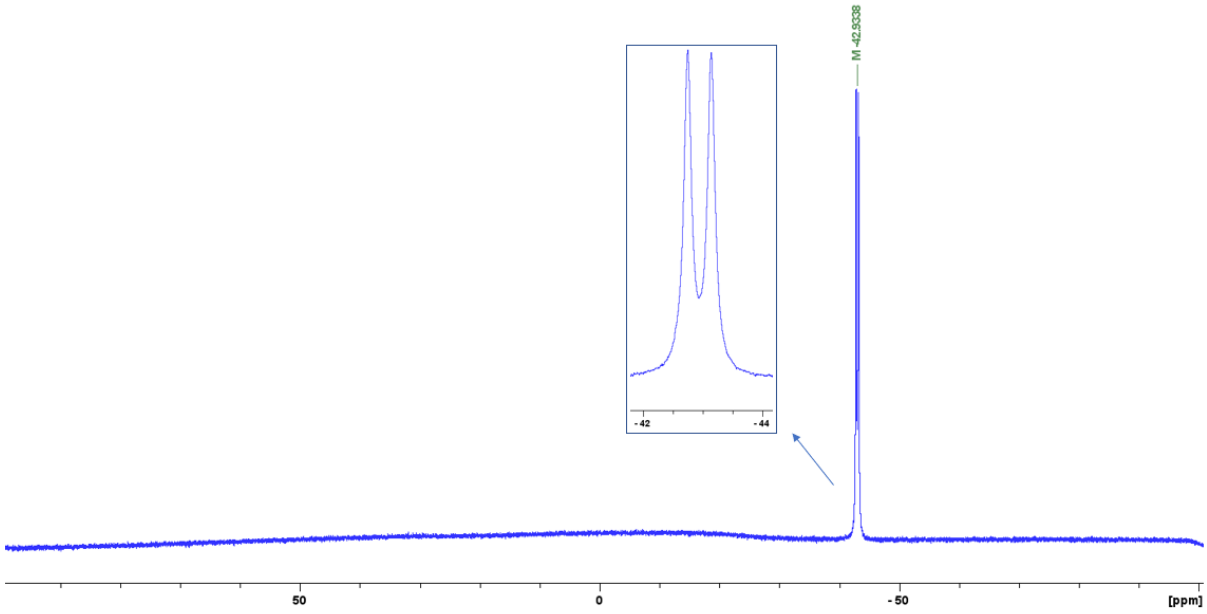

Figure A38. $^{11}B\{^1H\}$ spectrum of **8** in CD_3CN.

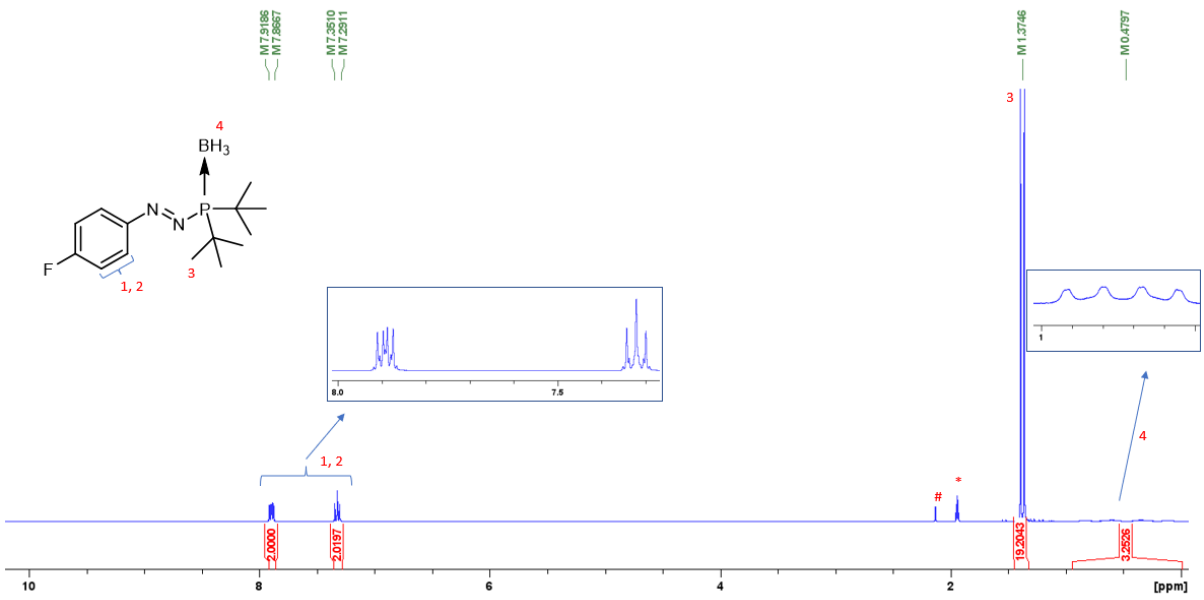

Figure A39. ^{1}H NMR spectrum of **9** in CD_3CN. * = residual CHD_2CN; # = water in CD_3CN.

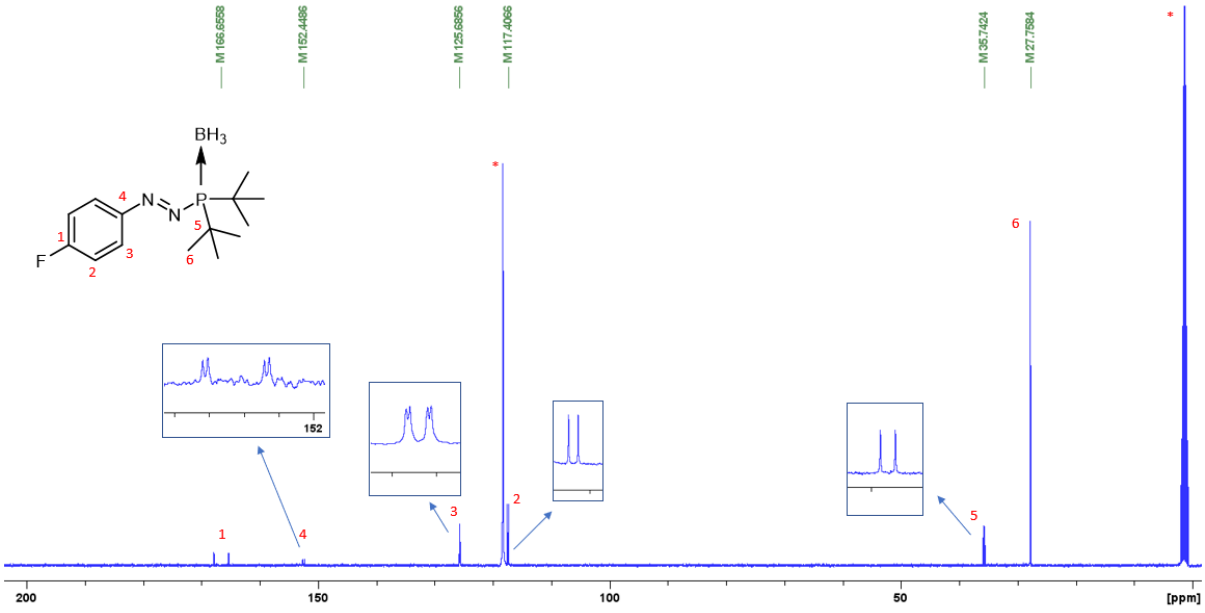

Figure A40. $^{13}C\{^{1}H\}$ spectrum of **9** in CD_3CN. * = CD_3CN.

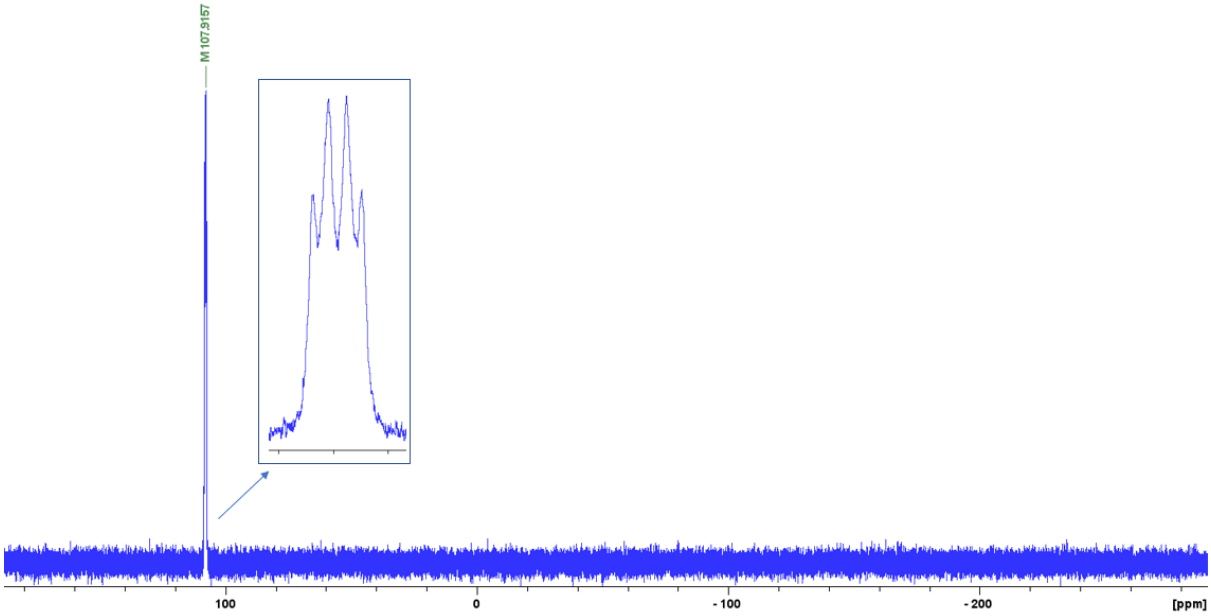

Figure A41. $^{31}P\{^{1}H\}$ spectrum of **9** in CD_3CN.

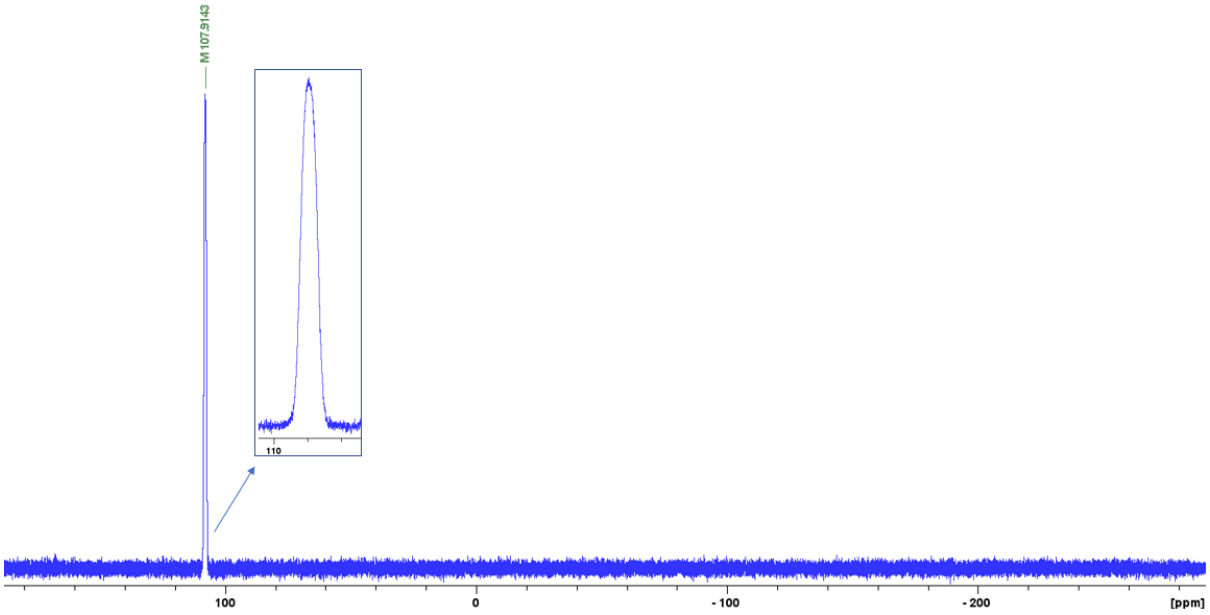

Figure A42. ^{31}P spectrum of **9** in CD_3CN.

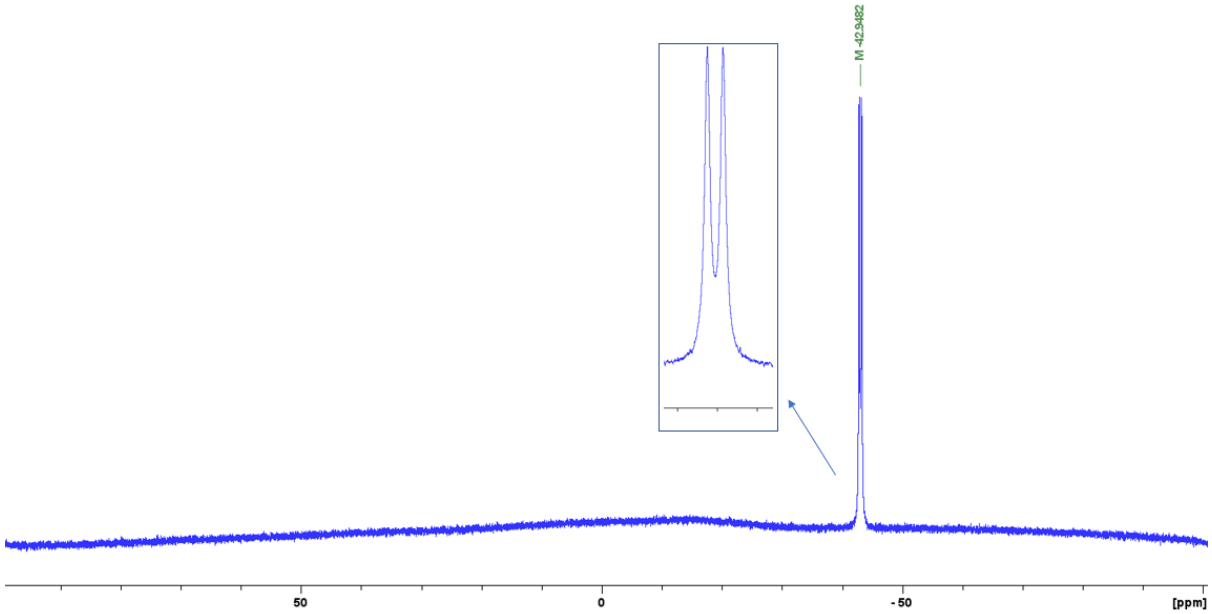

Figure A43. $^{11}B\{^{1}H\}$ spectrum of **9** in CD_3CN.

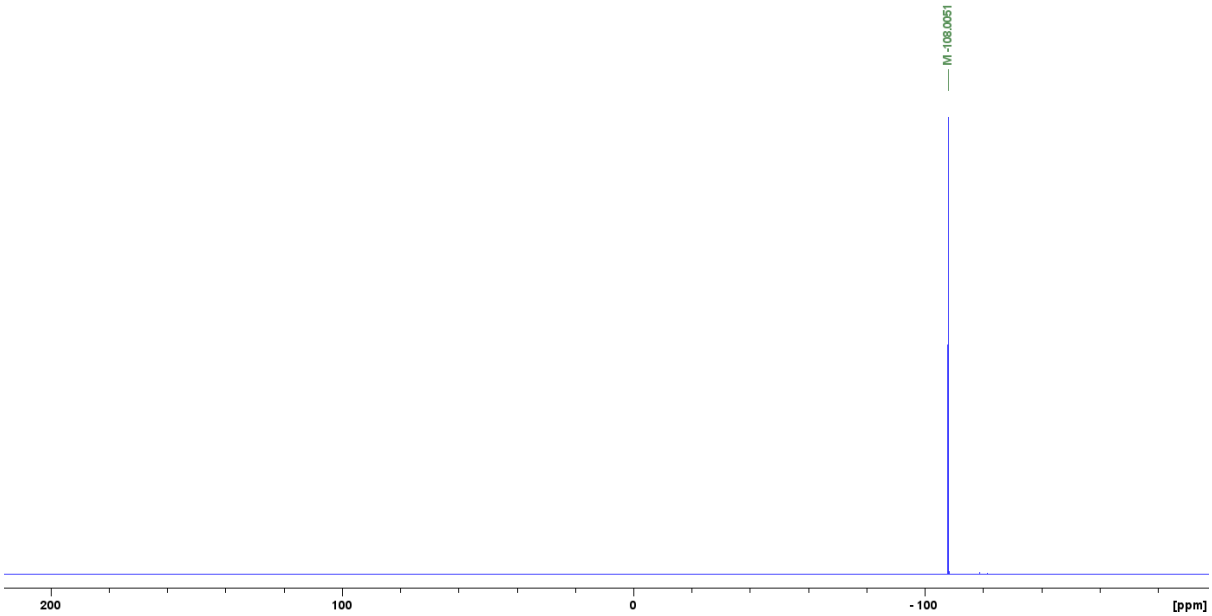

Figure A44. $^{19}F\{^{1}H\}$ spectrum of **9** in CD_3CN.

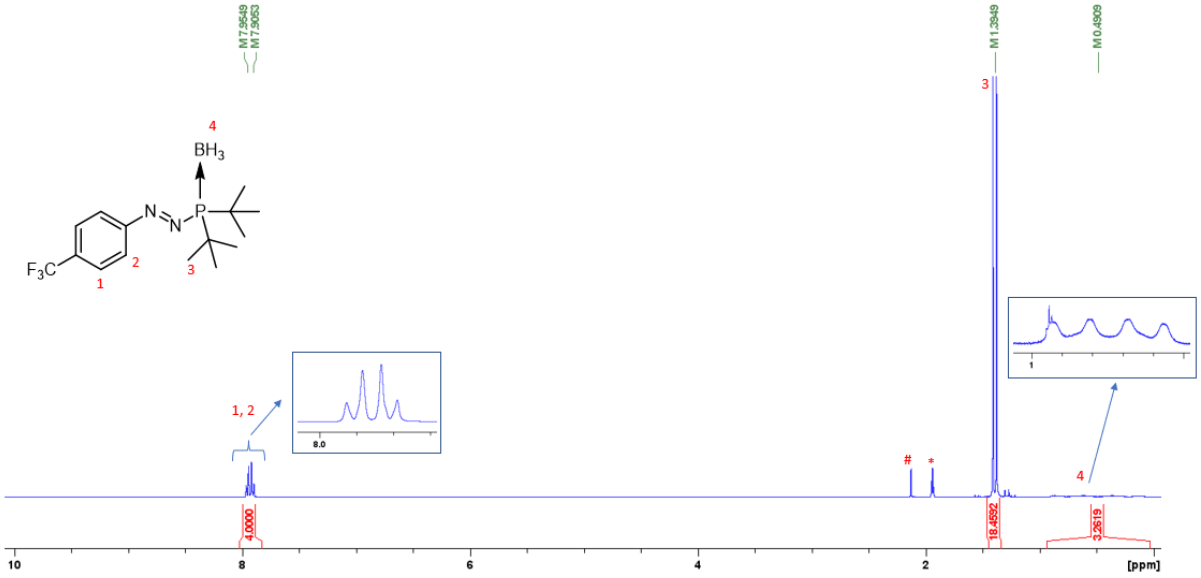

Figure A45. ^{1}H NMR spectrum of **10** in CD_3CN. * = residual CHD_2CN; # = water in CD_3CN.

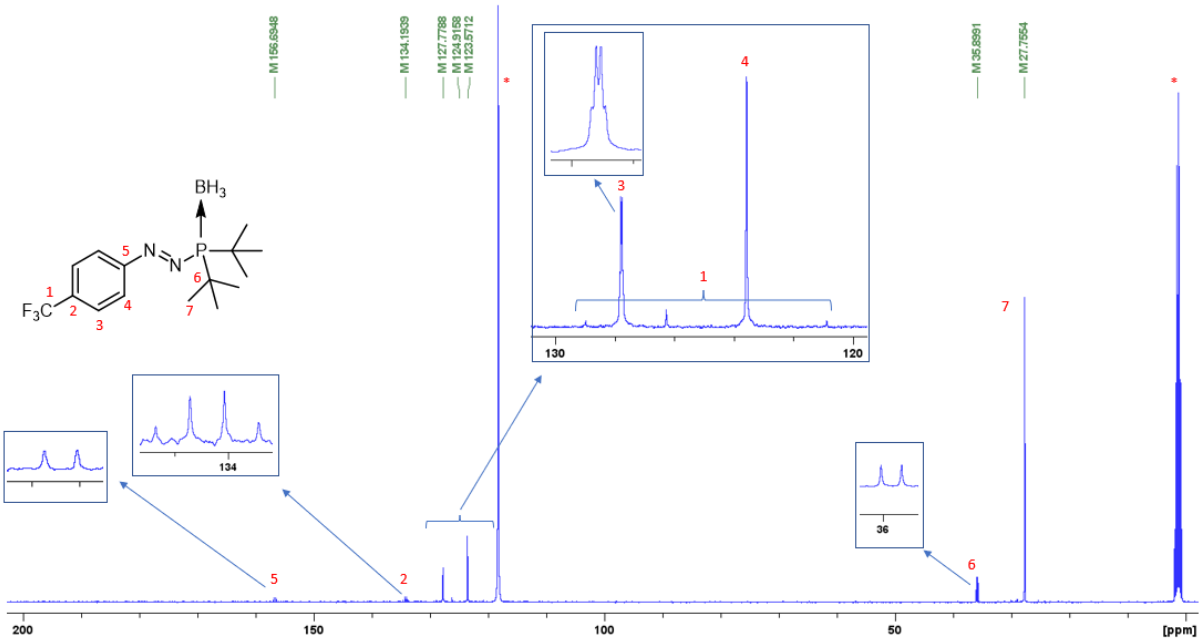

Figure A46. $^{13}C\{^{1}H\}$ spectrum of **10** in CD_3CN. * = CD_3CN.

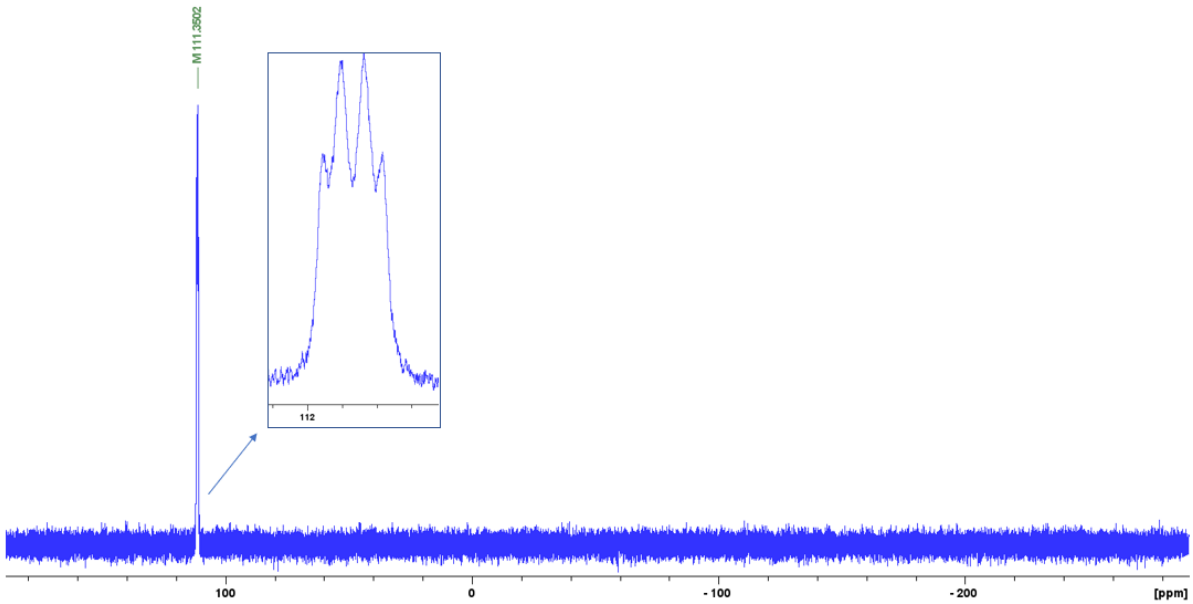

Figure A47. $^{31}P\{^{1}H\}$ spectrum of **10** in CD_3CN.

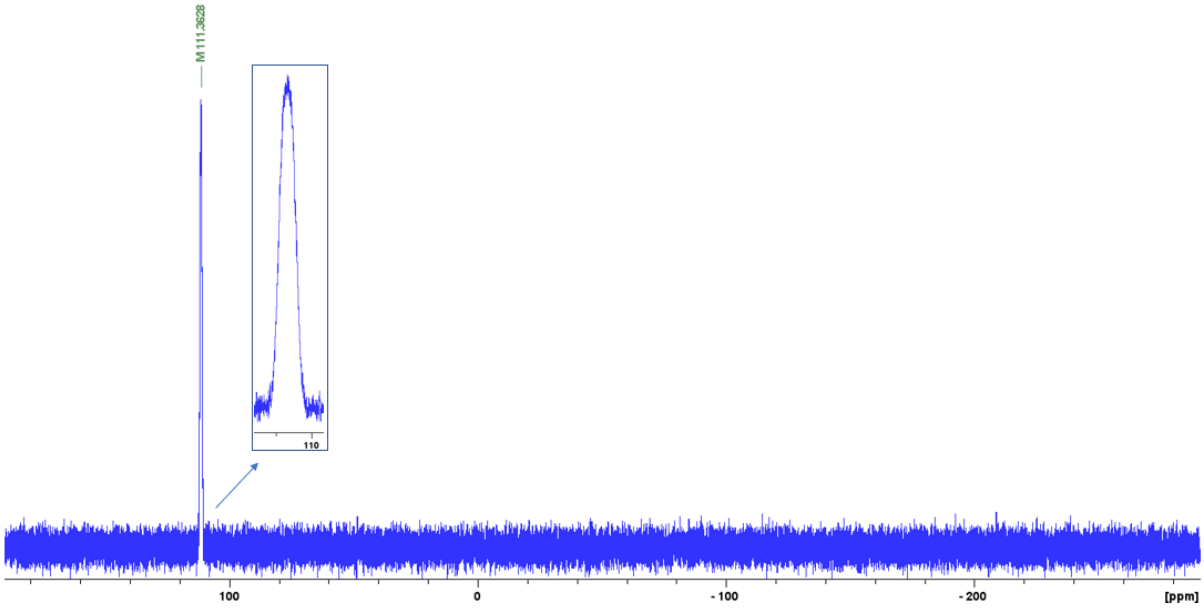

Figure A48. ^{31}P spectrum of **10** in CD_3CN.

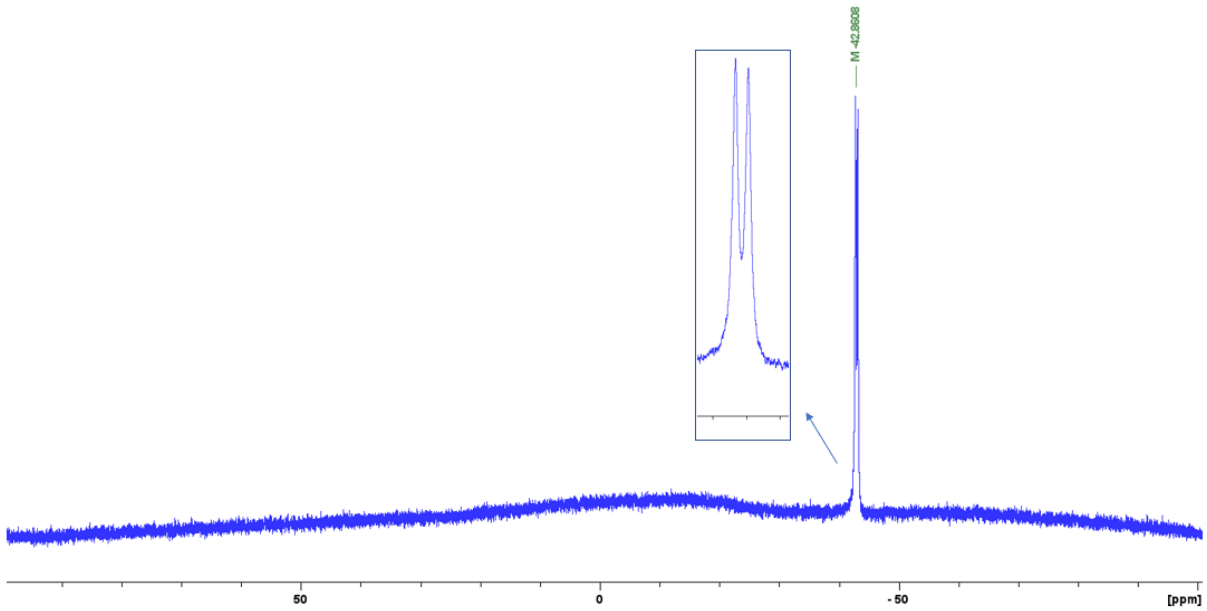

Figure A49. $^{11}B\{^{1}H\}$ spectrum of **10** in CD_3CN.

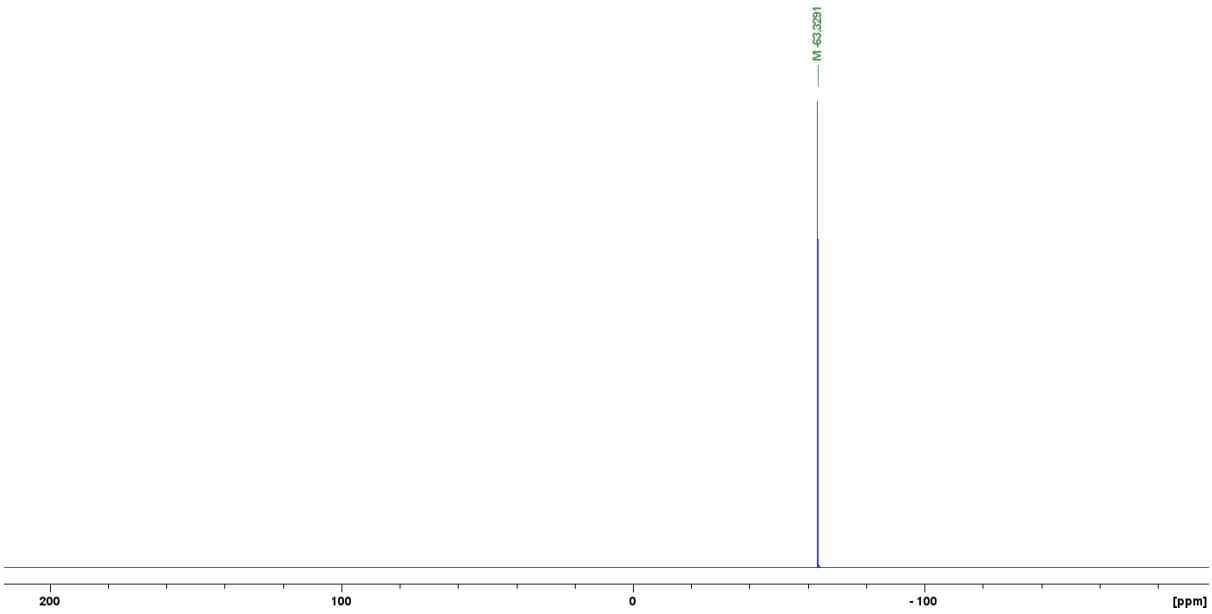

Figure A50. $^{19}F\{^{1}H\}$ spectrum of **10** in CD_3CN.

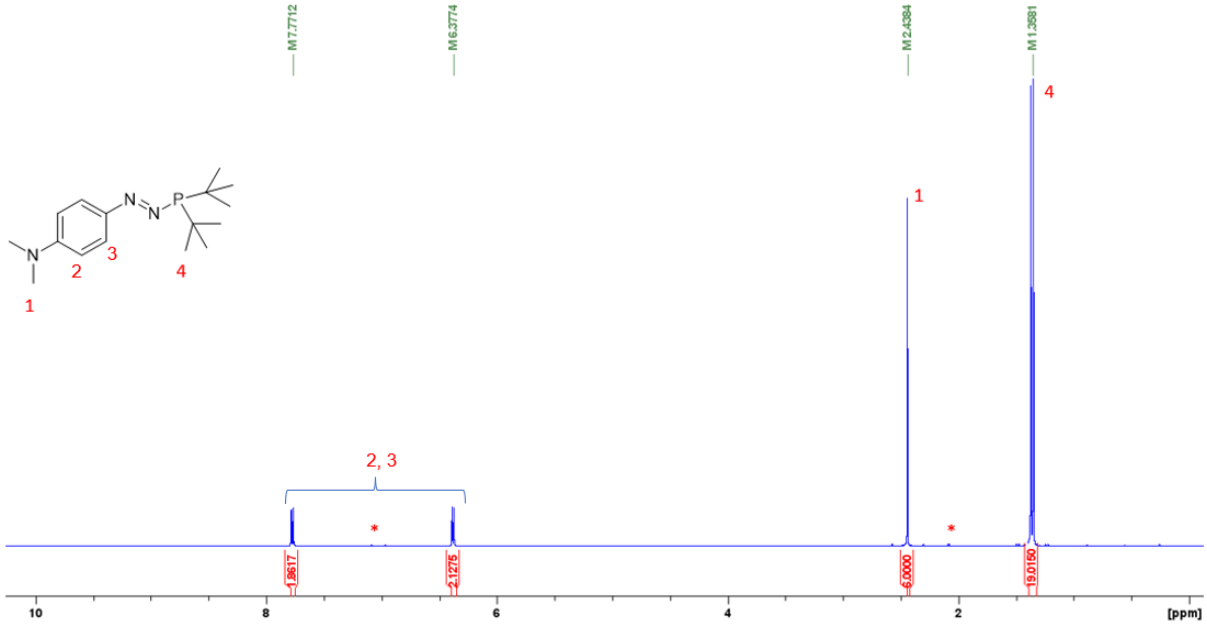

Figure A51. ^{1}H NMR spectrum of **11** in toluene-d_8. * = residual toluene-d_7H.

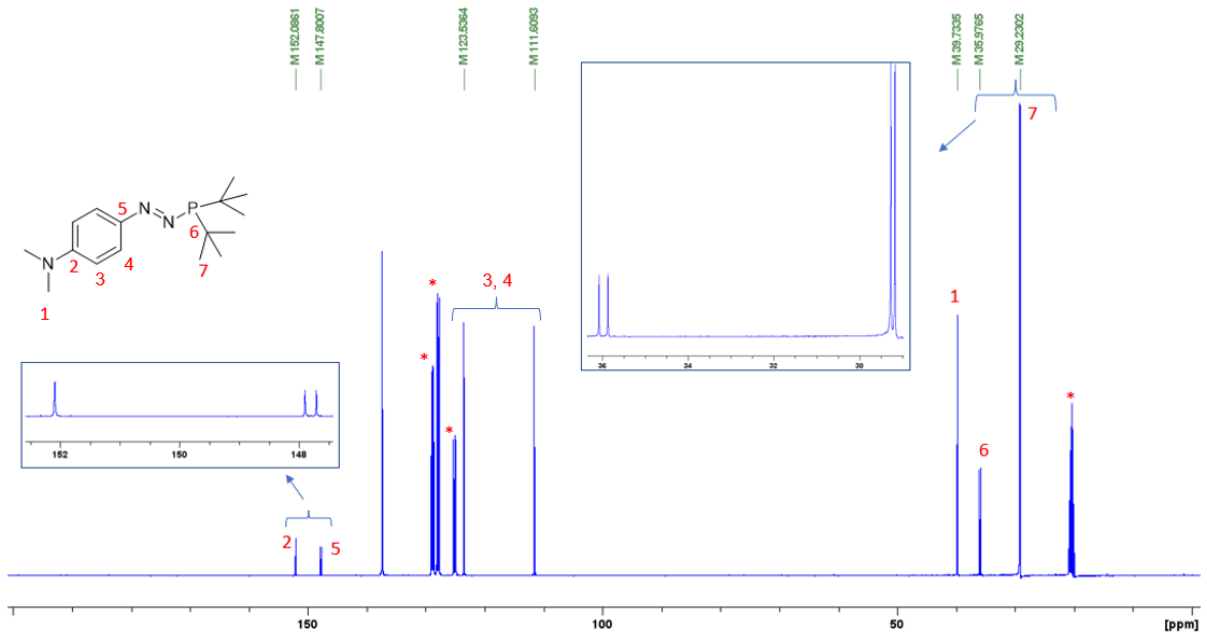

Figure A52. ^{13}C NMR spectrum of **11** in toluene-d_8. * = toluene-d_8.

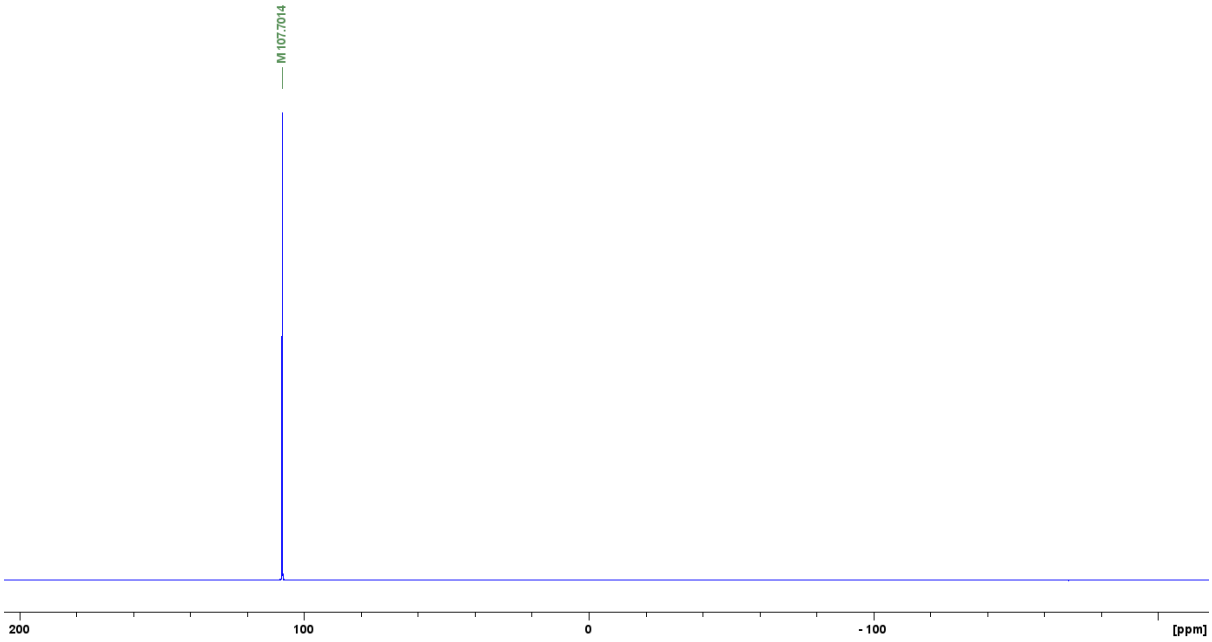

Figure A53. $^{31}P\{^{1}H\}$ NMR spectrum of **11** in toluene-d_8.

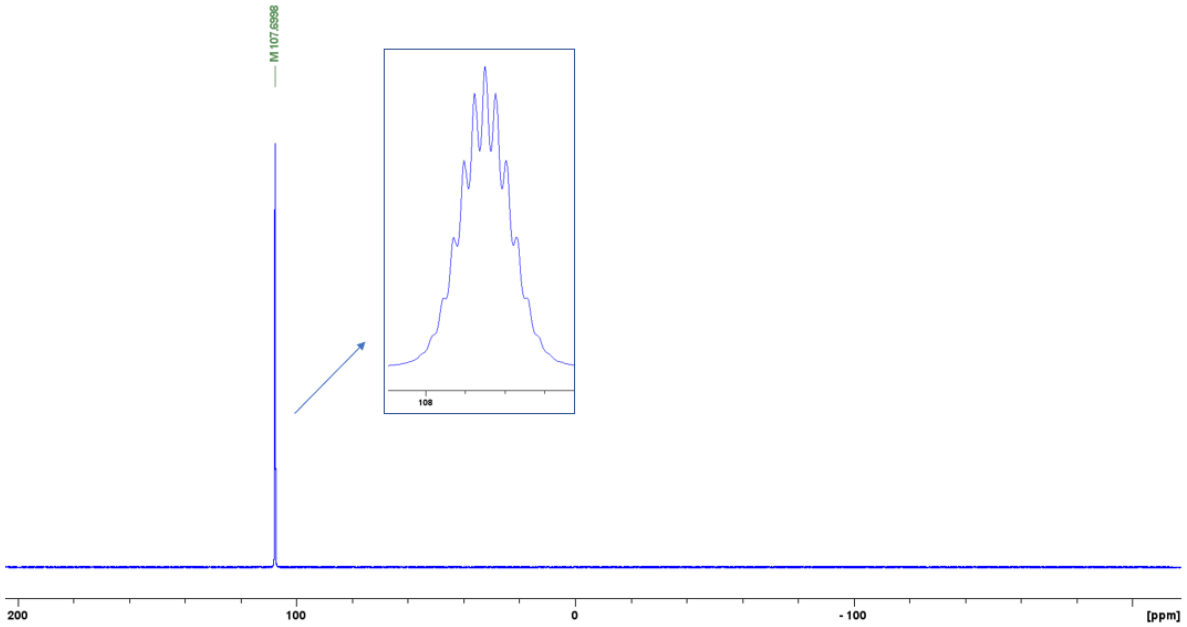

Figure A54. ^{31}P NMR spectrum of **11** in toluene-d_8.

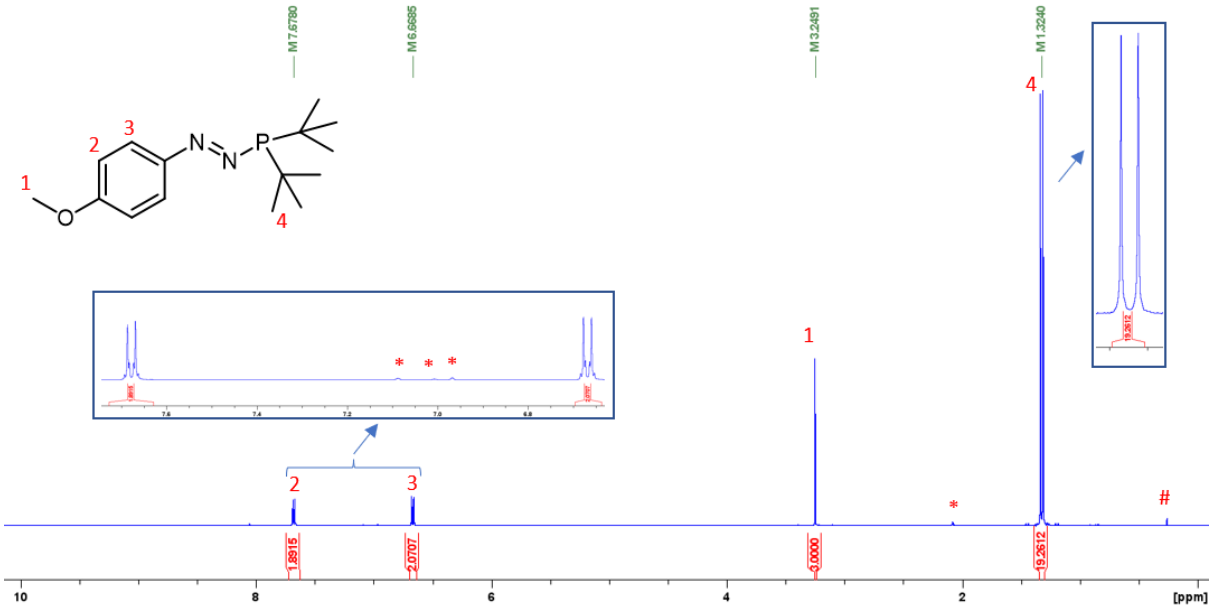

Figure A55. ^{1}H NMR spectrum of **12** in toluene-d_8. * = residual toluene-d_7H, # = silicon grease.

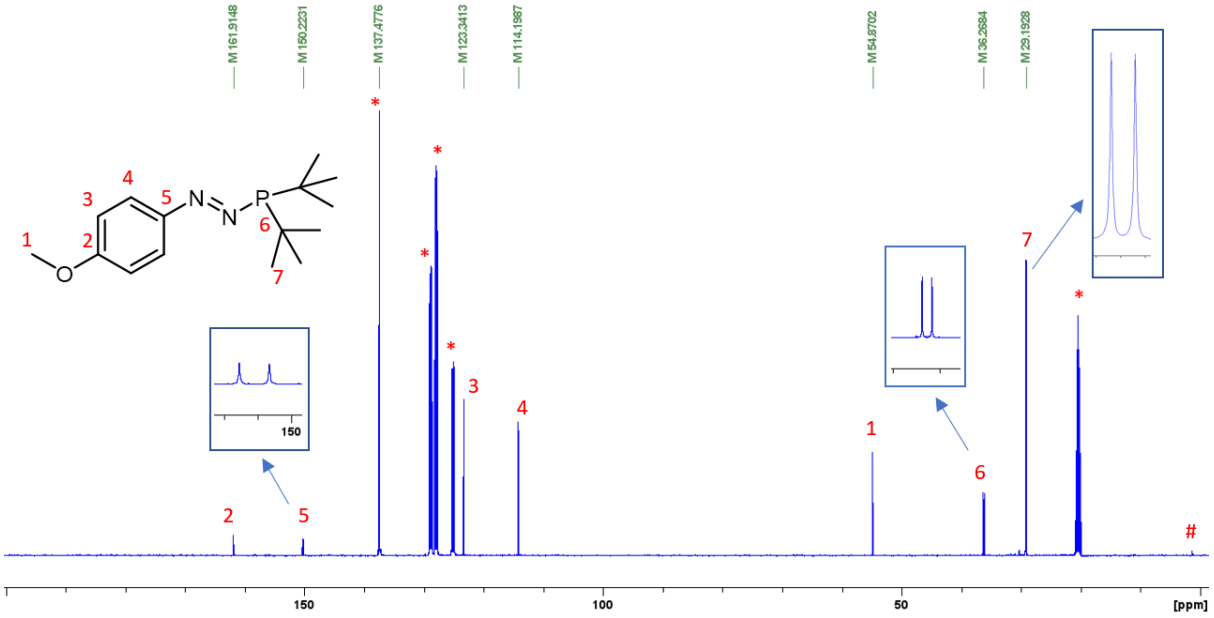

Figure A56. ^{13}C{^{1}H} NMR spectrum of **12** in toluene-d_8. * = toluene-d_8, # = silicon grease.

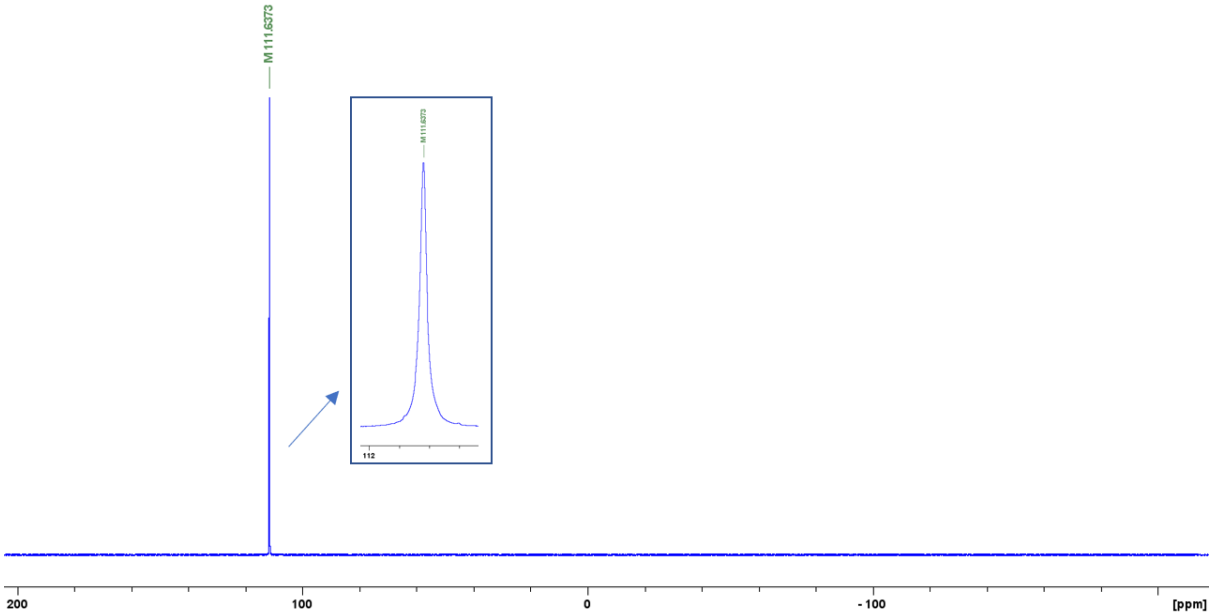

Figure A57. $^{31}P\{^{1}H\}$ NMR spectrum of **12** in toluene-d_8.

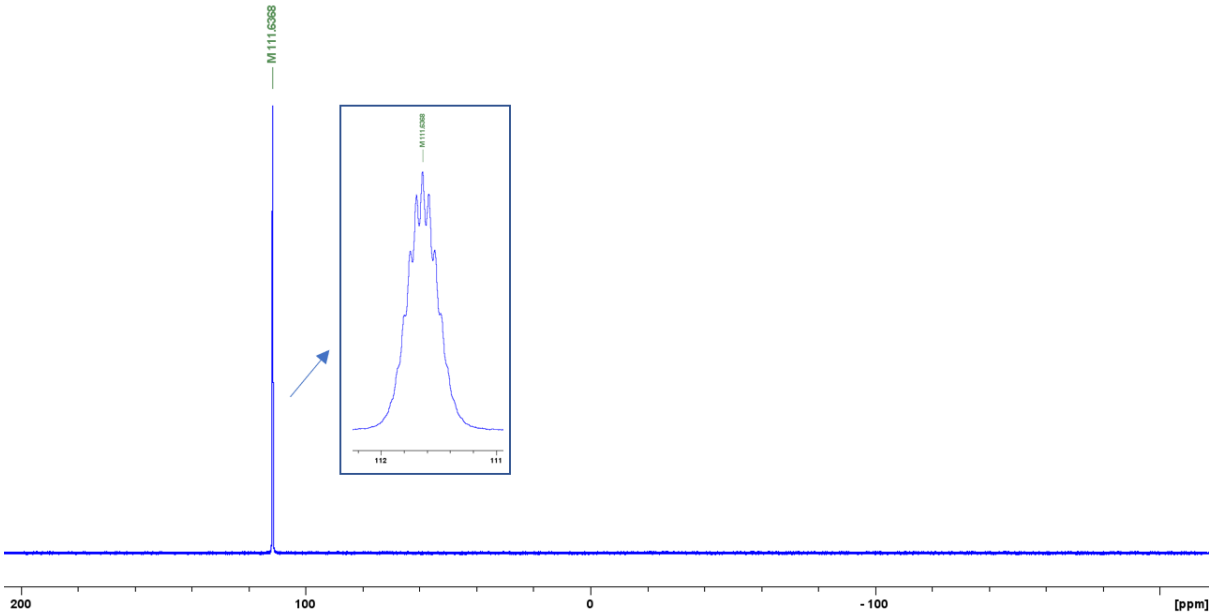

Figure A58. ^{31}P NMR spectrum of **12** in toluene-d_8.

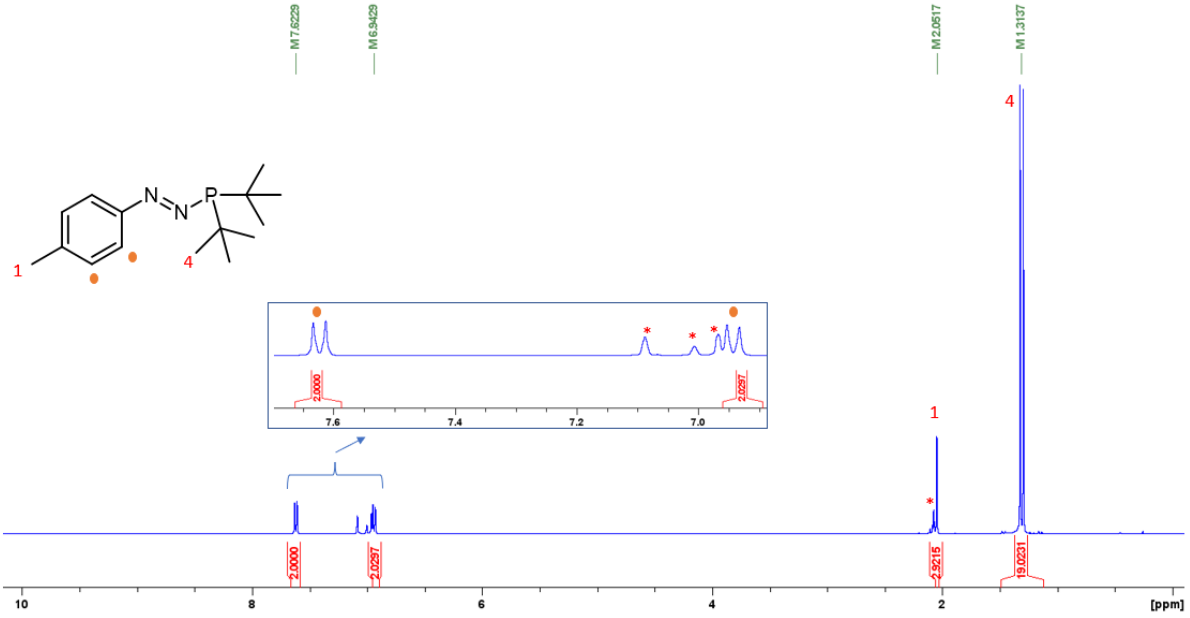

Figure A59. ^{1}H NMR spectrum of **13** in toluene-d_8. * = residual toluene-d_7H.

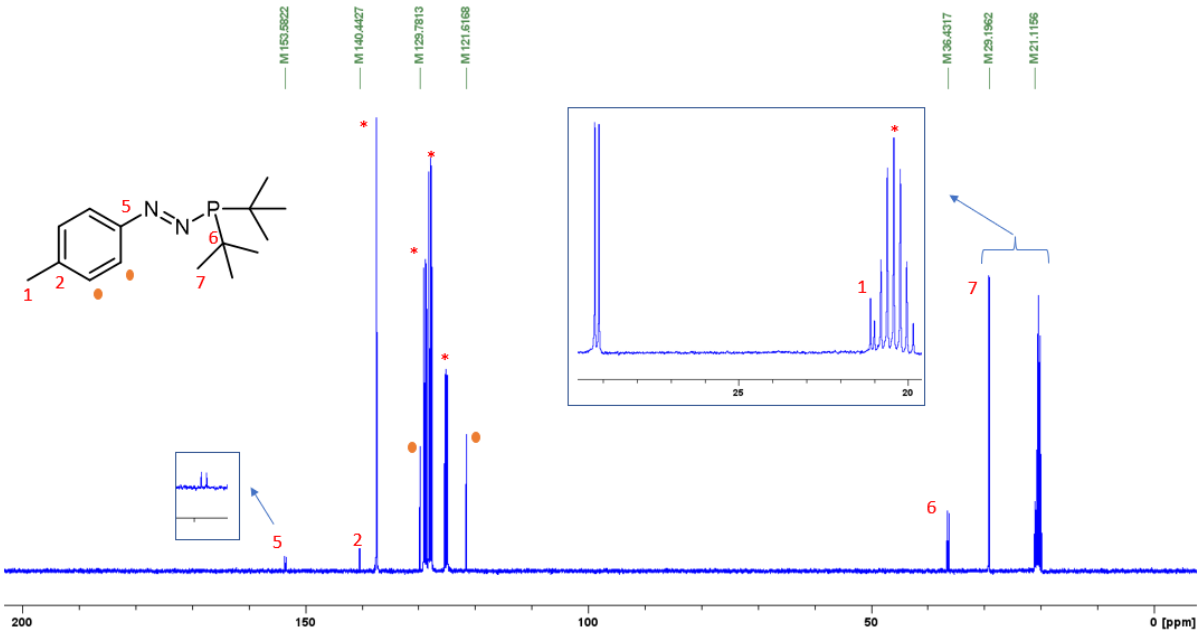

Figure A60. ^{13}C{^{1}H} NMR spectrum of **13** in toluene_d_8. * = toluene-d_8.

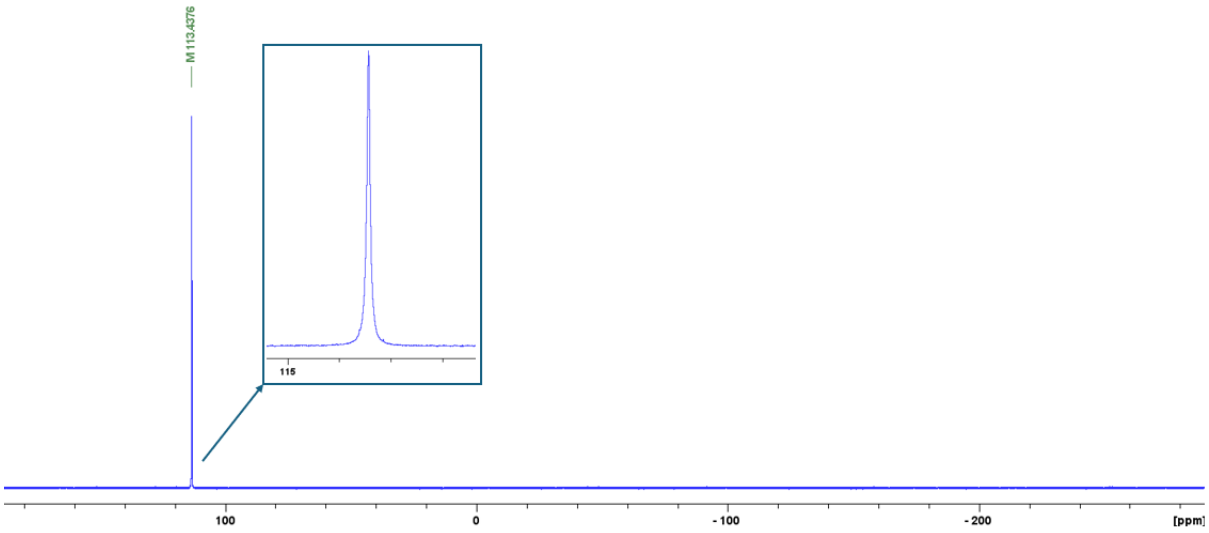

Figure A61. $^{31}P\{^{1}H\}$ NMR spectrum of **13** in toluene-d_8.

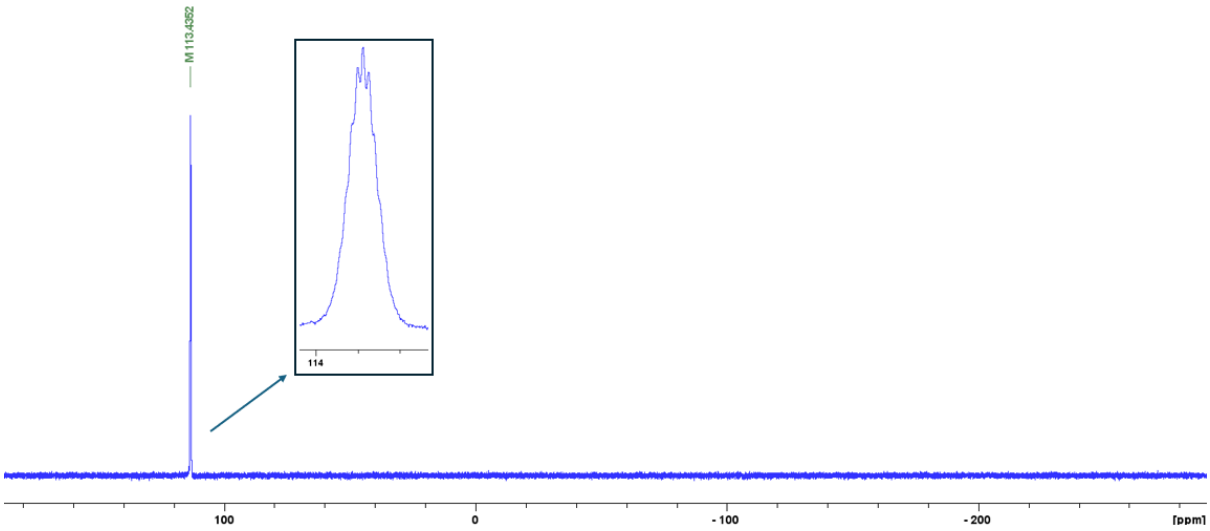

Figure A62. ^{31}P NMR spectrum of **13** in toluene-d_8.

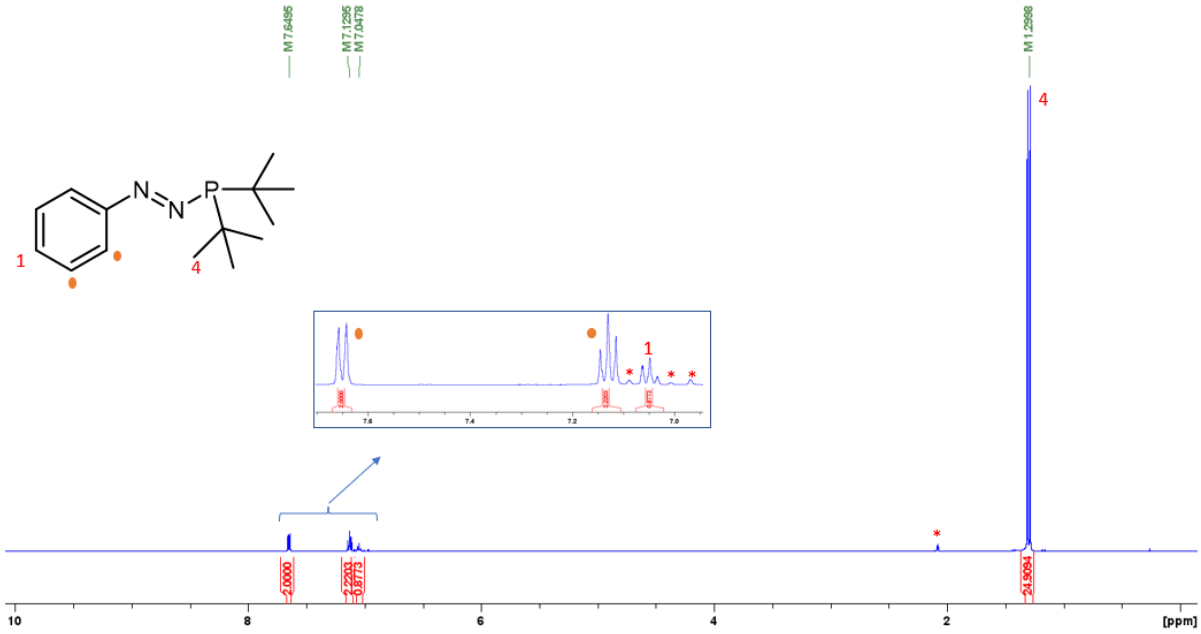

Figure A63. ^{1}H NMR spectrum of **14** in toluene-d_8. * = residual toluene-d_7H.

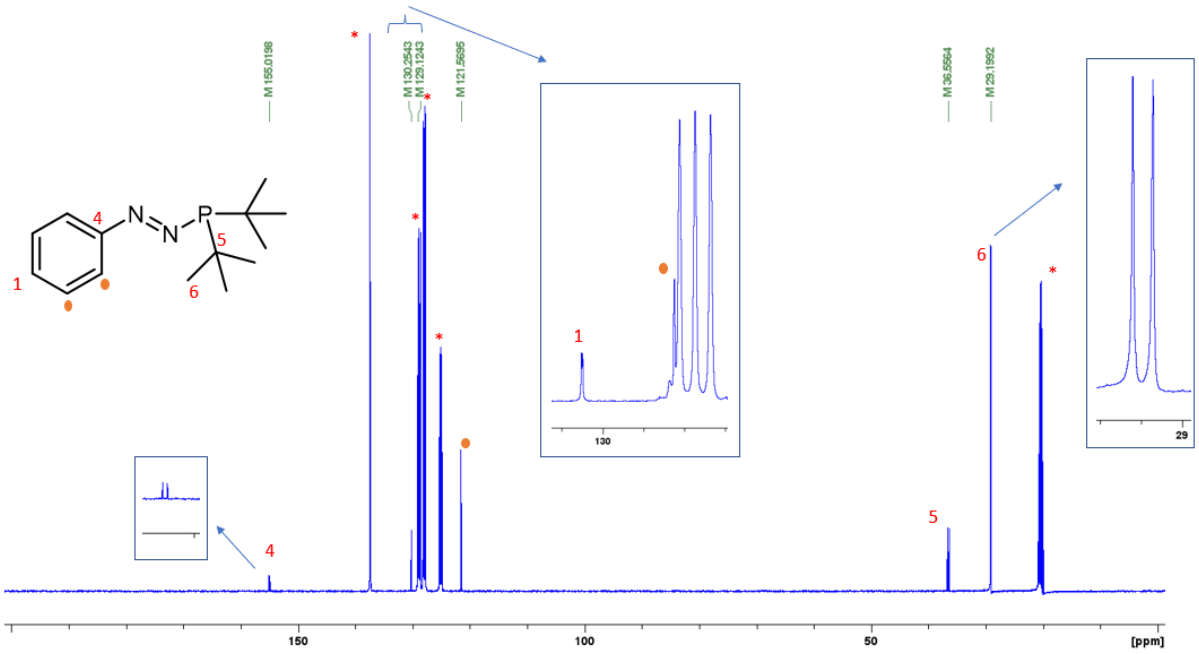

Figure A64. ^{13}C{^{1}H} NMR spectrum of **14** in toluene-d_8. * = toluene-d_8.

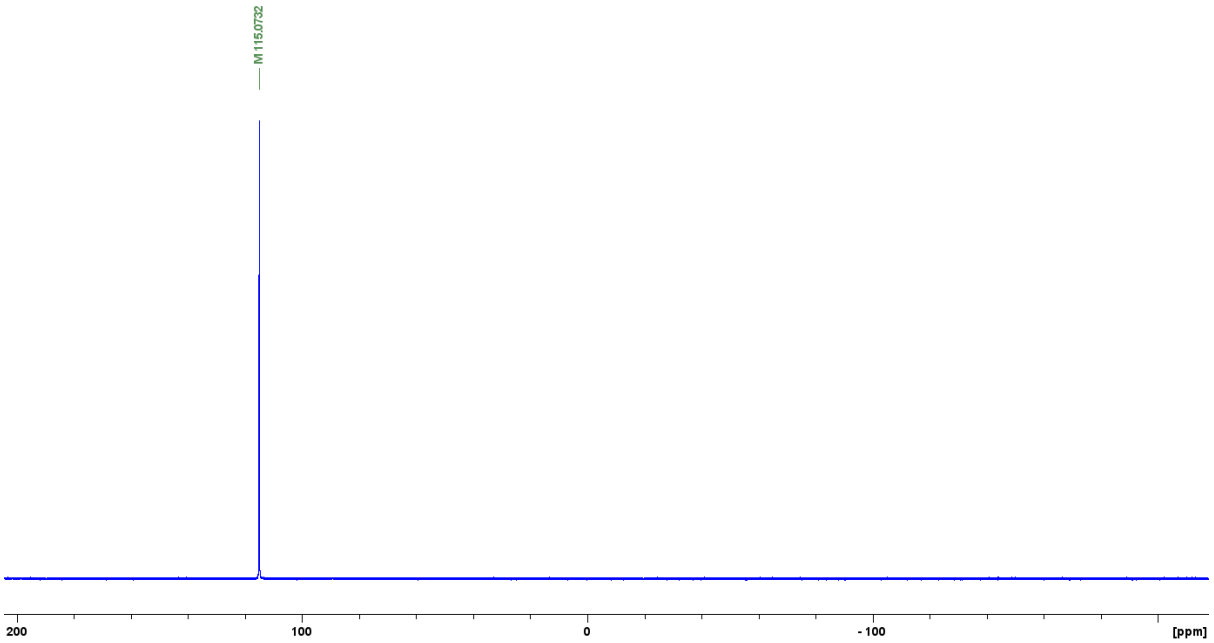

Figure A65. $^{31}P\{^{1}H\}$ NMR spectrum of **14** in toluene-d_8.

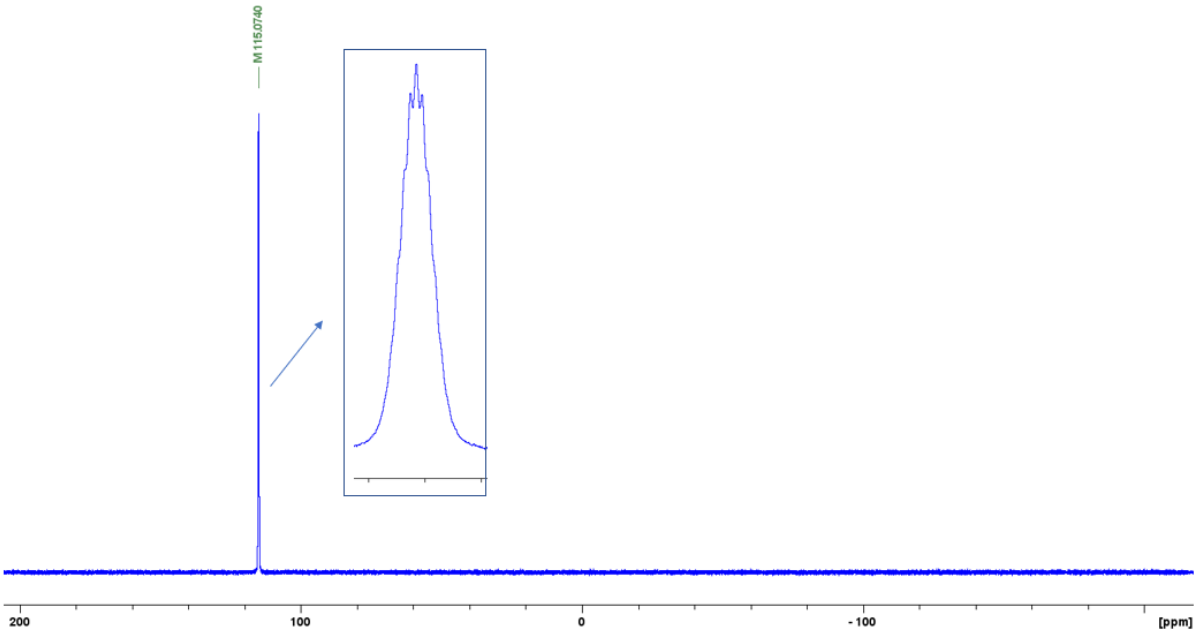

Figure A66. ^{31}P NMR spectrum of **14** in toluene-d_8.

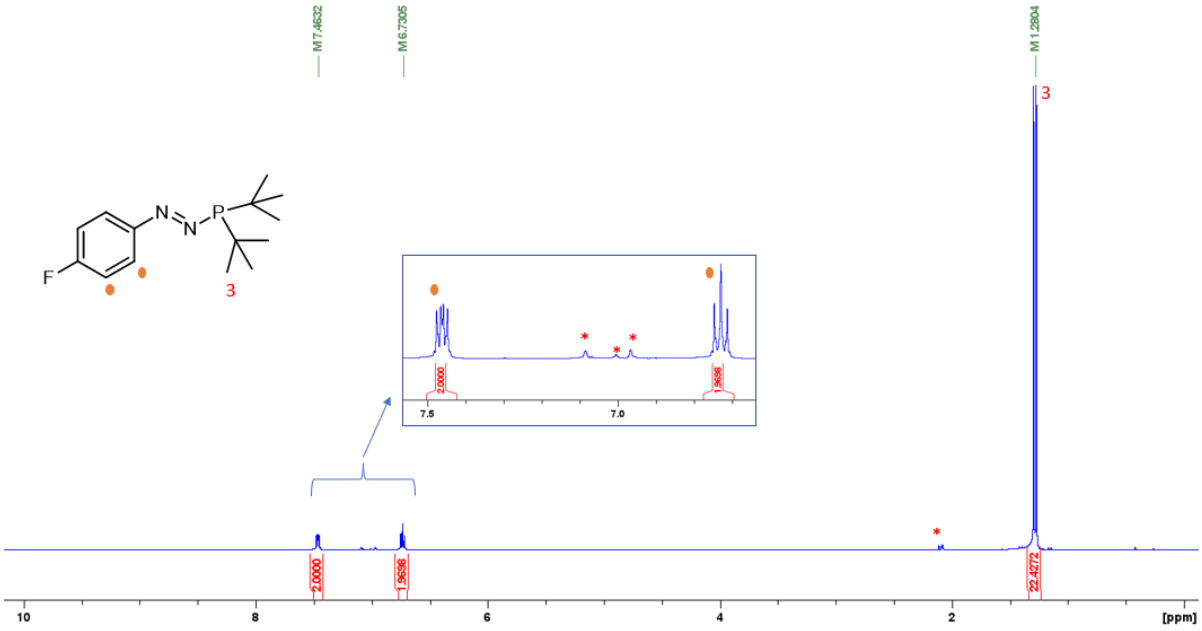

Figure A67. ^{1}H NMR spectrum of **15** in toluene-d_8. * = residual toluene-d_7H.

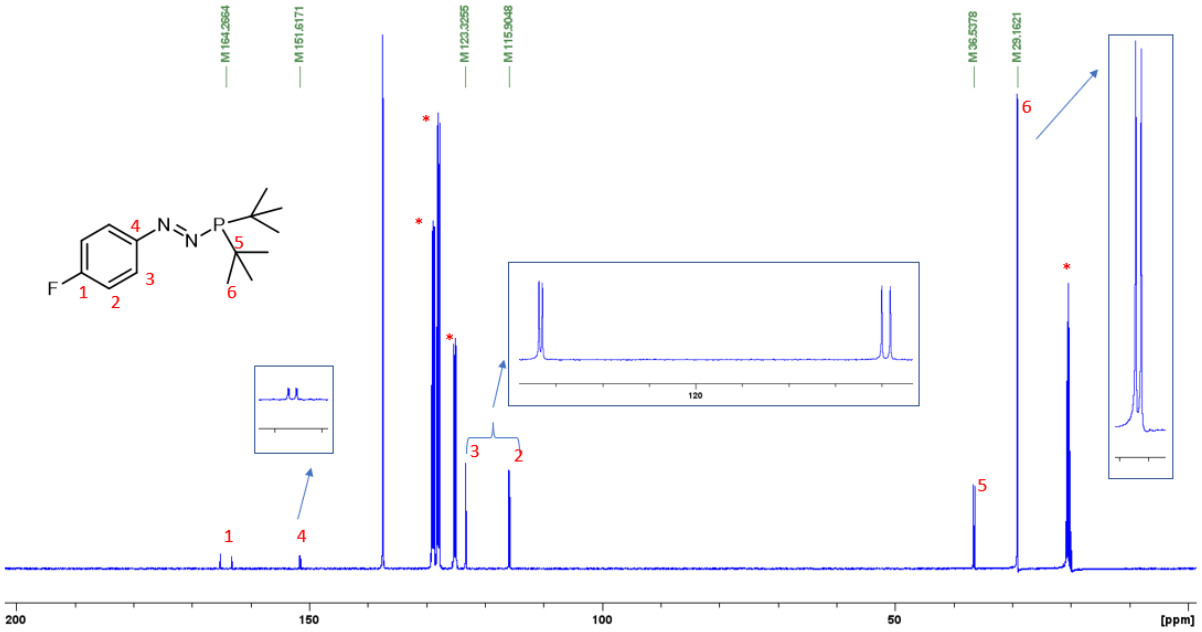

Figure A68. ^{13}C{^{1}H} NMR spectrum of **15** in toluene-d_8. * = toluene-d_8.

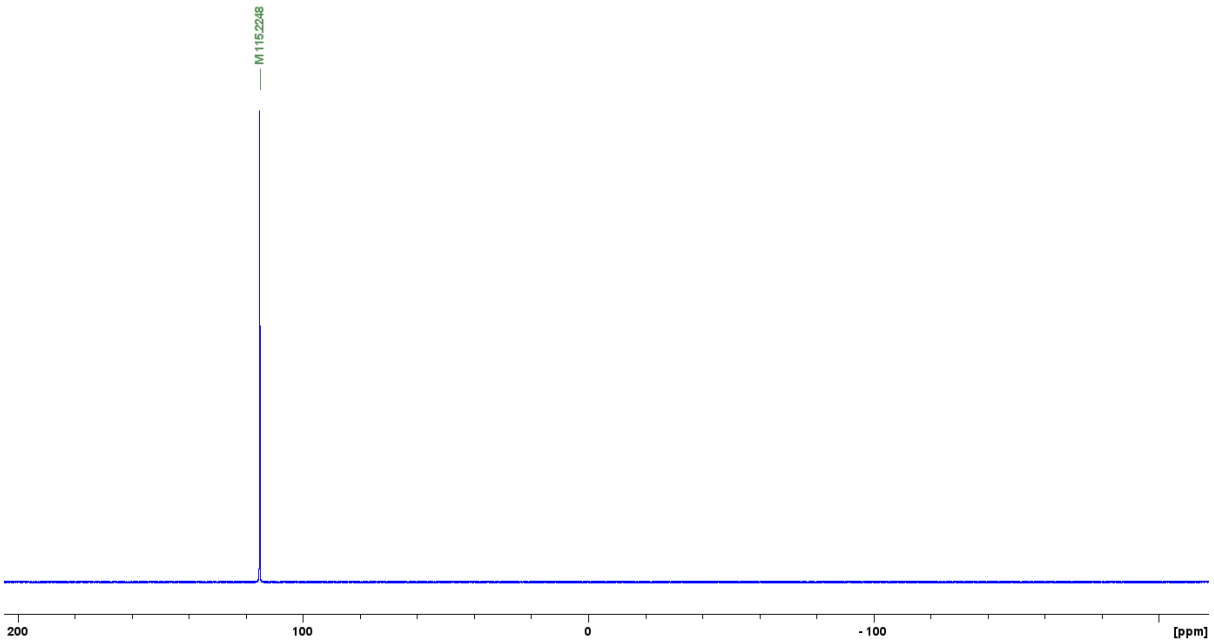

Figure A69. $^{31}P\{^{1}H\}$ NMR spectrum of **15** in toluene-d_8.

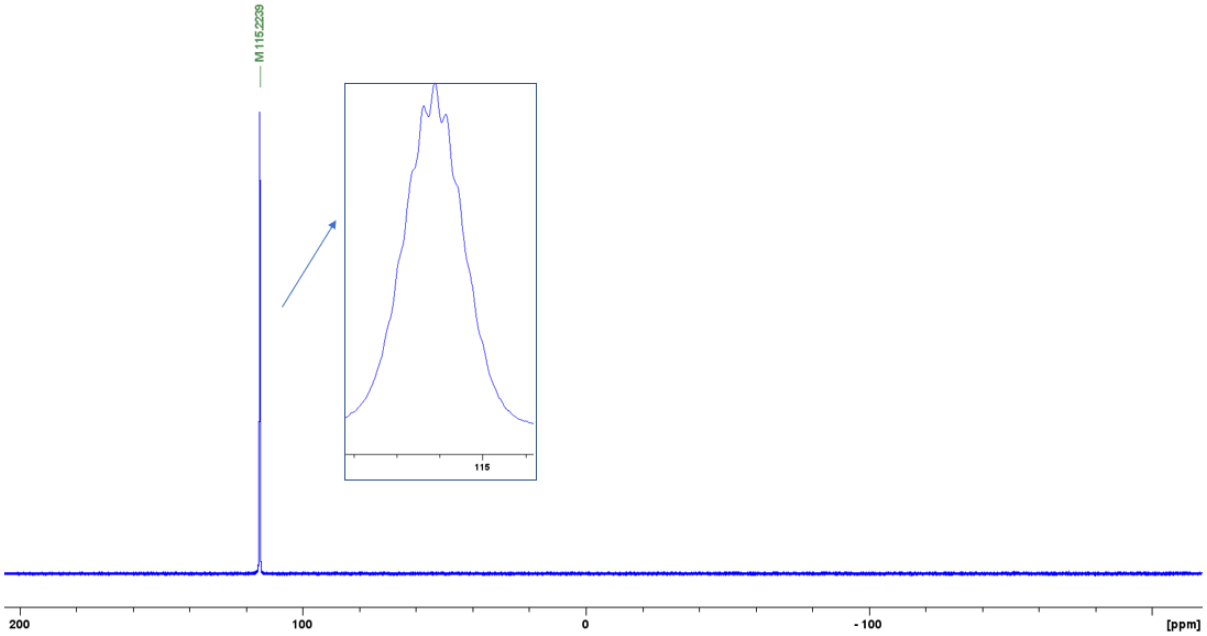

Figure A70. ^{31}P NMR spectrum of **15** in toluene-d_8.

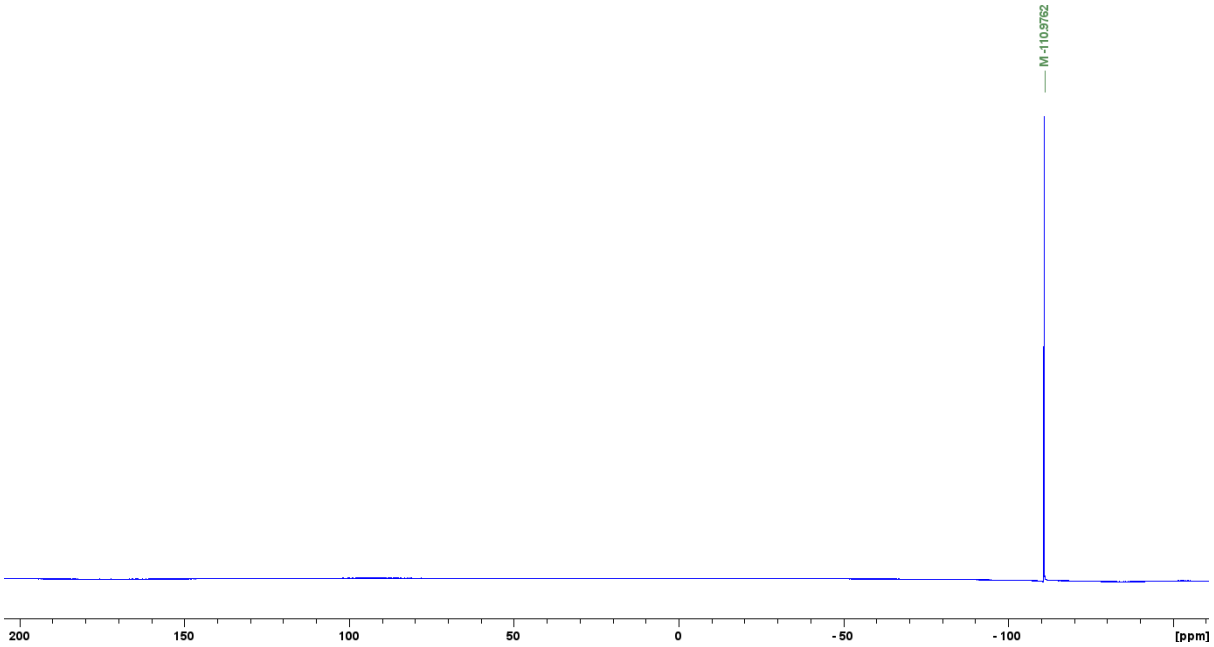

Figure A71. $^{19}F\{^{1}H\}$ NMR spectrum of **15** in toluene-d_8.

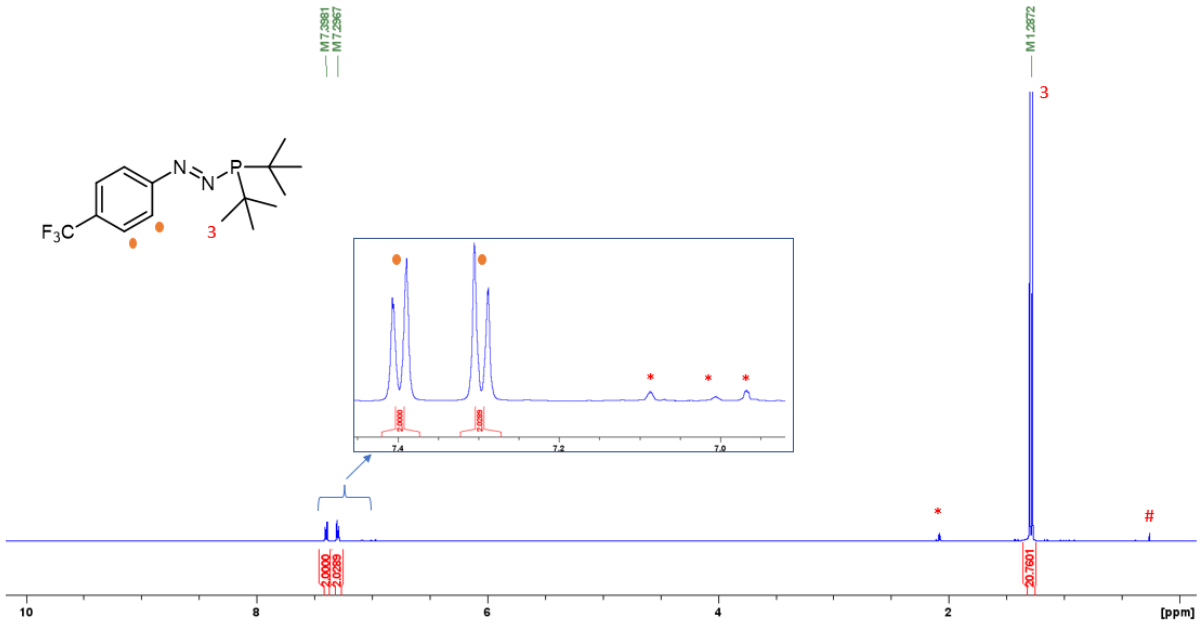

Figure A72. ^{1}H NMR spectrum of **16** in toluene-d_8. * = residual toluene-d_7H, # = silicon grease.

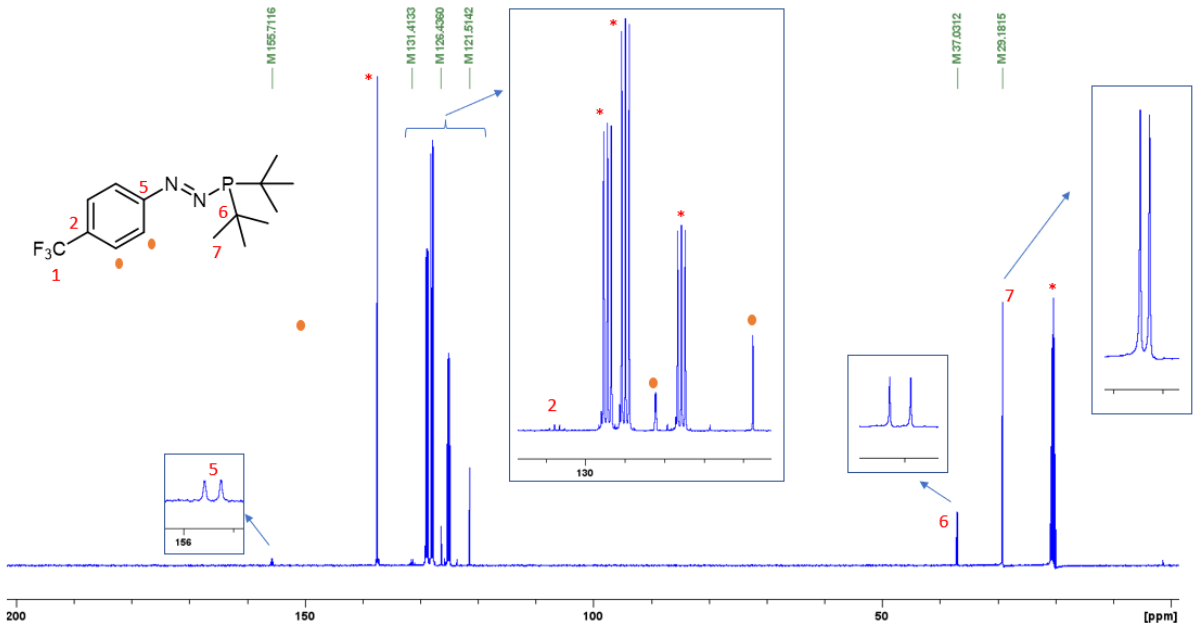

Figure A73. $^{31}C\{^{1}H\}$ NMR spectrum of **16** in toluene-d_8. * = toluene-d_8.

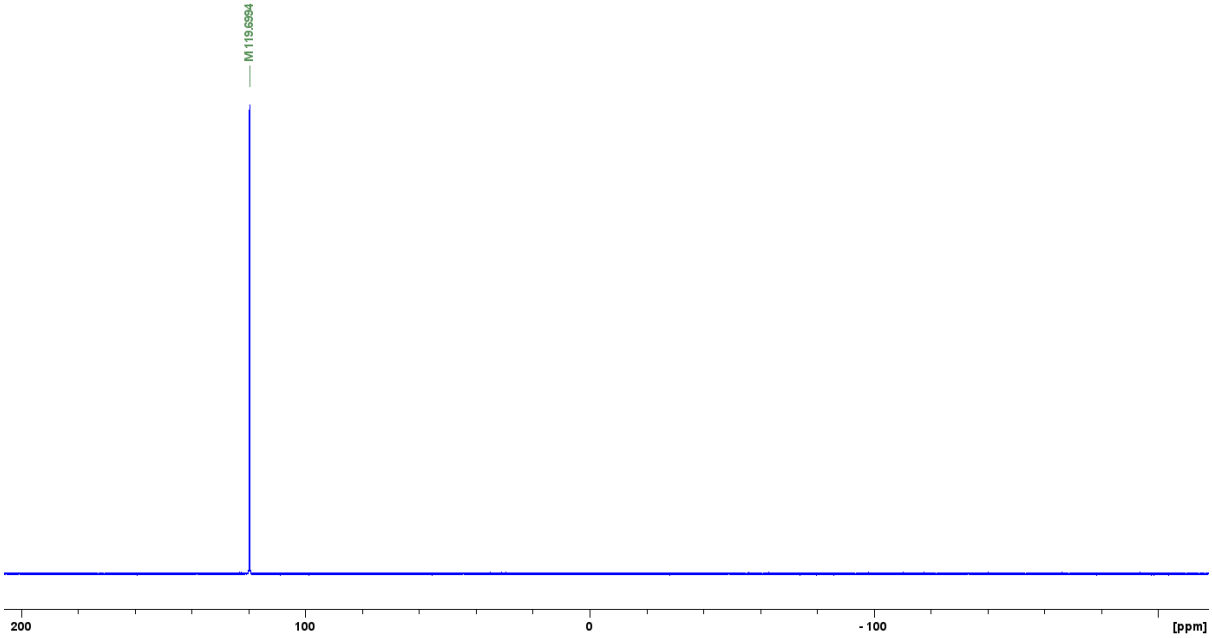

Figure A74. $^{31}P\{^{1}H\}$ NMR spectrum of **16** in toluene-d_8.

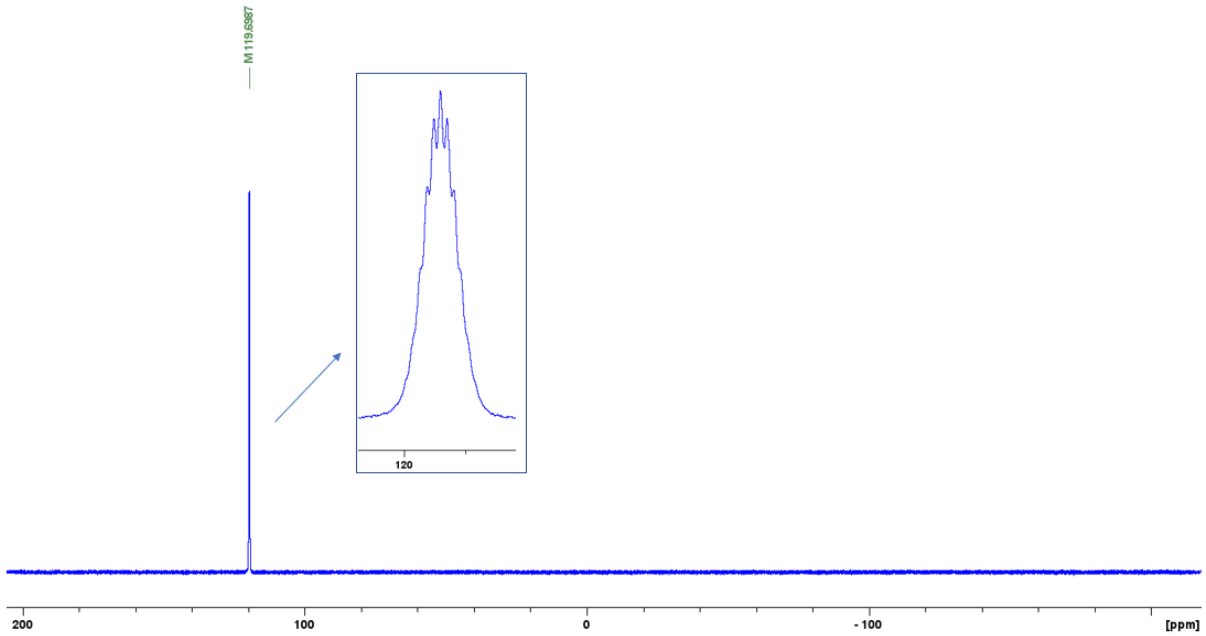

Figure A75. ^{31}P NMR spectrum of **16** in toluene-d_8.

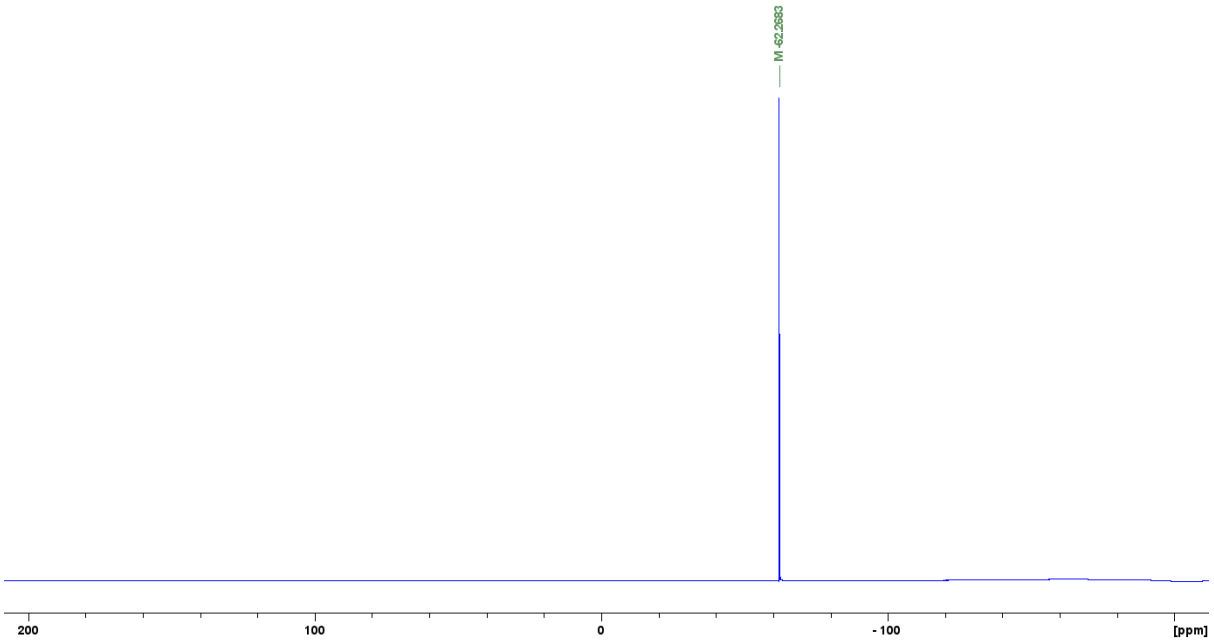

Figure A76. $^{19}F\{^1H\}$ NMR spectrum of **16** in toluene-d_8.

1.1.2 UV/Vis Spectra

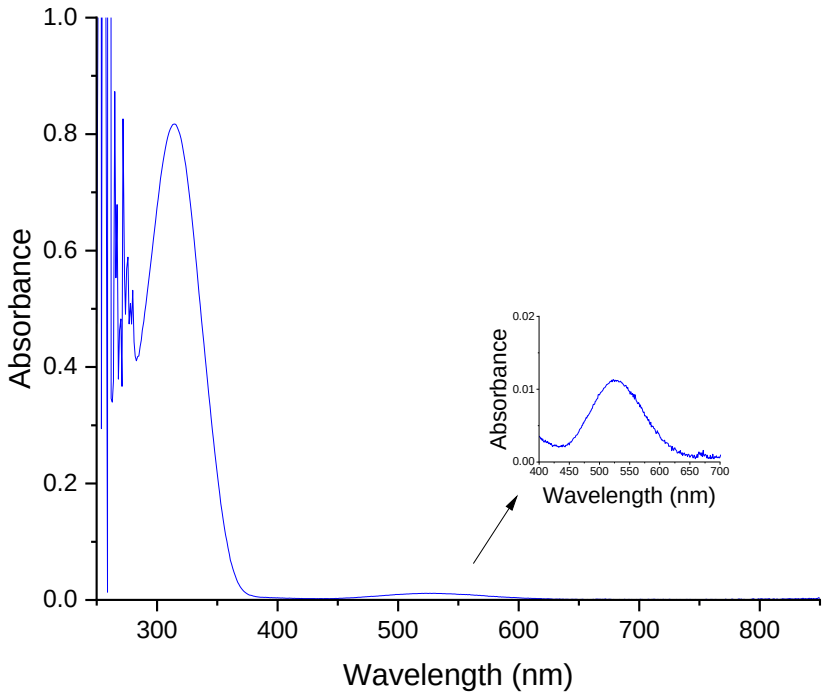

Figure A77. UV/Vis spectrum of **1** (5 x 10^{-5} M in toluene)

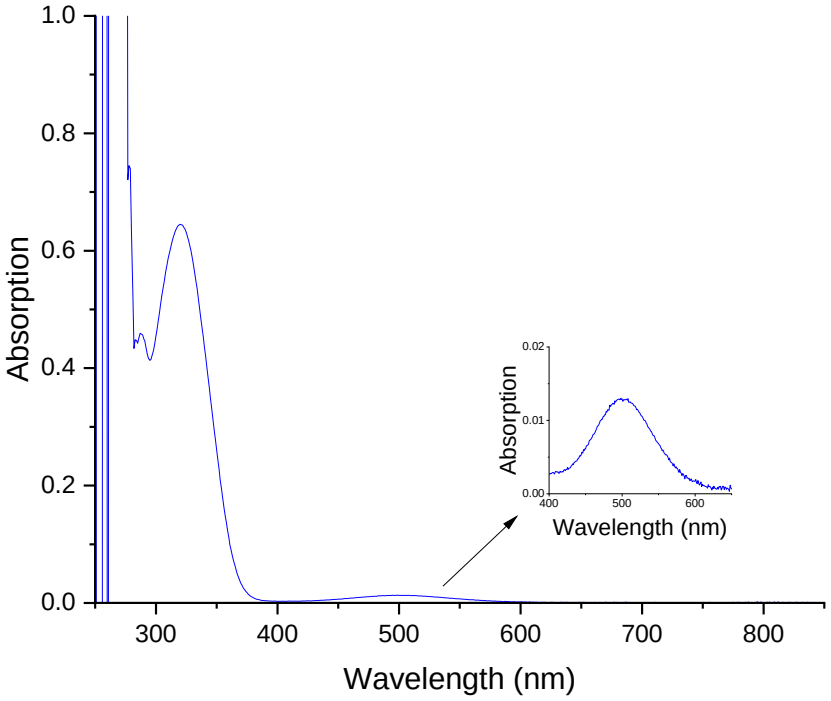

Figure A78. UV/Vis spectrum of **2** (5 x 10^{-5} M in toluene)

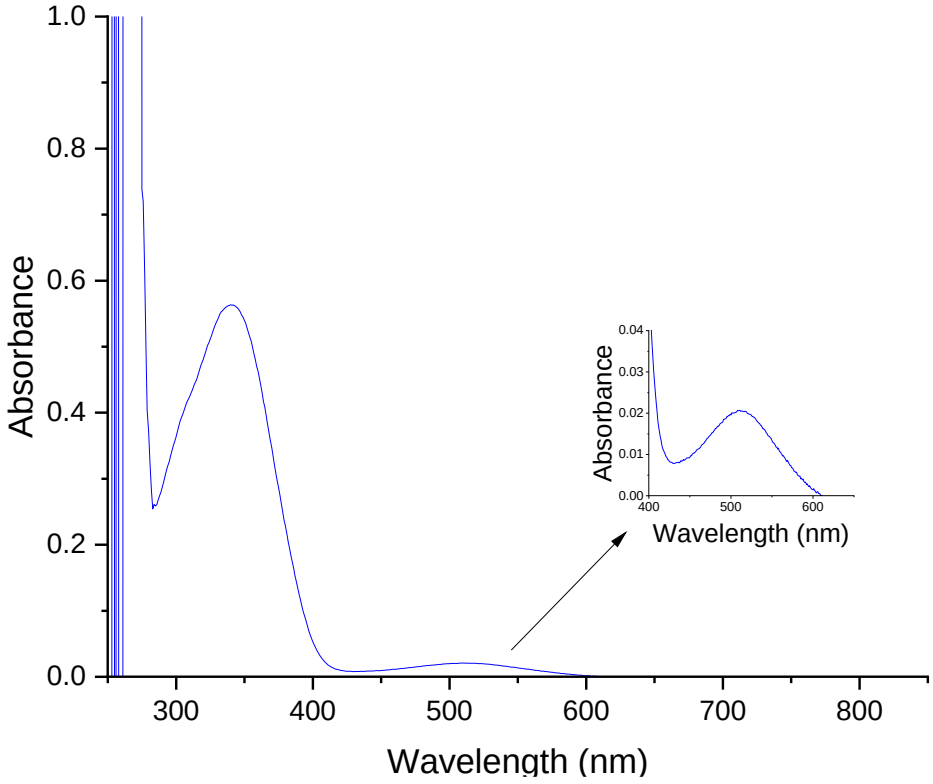

Figure A79. UV/Vis spectrum of **3** (5 x 10^{-5} M in toluene)

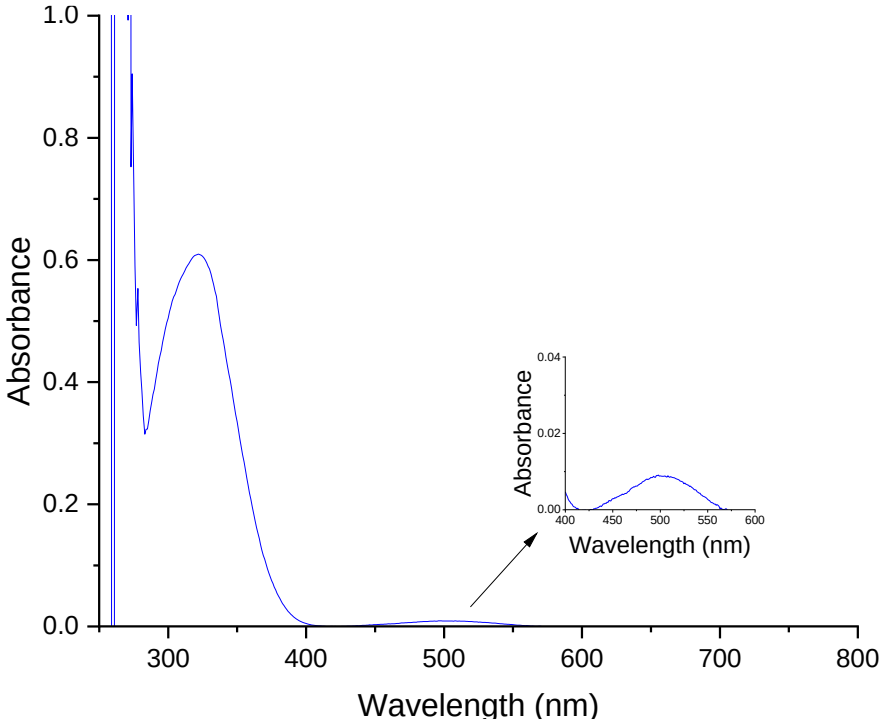

Figure A80. UV/Vis spectrum of **4** (5 x 10^{-5} M in toluene)

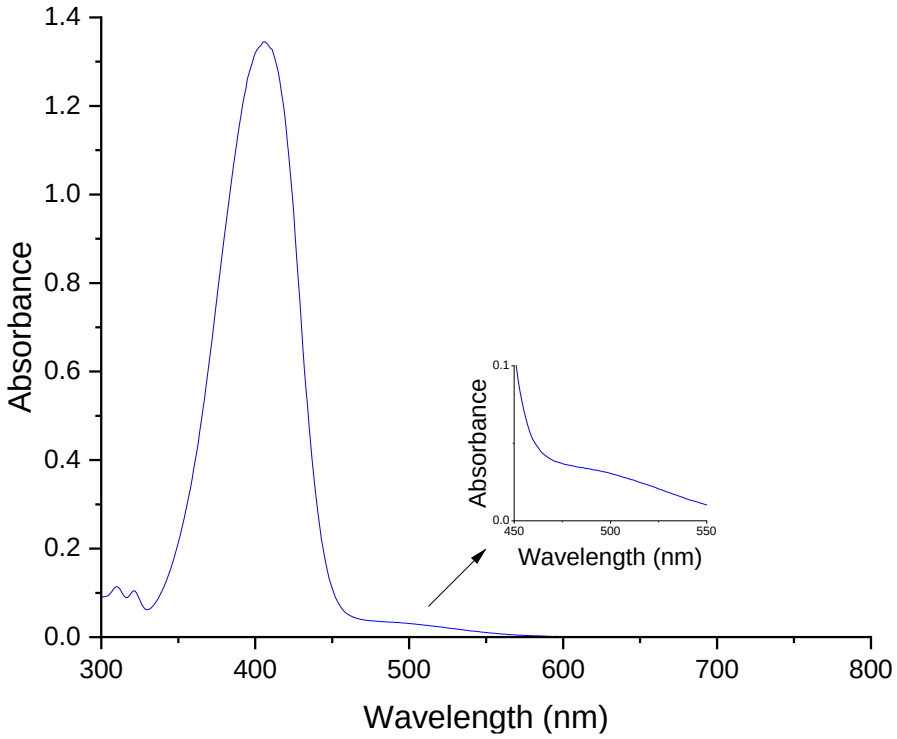

Figure A81. UV/Vis spectrum of **5** (5 x 10^{-5} M in toluene)

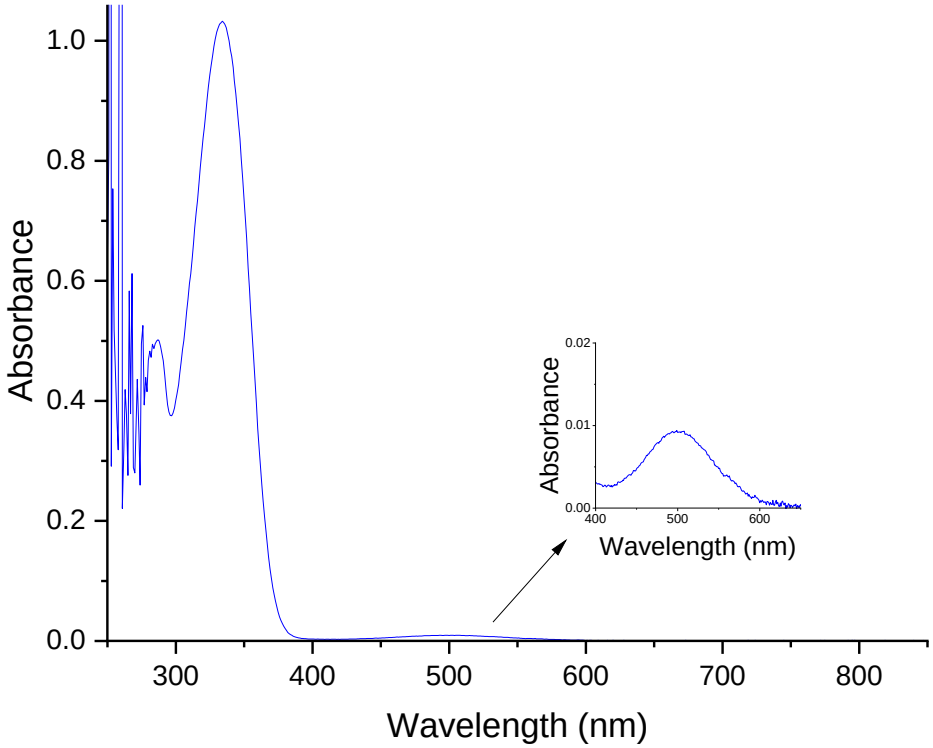

Figure A82. UV/Vis spectrum of **6** (5 x 10^{-5} M in toluene)

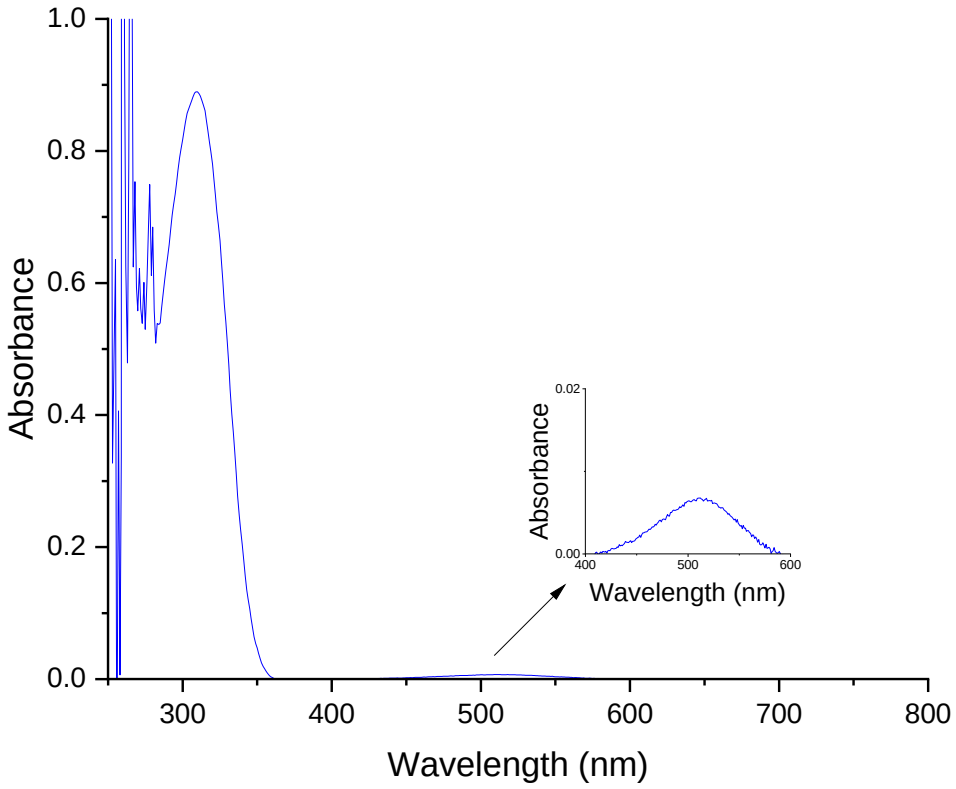

Figure A83. UV/Vis spectrum of **7** (5 x 10^{-5} M in toluene)

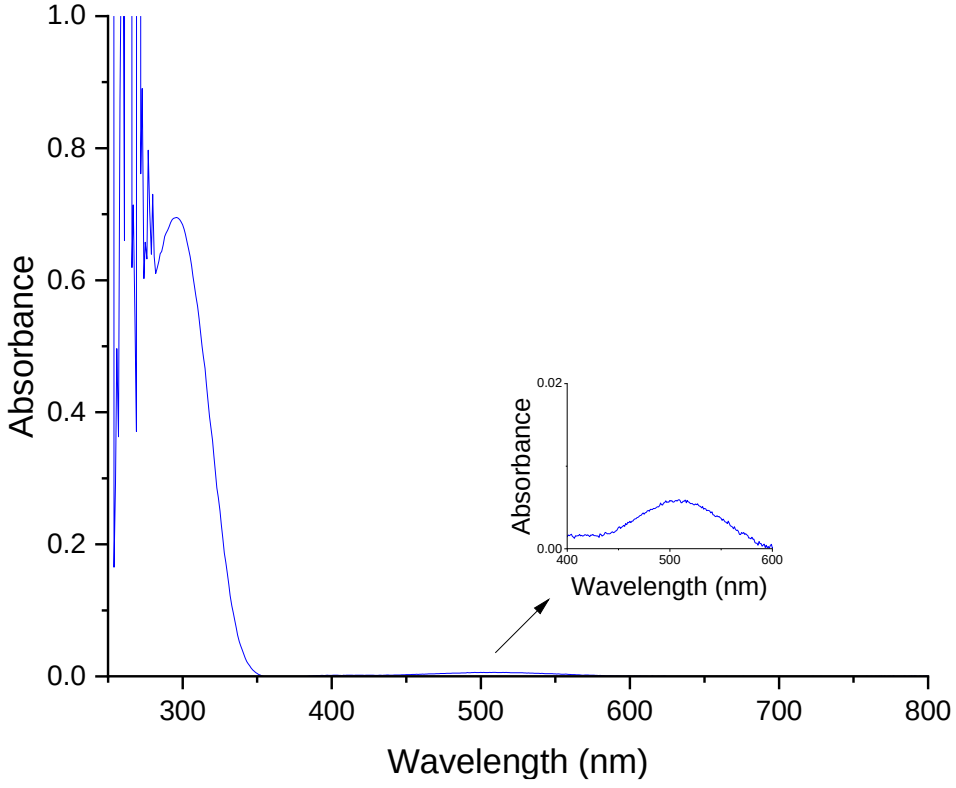

Figure A84. UV/Vis spectrum of **8** (5 x 10^{-5} M in toluene)

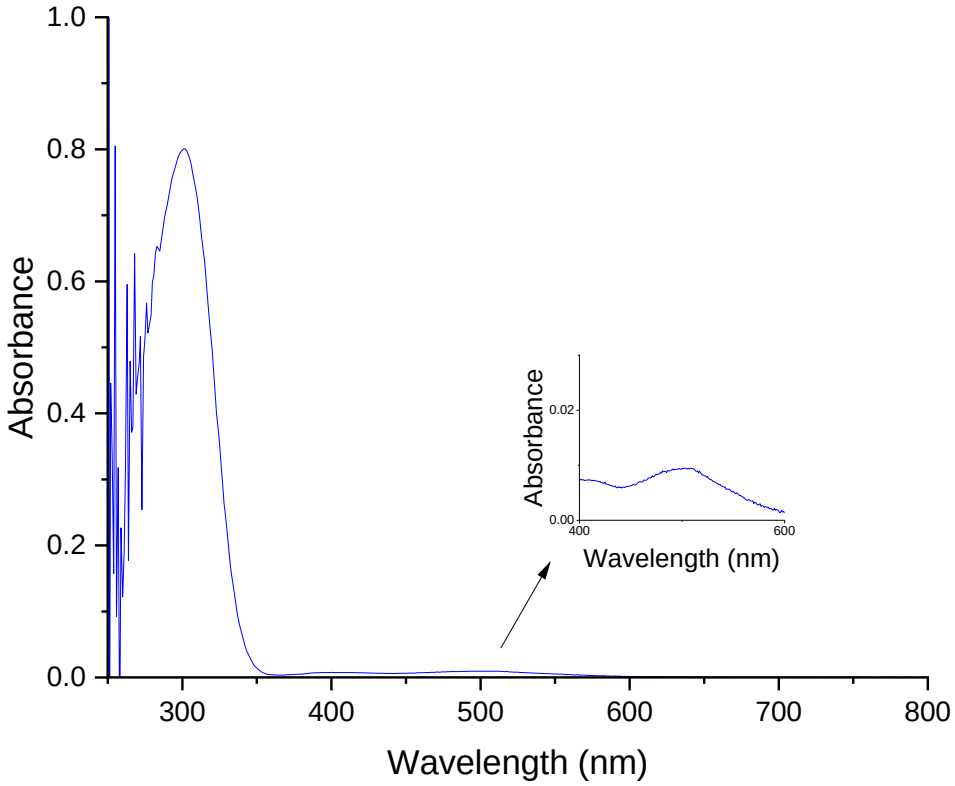

Figure A85. UV/Vis spectrum of **9** (5 x 10^{-5} M in toluene)

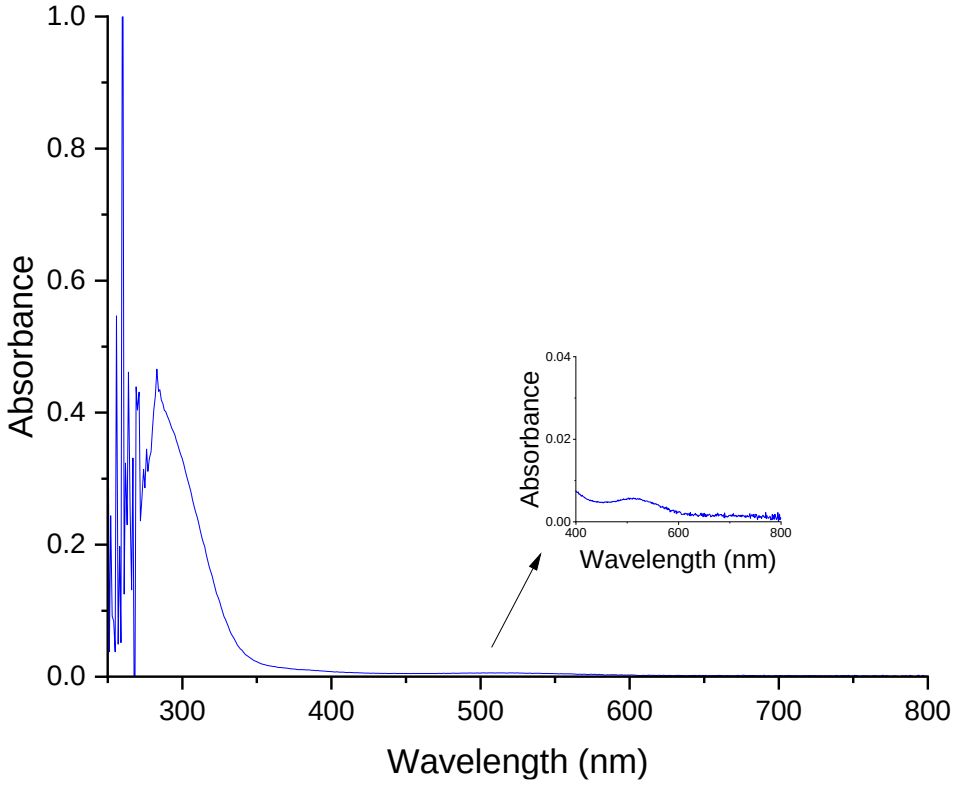

Figure A86. UV/Vis spectrum of **10** (5 x 10^{-5} M in toluene)

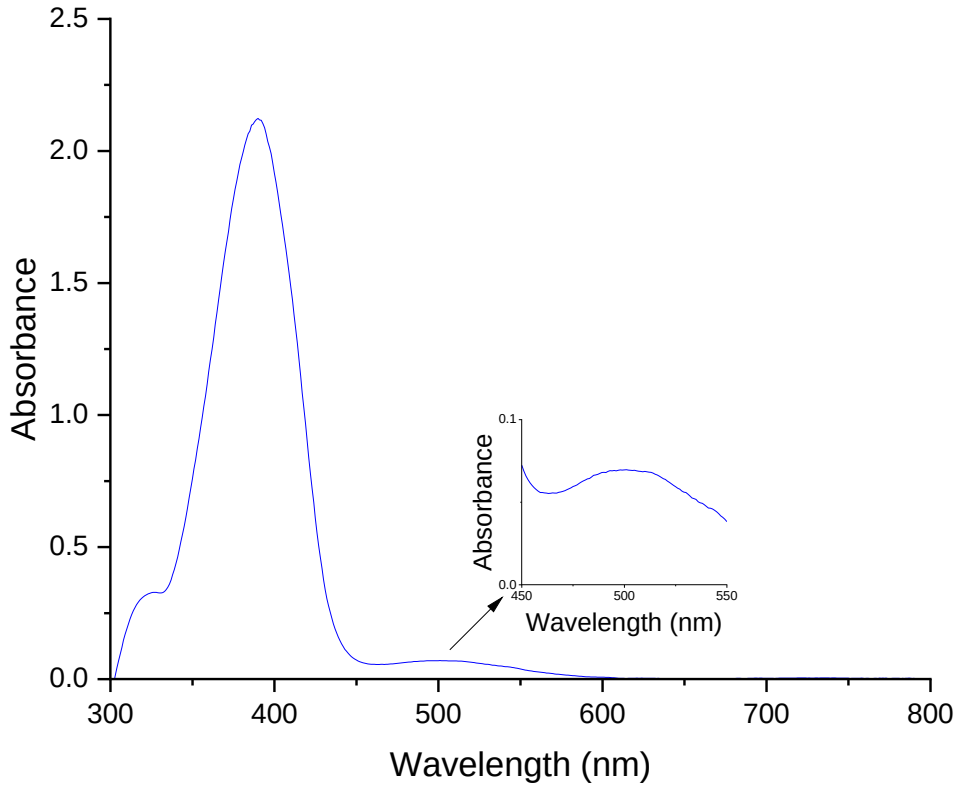

Figure A87. UV/Vis spectrum of **11** (5 x 10^{-5} M in toluene)

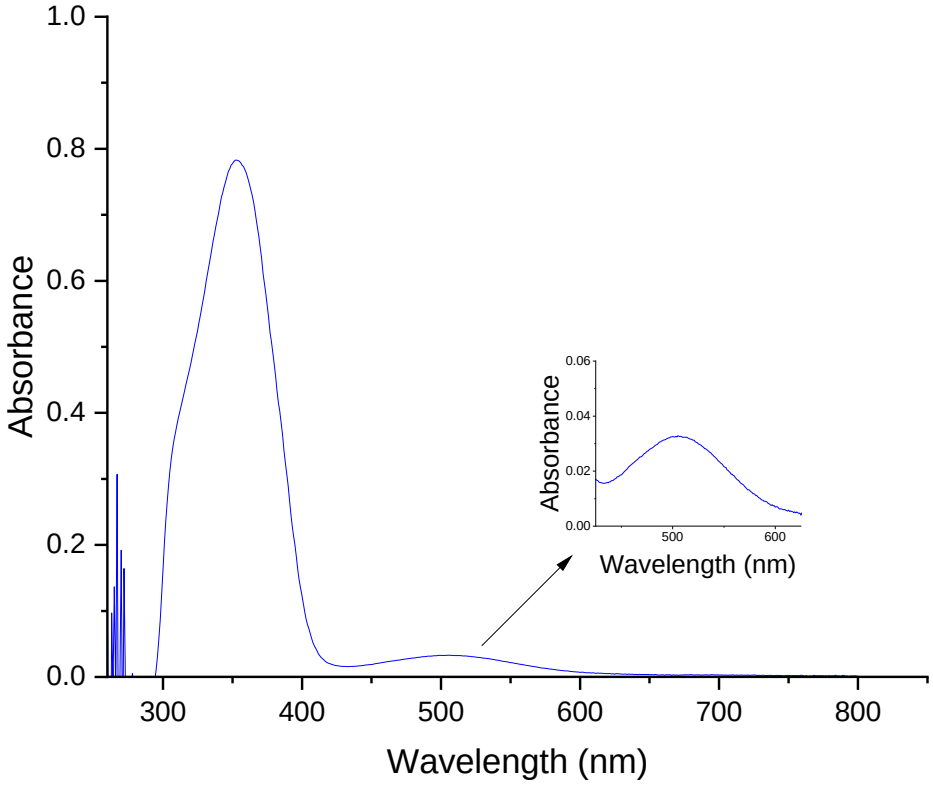

Figure A88. UV/Vis spectrum of **12** (5 x 10^{-5} M in toluene)

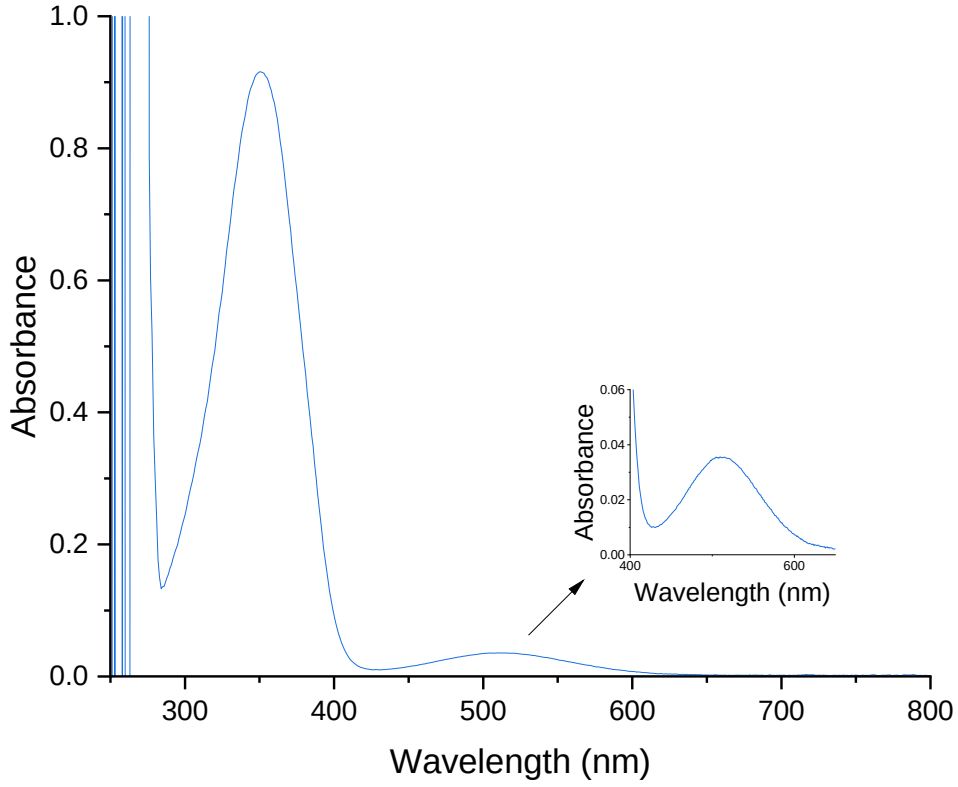

Figure A89. UV/Vis spectrum of **13** (5 x 10^{-5} M in toluene)

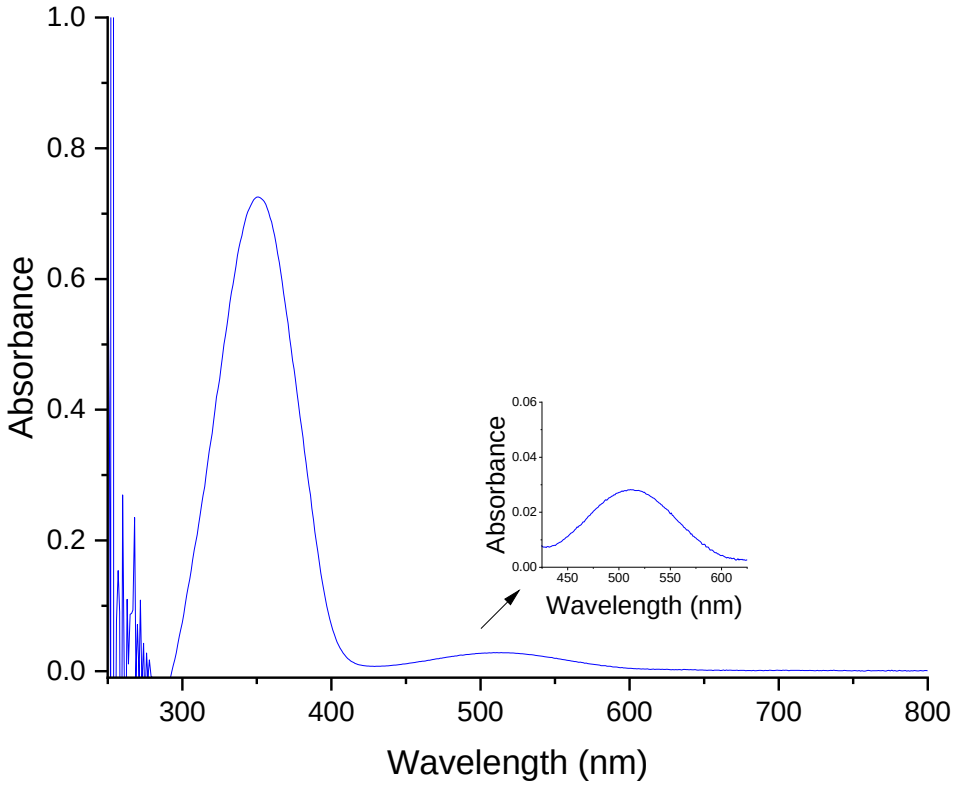

Figure A90. UV/Vis spectrum of **14** (5 x 10^{-5} M in toluene)

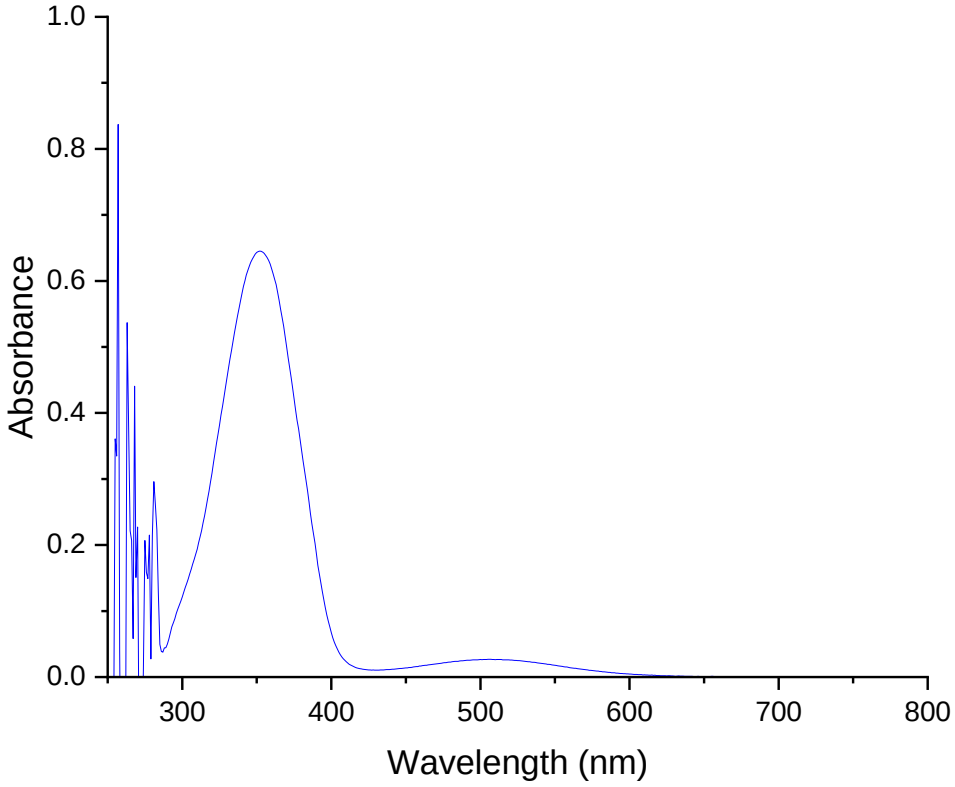

Figure A91. UV/Vis spectrum of **15** (5 x 10^{-5} M in toluene)

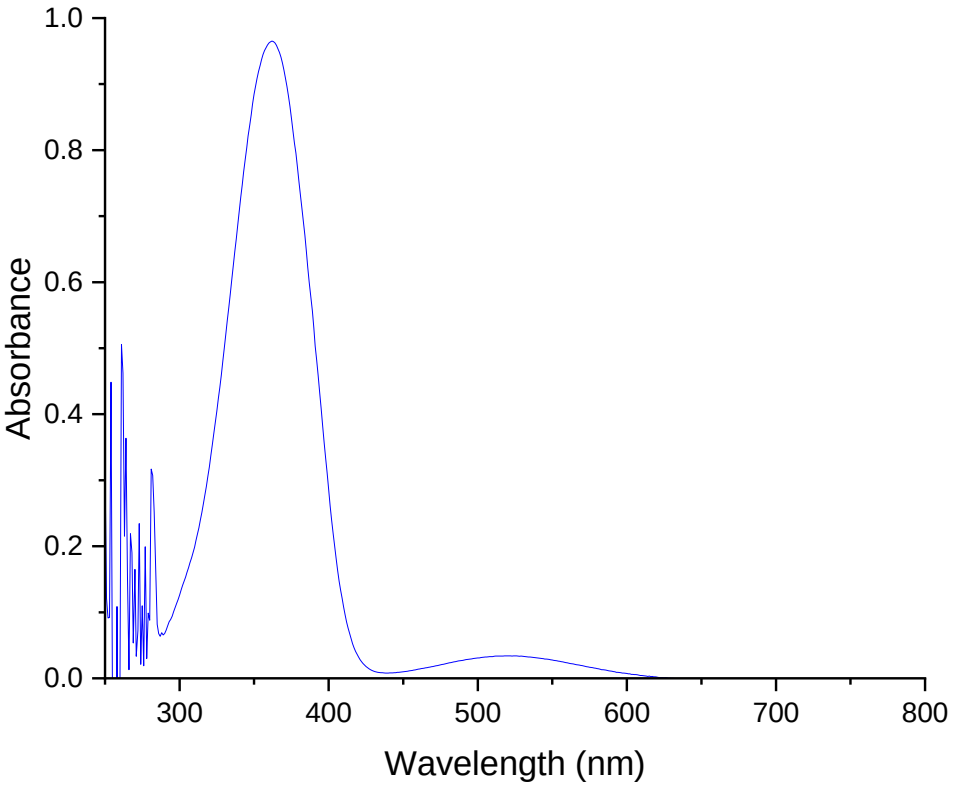

Figure A92. UV/Vis spectrum of **16** (5 x 10^{-5} M in toluene)

1.1.3 High-Resolution Mass Spectra

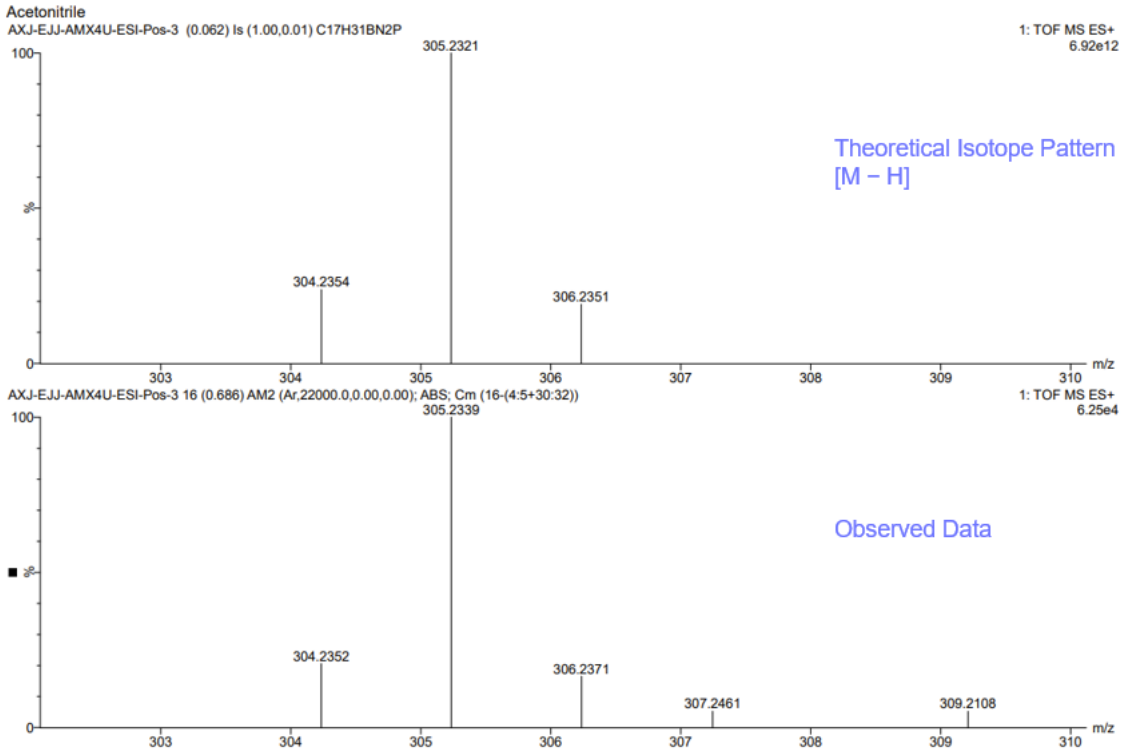

Figure A93. High Resolution Mass Spectrum of **1**

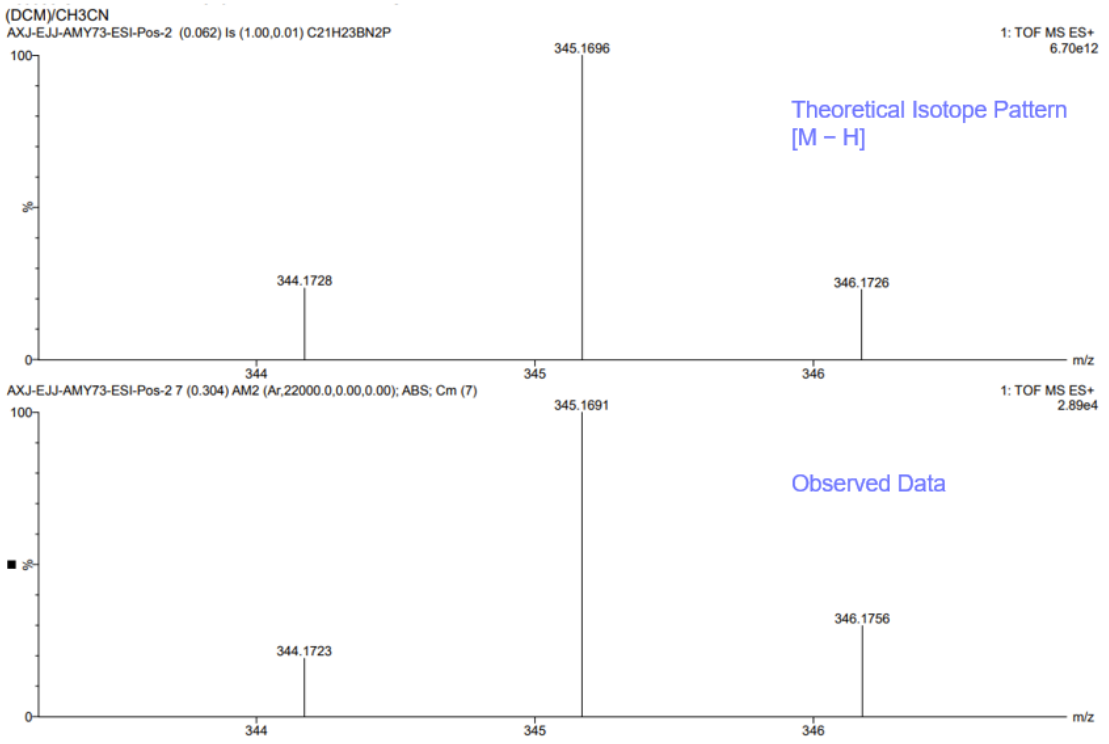

Figure A94. High Resolution Mass Spectrum of **2**

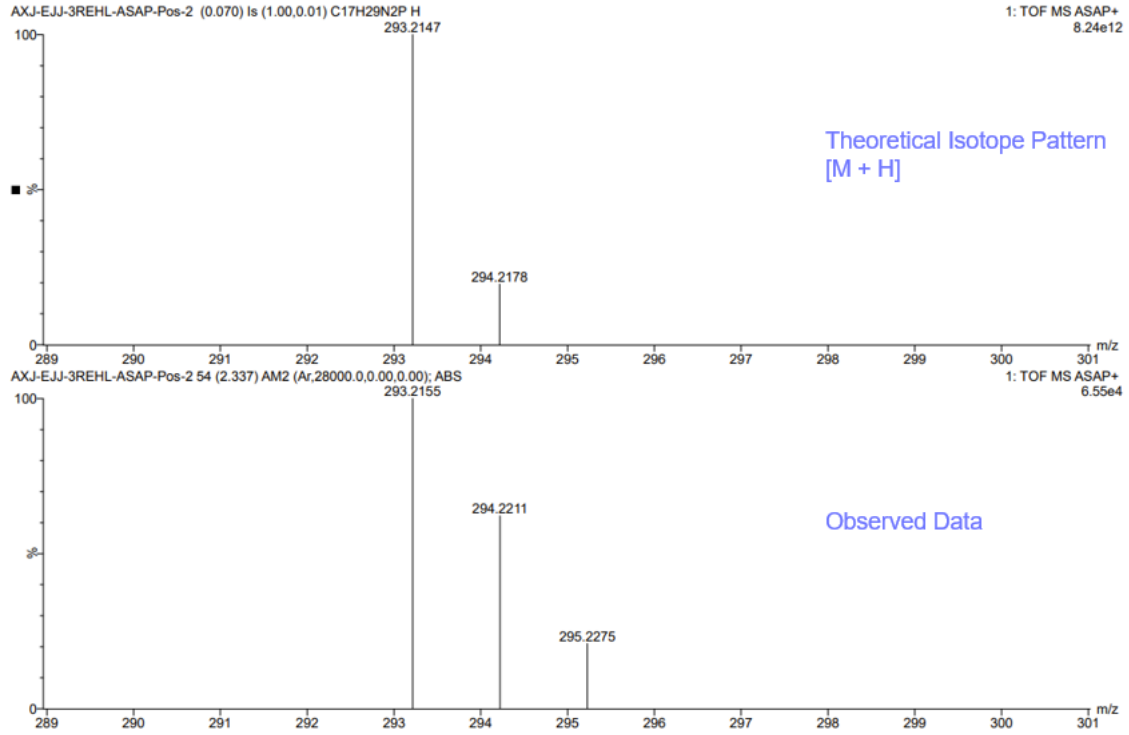

Figure A95. High Resolution Mass Spectrum of **3**

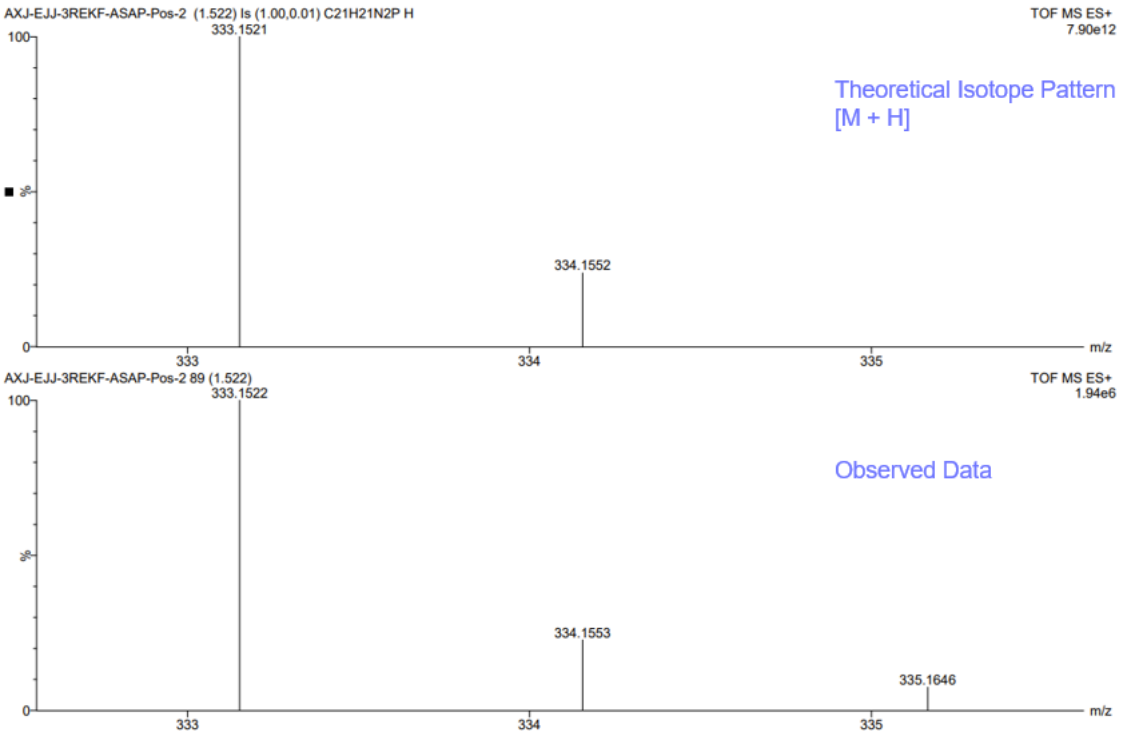

Figure A96. High Resolution Mass Spectrum of **4**

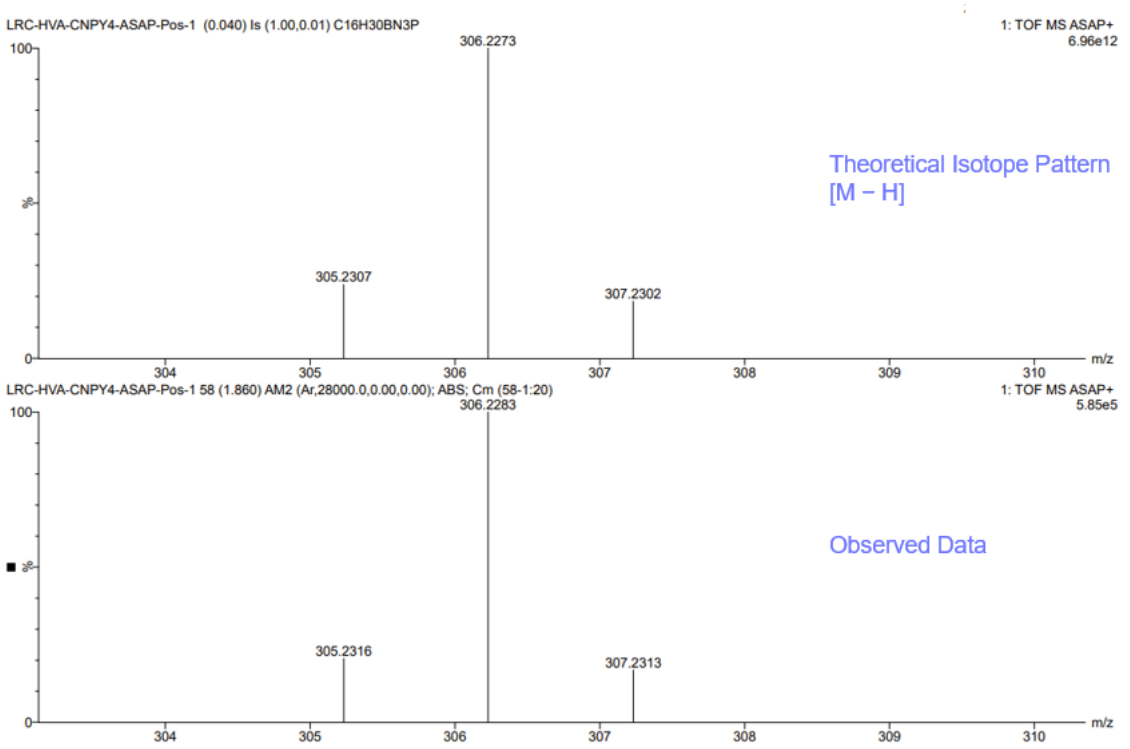

Figure A97. High Resolution Mass Spectrum of **5**

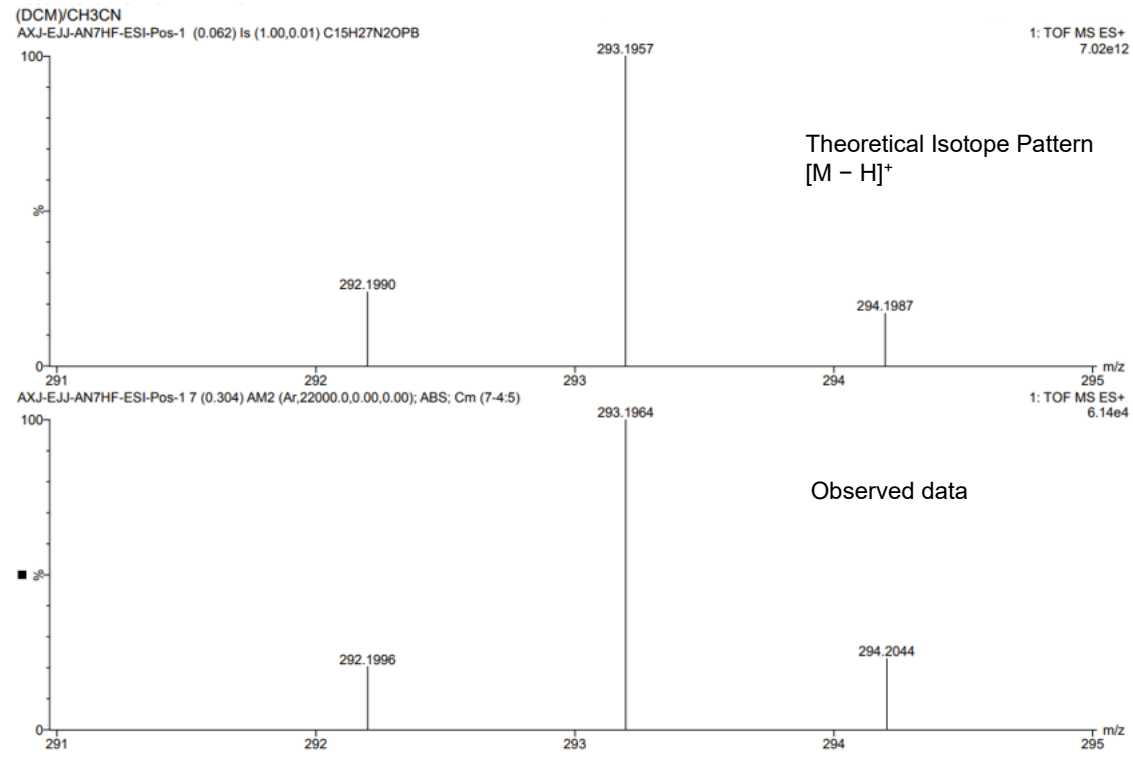

Figure A98. High-resolution Mass Spectrum of **6**

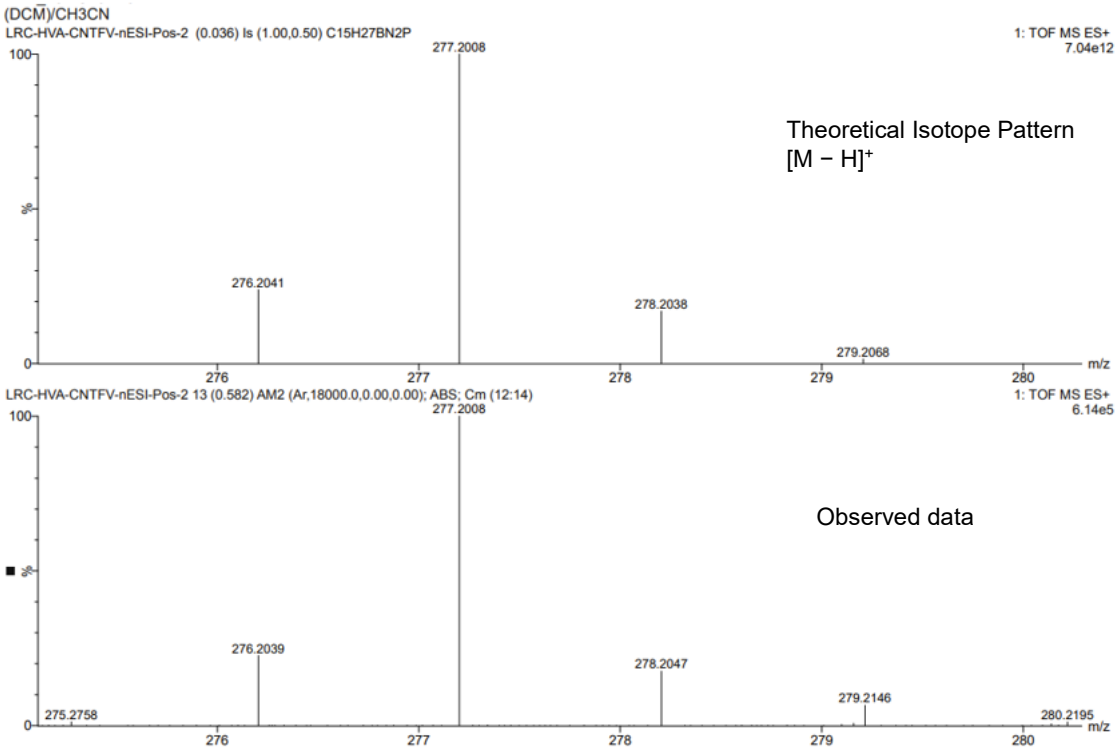

Figure A99. High-resolution Mass Spectrum of **7**

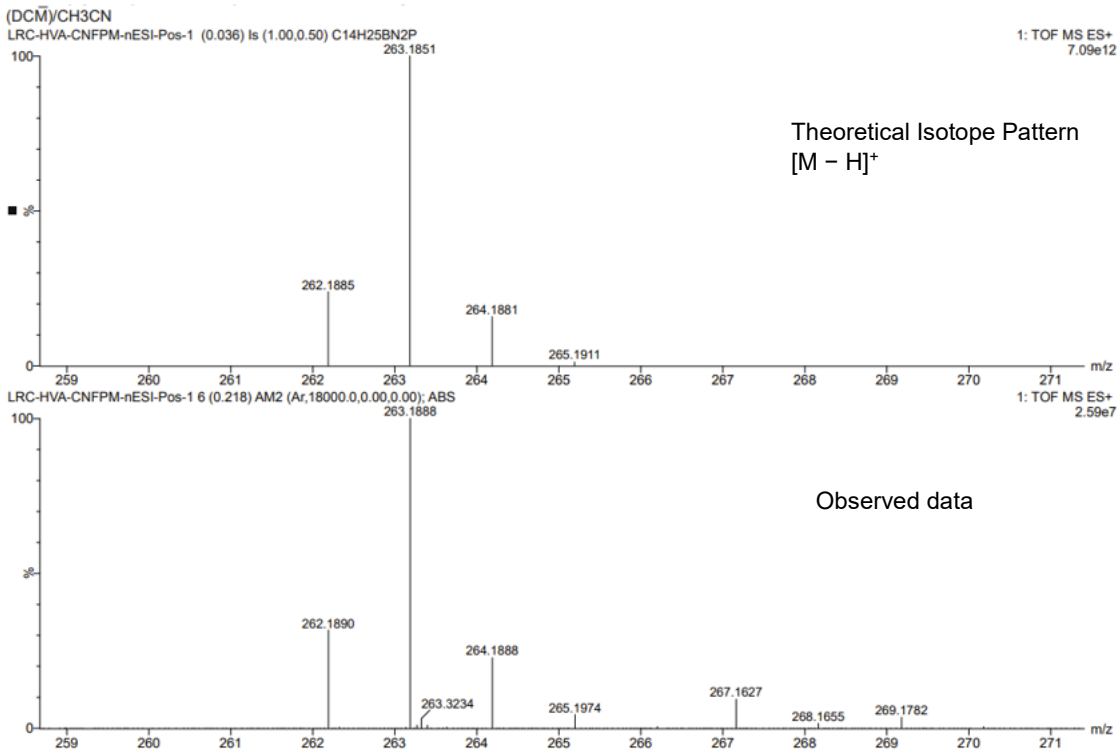

Figure A100. High-resolution Mass Spectrum of **8**

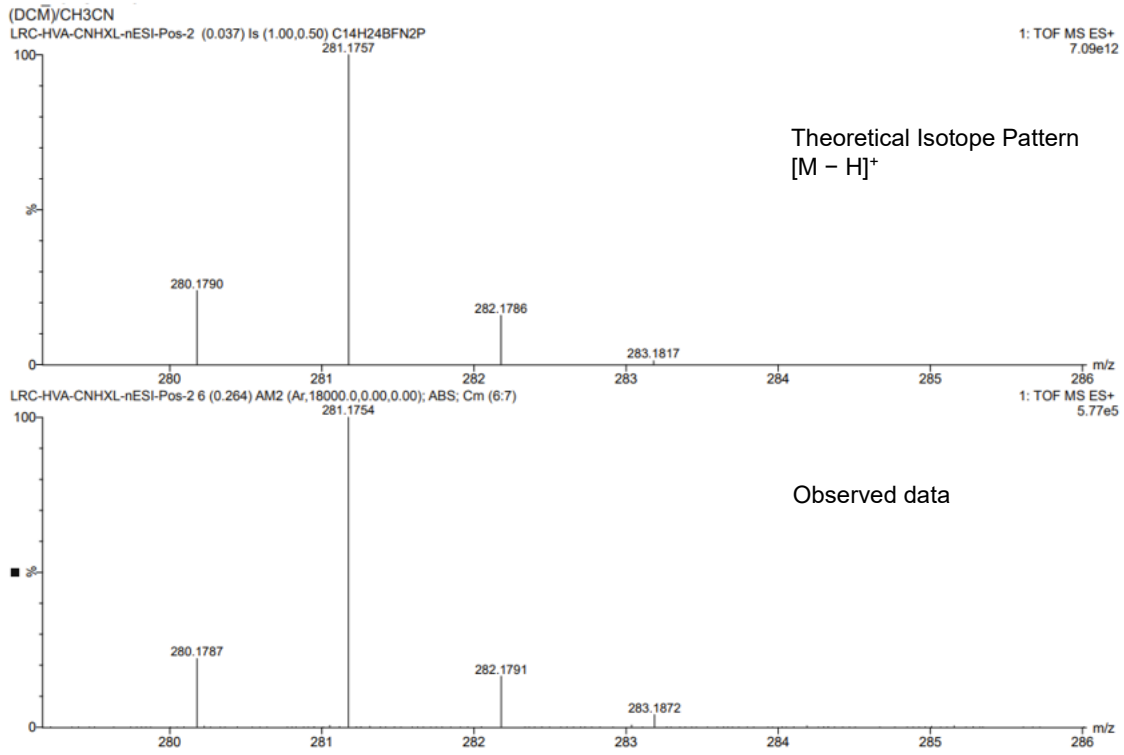

Figure A101. High-resolution Mass Spectrum of **9**

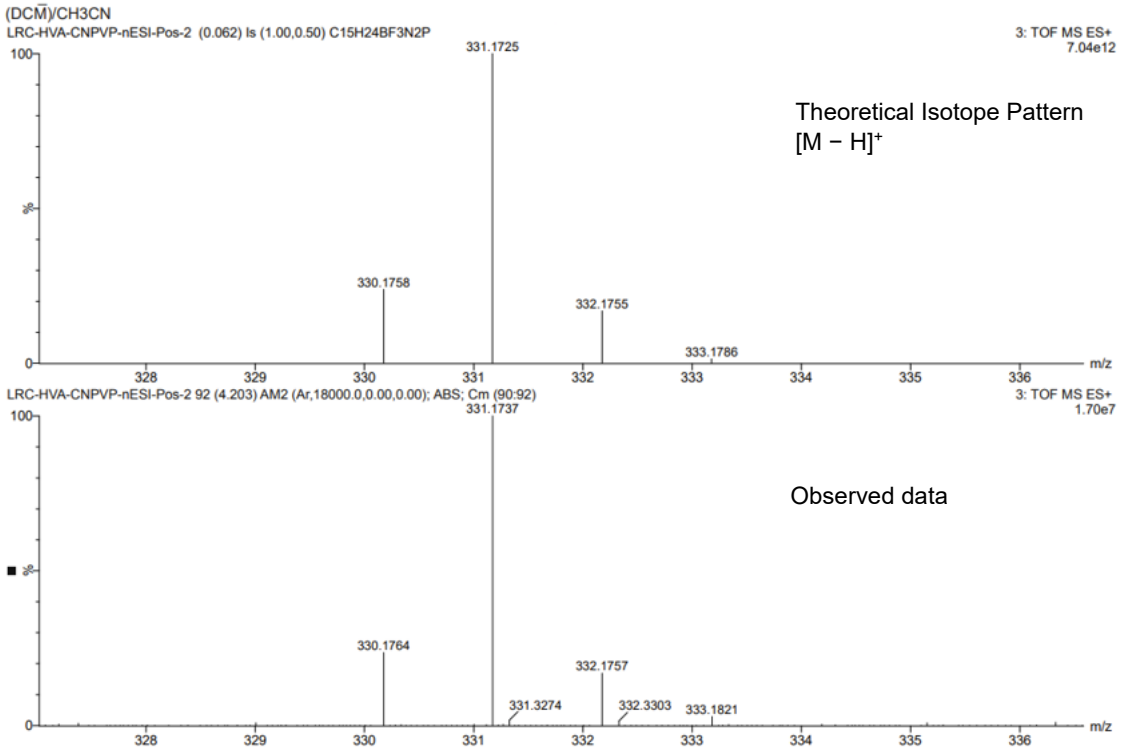

Figure A102. High-resolution Mass Spectrum of **10**

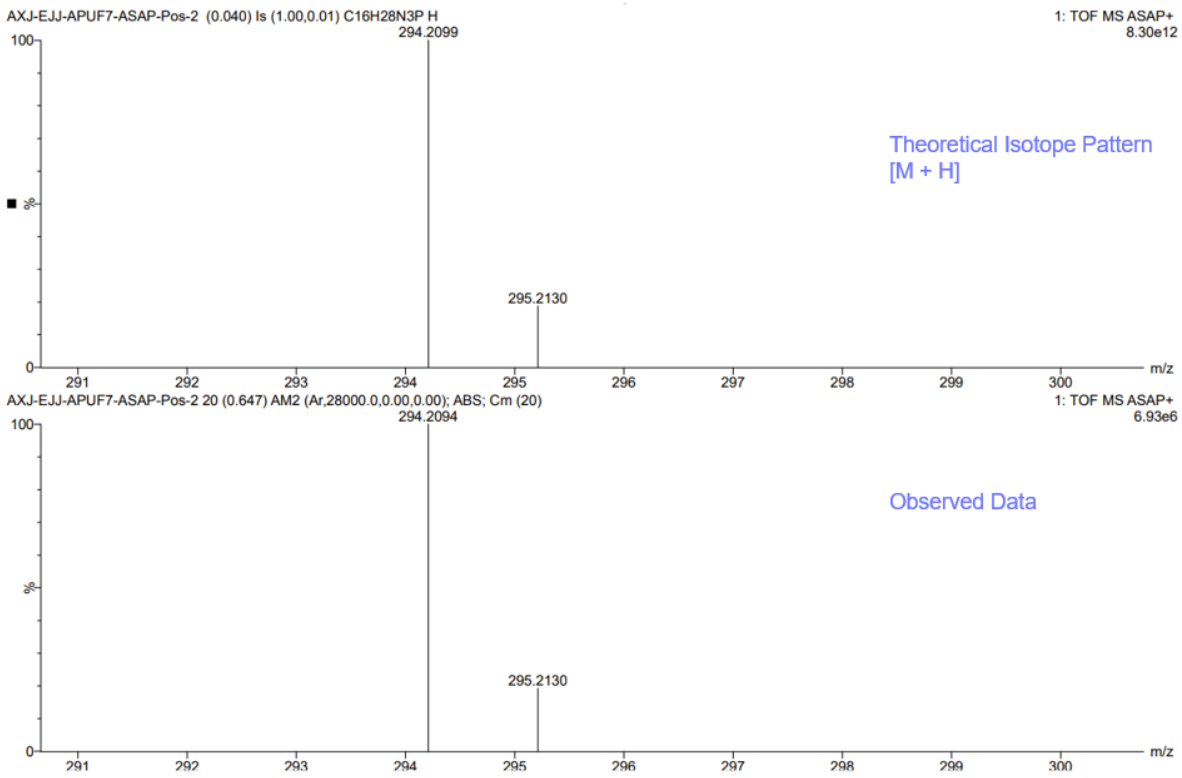

Figure A103. High Resolution Mass Spectrum of **11**

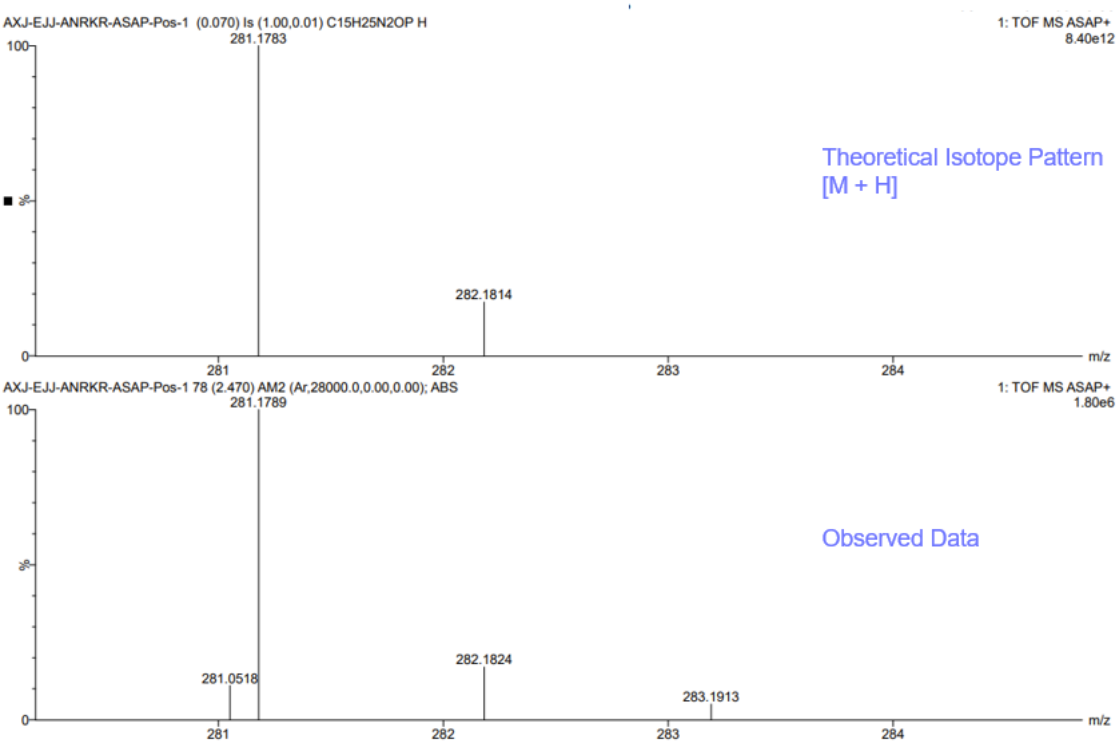

Figure A104. High-resolution Mass Spectrum of **12**

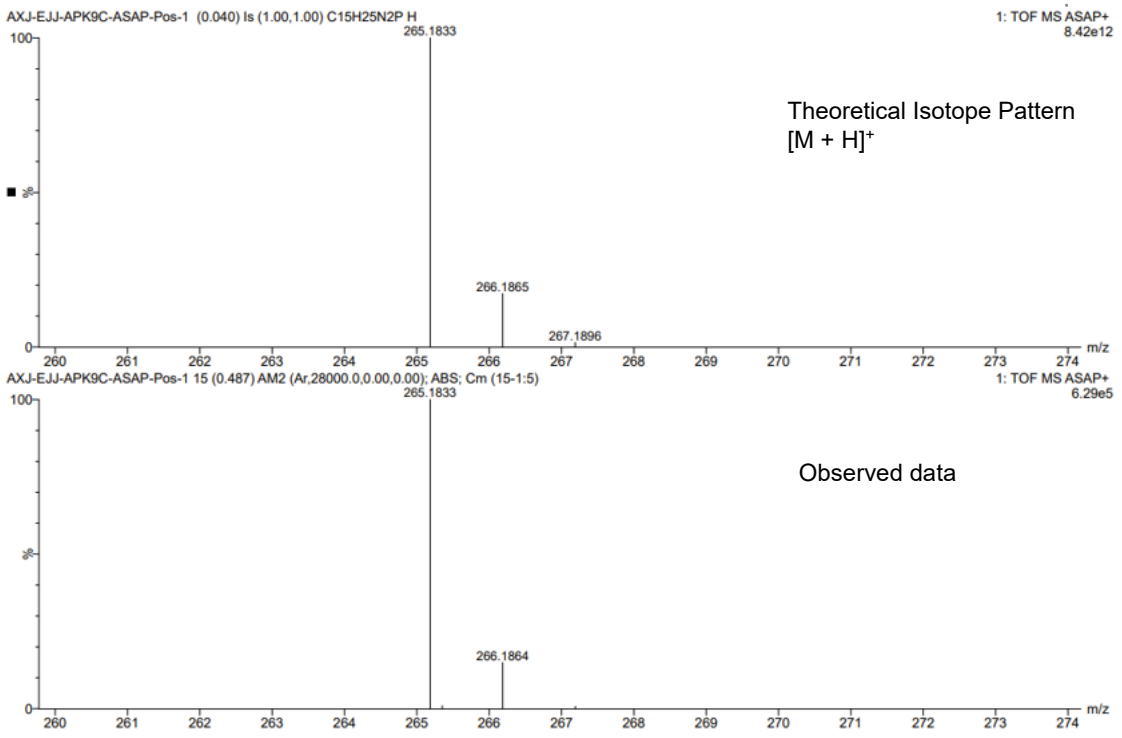

Figure A105. High-resolution Mass Spectrum of **13**

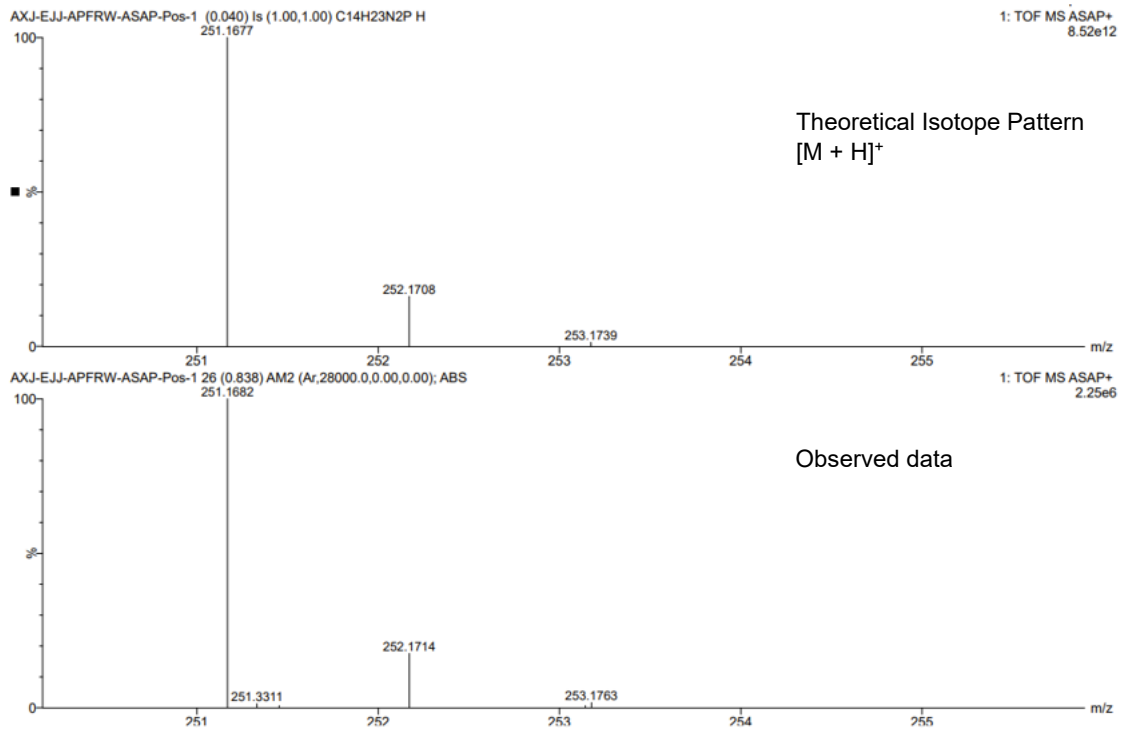

Figure A106. High-resolution Mass Spectrum of **14**

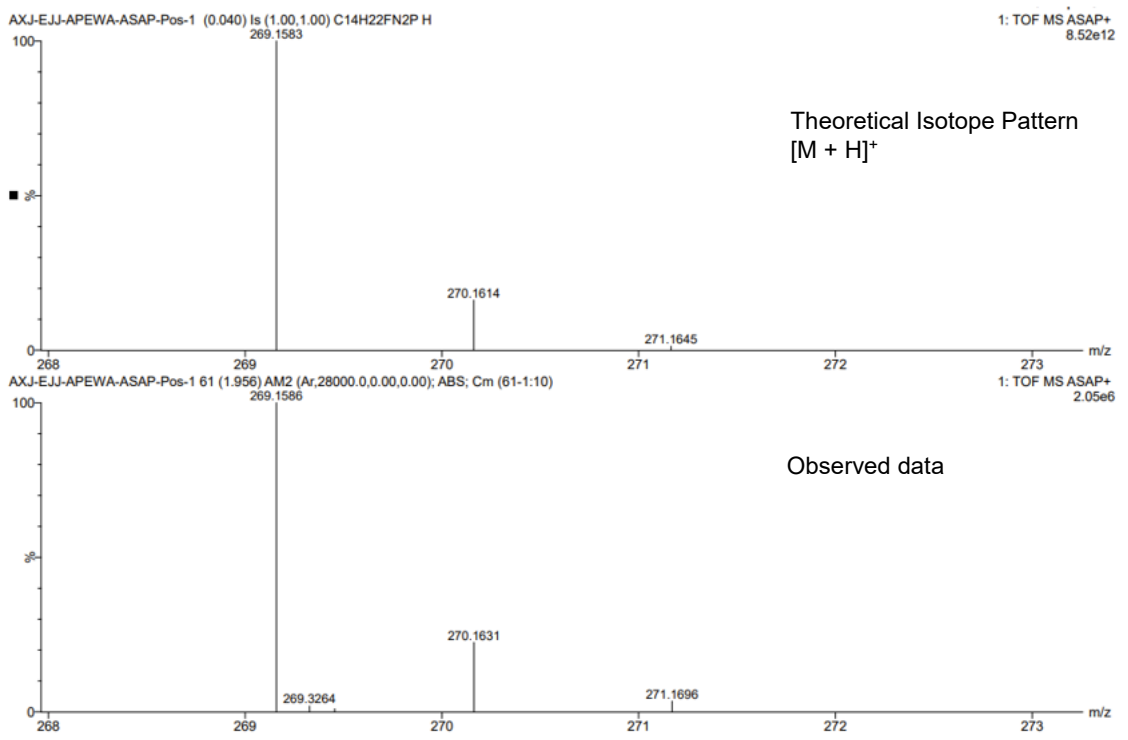

Figure A107. High-resolution Mass Spectrum of **15**

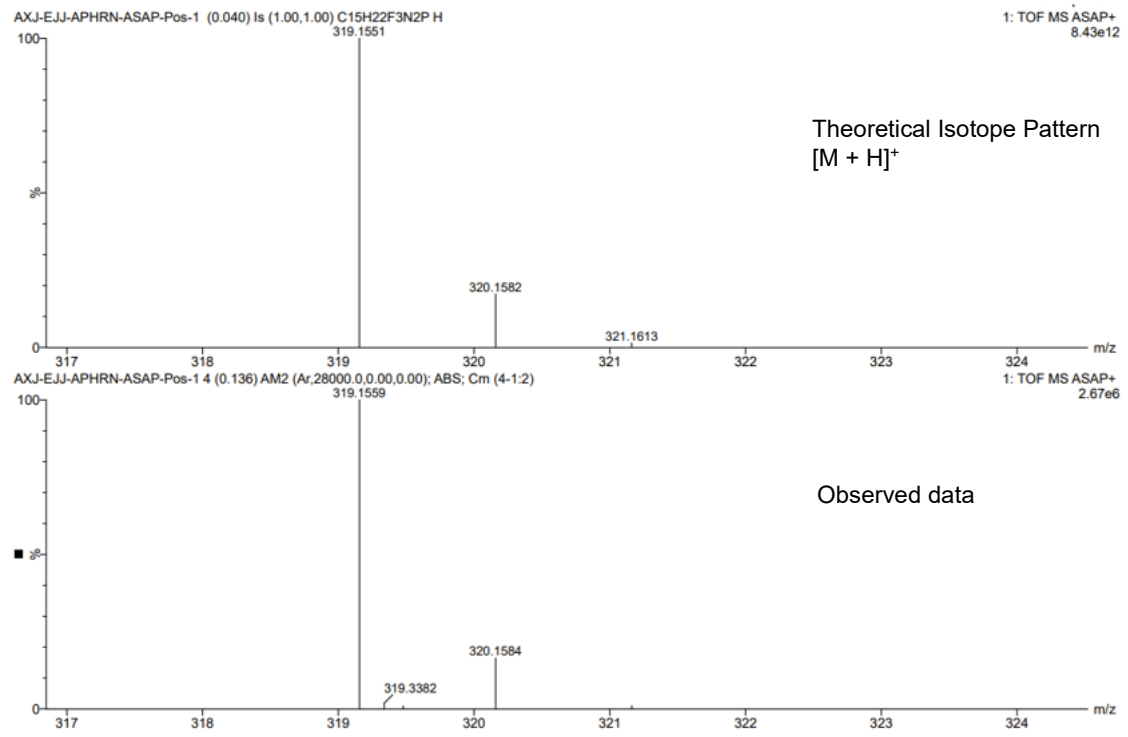

Figure A108. High-resolution Mass Spectrum of **16**

1.1.4 IR spectra

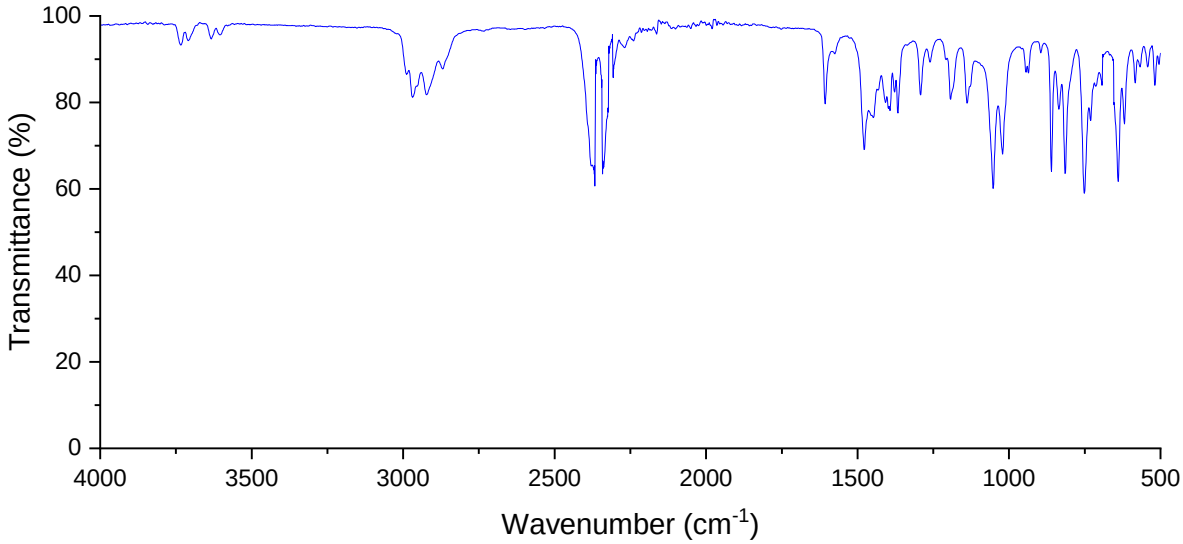

Figure A109. IR spectrum of **1**

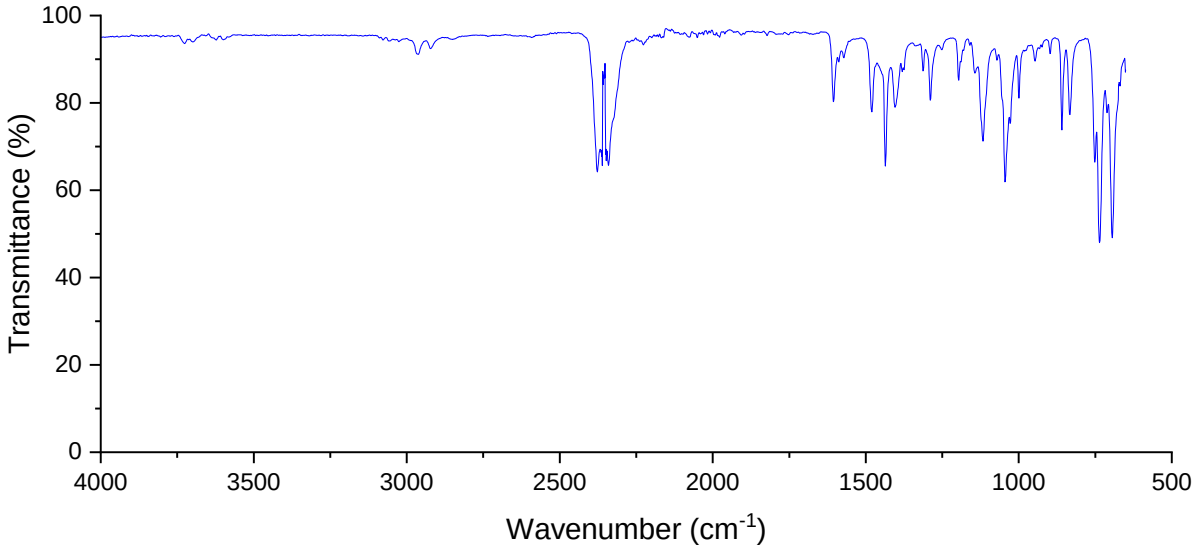

Figure A110. IR spectrum of **2**

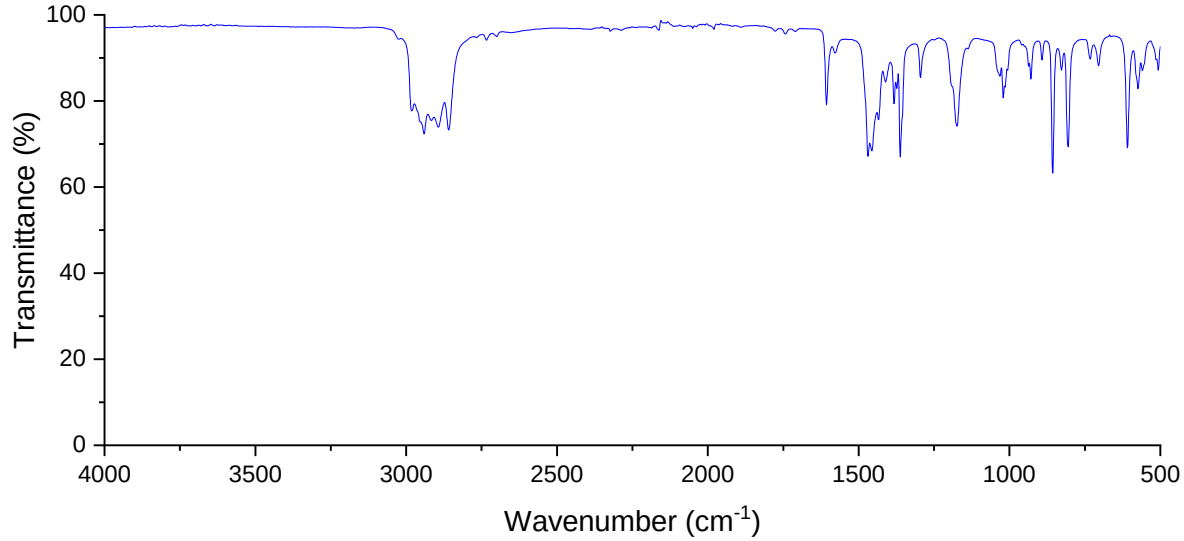

Figure A111. IR spectrum of **3**

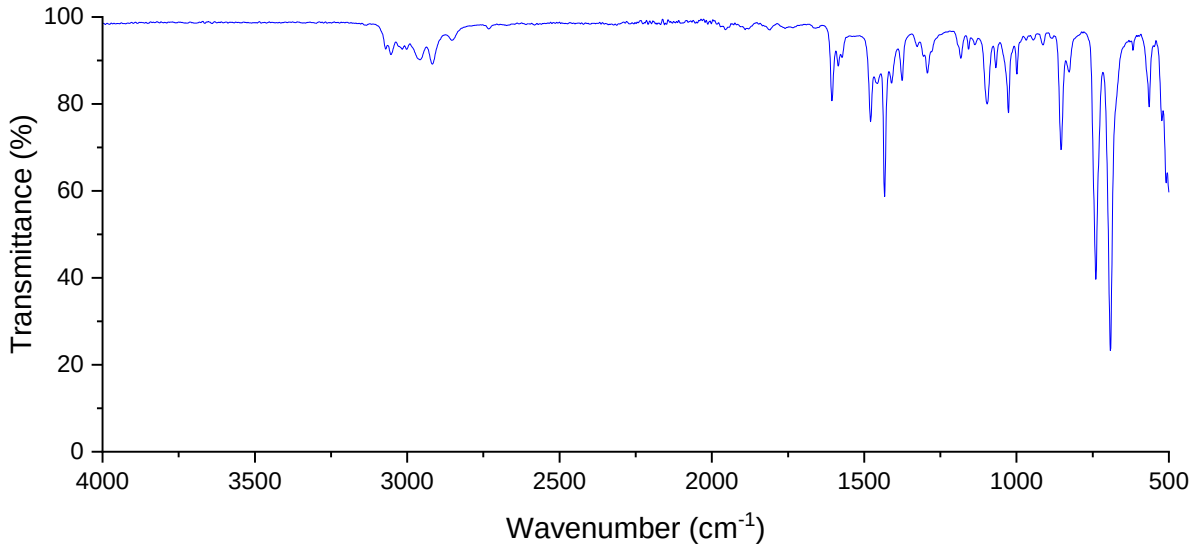

Figure A112. IR spectrum of 4

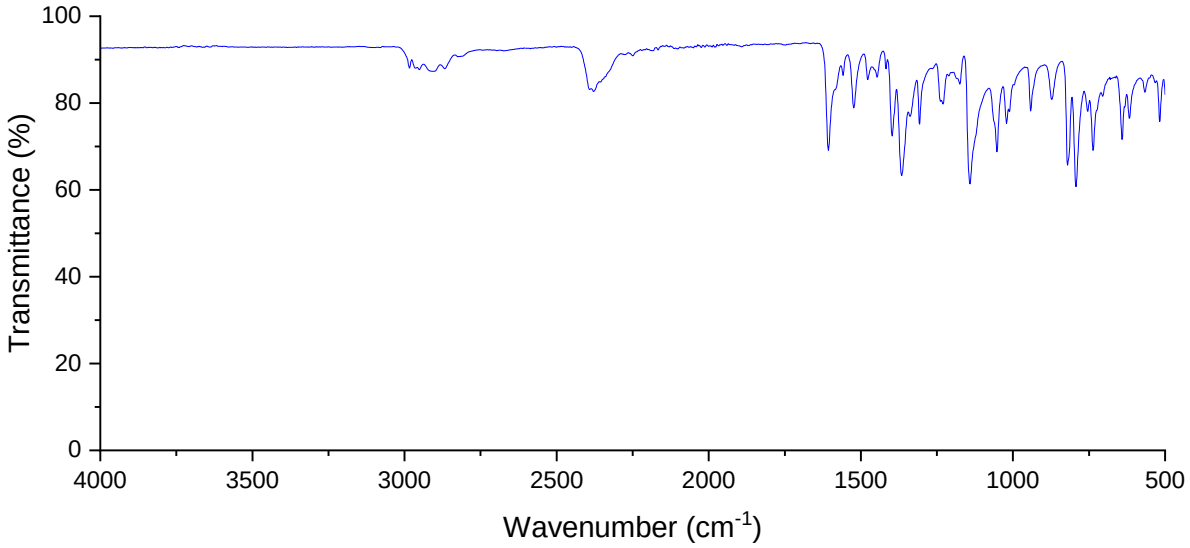

Figure A113. IR spectrum of **5**

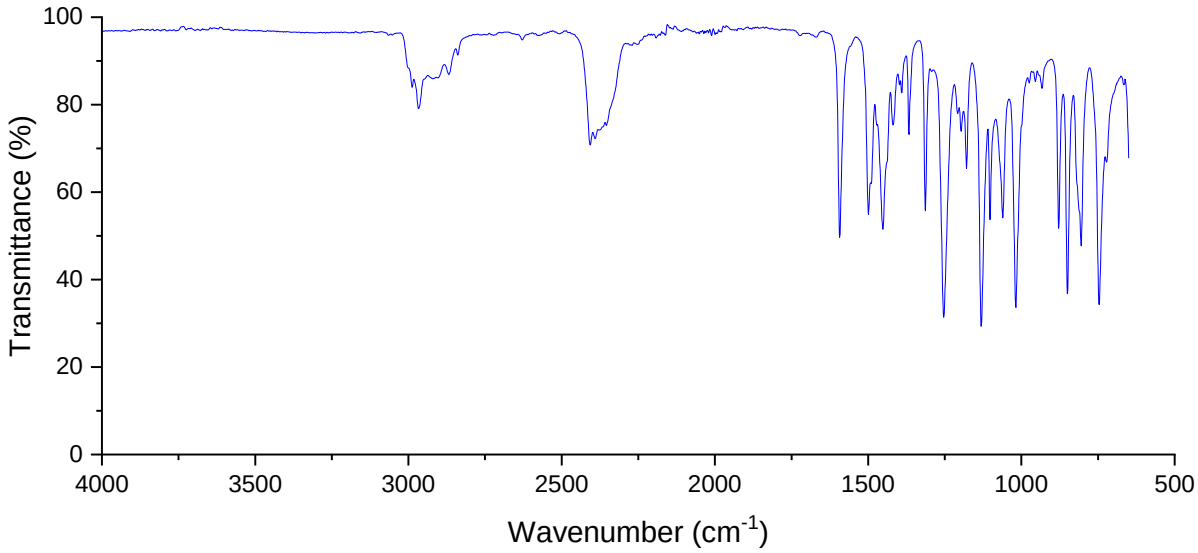

Figure A114. IR Spectrum of **6**

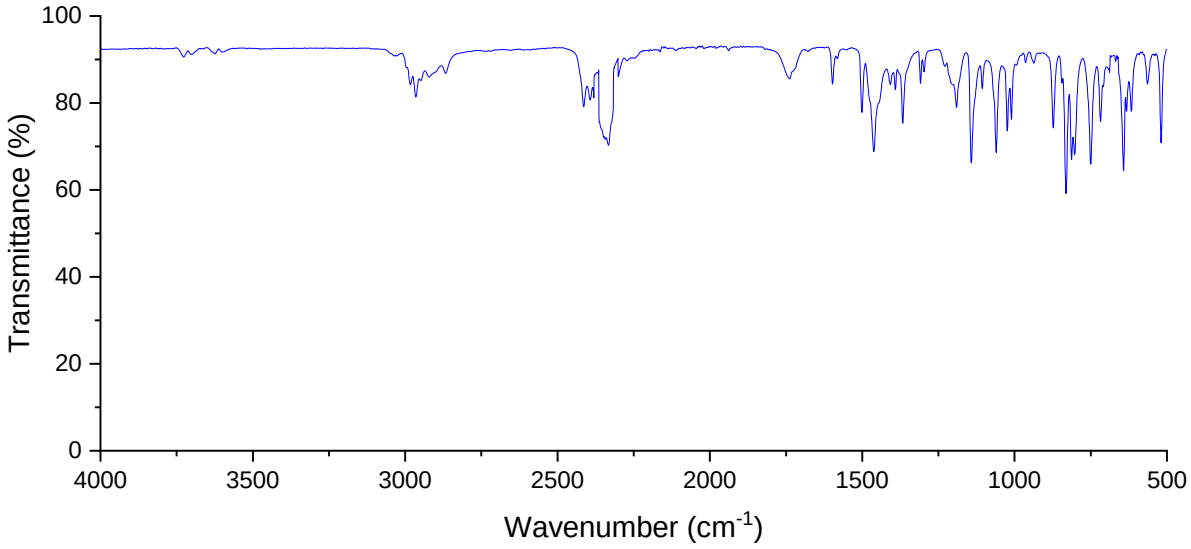

Figure A115. IR Spectrum of **7**

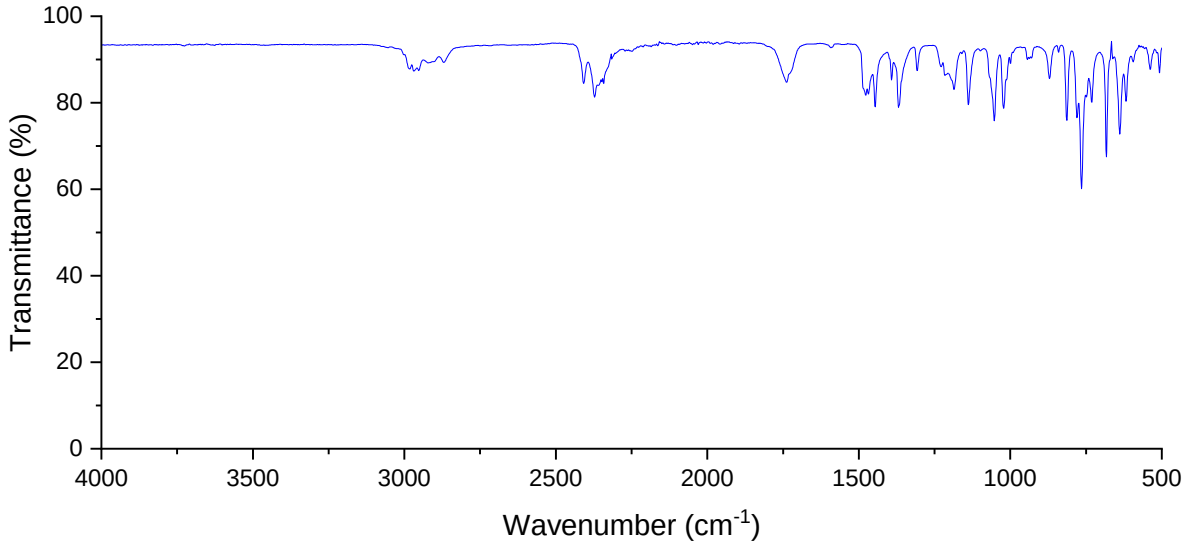

Figure A116. IR Spectrum of **8**

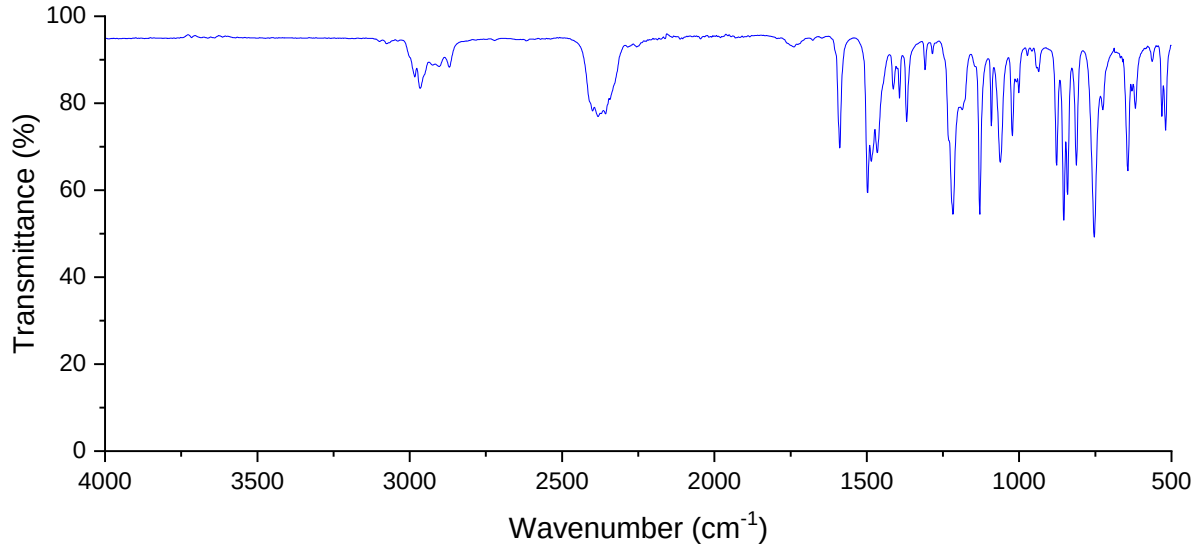

Figure A117. IR Spectrum of **9**

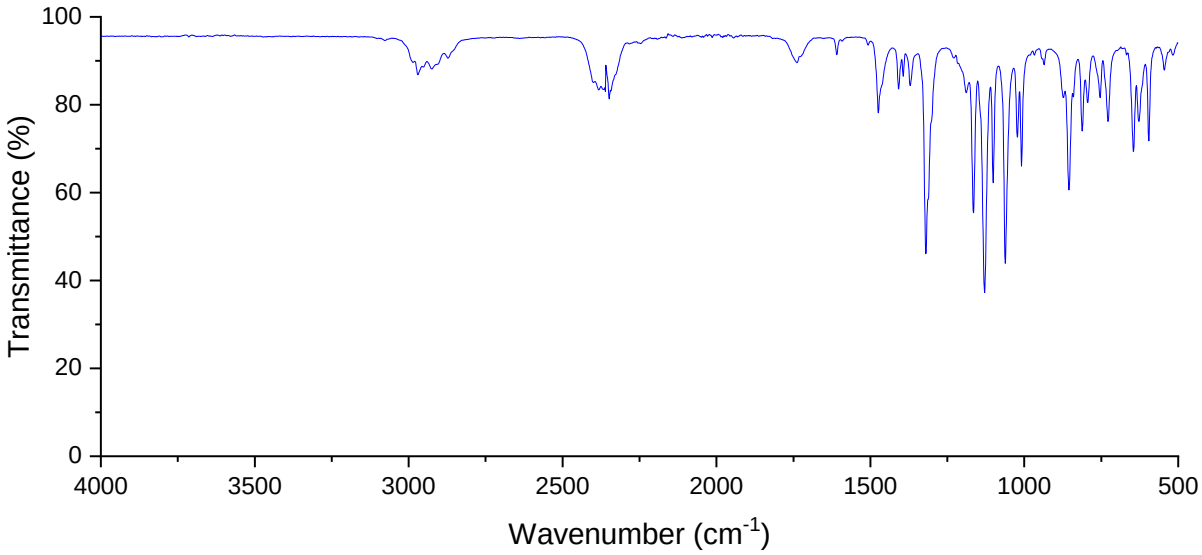

Figure A118. IR Spectrum of **10**

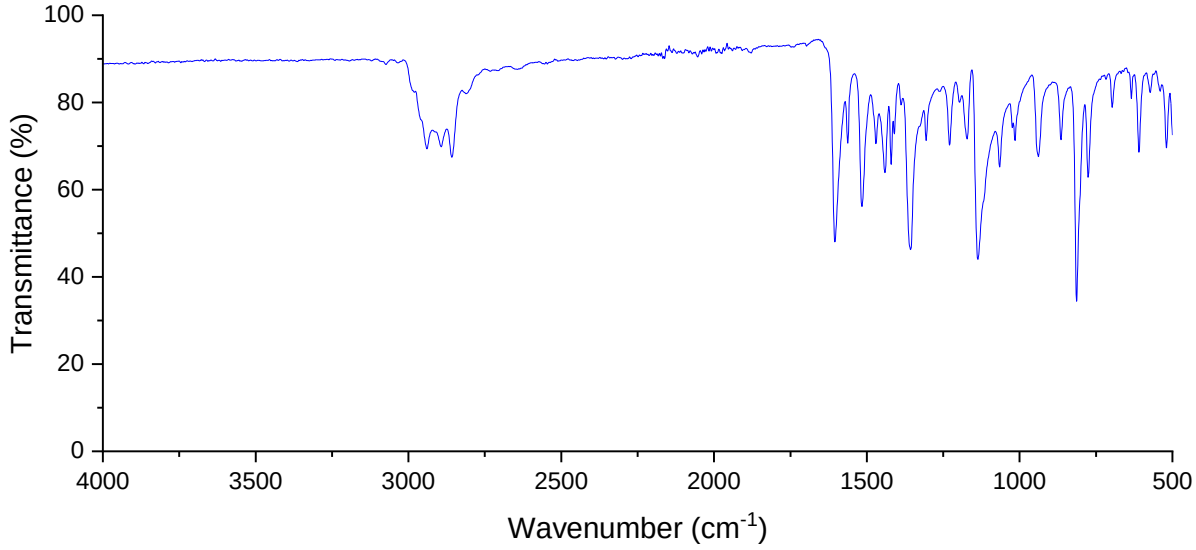

Figure A119. IR spectrum of **11**

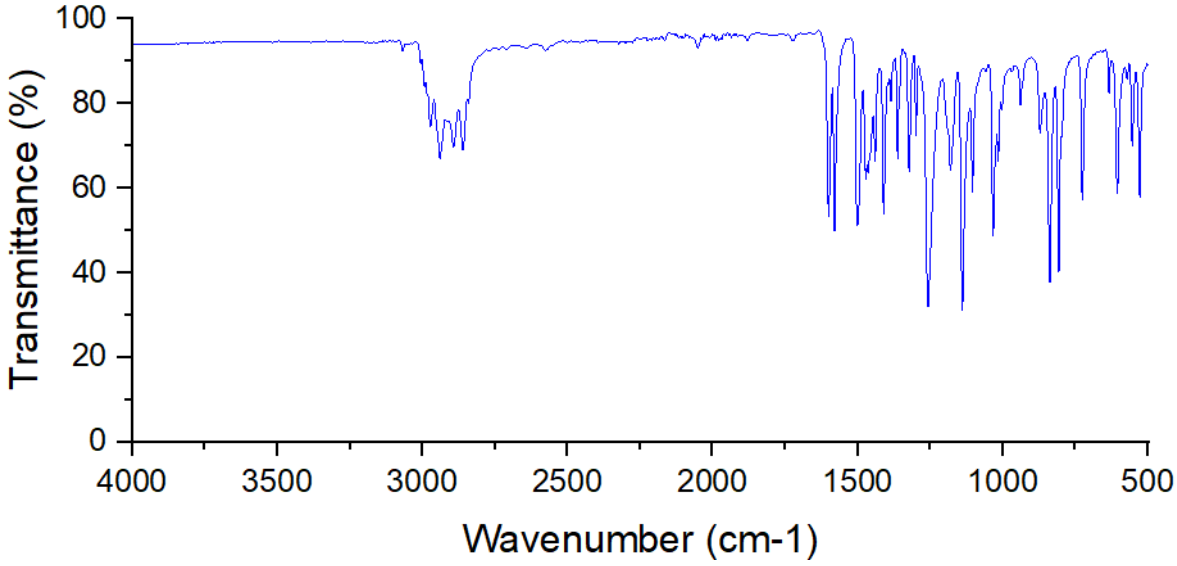

Figure A120. IR Spectrum of **12**

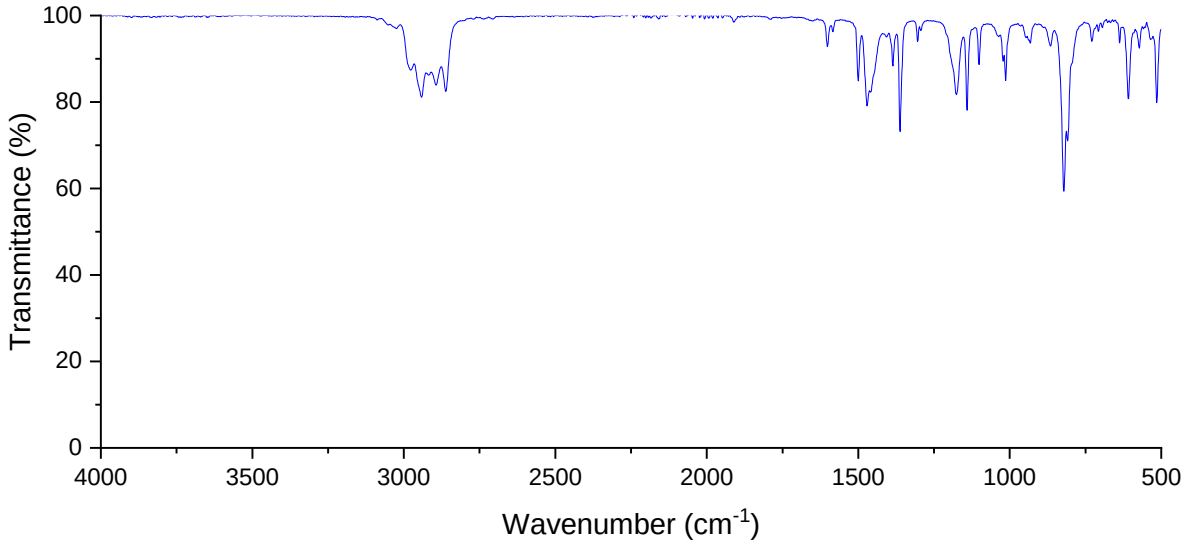

Figure A121. IR Spectrum of **13**

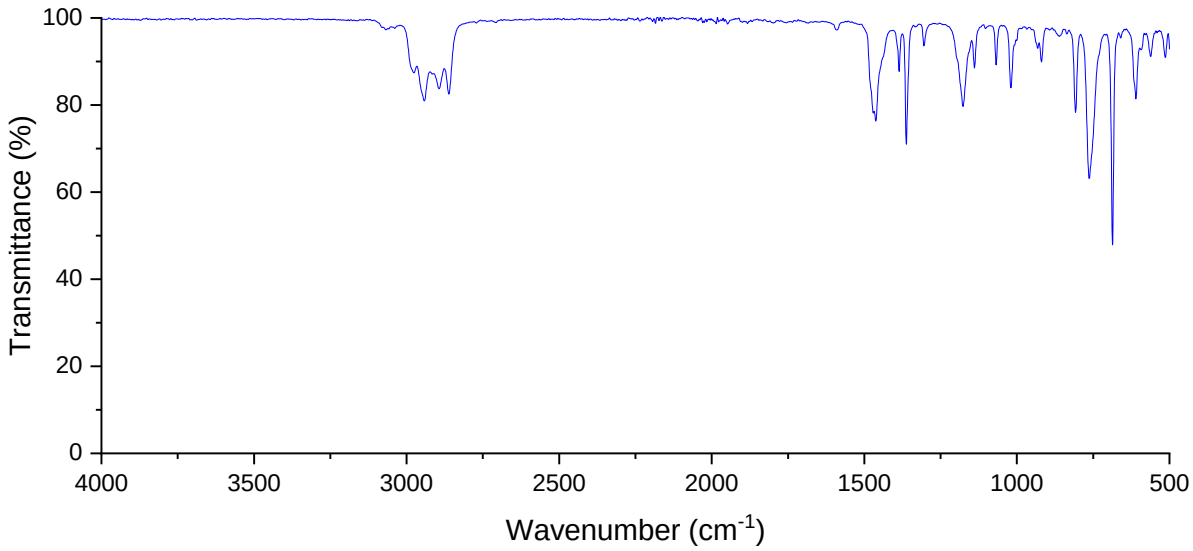

Figure A122. IR Spectrum of **14**

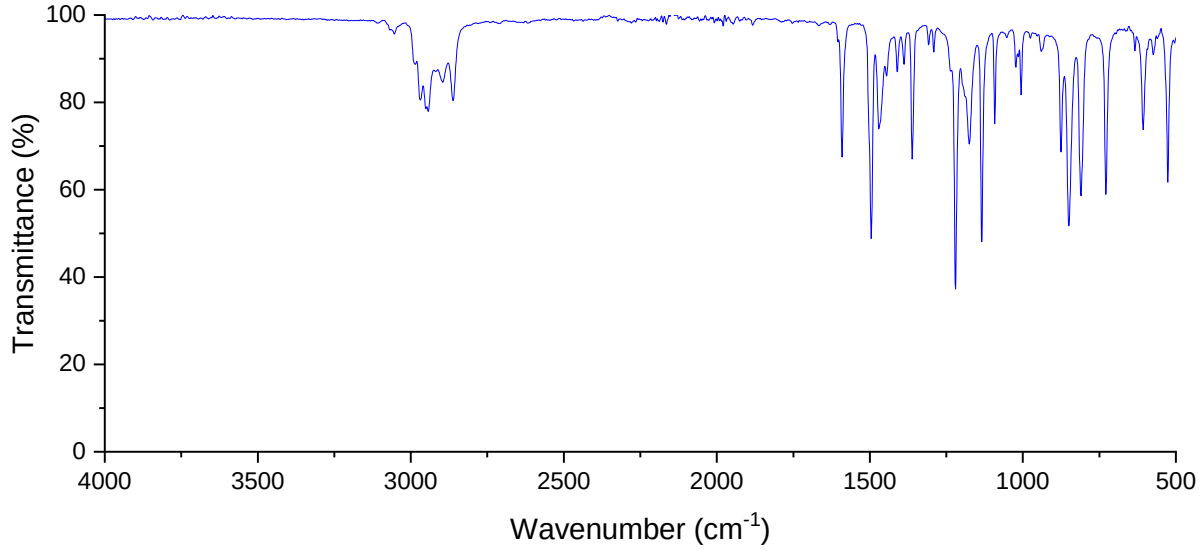

Figure A123. IR Spectrum of **15**

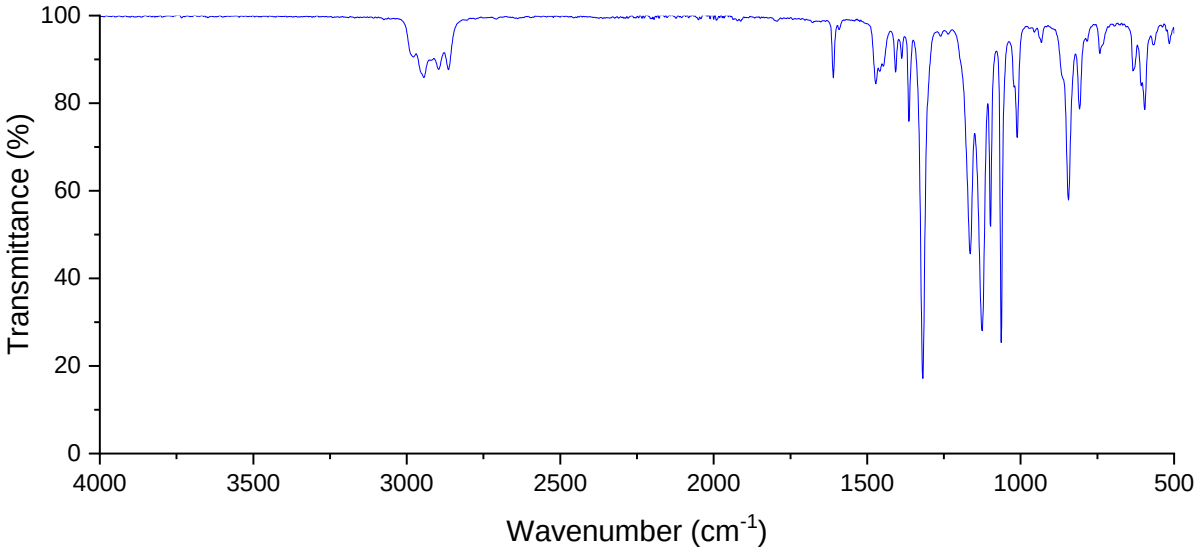

Figure A124. IR Spectrum of **16**

1.2 Azophosphine-Selenides **17** – **22**

1.2.1 NMR Spectra

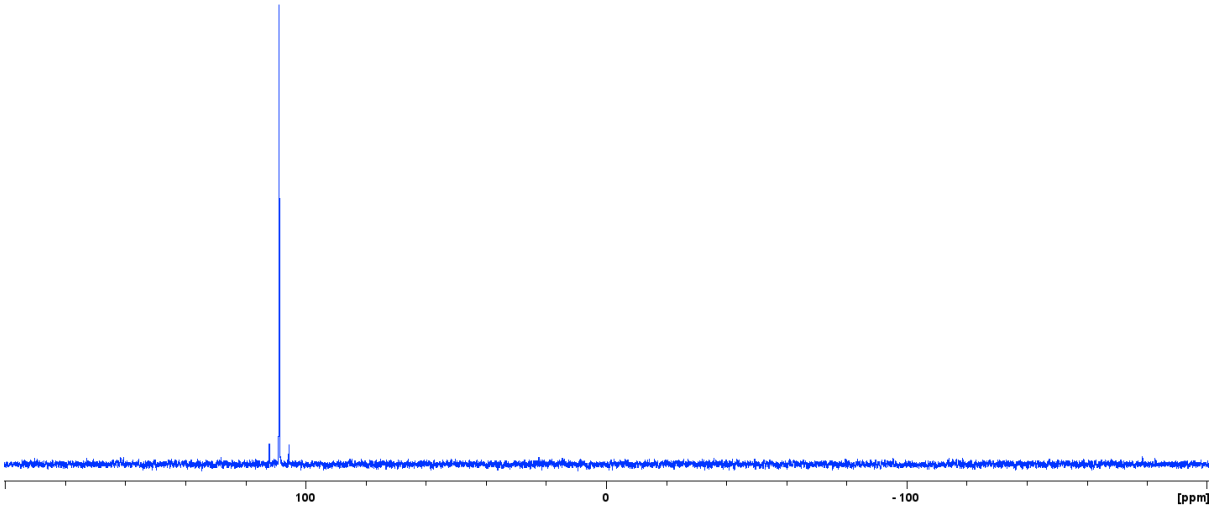

Figure A125. Crude $^{31}P\{^{1}H\}$ NMR spectrum of **17** in toluene. $^{1}J_{P-Se}$ = 794 Hz.

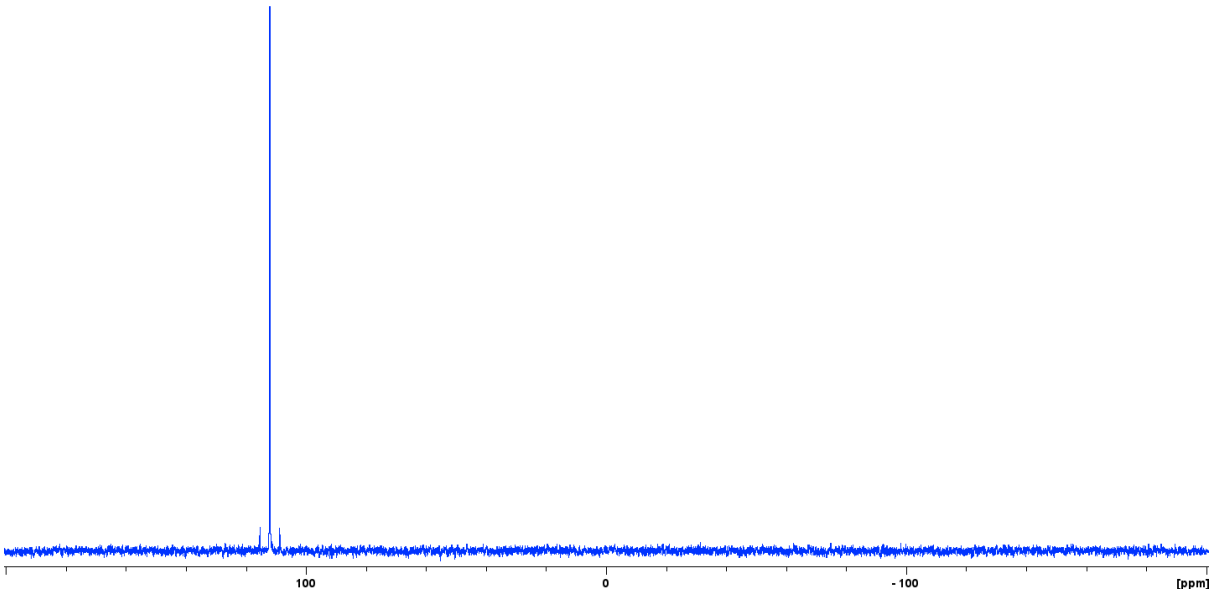

Figure A126. $^{31}P\{^{1}H\}$ NMR spectrum of **18** in toluene. $^{1}J_{P-Se}$ = 801 Hz.

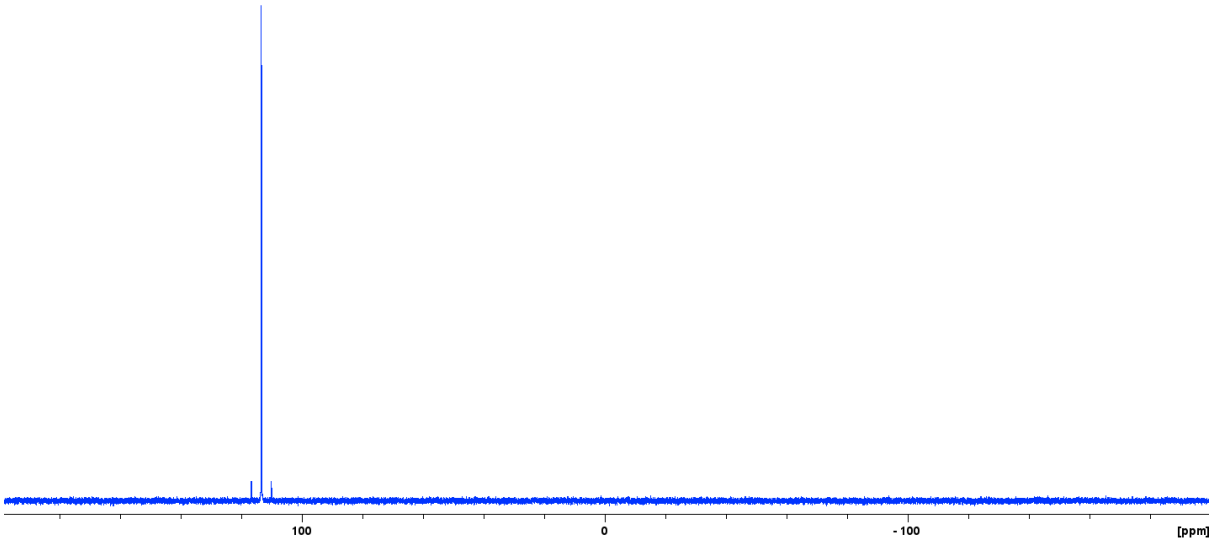

Figure A127. $^{31}P\{^{1}H\}$ NMR spectrum of **19** in toluene. $^{1}J_{P-Se}$ = 804 Hz.

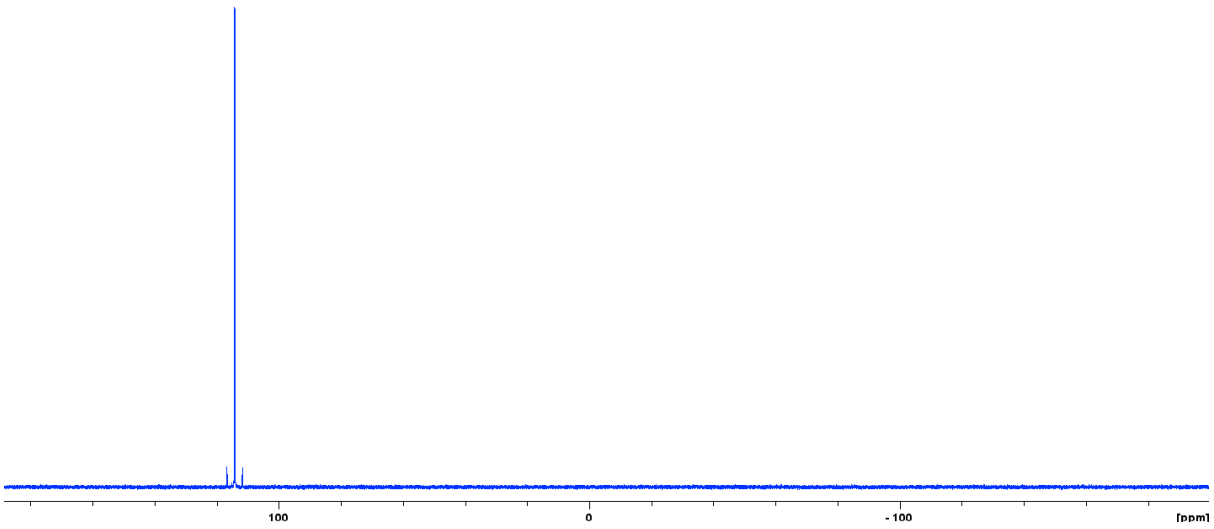

Figure A128. $^{31}P\{^{1}H\}$ NMR spectrum of **20** in toluene. $^{1}J_{P-Se}$ = 806 Hz.

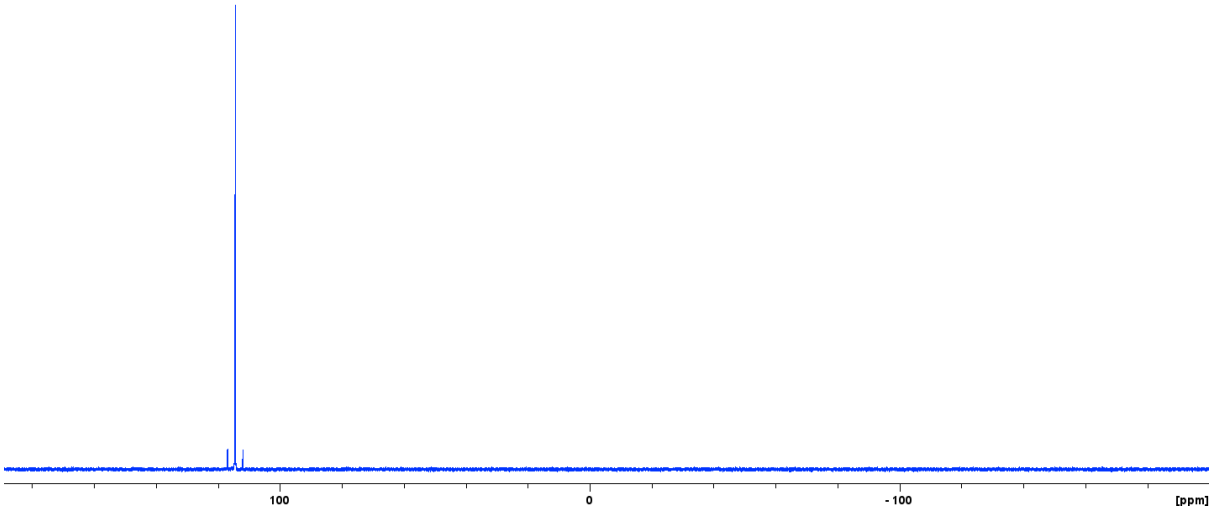

Figure A129. $^{31}P\{^{1}H\}$ NMR spectrum of **21** in toluene. $^{1}J_{P-Se}$ = 806 Hz.

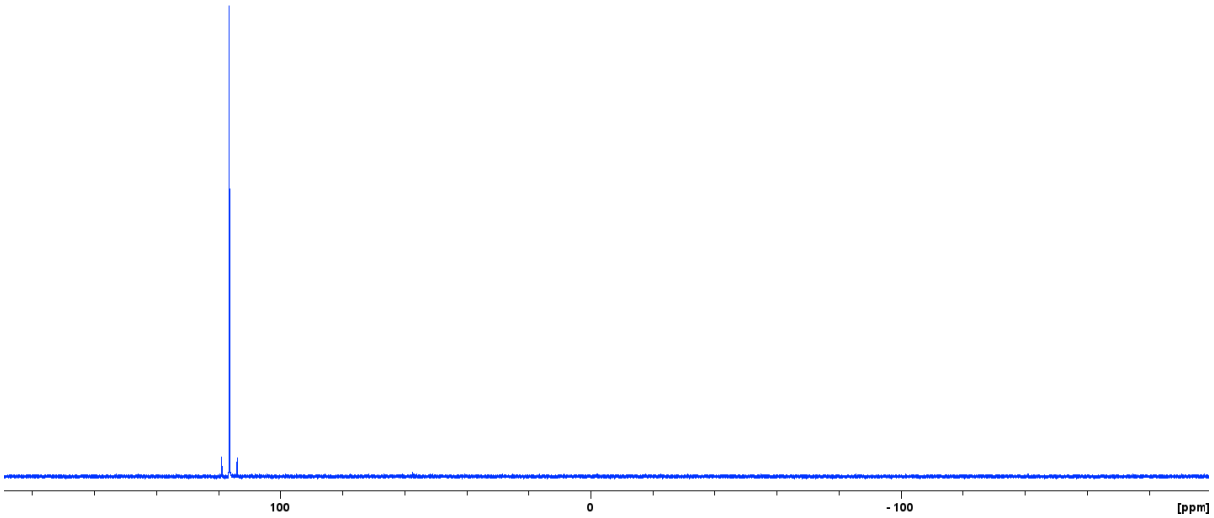

Figure A130. $^{31}P\{^{1}H\}$ NMR spectrum of **22** in toluene. $^{1}J_{P-Se}$ = 810 Hz.

1.3 Coordination Complexes **23** – **27, 29** and **30**

1.3.1 NMR Spectra

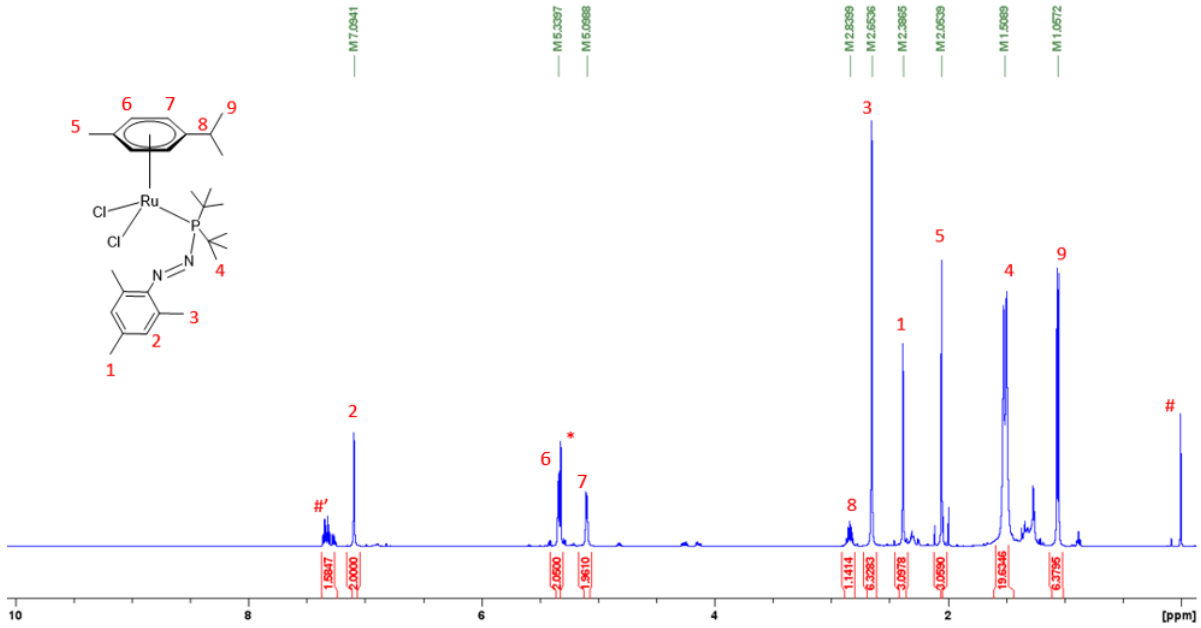

Figure A131. ^{1}H NMR spectrum of **23** in CD_2Cl_2. * = residual $CDHCl_2$, # = silicone grease and TMS internal standard, #' = residual chlorobenzene.

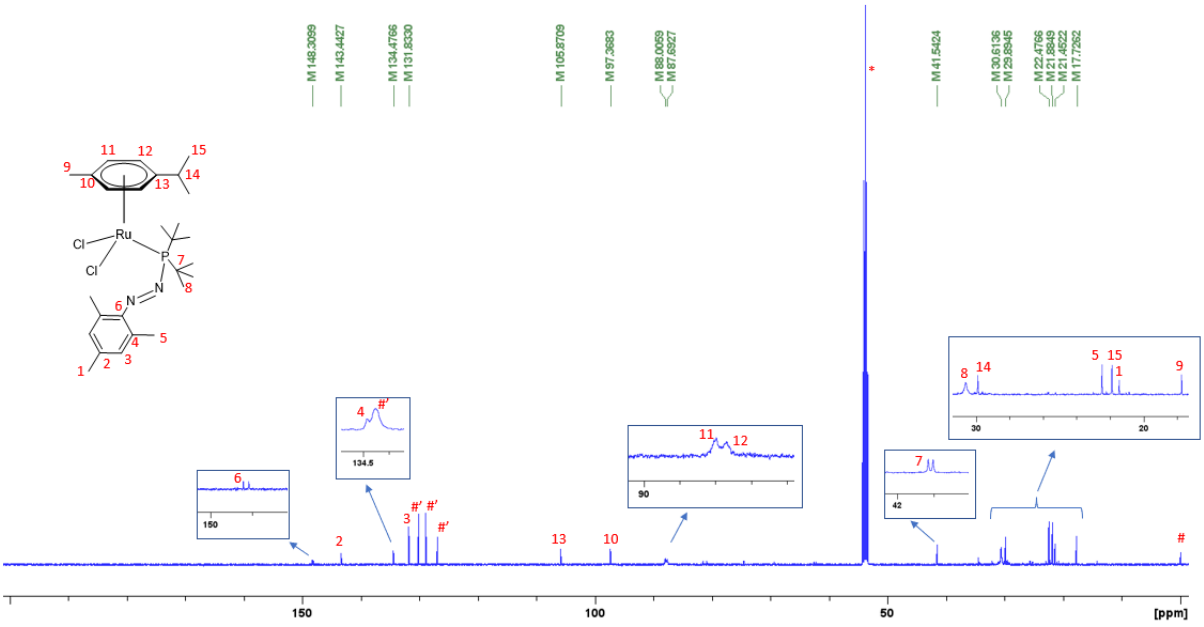

Figure A132. ^{13}C NMR spectrum of **23** in CD_2Cl_2. * = CD_2Cl_2, # = TMS internal standard, #' = residual chlorobenzene.

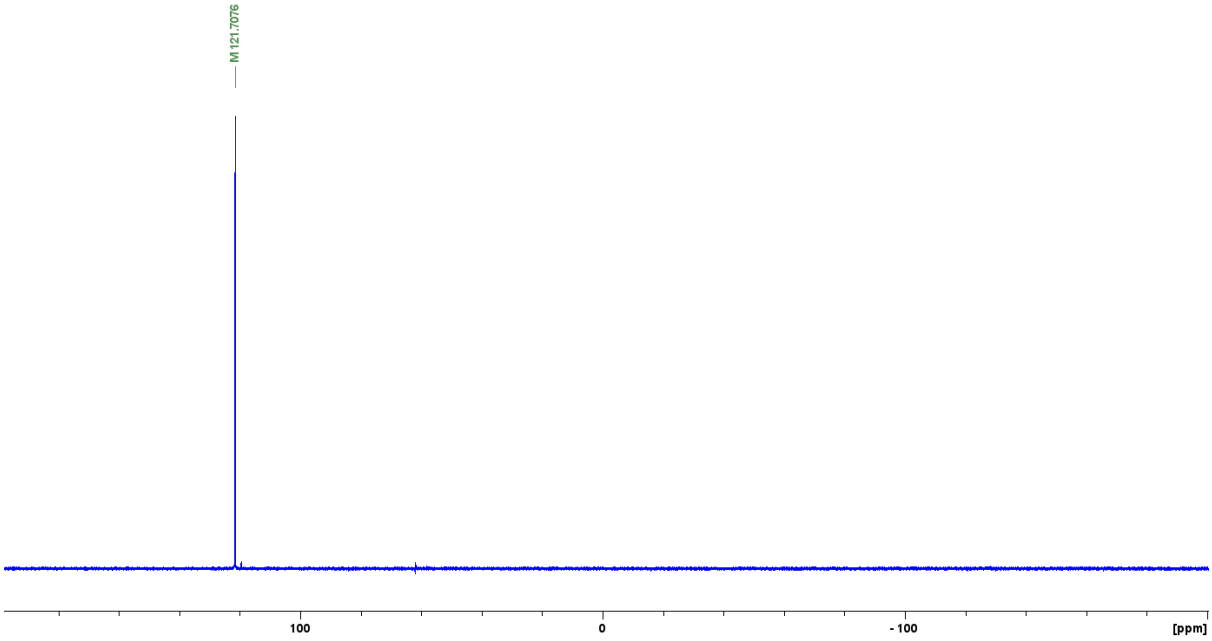

Figure A133. $^{31}P\{^{1}H\}$ NMR spectrum of **23** in CD_2Cl_2.

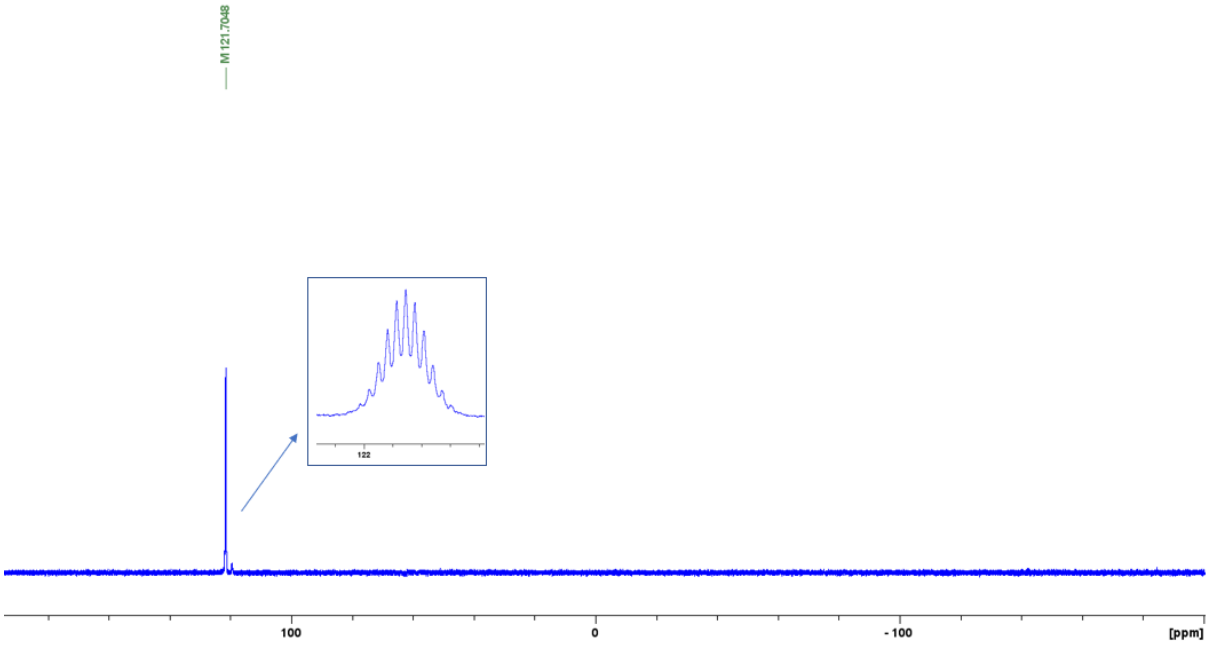

Figure A134. ^{31}P NMR spectrum of **23** in CD_2Cl_2.

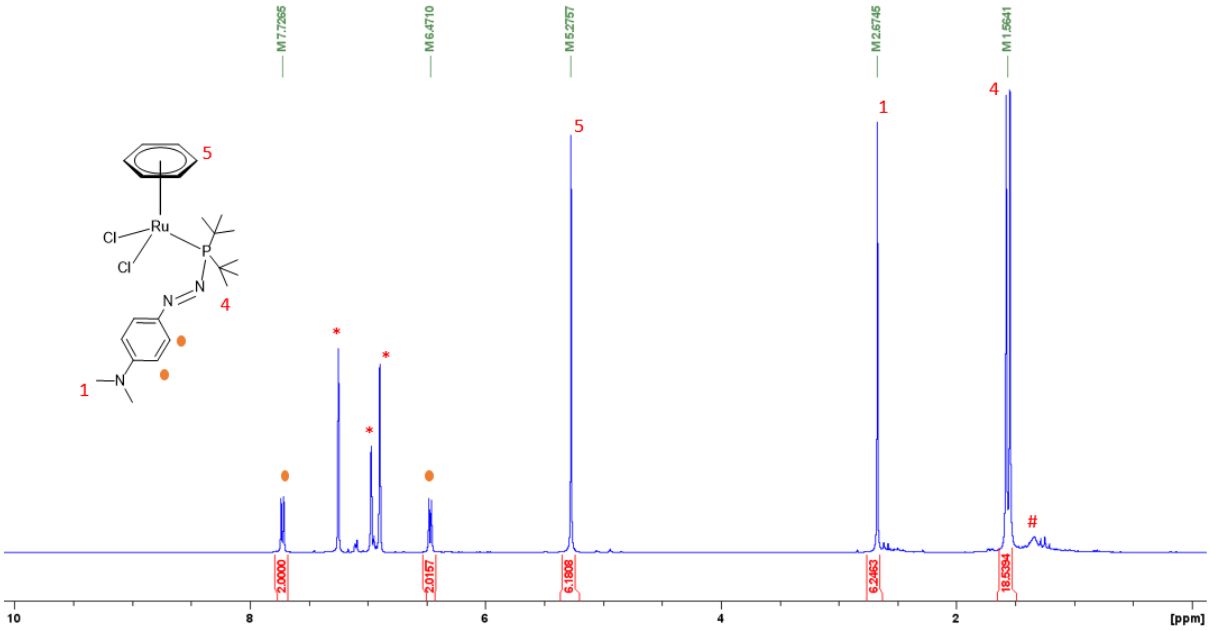

Figure A135. ^{1}H NMR spectrum of **24** in bromobenzene-d_5. * = residual bromobenzene-d_4H, # = water in solvent.

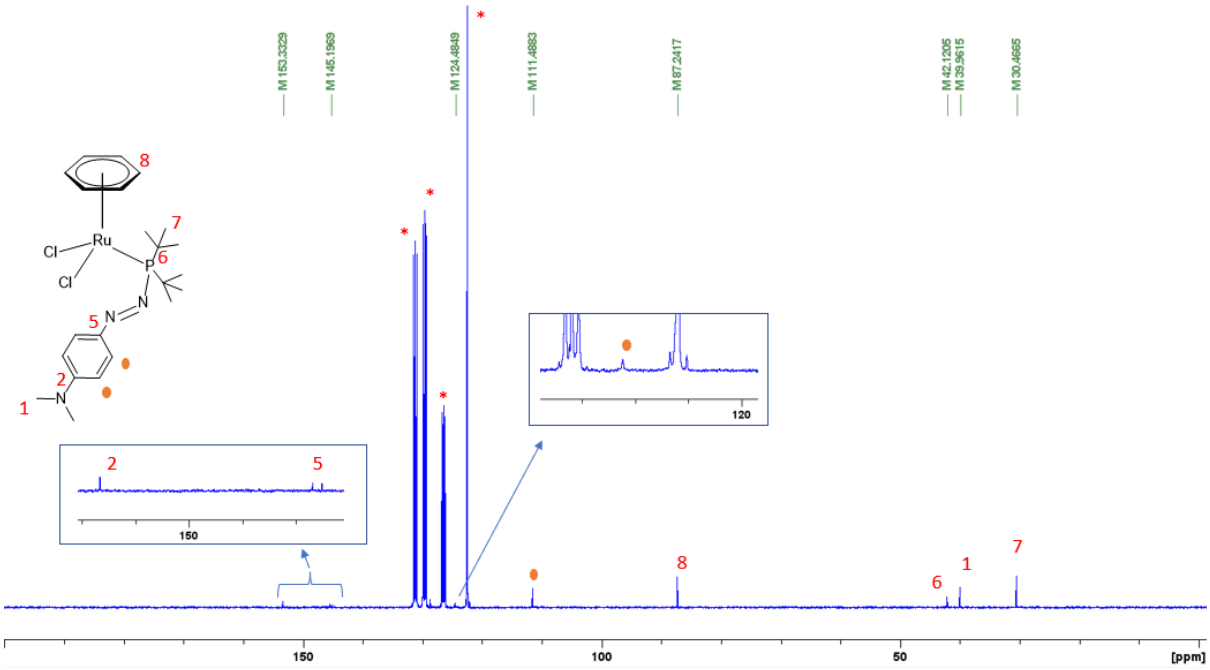

Figure A136. ^{13}C NMR spectrum of **24** in bromobenzene-d_5. * = residual bromobenzene-d_5.

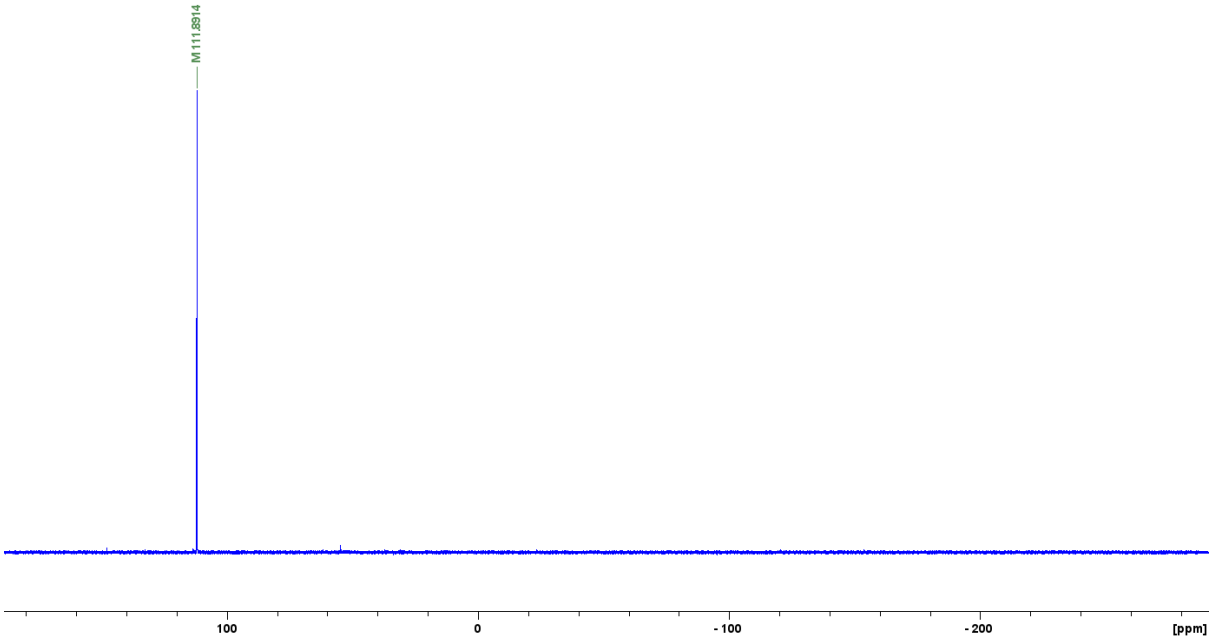

Figure A137. $^{31}P\{^{1}H\}$ NMR spectrum of **24** in bromobenzene-d_5.

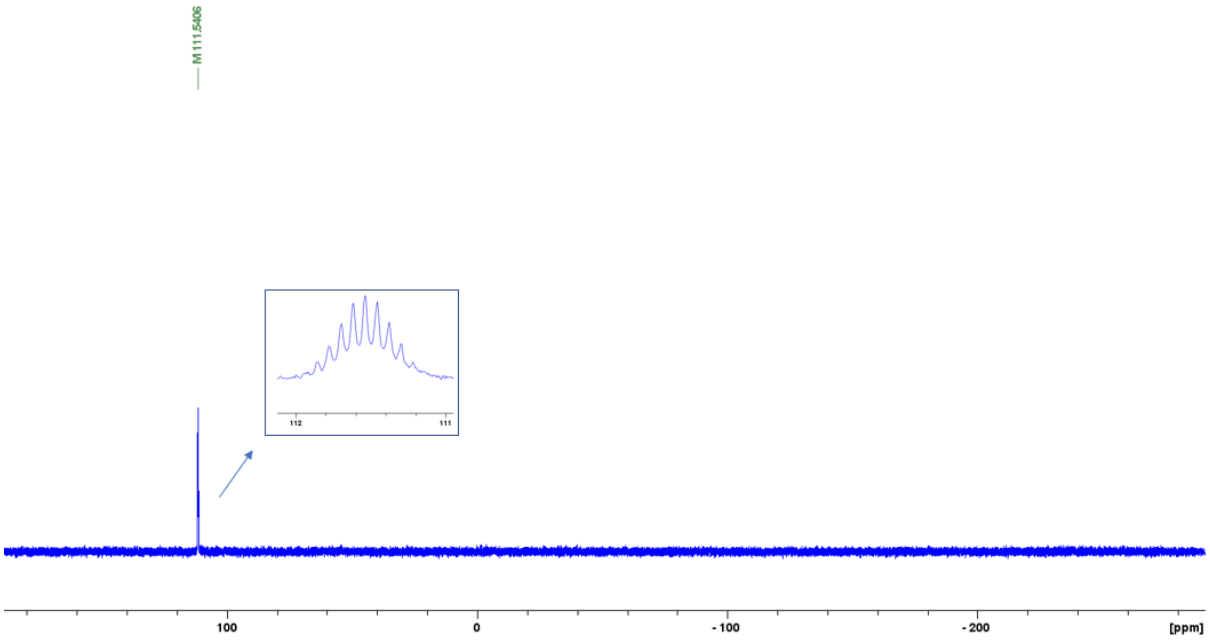

Figure A138. ^{31}P NMR spectrum of **24** in bromobenzene-d_5.

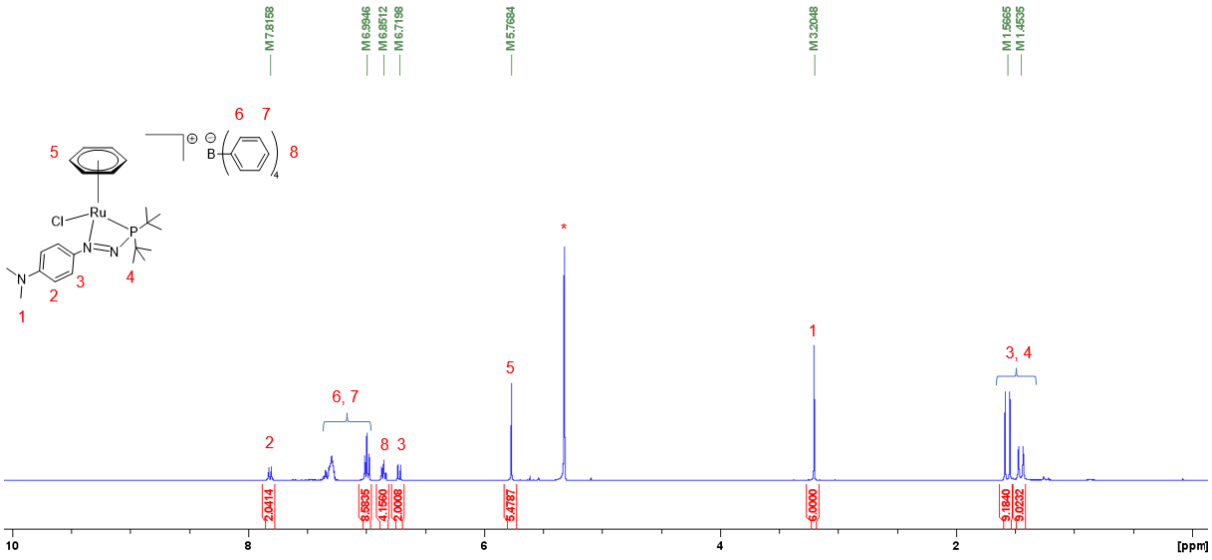

Figure A139. ^{1}H NMR spectrum of **25** in CD_2Cl_2. * = residual $CDHCl_2$.

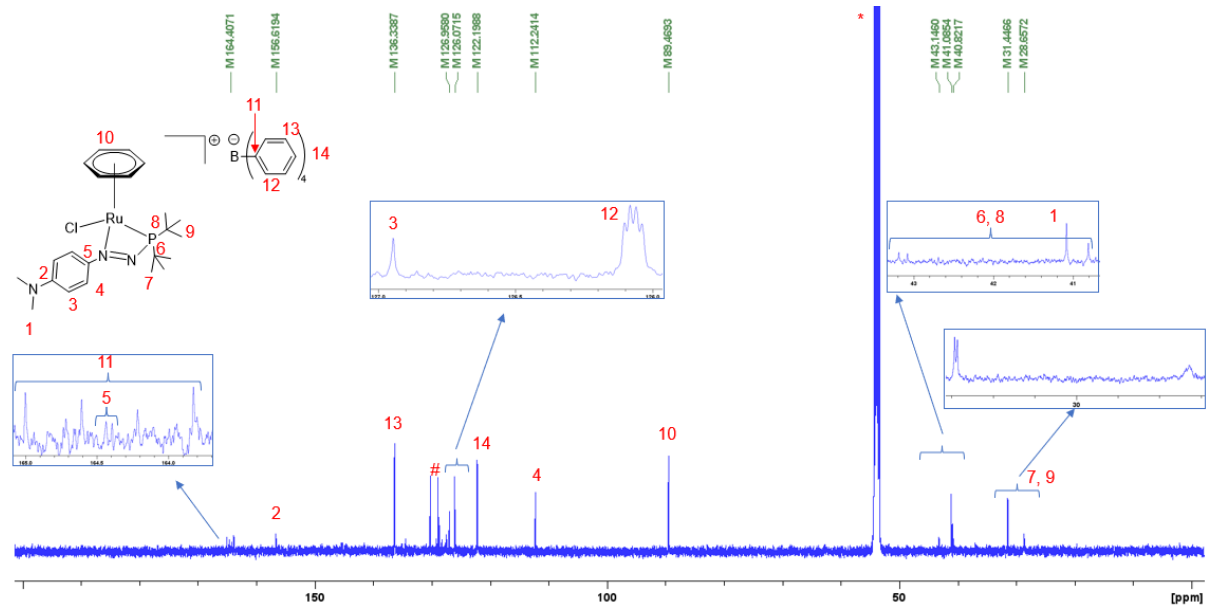

Figure A140. ^{13}C NMR spectrum of **25** in CD_2Cl_2. * = CD_2Cl_2, # = residual chlorobenzene.

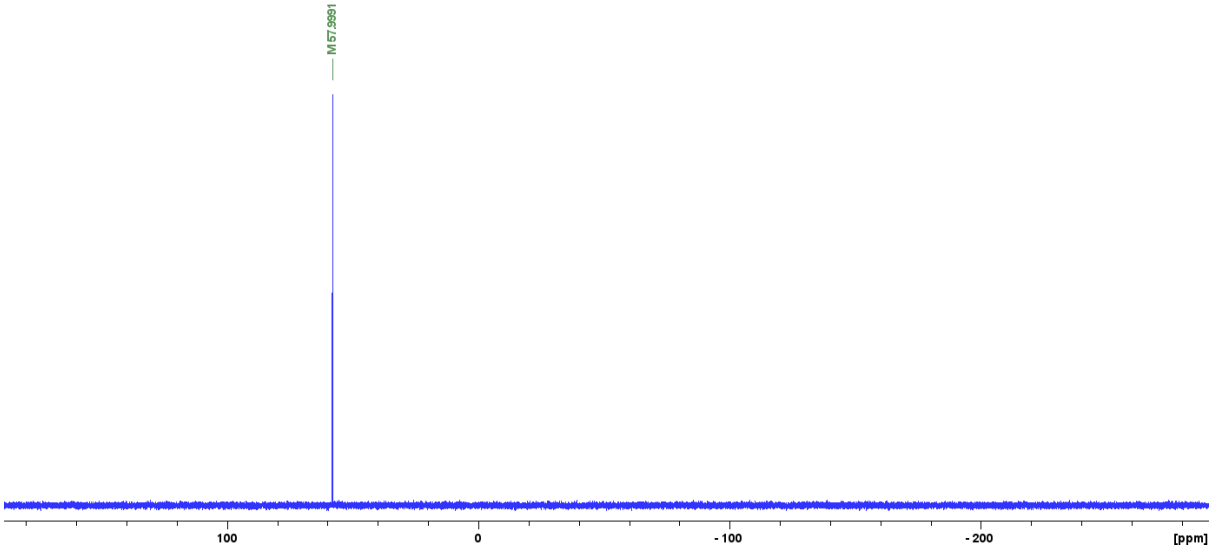

Figure A141. $^{31}P\{^{1}H\}$ NMR spectrum of **25** in CD_2Cl_2.

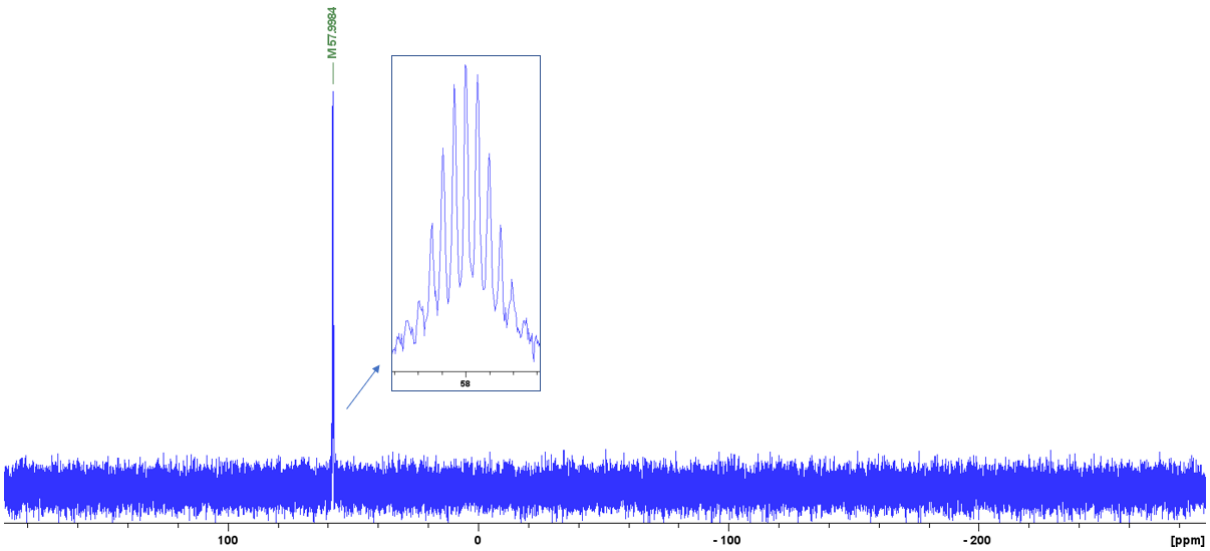

Figure A142. ^{31}P NMR spectrum of **25** in CD_2Cl_2.

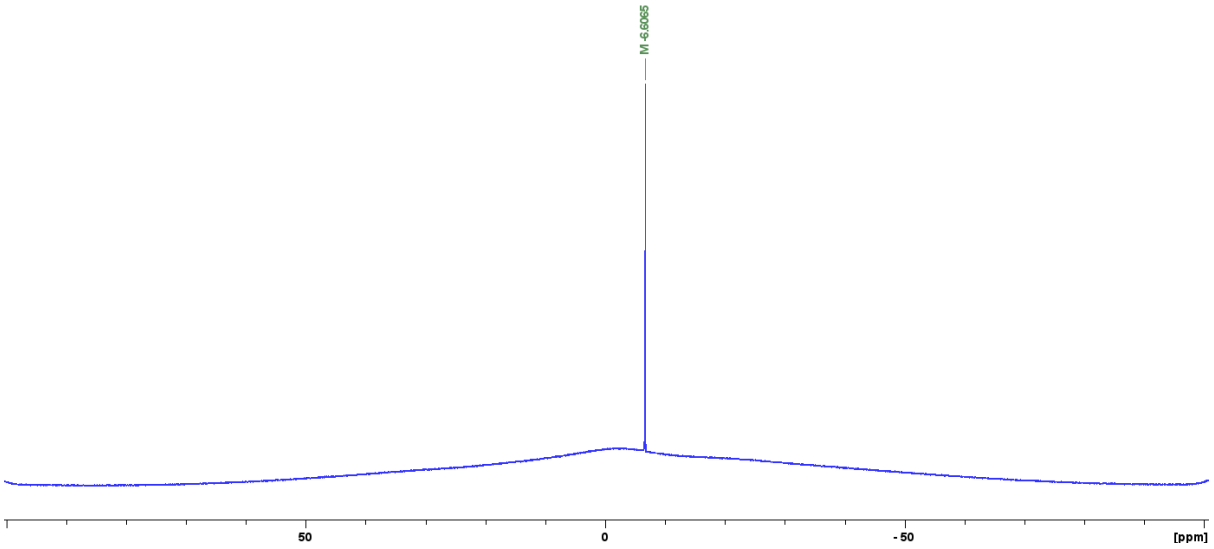

Figure A143. $^{11}B\{^{1}H\}$ NMR spectrum of **25** in CD_2Cl_2.

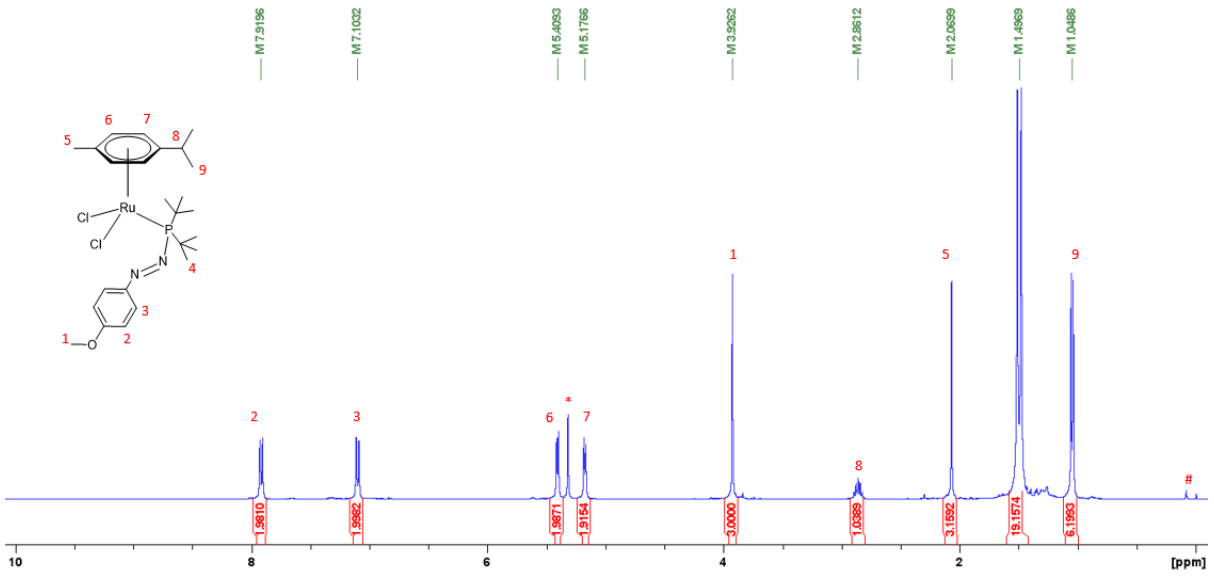

Figure A144. ^{1}H NMR spectrum of **26** in CD_2Cl_2. * = residual $CDHCl_2$, # = silicone grease and TMS internal reference.

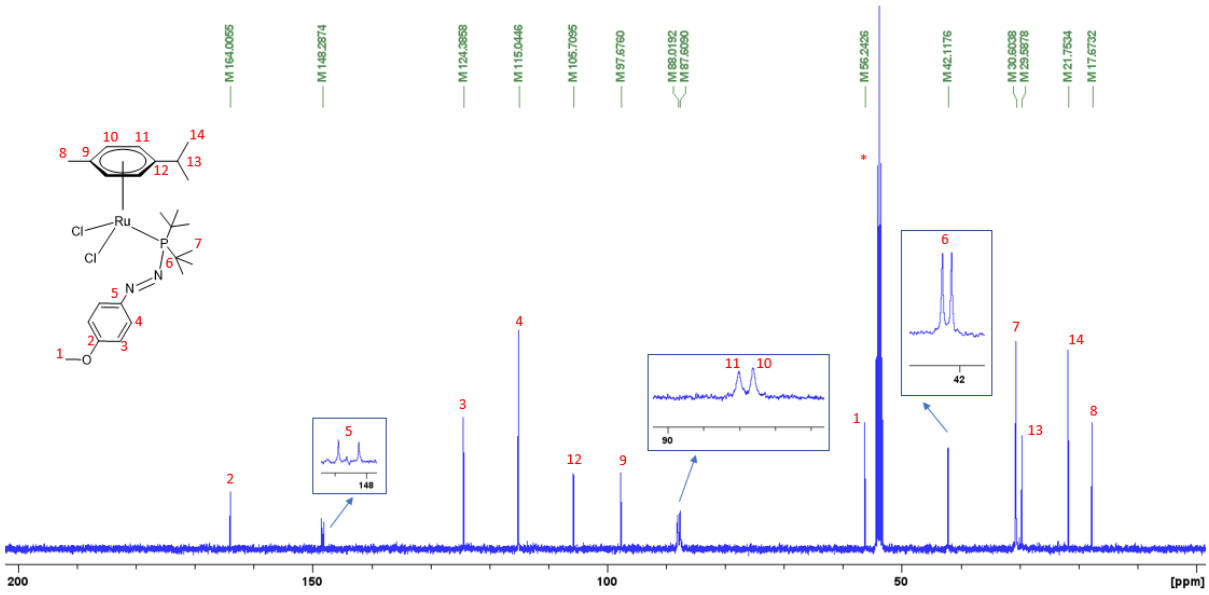

Figure A145. $^{13}C\{^{1}H\}$ NMR spectrum of **26** in CD_2Cl_2. * = CD_2Cl_2.

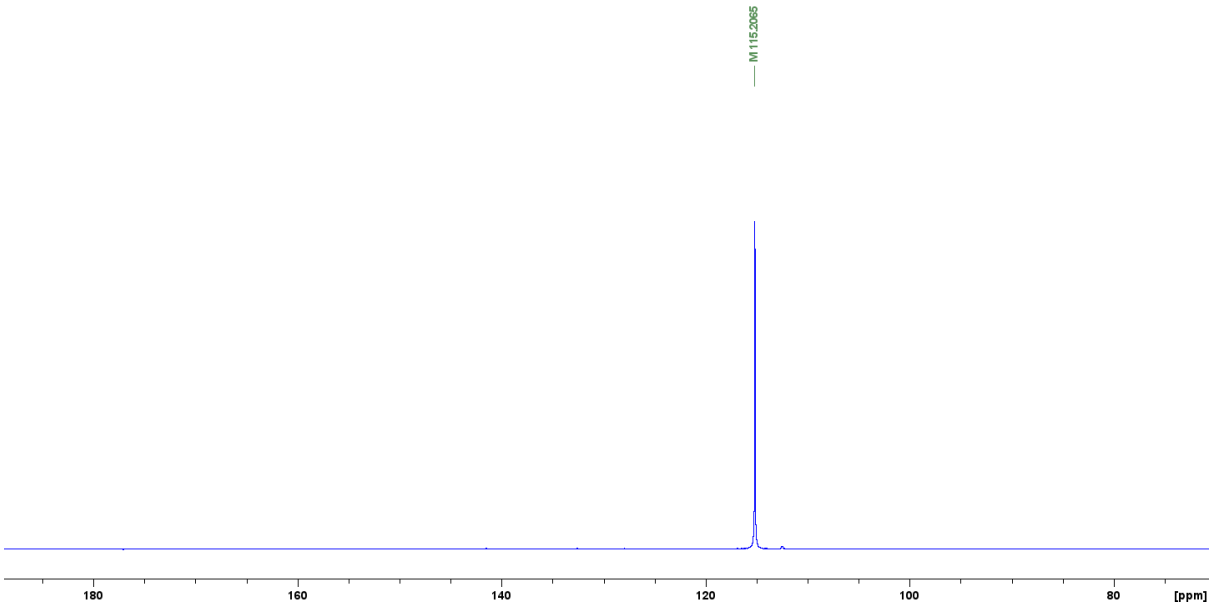

Figure A146. $^{31}P\{^{1}H\}$ NMR spectrum of **26** in CD_2Cl_2.

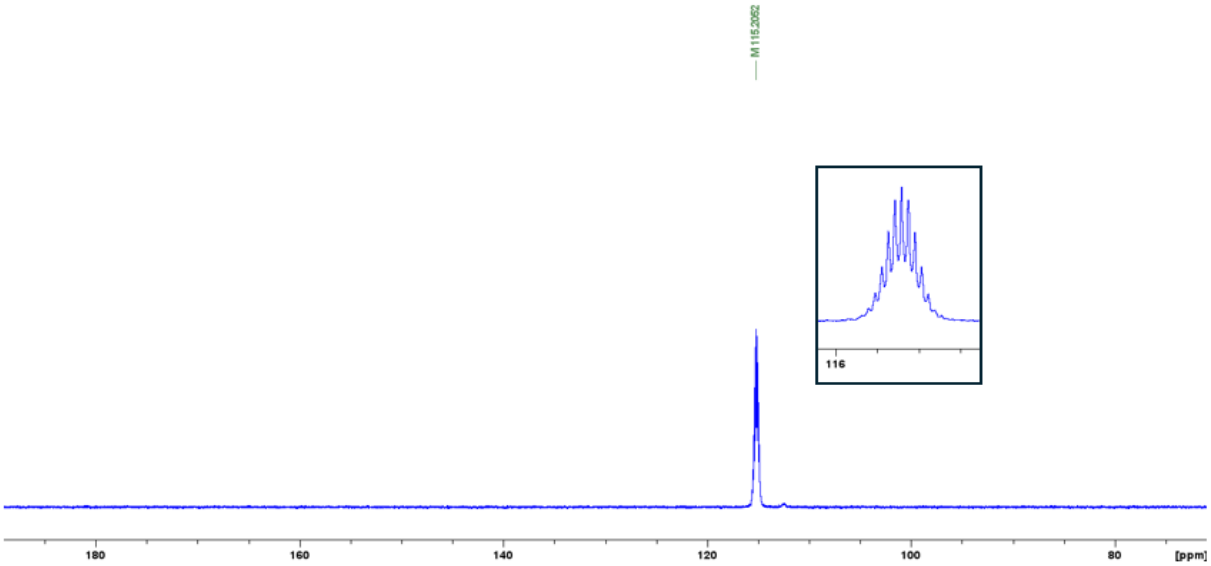

Figure A147. ^{31}P NMR spectrum of **26** in CD_2Cl_2.

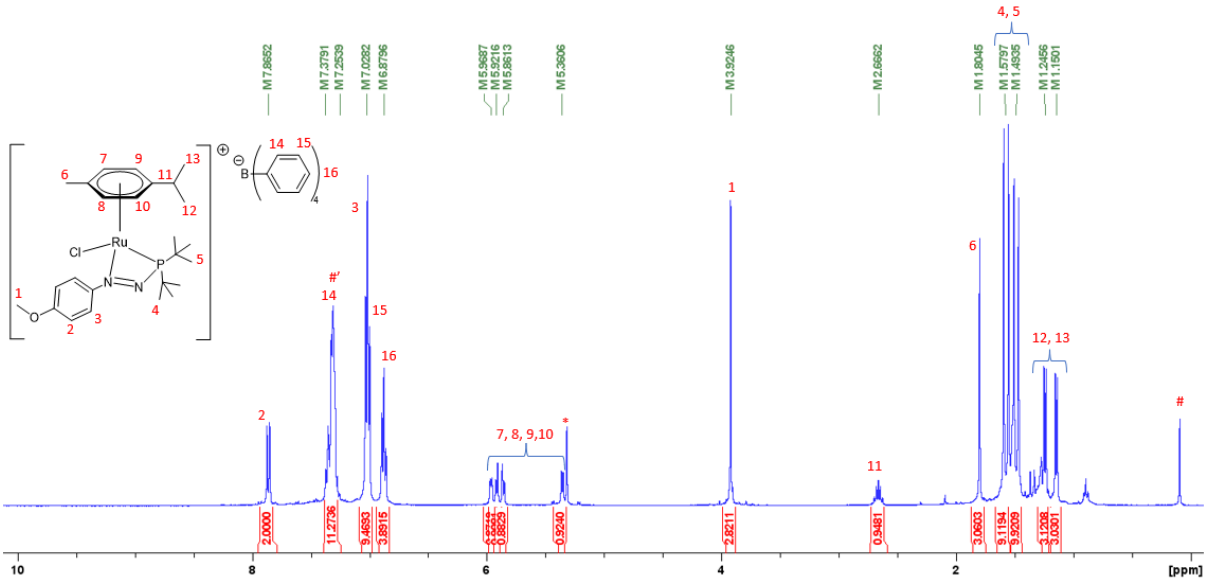

Figure A148. ^{1}H NMR spectrum of **27** in CD2Cl2. * = residual $CDHCl_2$, # = silicone grease, #' = residual chlorobenzene.

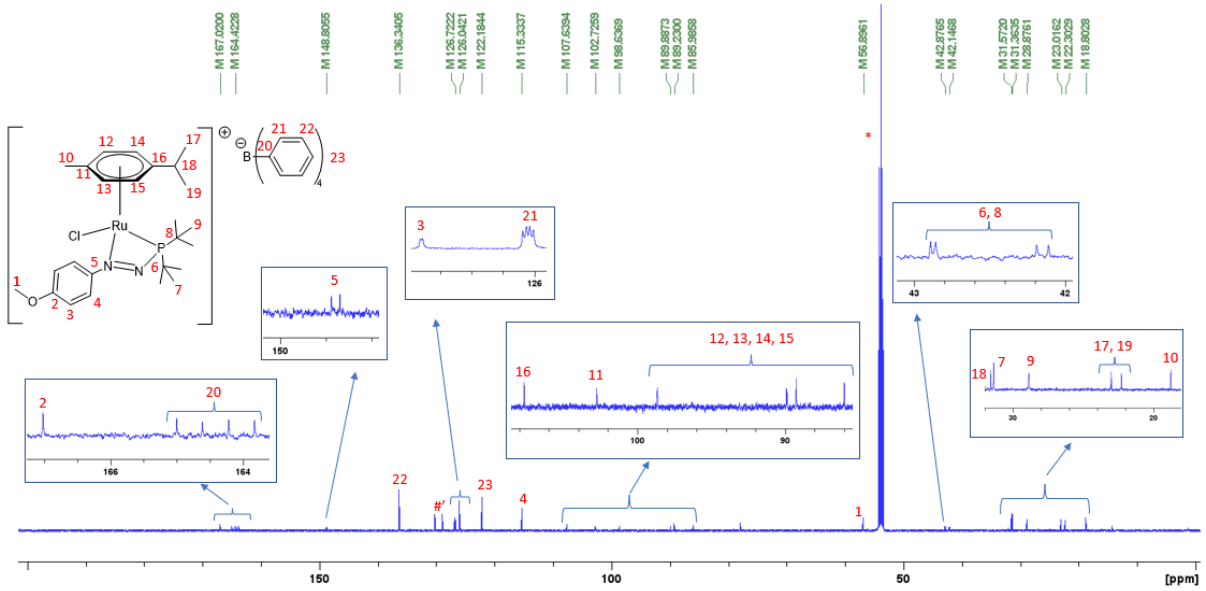

Figure A149. $^{13}C\{^{1}H\}$ NMR spectrum of **27** in CD_2Cl_2. * = CD_2Cl_2, #' = residual chlorobenzene.

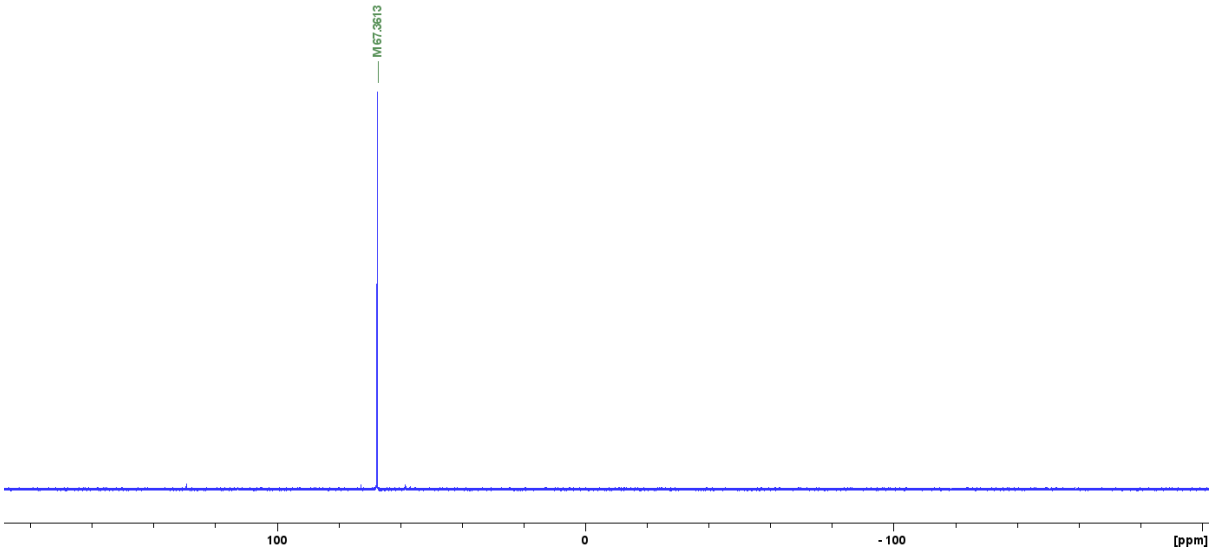

Figure A150. $^{31}P\{^{1}H\}$ NMR spectrum of **27** in CD_2Cl_2.

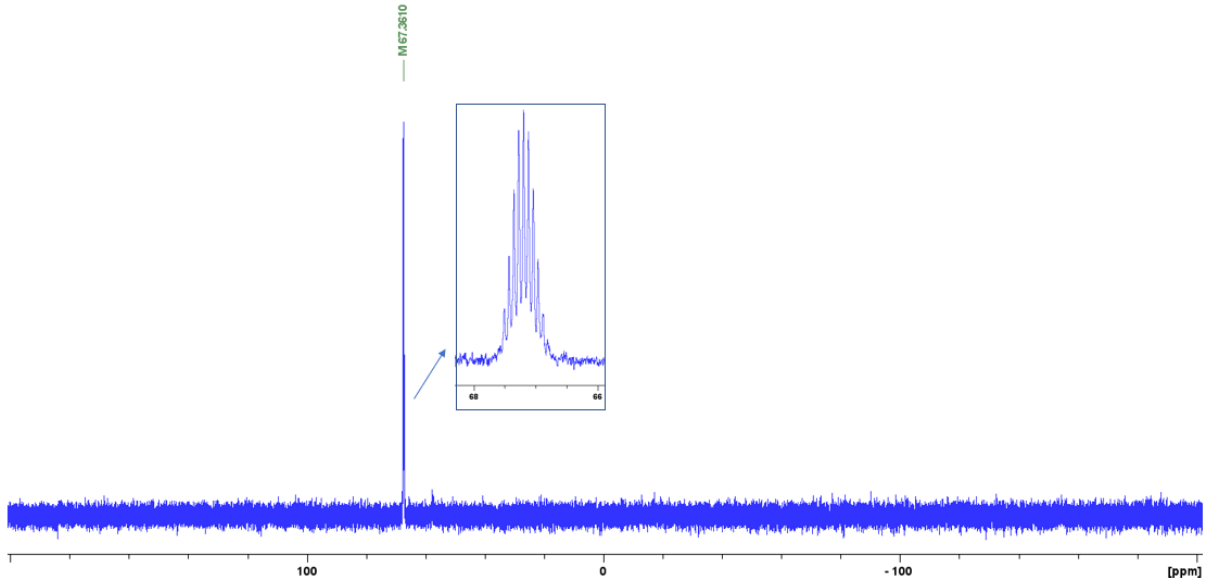

Figure A151. ^{31}P NMR spectrum of **27** in CD_2Cl_2.

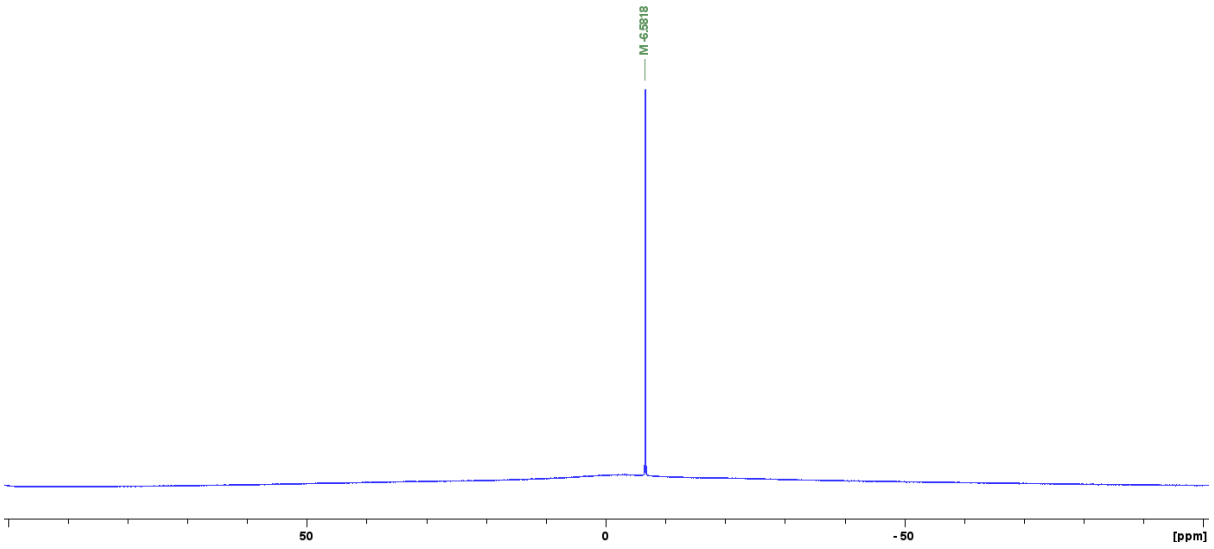

Figure A152. $^{11}B\{^1H\}$ NMR spectrum of **27** in CD_2Cl_2.

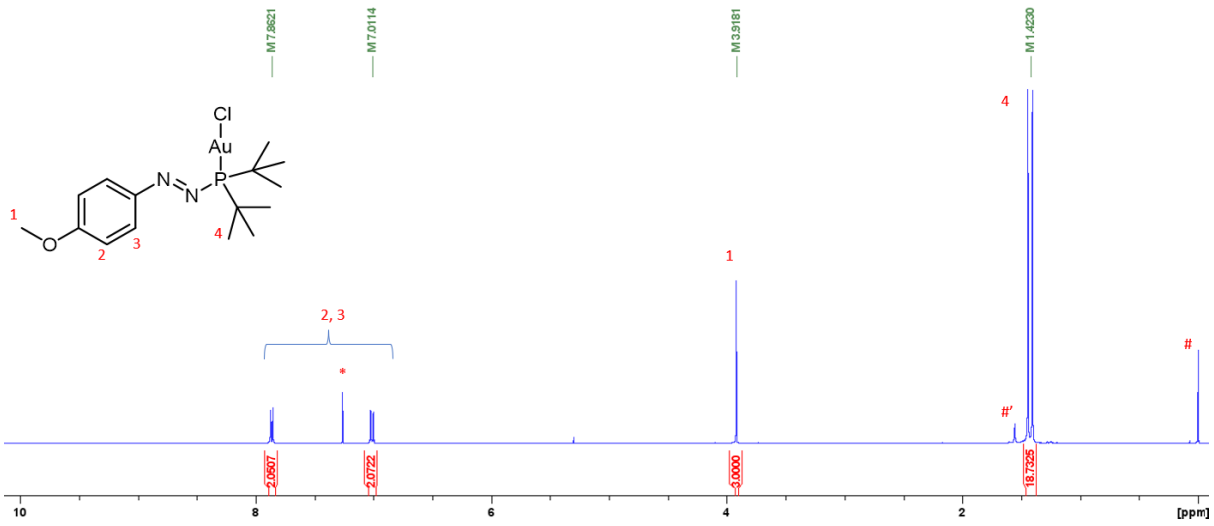

Figure A153. ^{1}H NMR spectrum of **29** in $CDCl_3$. * = residual $CHCl_3$, # = silicone grease, #' = water in solvent.

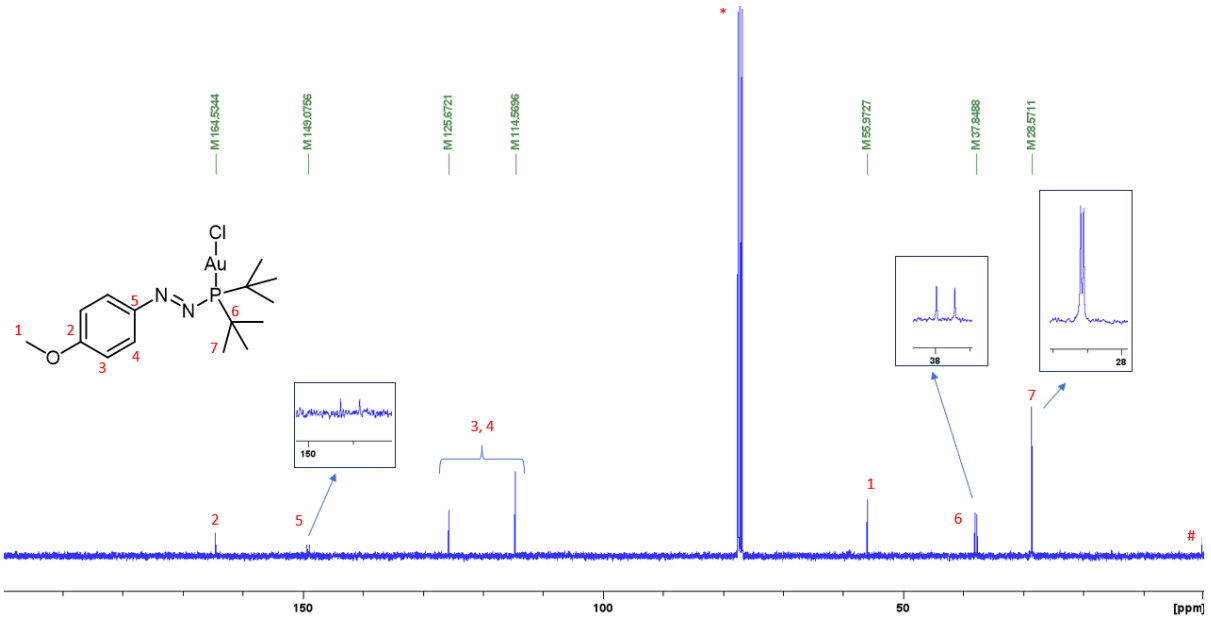

Figure A154. $^{13}C\{^{1}H\}$ NMR spectrum of **29** in $CDCl_3$. * = $CDCl_3$, # = silicone grease.

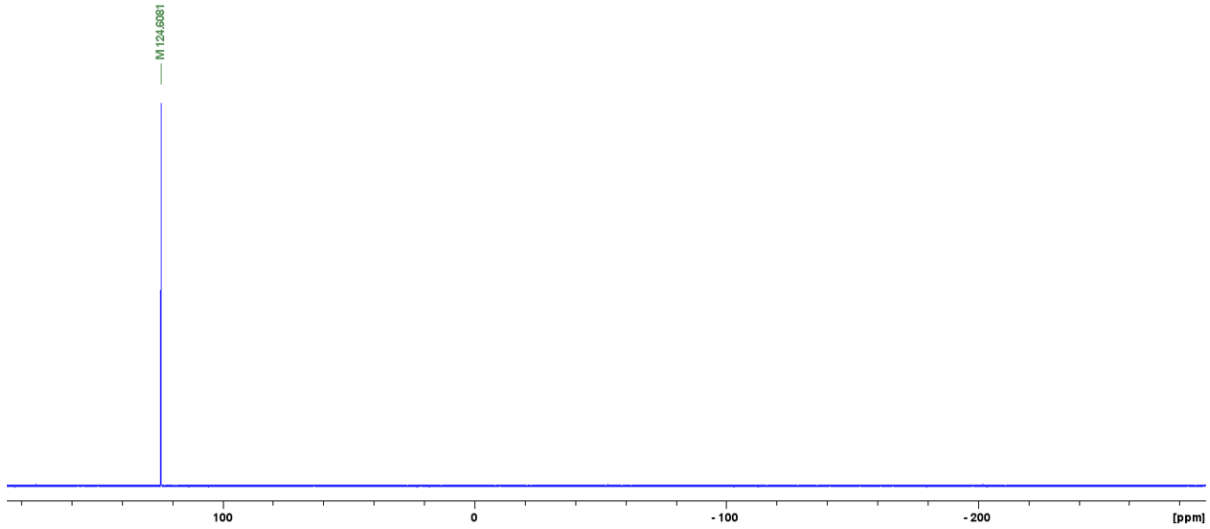

FigureA155. $^{31}P\{^{1}H\}$ NMR spectrum of **29** in $CDCl_3$.

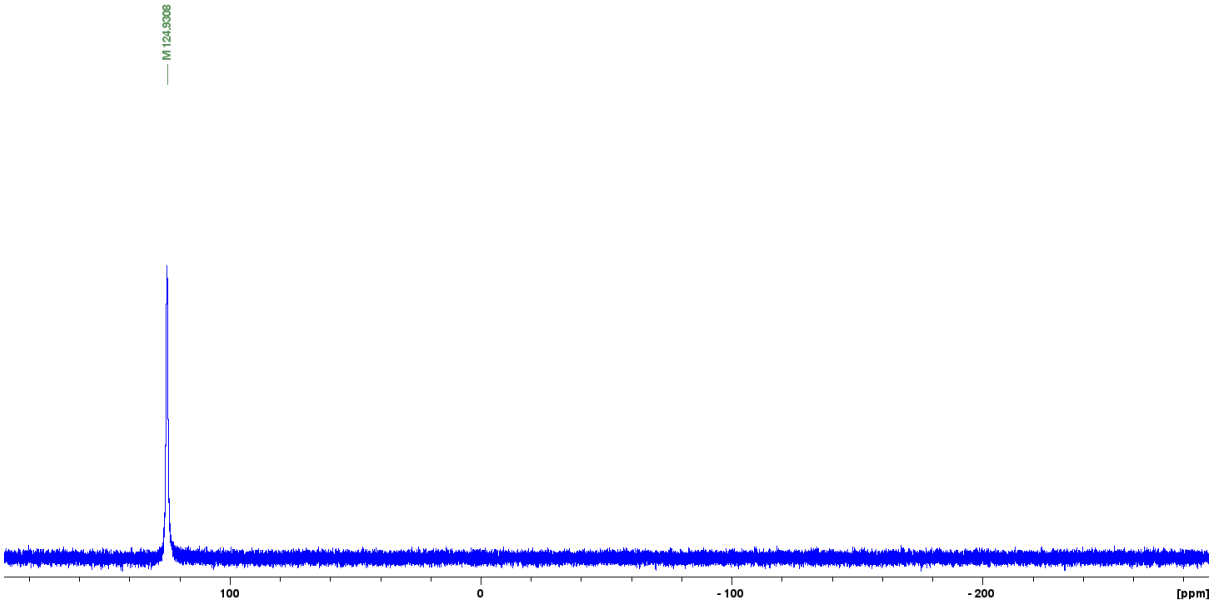

Figure A156. ^{31}P NMR spectrum of **29** in $CDCl_3$.

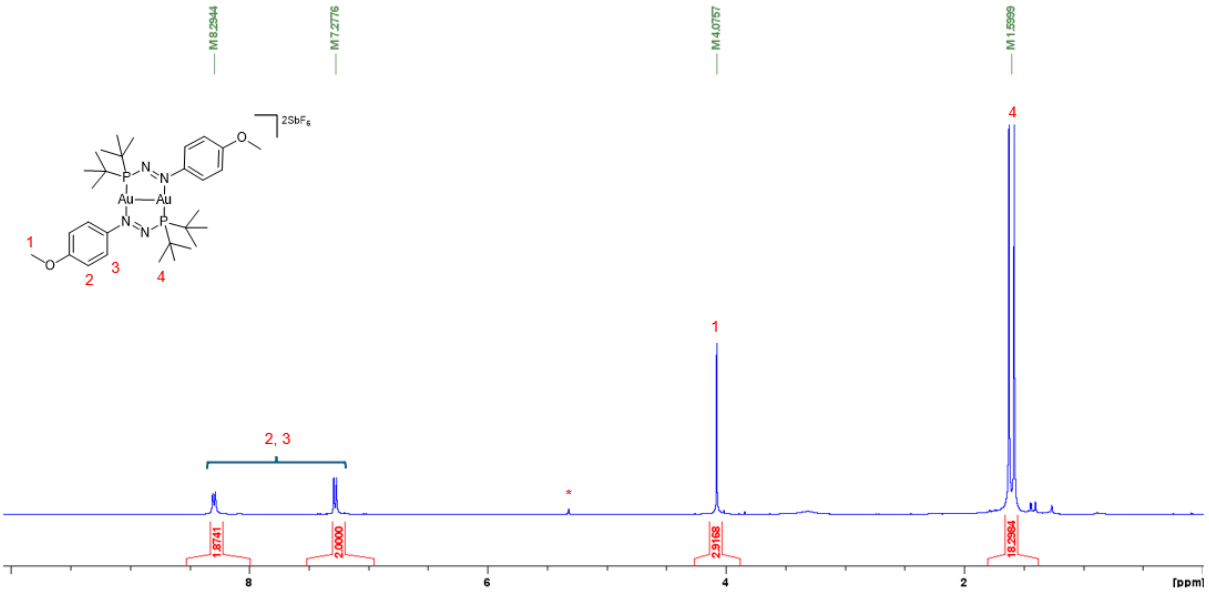

Figure A157. ^{1}H NMR spectrum of **30** in CD_2Cl_2. * = residual $CDHCl_2$

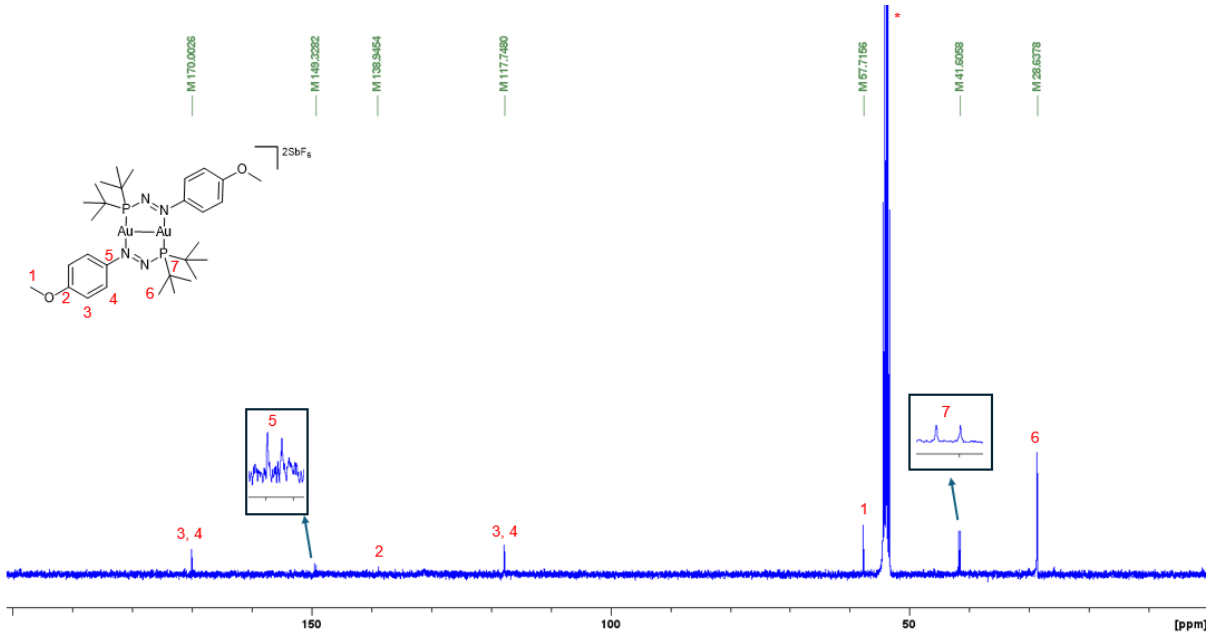

Figure A158. $^{13}C\{^{1}H\}$ NMR spectrum of **30** in CD_2Cl_2. * = CD_2Cl_2

Figure A159. $^{31}P\{^{1}H\}$ NMR spectrum of **30** in CD_2Cl_2

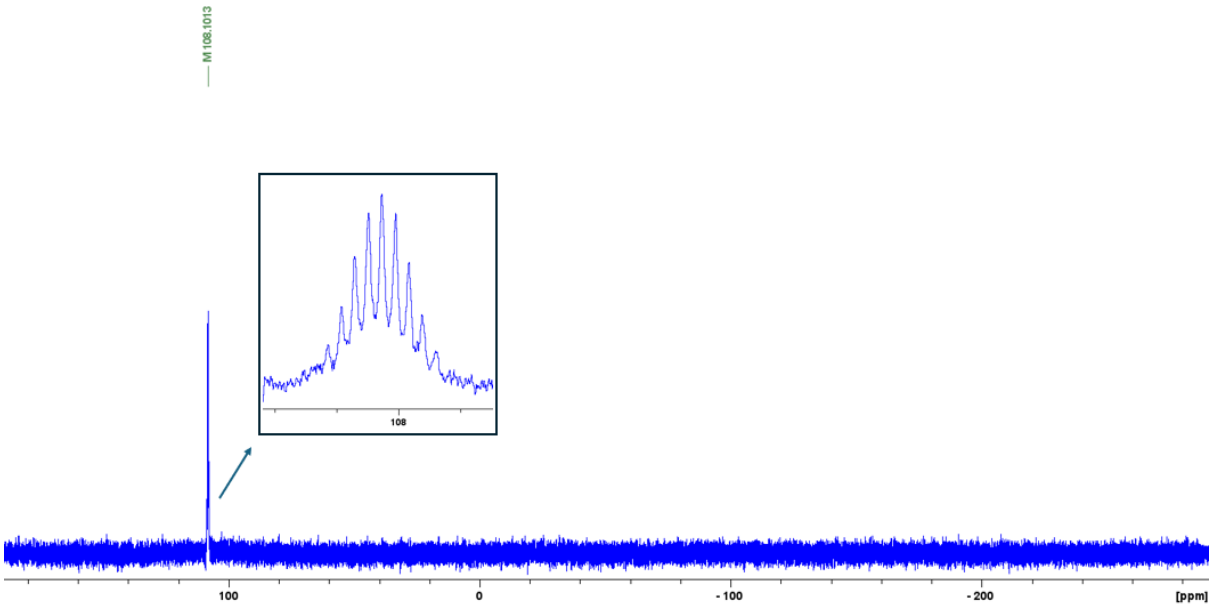

Figure A160. ^{31}P NMR spectrum of **30** in CD_2Cl_2

1.3.2 UV/Vis Spectra

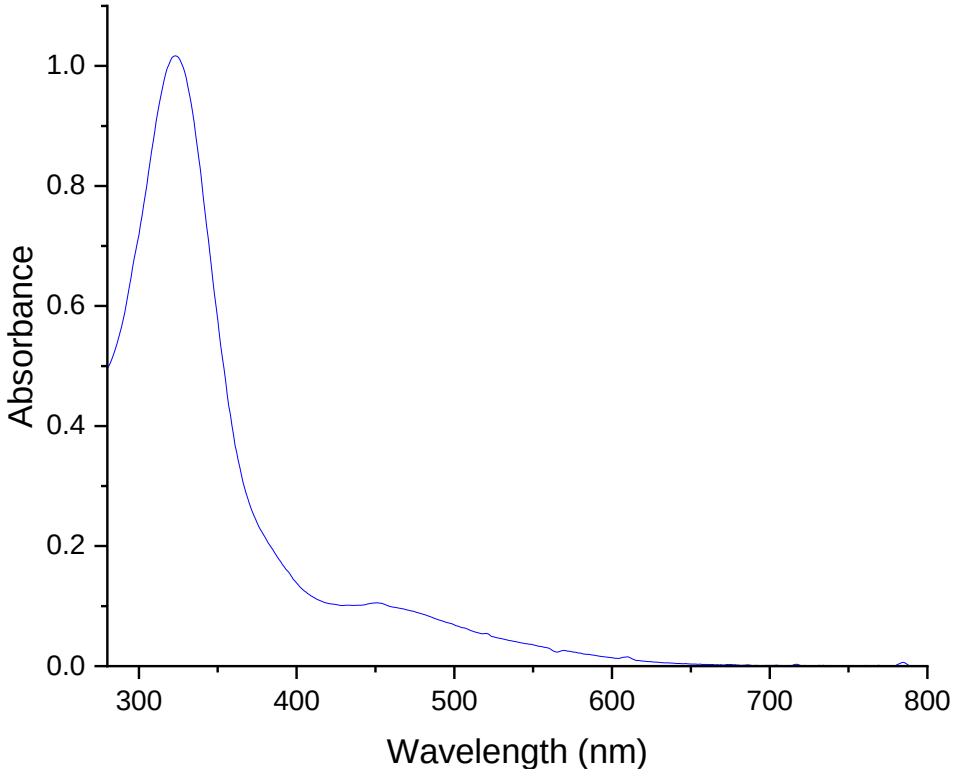

Figure A161. UV/Vis spectrum of **23** (5 x 10^{-5} M in DCM)

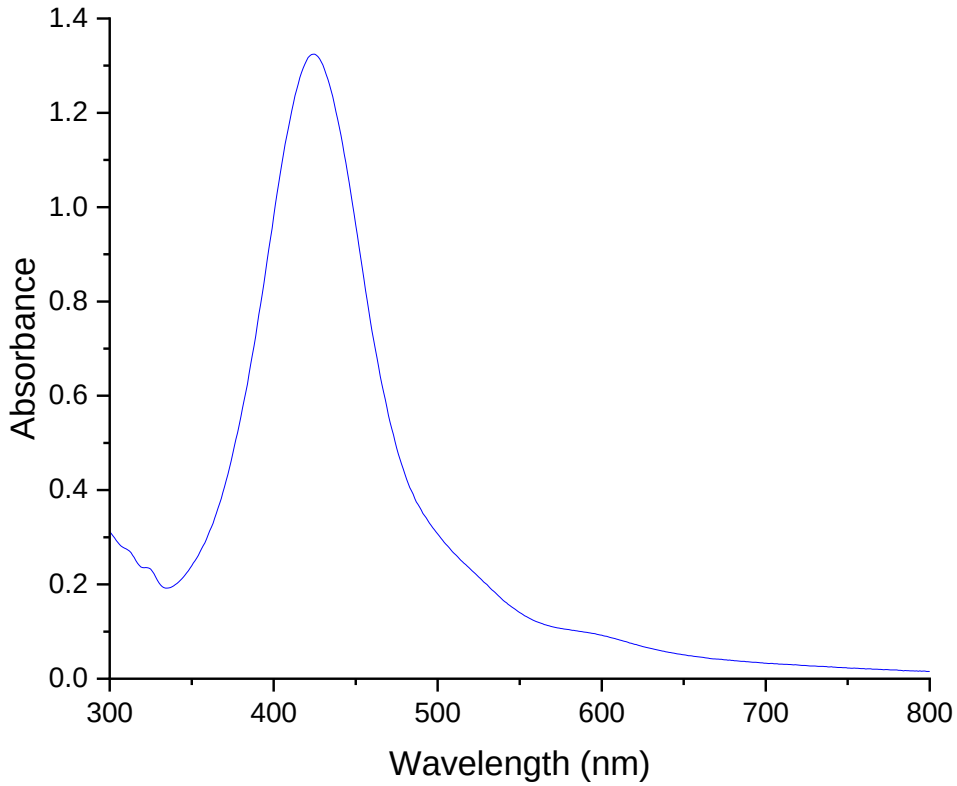

Figure A162. UV/Vis spectrum of **24** (5 x 10^{-5} M in DCM)

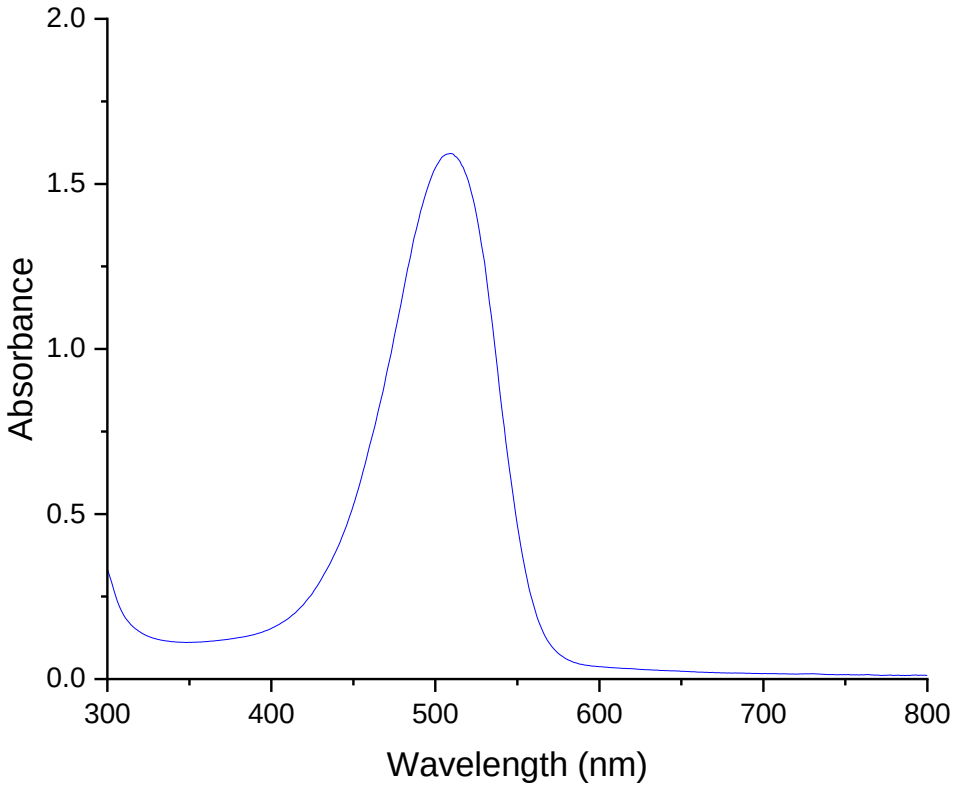

Figure A163. UV/Vis spectrum of **25** (5 x 10^{-5} M in DCM)

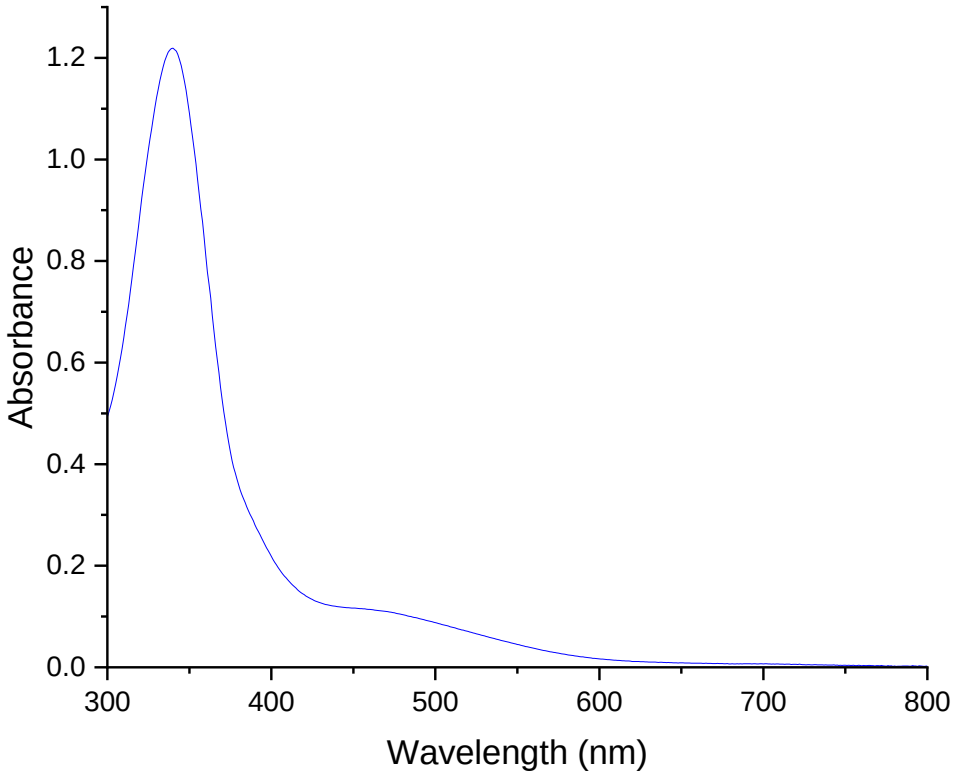

Figure A164. UV/Vis spectrum of **26** (5 x 10^{-5} M in DCM)

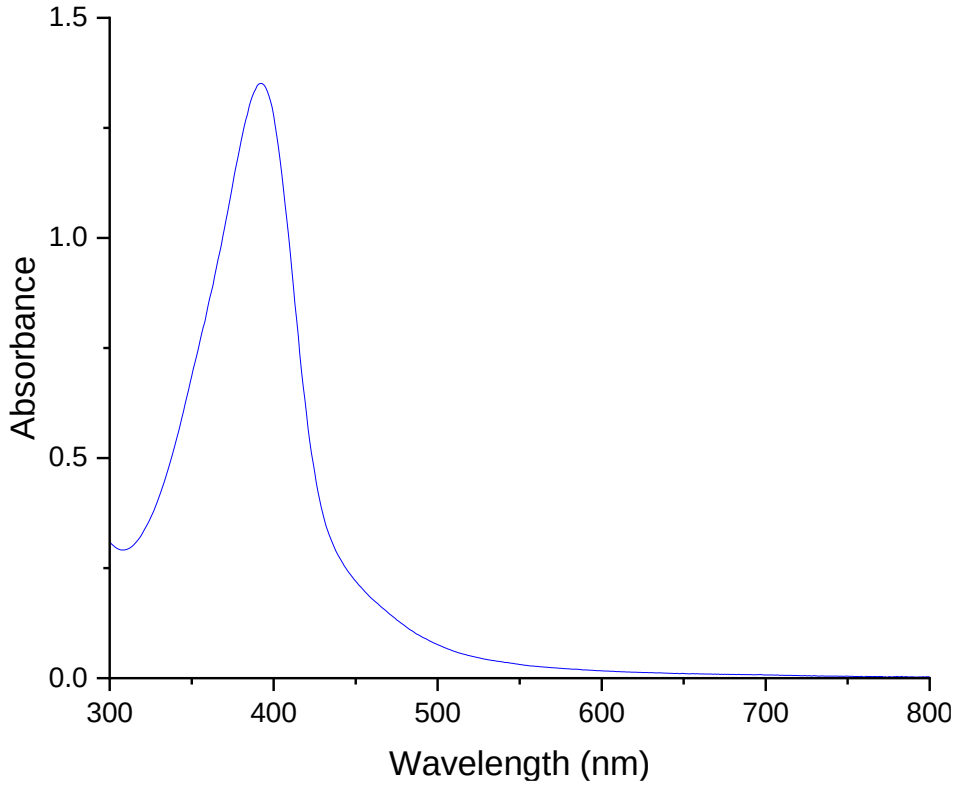

Figure A165. UV/Vis spectrum of **27** (5 x 10^{-5} M in DCM)

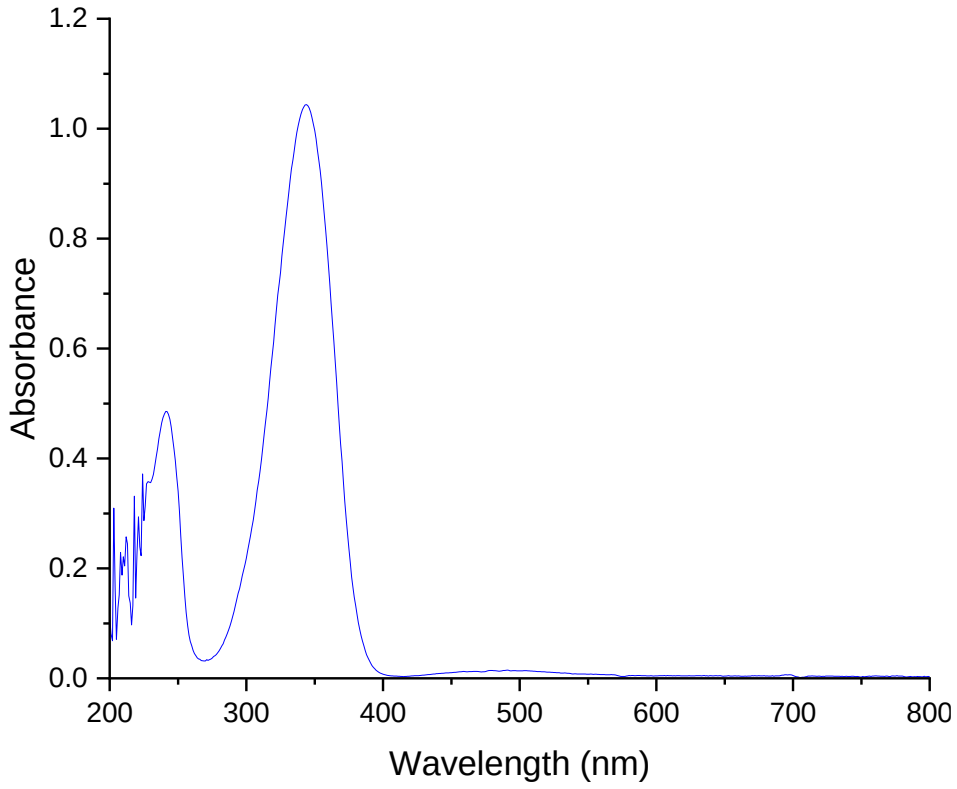

Figure A166. UV/Vis spectrum of **29** in DCM (5 x 10^{-5} M)

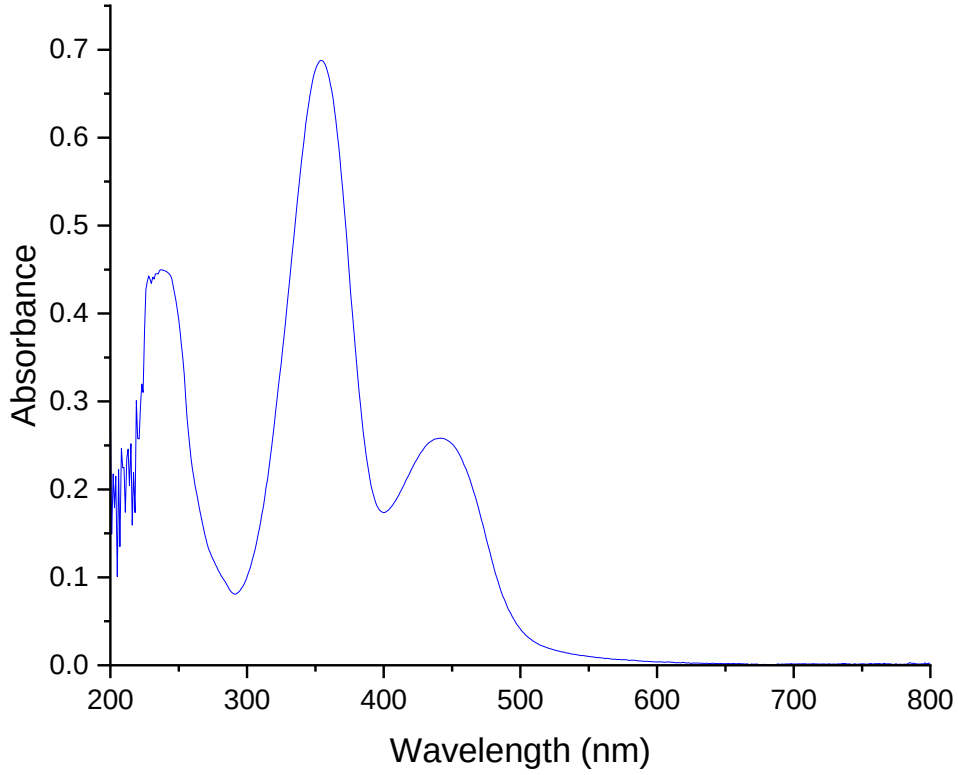

Figure A167. UV/Vis spectrum of **30** in CH_2Cl_2. (5 x 10^{-5} M)

1.3.3 High Resolution Mass Spectra

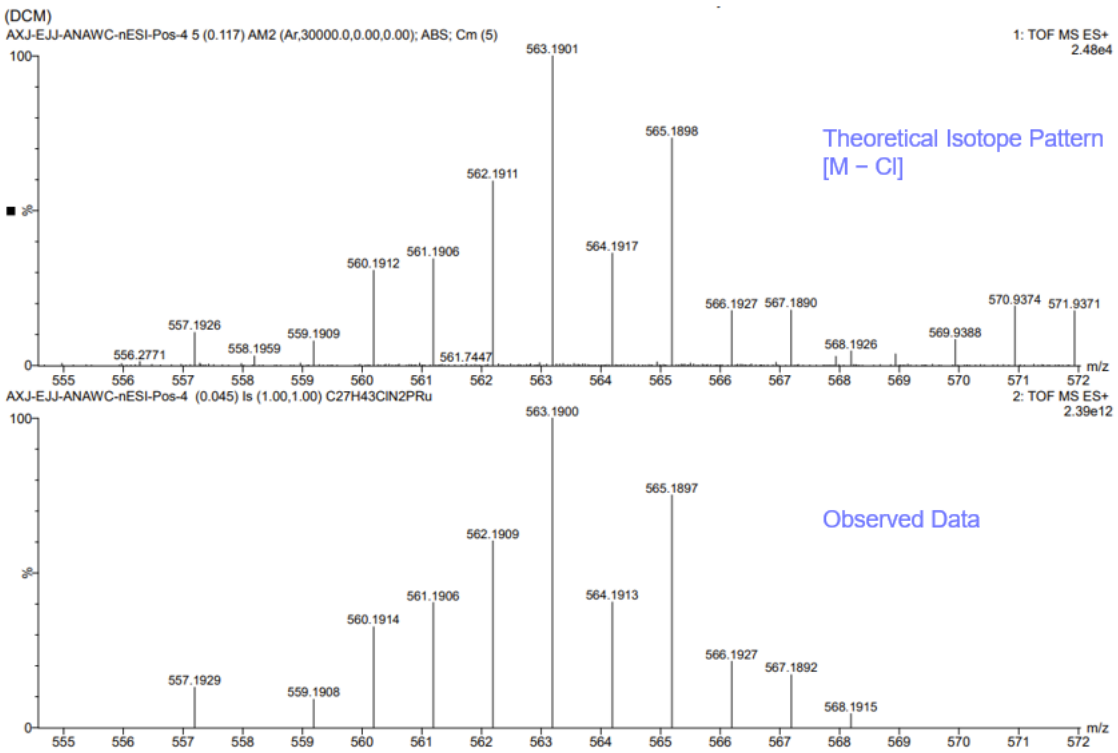

Figure A168. High Resolution Mass Spectrum of **23**

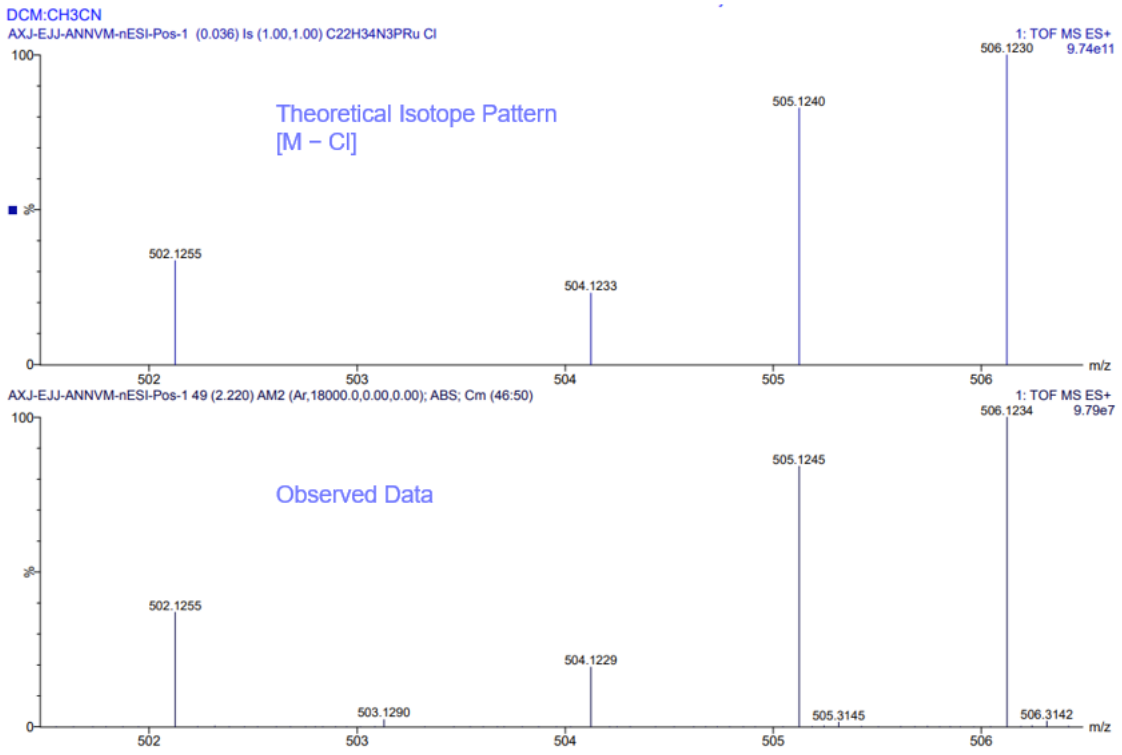

Figure A169. High Resolution Mass Spectrum of **24**

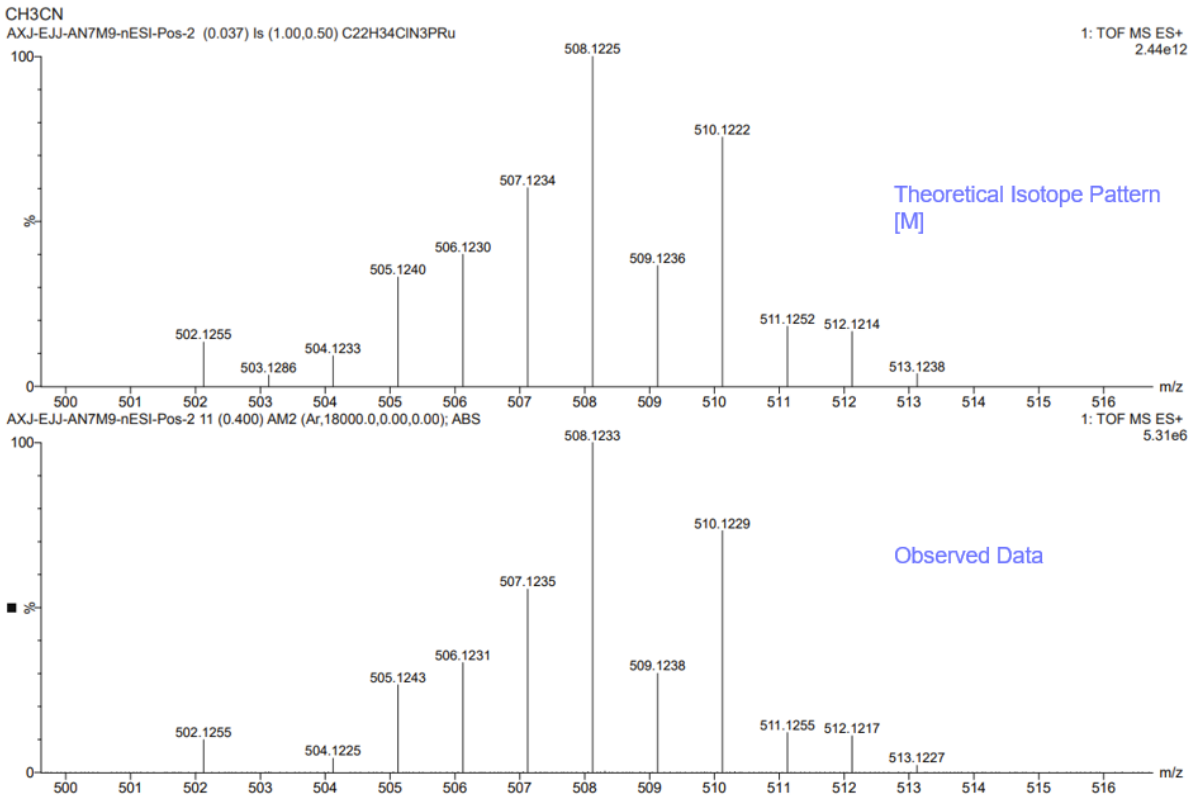

Figure A170. High Resolution Mass Spectrum of **25** (positive mode)

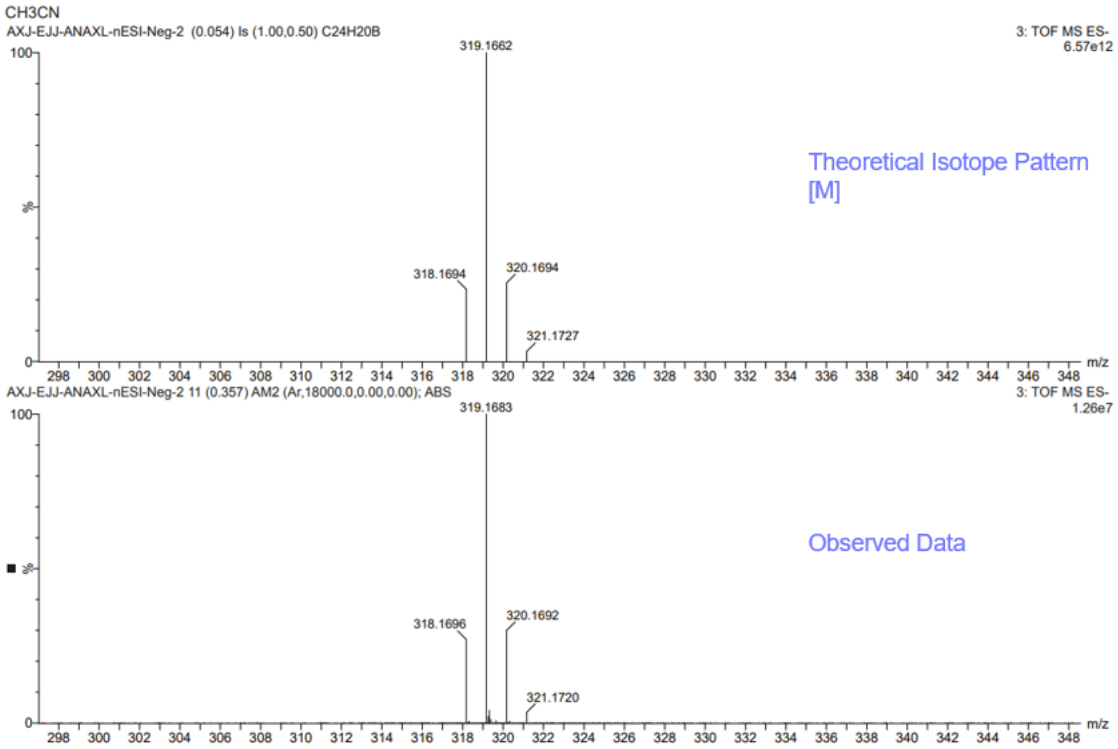

Figure A171. High Resolution Mass Spectrum of **25** (negative mode to observe $^{-}BPh_4$)

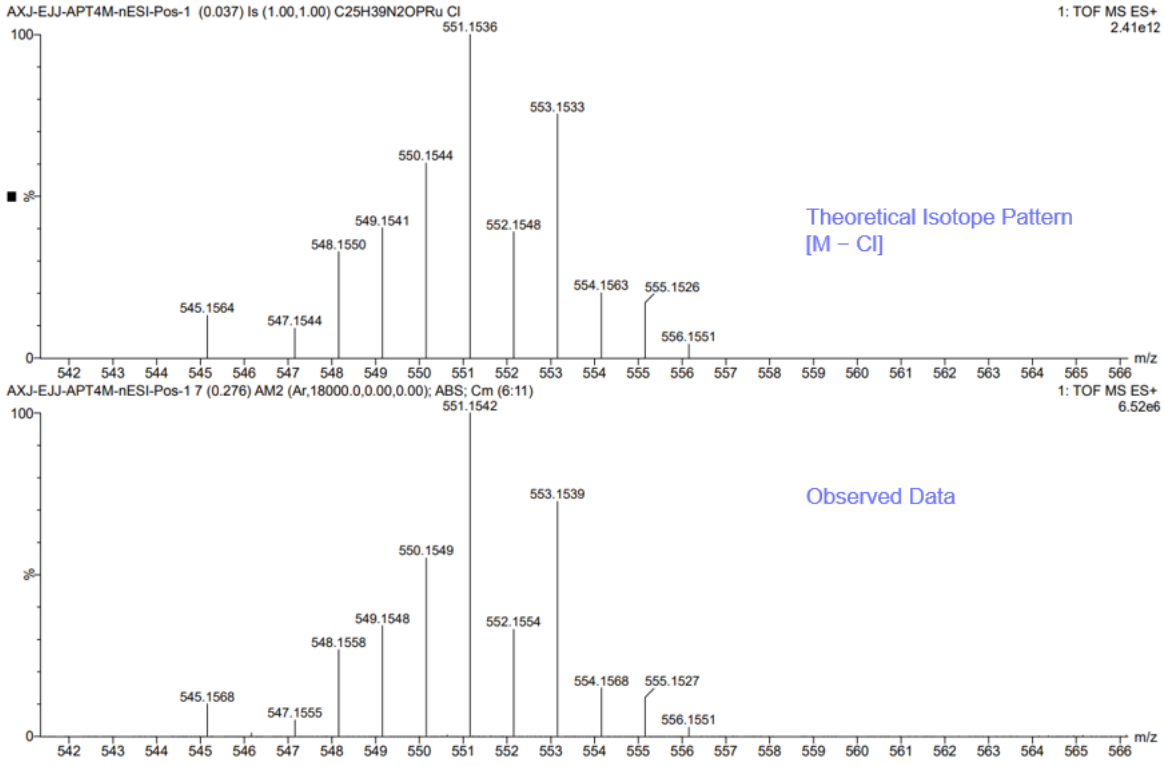

Figure A172. High-resolution Mass Spectrum of **26**

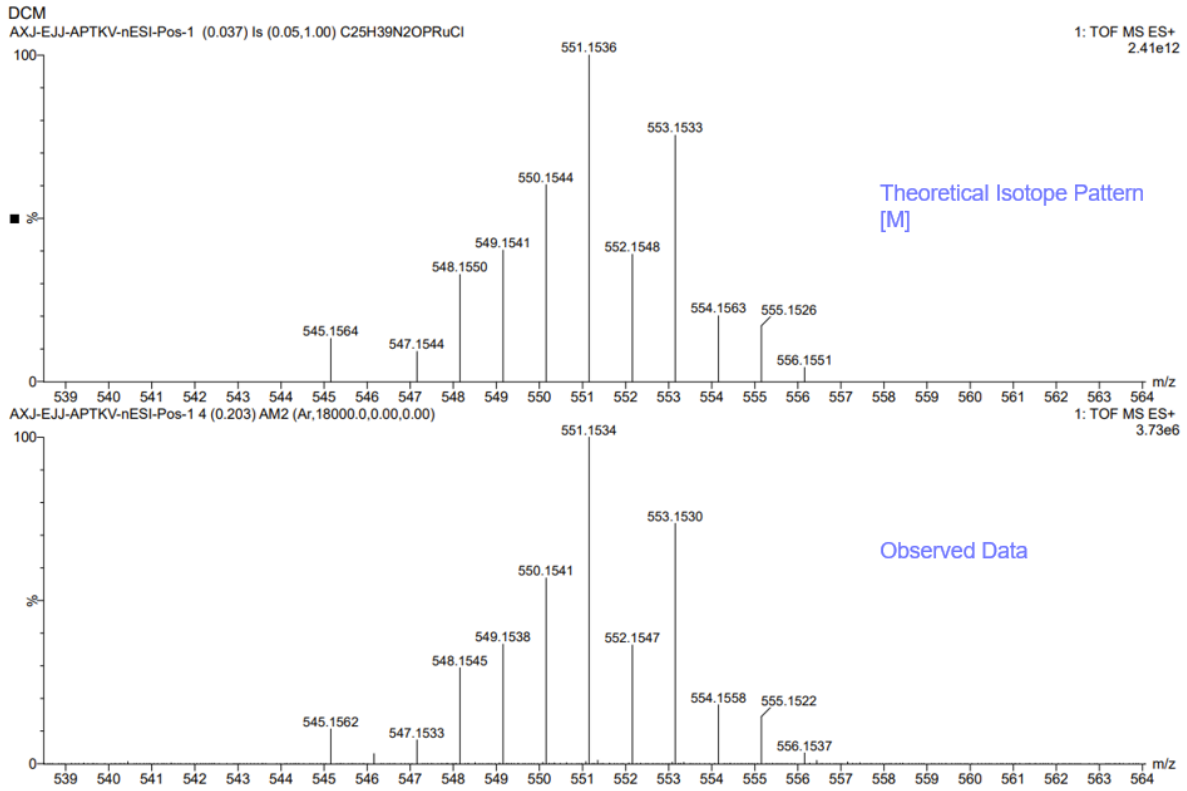

Figure A173. High-resolution Mass Spectrum of **27** (positive mode)

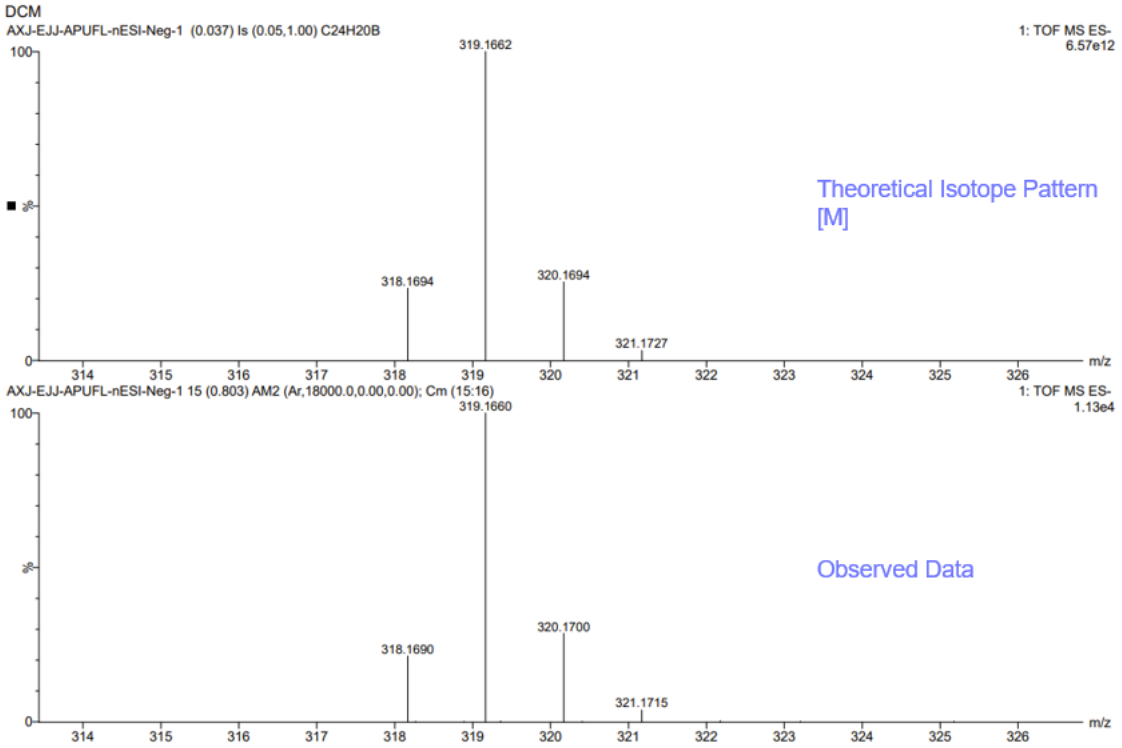

Figure A174. High-resolution Mass Spectrum of **27** (negative mode)

1.3.4 IR Spectra

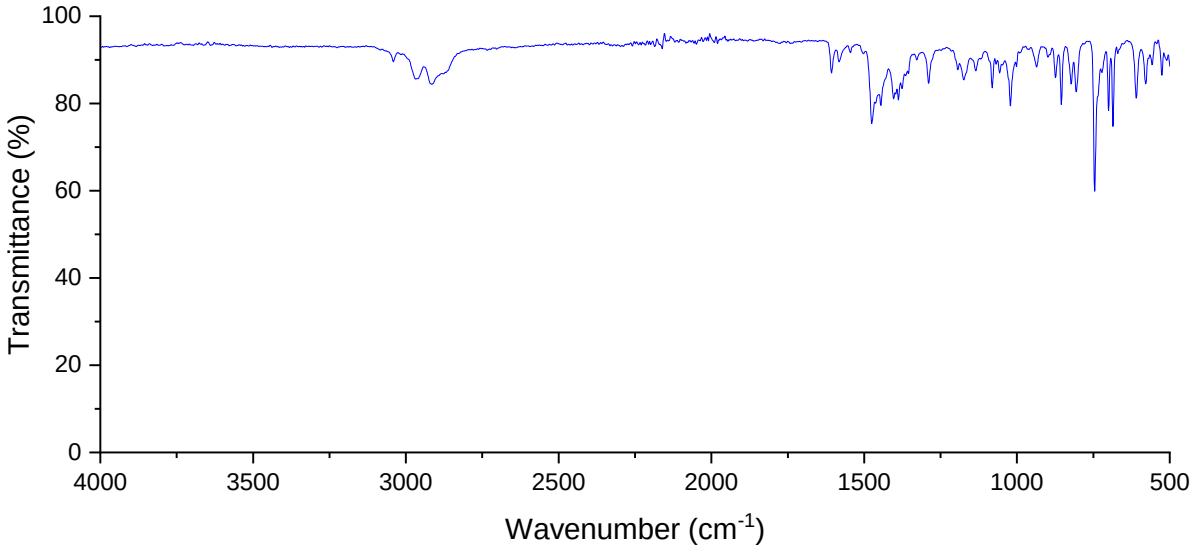

Figure A175. IR spectrum of **23**

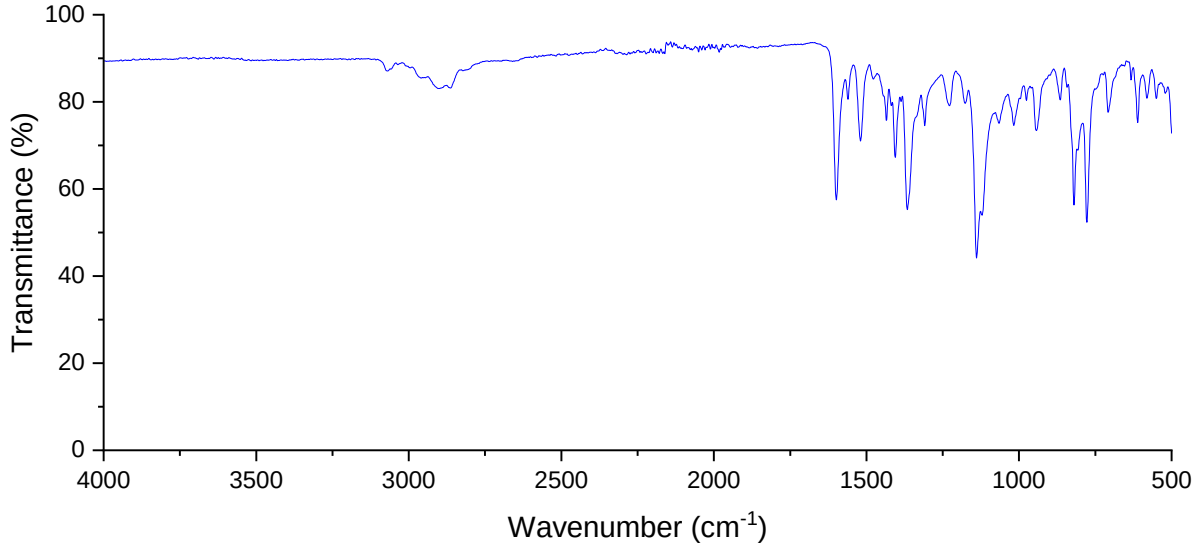

Figure A176. IR spectrum of **24**

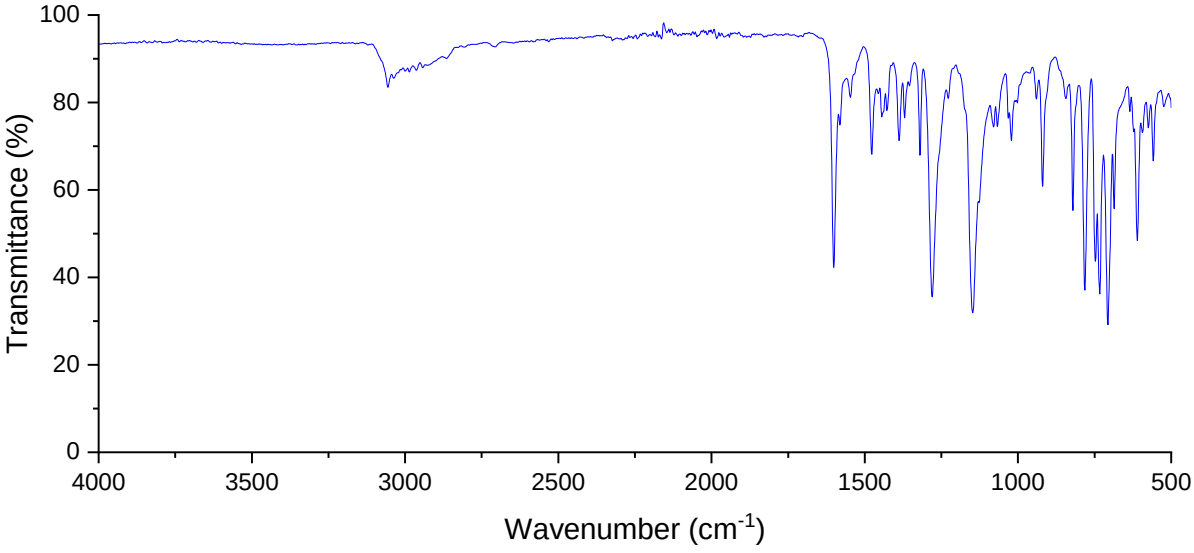

Figure A177. IR spectrum of **25**

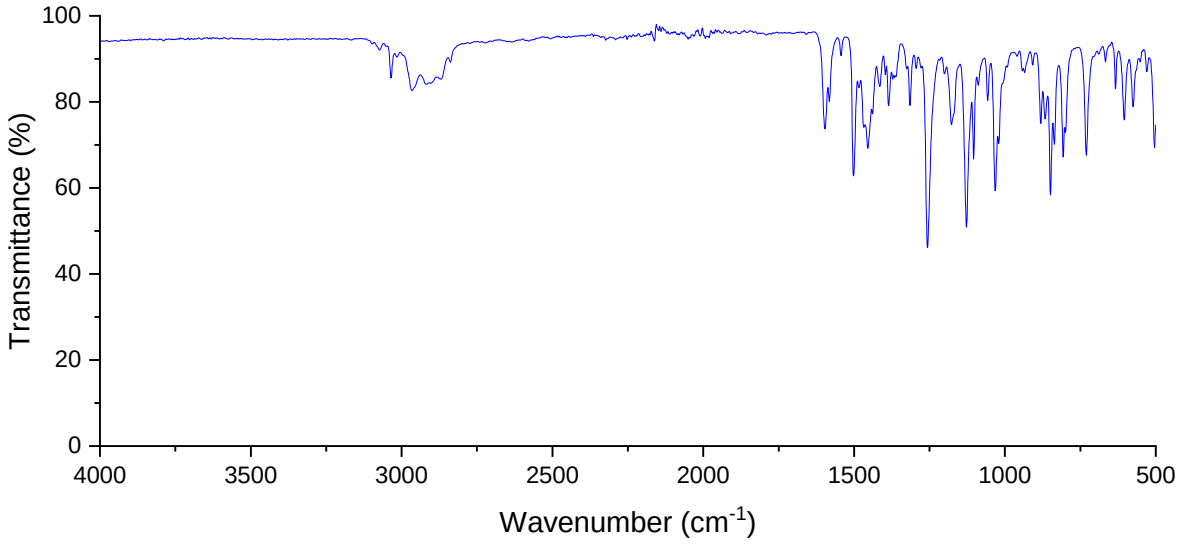

Figure A178. IR Spectrum of **26**

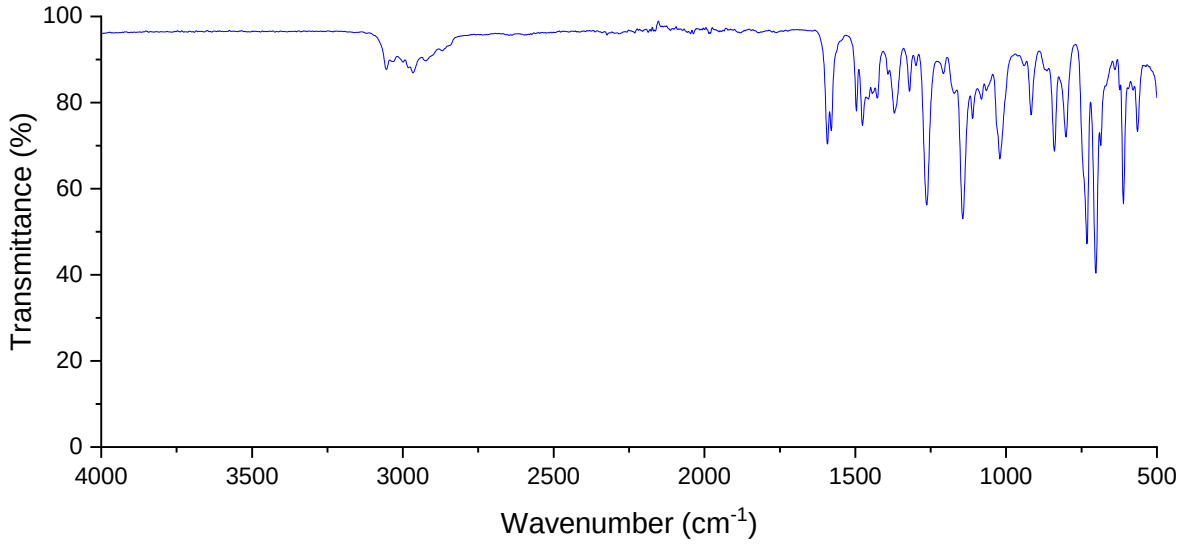

Figure A179. IR Spectrum of **27**

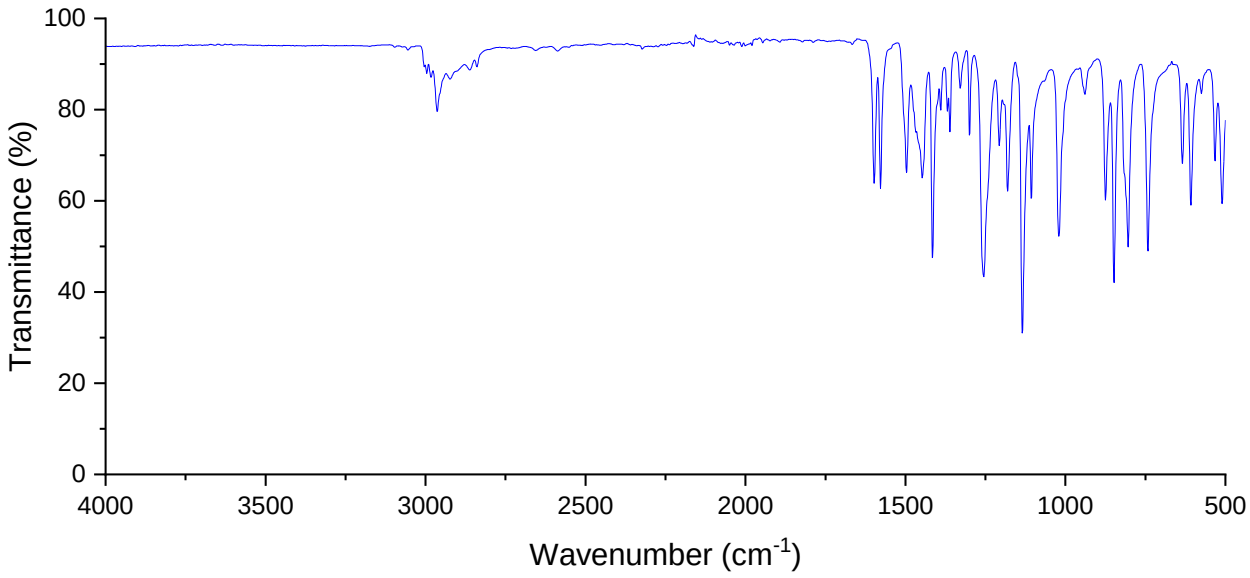

Figure A180. IR spectrum of **29**

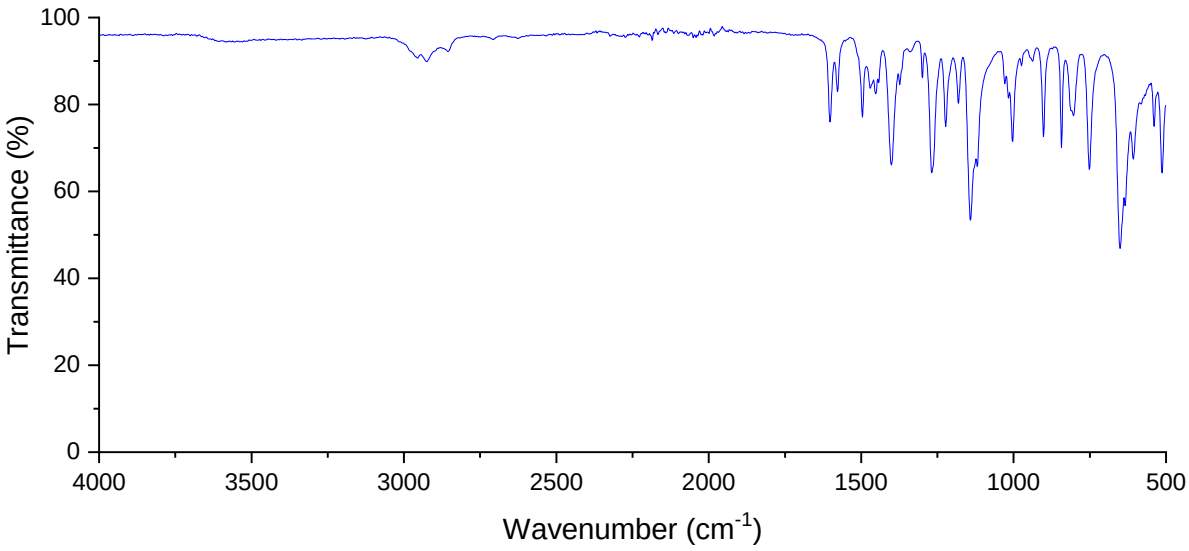

Figure A181. IR spectrum of **30**

2.0 Single-Crystal X-Ray Diffraction Data

2.1 Tables of Crystallographic Data and Structure Refinement

Table A1. Crystallographic data and structure refinement for **1**, **2**, **5** and **6**.

Compound	1	2	5	6
Crystallographic Parameter				
Identification code	CCDC2334072	CCDC2190921	CCDC2334075	CCDC2358660
Empirical formula	$C_{17}H_{32}BN_2P$	$C_{21}H_{24}BN_2P$	$C_{16}H_{31}BN_3P$	$C_{15}H_{28}BN_2OP$
Formula weight	306.22	346.20	307.22	294.17
Temperature/K	100.01(10)	123(2)	100.00(10)	100.01(10)
Crystal system	Orthorhombic	Monoclinic	Monoclinic	monoclinic
Space group	P212121	P21/c	P21/c	$P2_1/n$
a/Å	19.0485(4)	11.5329(8)	11.8695(4)	10.7092(2)
b/Å	12.4823(3)	8.9214(6)	28.4830(7)	14.1255(3)
c/Å	8.00810(17)	19.2380(14)	11.0450(3)	11.1853(2)
α/°	90	90	90	90
β/°	90	98.892(2)	93.696(3)	97.554(2)
γ/°	90	90	90	90
Volume/$Å^3$	1904.08(7)	1955.6(2)	3726.32(19)	1677.35(6)
Z	4	4	8	4
$\rho_{calc}g/cm^3$	1.068	1.176	1.095	1.165
μ/mm^{-1}	1.222	1.262	1.266	1.416
F(000)	672.0	736.0	1344.0	640.0
Crystal size/mm^3	0.131 × 0.102 × 0.049	0.24 x 0.2 x 0.08	0.33 × 0.21 × 0.12	0.205 × 0.173 × 0.116
Radiation	CuKα (λ = 1.54184)	CuKα (λ = 1.54178)	Cu Kα (λ = 1.54184)	Cu Kα (λ = 1.54184)
2Θ range for data collection/°	8.47 to 145.932	9.306 to 144.618	7.464 to 146.152	10.142 to 146.104
Index ranges	-23 ≤ h ≤ 23, -15 ≤ k ≤ 15, -9 ≤ l ≤ 9	-14 ≤ h ≤ 13, -10 ≤ k ≤ 11, -23 ≤ l ≤ 23	-14 ≤ h ≤ 14, -35 ≤ k ≤ 35, -13 ≤ l ≤ 13	-11 ≤ h ≤ 13, -17 ≤ k ≤ 17, -13 ≤ l ≤ 13
Reflections collected	18092	18539	35532	31186
Independent reflections	3749 [Rint = 0.0329, Rsigma = 0.0230]	3815 [Rint = 0.0240, Rsigma = 0.0200]	7355 [Rint = 0.0397, Rsigma = 0.0269]	3331 [R_{int} = 0.0392, R_{sigma} = 0.0160]
Data/restraints/parameters	3749/3/212	3815/3/238	7355/2/419	3331/0/200
Goodness-of-fit on F^2	1.274	1.054	1.039	1.058
Final R indexes [I>=2σ (I)]	R1 = 0.0692, wR2 = 0.1681	R1 = 0.0305, wR2 = 0.0768	R1 = 0.0375, wR2 = 0.0904	R_1 = 0.0310, wR_2 = 0.0805
Final R indexes [all data]	R1 = 0.0698, wR2 = 0.1684	R1 = 0.0308, wR2 = 0.0771	R1 = 0.0481, wR2 = 0.0977	R_1 = 0.0332, wR_2 = 0.0827
Largest diff peak/hole / e $Å^{-3}$	0.33/-0.32	0.34/-0.27	0.39/-0.27	0.30/-0.29
Flack parameter	0.12(7)	-	-	-

Table A2. Crystallographic data and structure refinement for **7** – **10**.

Compound	7	8	9	10
Crystallographic Parameter				
Identification code	CCDC2358661	CCDC2358659	CCDC2358663	CCDC2358666
Empirical formula	C15H28BN2P	$C_{14}H_{26}BN_2P$	$C_{14}H_{25}BFN_2P$	$C_{15}H_{25}BF_3N_2P$
Formula weight	278.17	264.15	282.14	332.15
Temperature/K	99.94(18)	100.01(10)	100.01(10)	120.03(10)
Crystal system	monoclinic	monoclinic	Monoclinic	monoclinic
Space group	P21/n	$P2_1/n$	Ia	$P2_1/c$
a/Å	12.5144(6)	8.0589(4)	14.3543(3)	14.5020(4)
b/Å	10.7260(3)	24.6162(13)	20.1151(3)	16.3948(6)
c/Å	13.6865(6)	8.0997(5)	22.8612(3)	15.3881(5)
α/°	90	90	90	90
β/°	112.488(5)	95.435(5)	91.138(2)	93.858(3)
γ/°	90	90	90	90
Volume/$Å^3$	1697.43(13)	1599.59(15)	6599.60(19)	3650.3(2)
Z	4	4	16	8
$\rho_{calc}g/cm^3$	1.089	1.097	1.136	1.209
μ/mm^{-1}	1.328	1.386	1.464	1.562
F(000)	608.0	576.0	2432.0	1408.0
Crystal size/mm^3	0.2 × 0.16 × 0.1	0.228 × 0.128 × 0.077	0.314 × 0.166 × 0.069	0.245 × 0.151 × 0.086
Radiation	Cu Kα (λ = 1.54184)	Cu Kα (λ = 1.54184)	Cu Kα (λ = 1.54184)	Cu Kα (λ = 1.54184)
2Θ range for data collection/°	8.152 to 146.252	7.182 to 146.294	7.568 to 146.03	7.89 to 145.212
Index ranges	-15 ≤ h ≤ 15, -8 ≤ k ≤ 13, -16 ≤ l ≤ 16	-9 ≤ h ≤ 9, -30 ≤ k ≤ 22, -8 ≤ l ≤ 9	-14 ≤ h ≤ 17, -24 ≤ k ≤ 24, -28 ≤ l ≤ 28	-13 ≤ h ≤ 17, -20 ≤ k ≤ 19, -17 ≤ l ≤ 19
Reflections collected	9714	6582	38387	18188
Independent reflections	3327 [Rint = 0.0339, Rsigma = 0.0336]	3105 [R_{int} = 0.0185, R_{sigma} = 0.0226]	11296 [R_{int} = 0.0280, R_{sigma} = 0.0238]	7072 [R_{int} = 0.0379, R_{sigma} = 0.0474]
Data/restraints/parameters	3327/1/191	3105/0/181	11296/11/758	7072/4/433
Goodness-of-fit on F^2	1.021	1.054	1.023	1.015
Final R indexes [I>=2σ (I)]	R1 = 0.0354, wR2 = 0.0833	R_1 = 0.0299, wR_2 = 0.0758	R_1 = 0.0380, wR_2 = 0.1029	R_1 = 0.0426, wR_2 = 0.1011
Final R indexes [all data]	R1 = 0.0439, wR2 = 0.0887	R_1 = 0.0329, wR_2 = 0.0782	R_1 = 0.0397, wR_2 = 0.1049	R_1 = 0.0631, wR_2 = 0.1148
Largest diff peak/hole / e $Å^{-3}$	0.24/-0.31	0.30/-0.25	0.35/-0.24	0.54/-0.24
Flack parameter	-	-	0.448(19)	-

Table A3. Crystallographic data and structure refinement for **11** – **24**.

Compound	11	12	23	24
Crystallographic Parameter				
Identification code	CCDC2334076	CCDC2358664	CCDC2334073	CCDC2334074
Empirical formula	C16H28N3P	$C_{15}H_{25}N_2OP$	C30H45.5Cl2.5N2PRu	$C_{24}H_{38}Cl_6N_3PRu$
Formula weight	293.38	280.34	654.85	713.31
Temperature/K	99.97(10)	120.00(10)	100.01(12)	99.95(16)
Crystal system	Triclinic	triclinic	Triclinic	Triclinic
Space group	P-1	P-1	P-1	P-1
a/Å	5.9546(2)	6.3217(3)	9.01910(10)	11.4458(6)
b/Å	16.3492(7)	7.0360(3)	10.5425(2)	11.5645(6)
c/Å	18.7418(9)	19.1910(6)	17.8214(3)	12.7410(6)
α/°	105.450(4)	98.292(3)	101.167(2)	64.707(5)
β/°	96.456(3)	95.150(3)	94.9460(10)	87.314(4)
γ/°	90.354(3)	102.444(3)	110.645(2)	83.841(4)
Volume/Å^3	1746.24(13)	818.36(6)	1533.50(5)	1515.99(14)
Z	4	2	2	2
ρ_{calc}g/cm^3	1.116	1.138	1.418	1.563
μ/mm^{-1}	1.341	1.441	6.789	9.699
F(000)	640.0	304.0	682.0	728.0
Crystal size/mm^3	0.412 × 0.095 × 0.043	0.273 × 0.124 × 0.025	0.093 × 0.078 × 0.014	0.232 × 0.178 × 0.095
Radiation	Cu Kα (λ = 1.54184)	Cu Kα (λ = 1.54184)	Cu Kα (λ = 1.54184)	Cu Kα (λ = 1.54184)
2Θ range for data collection/°	8.408 to 145.644	9.388 to 154.532	9.234 to 144.124	7.674 to 145.492
Index ranges	-5 ≤ h ≤ 7, -20 ≤ k ≤ 20, -22 ≤ l ≤ 23	-7 ≤ h ≤ 7, -8 ≤ k ≤ 8, -24 ≤ l ≤ 24	-10 ≤ h ≤ 11, -13 ≤ k ≤ 12, -18 ≤ l ≤ 21	-14 ≤ h ≤ 13, -14 ≤ k ≤ 14, -14 ≤ l ≤ 15
Reflections collected	18829	26935	22862	14075
Independent reflections	6829 [Rint = 0.0601, Rsigma = 0.0564]	3399 [R_{int} = 0.0582, R_{sigma} = 0.0318]	5886 [Rint = 0.0414, Rsigma = 0.0369]	5884 [R_{int} = 0.0386, R_{sigma} = 0.0427]
Data/restraints/parameters	6829/0/377	3399/0/179	5886/15/373	5884/0/324
Goodness-of-fit on F^2	1.024	1.047	1.091	1.037
Final R indexes [I>=2σ (I)]	R1 = 0.0520, wR2 = 0.1347	R_1 = 0.0379, wR_2 = 0.0949	R1 = 0.0304, wR2 = 0.0778	R_1 = 0.0357, wR_2 = 0.0838
Final R indexes [all data]	R1 = 0.0686, wR2 = 0.1499	R_1 = 0.0465, wR_2 = 0.1000	R1 = 0.0339, wR2 = 0.0793	R_1 = 0.0461, wR_2 = 0.0911
Largest diff peak/hole / e Å^{-3}	0.52/-0.40	0.40/-0.25	0.65/-0.80	1.12/-1.07
Flack parameter	-	-	-	-

Table A4. Crystallographic data and structure refinement for **25** – **28**.

Compound	25	26	27	28
Crystallographic Parameter				
Identification code	CCDC2334077	CCDC2358665	CCDC2358662	EJJ191
Empirical formula	$C_{52}H_{59}BCl_2N_3PRu$	$C_{25}H_{39}Cl_2N_2OPRu$	$C_{49}H_{59}BN_2OPClRu$	$C_{49}H_{59}BN_2PClRu$
Formula weight	939.77	586.52	870.28	854.28
Temperature/K	100.00(10)	99.95(15)	100.00(10)	120.00(10)
Crystal system	Monoclinic	triclinic	monoclinic	Monoclinic
Space group	$P2_1/c$	P-1	$P2_1/c$	$P2_1/c$
a/Å	18.0759(4)	9.2219(3)	16.53190(10)	10.9270(4)
b/Å	9.7552(2)	9.3766(4)	11.70170(10)	22.7541(6)
c/Å	26.0543(6)	16.9666(7)	23.41560(10)	18.2528(5)
α/°	90	102.406(3)	90	90
β/°	90.537(2)	97.481(3)	109.3460(10)	106.935(3)
γ/°	90	108.658(4)	90	90
Volume/$Å^3$	4594.06(17)	1325.80(10)	4274.01(5)	4341.5(2)
Z	4	2	4	4
$\rho_{calc}g/cm^3$	1.359	1.469	1.352	1.307
μ/mm^{-1}	4.452	7.359	4.189	4.096
F(000)	1960.0	608.0	1824.0	1792.0
Crystal size/mm^3	0.152 × 0.078 × 0.022	0.3 × 0.048 × 0.033	0.148 × 0.097 × 0.025	0.139 × 0.069 × 0.055
Radiation	Cu Kα (λ = 1.54184)	Cu Kα (λ = 1.54184)	Cu Kα (λ = 1.54184)	Cu Kα (λ = 1.54184)
2Θ range for data collection/°	8.33 to 145.416	10.302 to 136.498	5.666 to 157.958	7.77 to 140.148
Index ranges	-21 ≤ h ≤ 22, -11 ≤ k ≤ 12, -32 ≤ l ≤ 28	-11 ≤ h ≤ 11, -9 ≤ k ≤ 11, -20 ≤ l ≤ 20	-20 ≤ h ≤ 21, -14 ≤ k ≤ 14, -27 ≤ l ≤ 29	-12 ≤ h ≤ 13, -27 ≤ k ≤ 27, -22 ≤ l ≤ 19
Reflections collected	30660	14013	108193	23537
Independent reflections	8956 [R_{int} = 0.0415, R_{sigma} = 0.0387]	4830 [R_{int} = 0.0602, R_{sigma} = 0.0580]	8805 [R_{int} = 0.0424, R_{sigma} = 0.0181]	7958 [R_{int} = 0.0400, R_{sigma} = 0.0451]
Data/restraints/parameters	8956/273/675	4830/0/299	8805/0/515	7958/0/506
Goodness-of-fit on F^2	1.052	1.063	1.085	1.048
Final R indexes [I>=2σ (I)]	R_1 = 0.0337, wR_2 = 0.0734	R_1 = 0.0515, wR_2 = 0.1268	R_1 = 0.0265, wR_2 = 0.0679	R_1 = 0.0356, wR_2 = 0.0797
Final R indexes [all data]	R_1 = 0.0449, wR_2 = 0.0734	R_1 = 0.0633, wR_2 = 0.1349	R_1 = 0.0287, wR_2 = 0.0692	R_1 = 0.0487, wR_2 = 0.0876
Largest diff peak/hole / e $Å^{-3}$	0.49/-0.47	2.51/-1.46	0.42/-0.63	0.55/-0.74
Flack parameter	-	-	-	-

Table A5. Crystallographic data and structure refinement for **29** – **32**.

Compound	29	30	31	32
Crystallographic Parameter				
Identification code	ET16	Et_Ag_C	MGB002	EJJ135
Empirical formula	$C_{15}H_{25}AuClN_2OP$	$C_{30}H_{50}Au_2F_{12}N_4O_2P_2Sb_2$	$C_{38}H_{58}N_4O_4P_2W$	$C_{32}H_{56}Cl_2N_6P_2Pd$
Formula weight	512.76	1426.11	880.67	764.06
Temperature/K	99.95(15)	99.97(12)	100.00(10)	100.00(10)
Crystal system	Monoclinic	Monoclinic	Triclinic	Triclinic
Space group	$P2_1/c$	$P2_1/c$	P-1	P-1
a/Å	12.2138(3)	12.4548(6)	12.1907(3)	8.9556(6)
b/Å	11.6076(3)	12.6126(5)	17.3422(2)	9.1518(7)
c/Å	14.2495(4)	14.7731(6)	21.2969(3)	11.7895(8)
α/°	90	90	105.2710(10)	100.818(6)
β/°	114.331(3)	112.161(5)	97.648(2)	94.711(5)
γ/°	90	90	110.510(2)	97.988(6)
Volume/Å^3	1840.76(9)	2149.23(17)	3939.56(13)	934.05(12)
Z	4	2	4	1
ρ_{calc}g/cm^3	1.850	2.204	1.485	1.358
μ/mm^{-1}	17.174	23.875	6.541	6.358
F(000)	992.0	1344.0	1800.0	400.0
Crystal size/mm^3	0.129 × 0.1 × 0.075	0.122 × 0.095 × 0.039	0.165 × 0.105 × 0.087	0.113 × 0.08 × 0.035
Radiation	Cu Kα (λ = 1.54184)	Cu Kα (λ = 1.54184)	Cu Kα (λ = 1.54184)	Cu Kα (λ = 1.54184)
2Θ range for data collection/°	7.944 to 145.508	7.664 to 146.212	5.772 to 140.142	7.682 to 145.796
Index ranges	-15 ≤ h ≤ 13, -13 ≤ k ≤ 14, -17 ≤ l ≤ 17	-14 ≤ h ≤ 15, -15 ≤ k ≤ 14, -15 ≤ l ≤ 18	-14 ≤ h ≤ 13, -21 ≤ k ≤ 21, -25 ≤ l ≤ 25	-10 ≤ h ≤ 7, -11 ≤ k ≤ 10, -14 ≤ l ≤ 14
Reflections collected	33476	12151	118228	6387
Independent reflections	3631 [R_{int} = 0.0448, R_{sigma} = 0.0208]	4194 [R_{int} = 0.0511, R_{sigma} = 0.0485]	14877 [R_{int} = 0.0406, R_{sigma} = 0.0202]	3596 [R_{int} = 0.0901, R_{sigma} = 0.1032]
Data/restraints/parameters	3631/0/197	4194/0/251	14877/0/922	3596/0/204
Goodness-of-fit on F^2	1.059	1.042	1.041	1.032
Final R indexes [I>=2σ (I)]	R_1 = 0.0227, wR_2 = 0.0519	R_1 = 0.0356, wR_2 = 0.0897	R_1 = 0.0206, wR_2 = 0.0527	R_1 = 0.0731, wR_2 = 0.1835
Final R indexes [all data]	R_1 = 0.0293, wR_2 = 0.0559	R_1 = 0.0438, wR_2 = 0.0958	R_1 = 0.0228, wR_2 = 0.0541	R_1 = 0.0993, wR_2 = 0.2046
Largest diff peak/hole / e Å^{-3}	0.86/-1.16	2.25/-1.47	0.59/-0.74	1.84/-1.56
Flack parameter	-	-	-	-

Table A6. Crystallographic data and structure refinement for **33** – **35**.

Compound	33	34	35
Crystallographic Parameter			
Identification code	EJJ135_V1	EJJ134	ET08
Empirical formula	$C_{24}H_{40}N_5PCl_2Pd$	$C_{27}H_{44}Cl_5IrN_3P$	$C_{25}H_{40}Cl_2IrN_2OP$
Formula weight	606.88	811.07	678.66
Temperature/K	100.00(10)	100.00(10)	99.99(10)
Crystal system	Monoclinic	Monoclinic	Orthorhombic
Space group	$P2_1$	$P2_1/c$	$Cmc2_1$
a/Å	12.3068(2)	16.6142(3)	13.1031(7)
b/Å	7.9523(2)	9.0294(2)	16.0077(8)
c/Å	15.1327(3)	21.6683(3)	12.7411(6)
α/°	90	90	90
β/°	108.797(2)	93.0920(10)	90
γ/°	90	90	90
Volume/$Å^3$	1402.01(5)	3245.86(10	2672.5(2)
Z	2	4	4
$\rho_{calc}g/cm^3$	1.438	1.660	1.687
μ/mm^{-1}	7.790	12.379	5.276
F(000)	628.0	1616.0	1352.0
Crystal size/mm^3	0.098 × 0.086 × 0.048	0.465 × 0.121 × 0.035	0.257 × 0.157 × 0.108
Radiation	Cu Kα (λ = 1.54184)	Cu Kα (λ = 1.54184)	Mo Kα (λ = 0.71073)
2Θ range for data collection/°	7.588 to 145.816	8.172 to 136.47	7.554 to 59.14
Index ranges	-14 ≤ h ≤ 15, -8 ≤ k ≤ 9, -18 ≤ l ≤ 18	-20 ≤ h ≤ 20, -10 ≤ k ≤ 9, -26 ≤ l ≤ 26	-17 ≤ h ≤ 17, -22 ≤ k ≤ 21, -16 ≤ l ≤ 16
Reflections collected	25808	29658	14592
Independent reflections	5298 [R_{int} = 0.0475, R_{sigma} = 0.0389]	5909 [R_{int} = 0.0567, R_{sigma} = 0.0342]	3439 [R_{int} = 0.0373, R_{sigma} = 0.0299]
Data/restraints/parameters	5298/1/315	5909/12/384	3439/83/247
Goodness-of-fit on F^2	1.072	1.023	1.089
Final R indexes [I>=2σ (I)]	R_1 = 0.0395, wR_2 = 0.0992	R_1 = 0.0361, wR_2 = 0.0927	R_1 = 0.0249, wR_2 = 0.0582
Final R indexes [all data]	R_1 = 0.0414, wR_2 = 0.1014	R_1 = 0.0427, wR_2 = 0.0988	R_1 = 0.0256, wR_2 = 0.0586
Largest diff peak/hole / e $Å^{-3}$	0.69/-1.37	1.43/-2.00	1.13/-1.21
Flack parameter	0.355(13)	-	-0.008(9)

2.2 Crystal Structure Determinations

Unless otherwise stated, all hydrogen atoms not bonded to boron were fixed as riding models and the isotropic thermal parameters (U_{iso}) were based on the U_{eq} of the parent atom.

1 A Gaussian absorption correction was applied. The structure of **1** occupies a chiral space group and has been refined as an inversion twin with the refined percentage

occupancy of the twin domains being 88(7):12(7), respectively. The hydrogen atoms bonded to B1 were located in the electron density and refined subject to bond length restraints.

2 A semi-empirical absorption correction was applied.

5 An analytical absorption correction was applied. The structure of **5** contains two crystallographically independent molecules. The hydrogen atoms bonded to B1 were located in the electron density and freely refined.

6 A Gaussian absorption correction was applied. The hydrogen atoms bonded to B(1) were located in the electron density and freely refined.

7 A Gaussian absorption correction was applied. The hydrogen atoms bonded to B(1) were located in the electron density and freely refined, one of which is subject to B–H bond length restraints.

8 A Gaussian absorption correction was applied. The hydrogen atoms bonded to B(1) were located in the electron density and freely refined.

9 A Gaussian absorption correction was applied. The structure of **9** occupies a non-centrosymmetric space group and has been refined as an inversion twin, with the refined percentage ratio of domains being 55.2(19):44.8(19). The hydrogen atoms bonded to B(1), B(101), B(201) and B(301) were located in the electron density and freely refined, some of which are subject to B–H bond length restraints. The structure of **9** contains four crystallographically independent molecules.

10 A Gaussian absorption correction was applied. The hydrogen atoms bonded to B(1) and B(101) were located in the electron density and freely refined, four of which are subject to B–H bond length restraints. The structure of **10** contains two crystallographically independent molecules.

11 A SMART Gaussian absorption correction was applied. The structure of **11** contains two crystallographically independent molecules.

12 A Gaussian absorption correction was applied.

23 A Gaussian absorption correction was applied. The structure of **23** contains a ruthenium complex and a molecule of chlorobenzene disordered over an inversion centre, at exactly 50% occupancy per position, by symmetry.

24 A Gaussian absorption correction was applied. The structure of **23** contains a ruthenium complex and two molecules of dichloromethane.

25 A Gaussian absorption correction was applied. The structure of **25** contains a ruthenium complex and a molecule of tetraphenylborate. The structure also contains a molecule of chlorobenzene, Cl21, C201-C206 / Cl2', C21'-C26' / Cl3', C31'-C36', which is disordered over three positions at a percentage occupancy ratio of 70:15:15, respectively.

26 A Gaussian absorption correction was applied.

27 A Gaussian absorption correction was applied. The structure of **27** contains a ruthenium complex and a molecule of tetraphenylborate.

28 A Gaussian absorption correction was applied. The structure of **28** contains a ruthenium complex and a molecule of tetraphenylborate.

29 A Gaussian absorption correction was applied.

30 A Gaussian absorption correction was applied.

31 A Gaussian absorption correction was applied. The structure of **31** contains three crystallographically-independent tungsten complexes with two being located on inversion centres, such that, for both of these complexes only half is crystallographicaly-unique.

Symmetry codes used to generate equivalent atoms: $1: 1-x, -y, -z. $2: 1-x, 1-y, 2-z

32 A Gaussian absorption correction was applied. The structure of **32** contains a palladium complex with an inversion centre.

33 A Gaussian absorption correction was applied. The crystal of **33** was a two-component inversion twin with the refined ratio of the enantiomeric domains being 0.645(13):0.355(13). The hydrogen atoms bonded to N4 were located in the electron density and freely refined.

34 A Gaussian absorption correction was applied. The structure of **34** contains a molecule of chloroform which is disordered over two positions.

35 A Gaussian absorption correction was applied. The structure of **35** is sitting on a mirror plane running through Ir1 and P1. The Cp* and $N_2C_6H_4OCH_3$ fragments are disordered across the mirror plane at 50% occupancy by symmetry. Symmetry codes used to generate equivalent atoms: $1: 1-x, -y, -z.

3.0 Stability Study of **3** and **4**

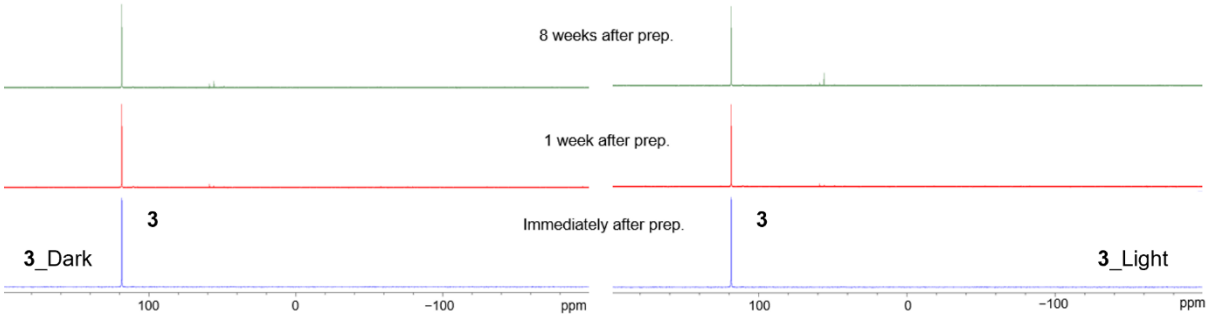

Figure A182. Stacked $^{31}P\{^{1}H\}$ NMR spectra of **3** in toluene-d_8. Stability of **3** in light/dark monitored over eight weeks.

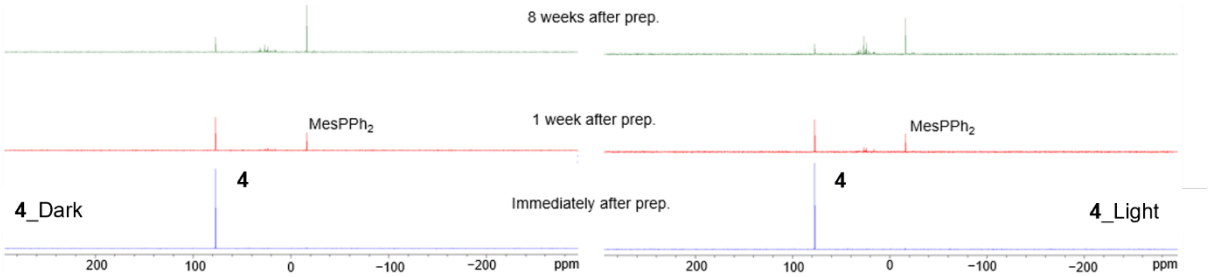

Figure A183. Stacked $^{31}P\{^{1}H\}$ NMR spectra of **4** in toluene-d_8. Stability of **4** in light/dark monitored over eight weeks.

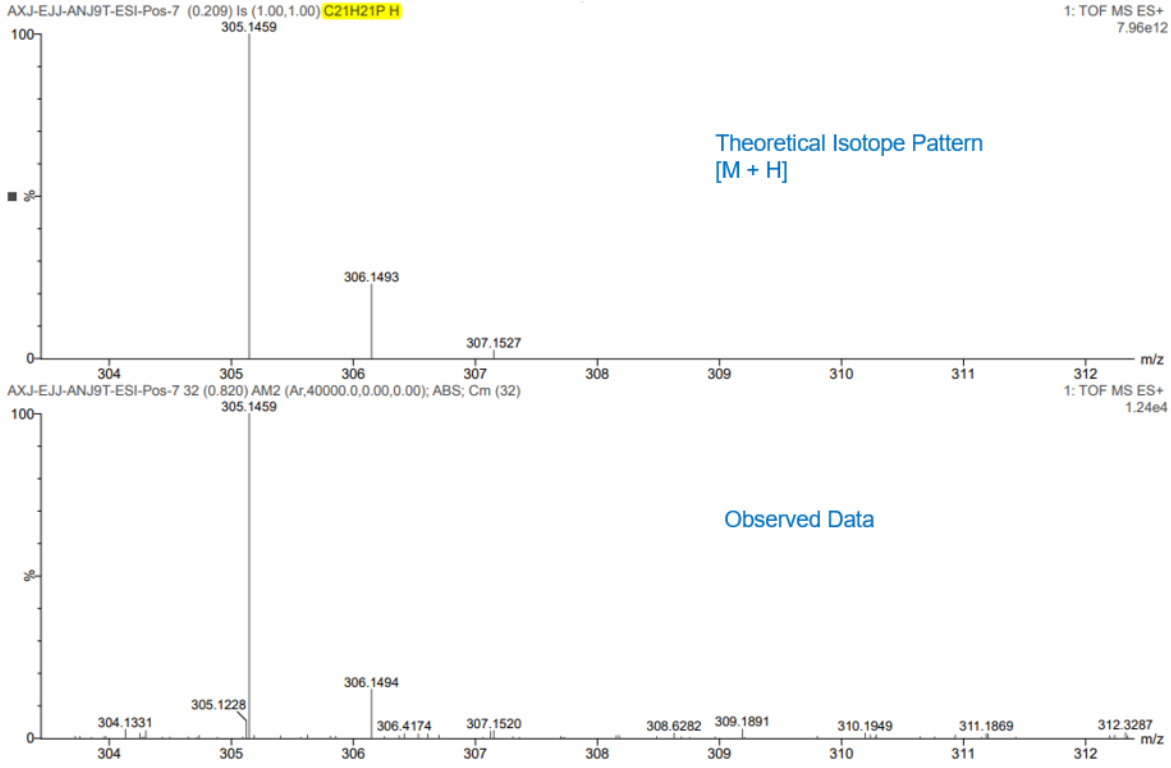

Figure A184. High Resolution Mass Spectrum of $MesPPh_2$ found in NMR sample **4**_Light.

4.0 Catalysis

4.1 Ruthenium

4.1.1 Transfer Hydrogenations

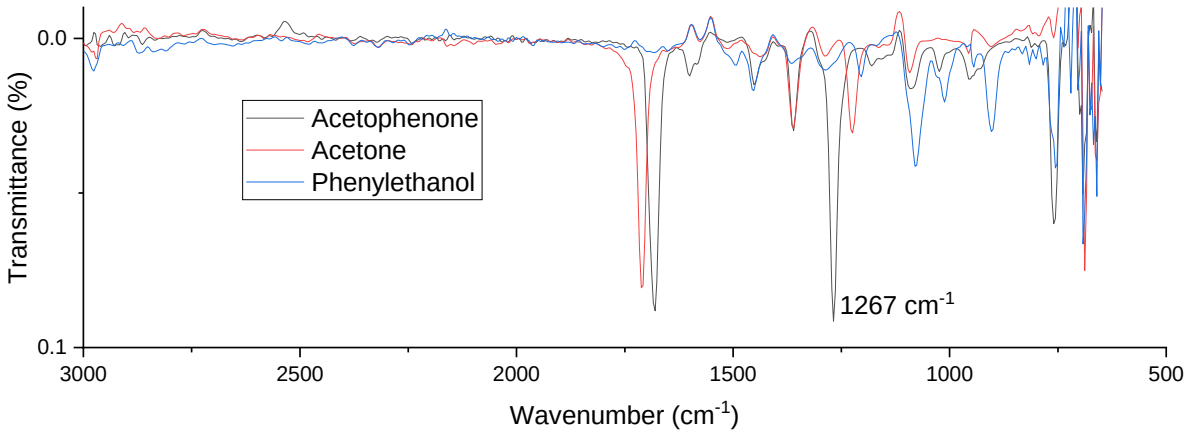

Figure A185. IR spectrum of acetophenone, acetone and 1-phenylethanol. The peak at 1267 cm^{-1} (C_{Ar}–C_{CO}–C_{Me} stretch) was tracked to measure the conversion of acetophenone with time.

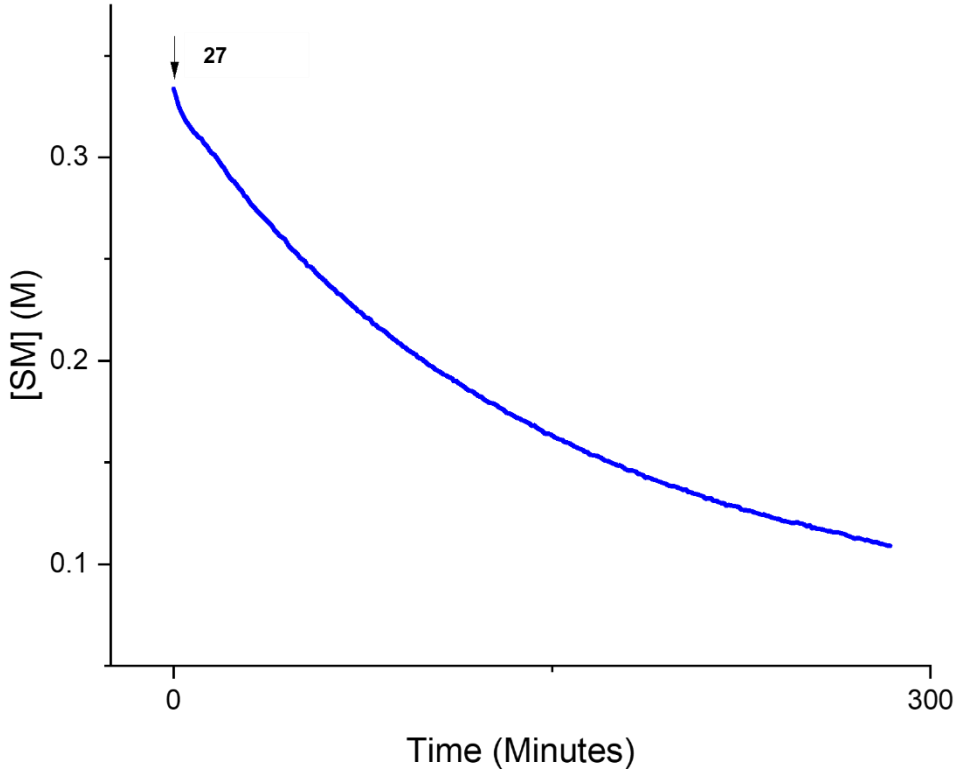

Figure A186. Conversion of acetophenone (SM) with time after addition of **27** as catalyst.

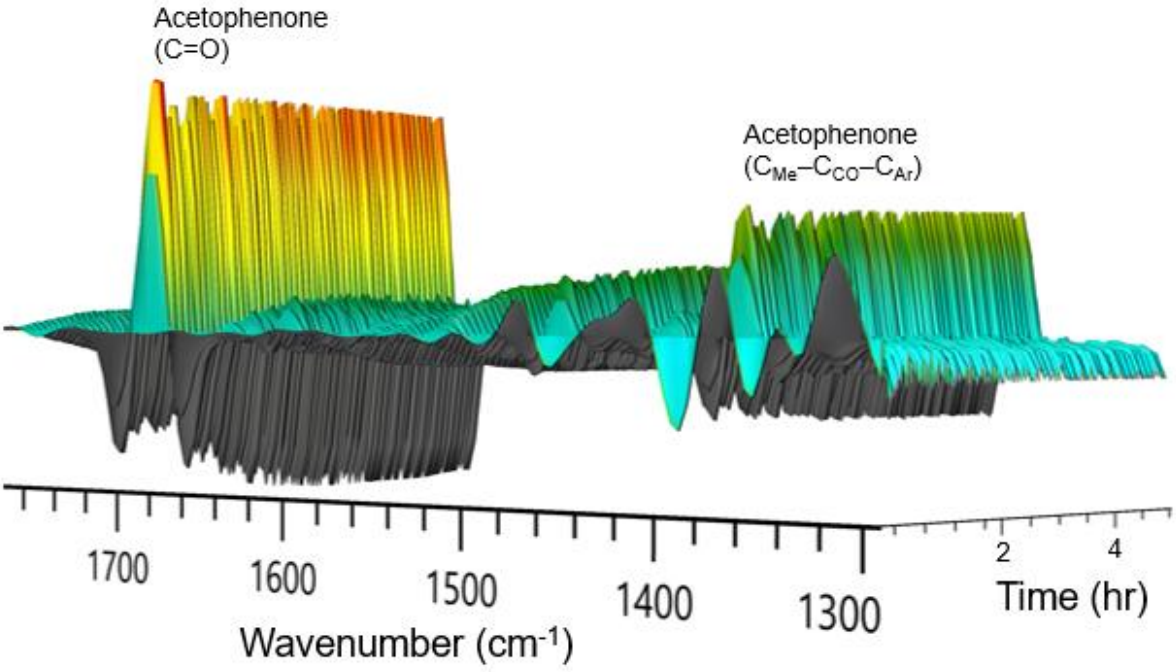

Figure A187. ReactIR surface plot of TH reaction using **26** as catalyst.

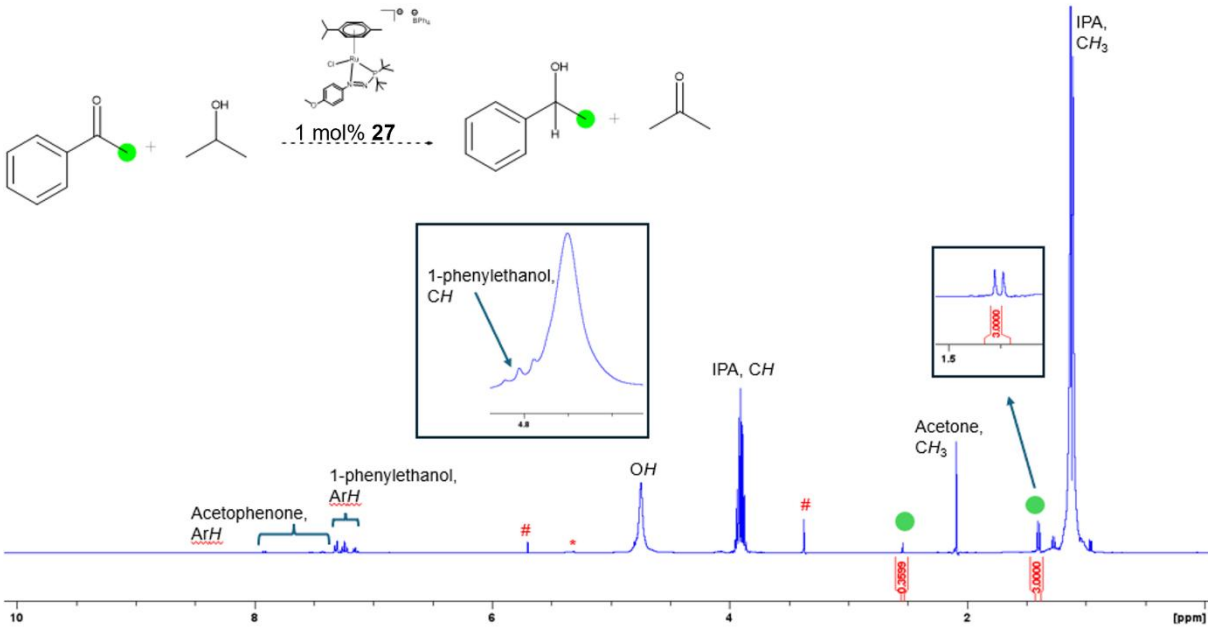

Figure A188. ^{1}H NMR spectrum of an aliquot of the TH reaction following ReactIR experiment using **27** as catalyst.

* = residual CDHCl2, # = internal standard (trimethoxybenzene in $CDCl_3$ within a sealed capillary tube).

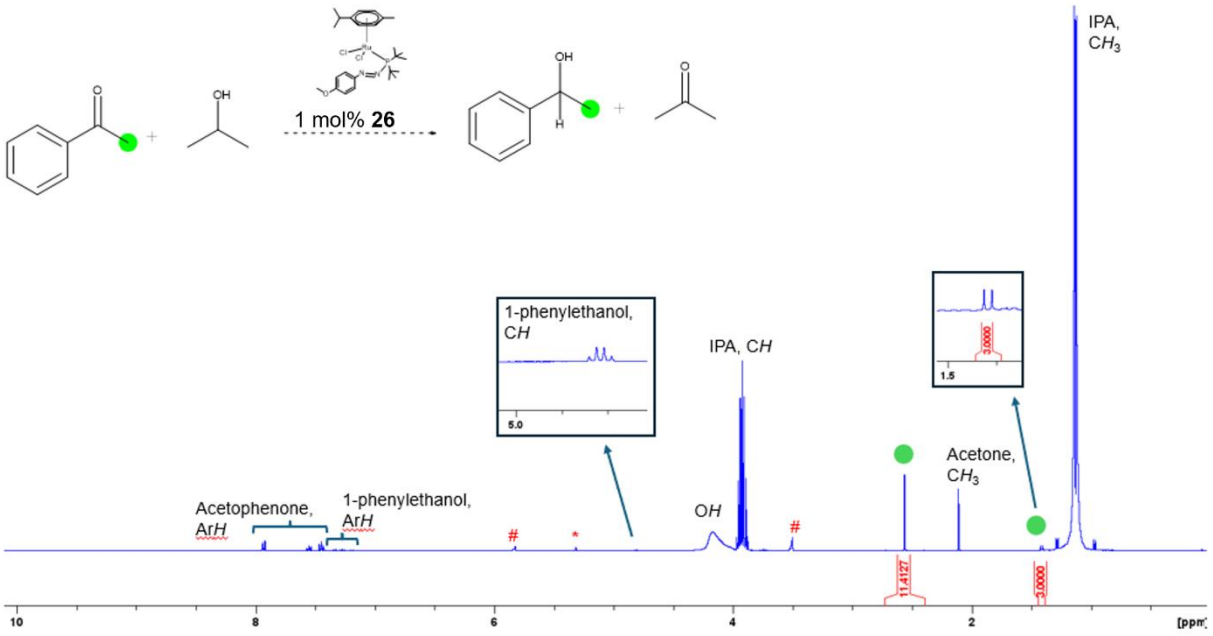

Figure A189. ^{1}H NMR spectrum of an aliquot of the TH reaction following ReactIR experiment using **26** as catalyst. * = residual CDHCl2, = internal standard (trimethoxybenzene in $CDCl_3$ within a sealed capillary tube).

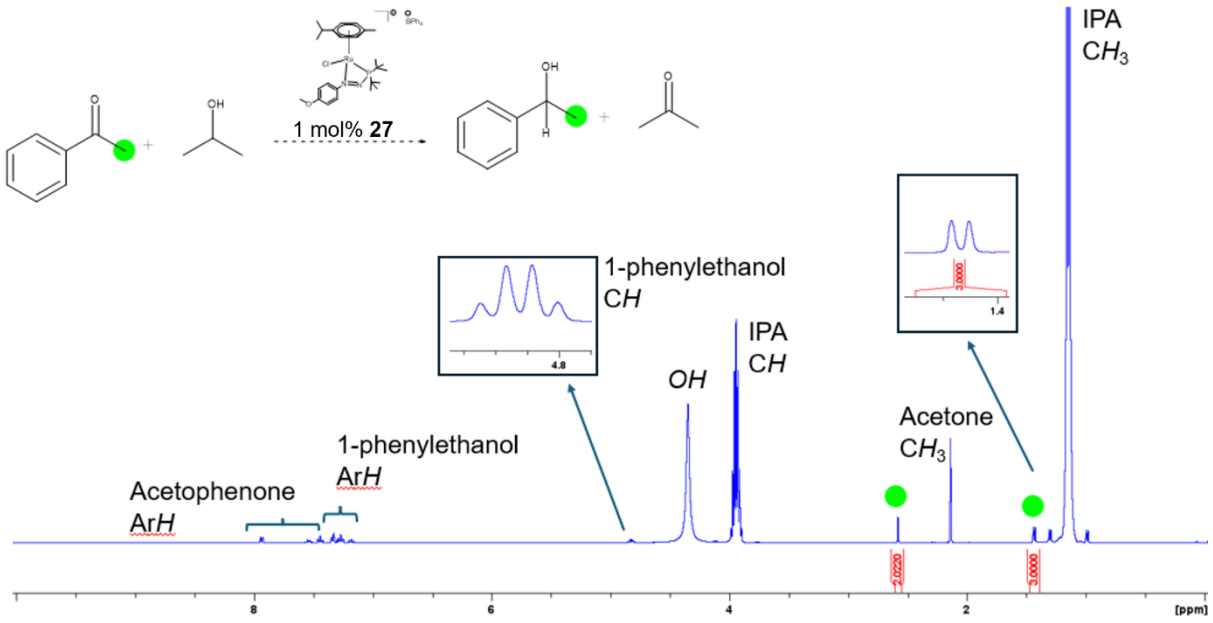

Figure A190. ^{1}H NMR spectrum of the TH of acetophenone using IPA as the proton source and **27** as catalyst (NMR spectroscopy scale).

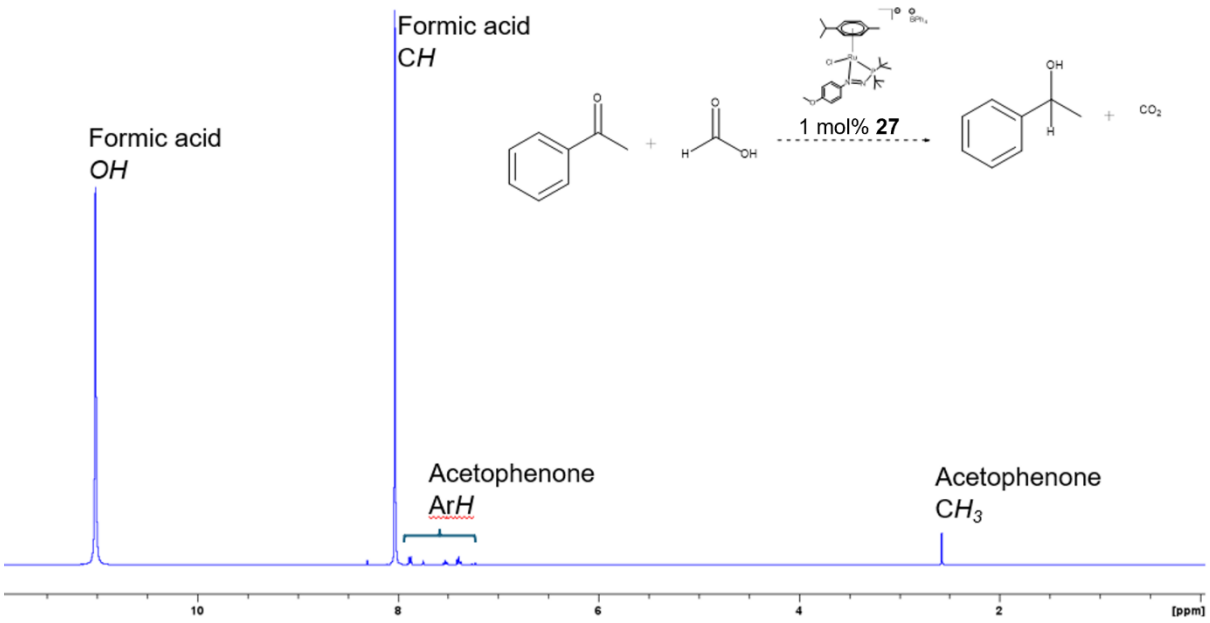

Figure A191. ^{1}H NMR spectrum of the TH of acetophenone using formic acid as the proton source and **27** as catalyst. (NMR spectroscopy scale).

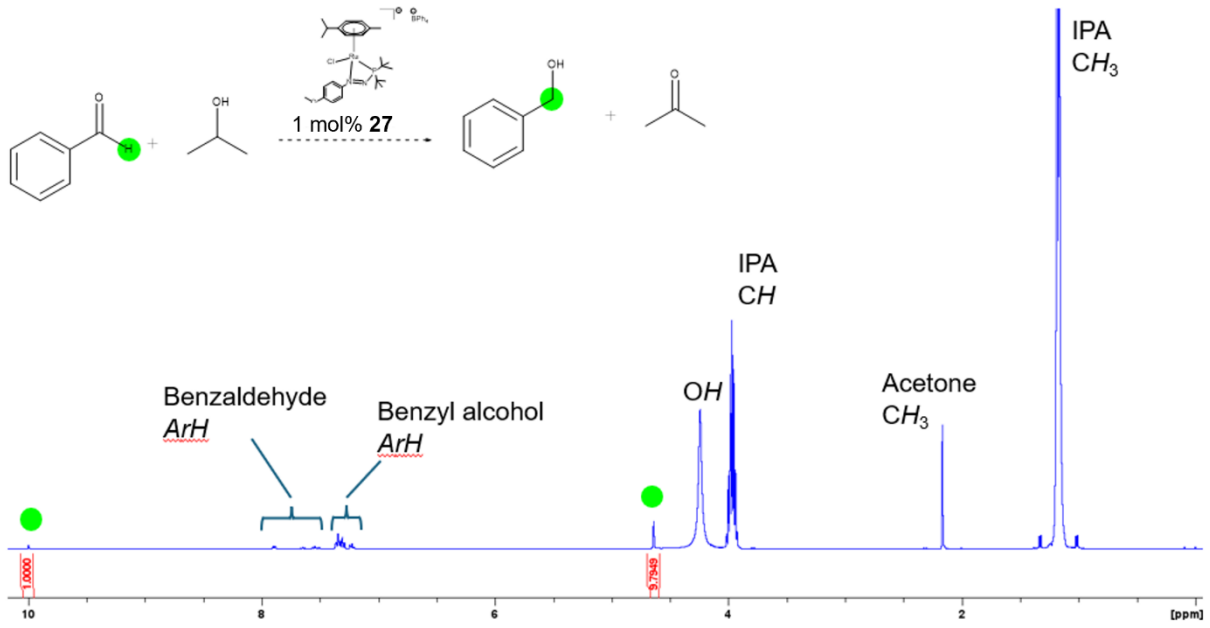

Figure A192. ^{1}H NMR spectrum of the TH of benzaldehyde using IPA as the proton source and **27** as catalyst. (NMR spectroscopy scale).

4.1.2 Oxidation of Styrene

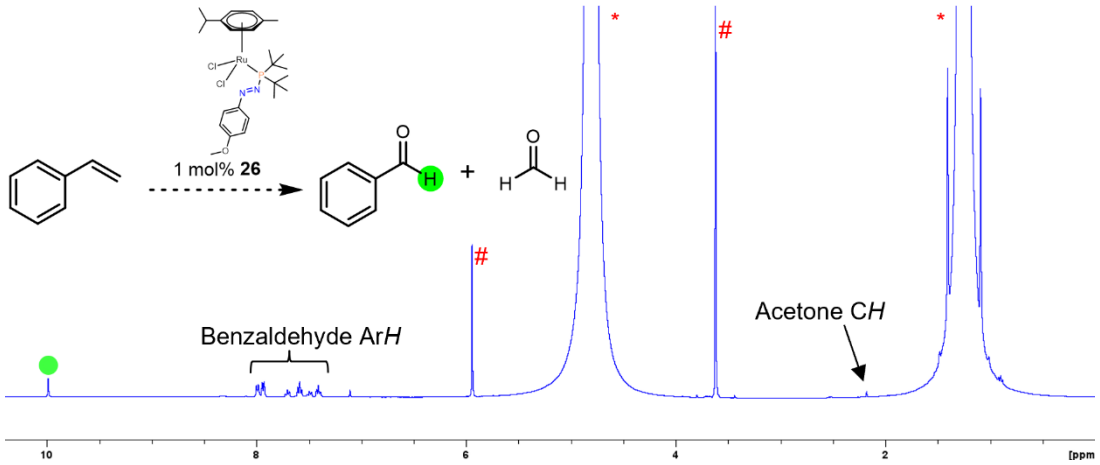

Figure A193. ^{1}H NMR spectrum of the oxidation of styrene using 1 mol% **26** as catalyst.

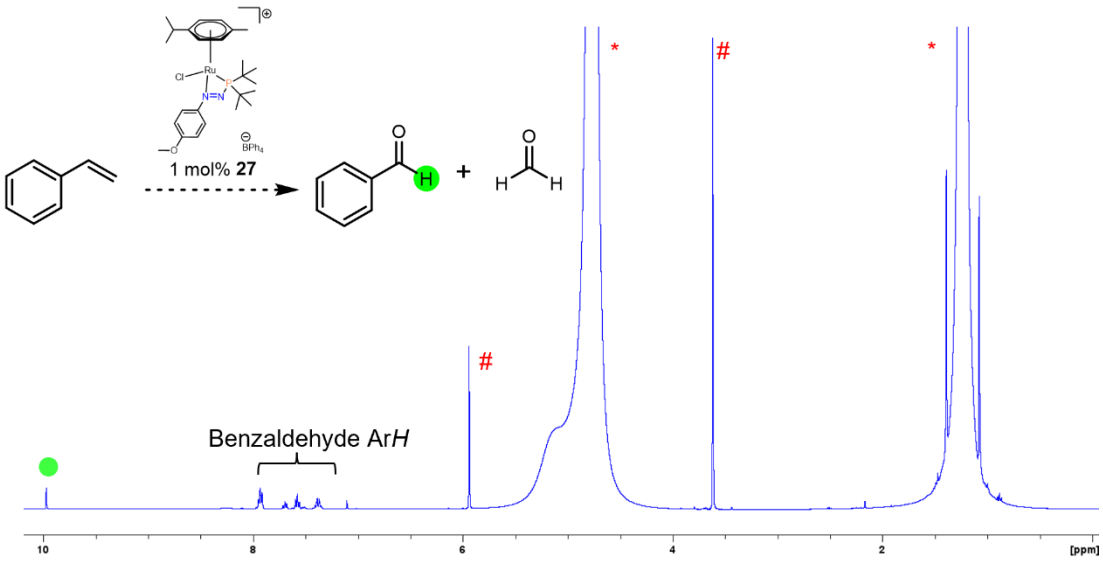

Figure A194. ^{1}H NMR spectrum of the oxidation of styrene using 1 mol% **27** as catalyst.

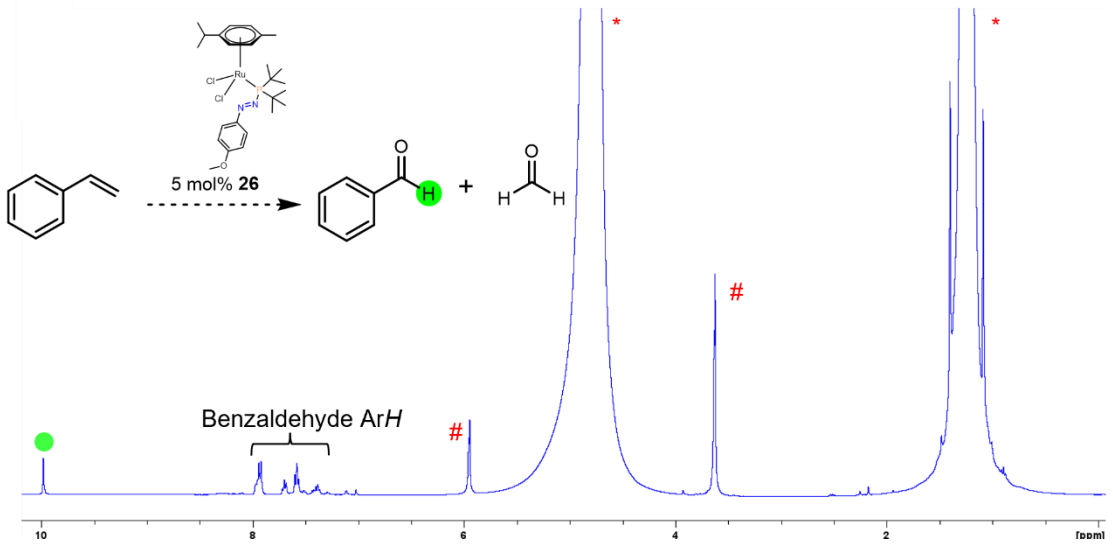

Figure A195. ^{1}H NMR spectrum of the oxidation of styrene using 5 mol% **26** as catalyst.

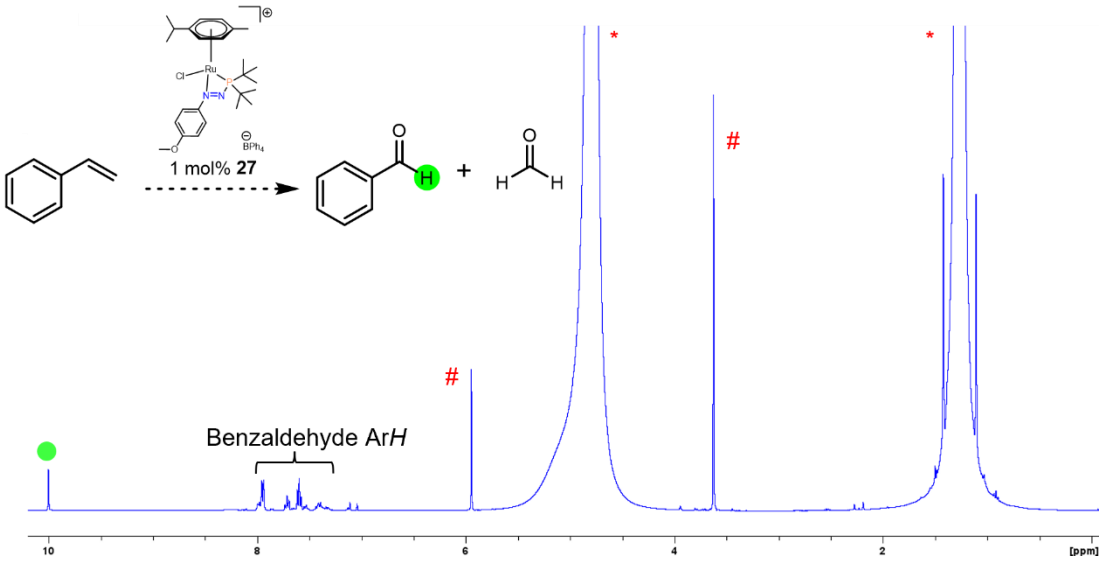

Figure A196. ^{1}H NMR spectrum of the oxidation of styrene using 5 mol% **27** as catalyst.

4.2 Gold

4.2.1 Reaction A

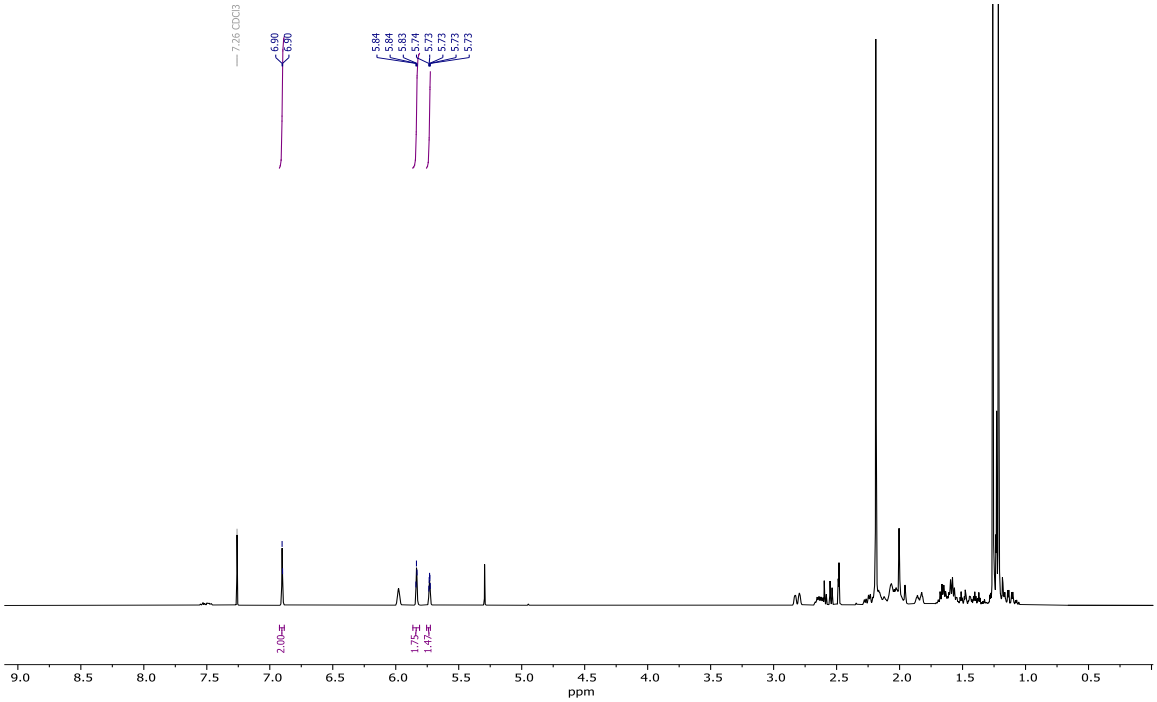

Figure A197. ^{1}H NMR spectrum of Reaction A using 1 mol% PPh_3AuCl as catalyst. Run 1.

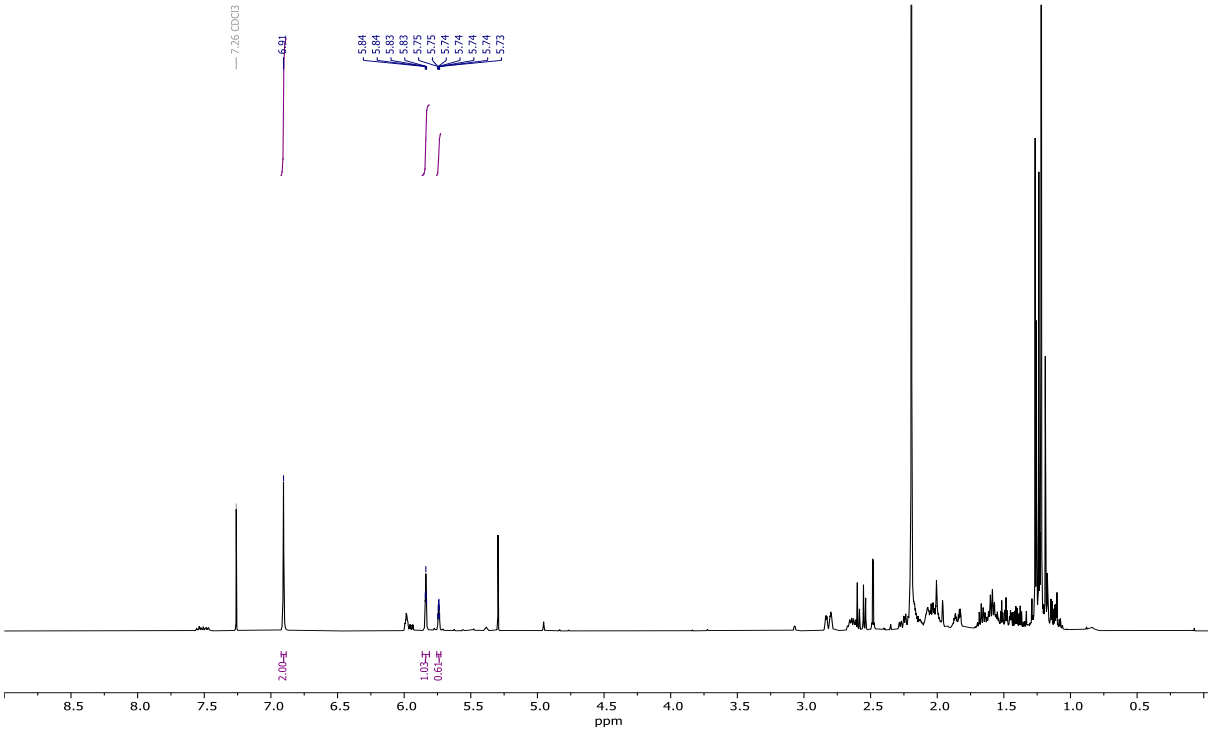

Figure A198. ^{1}H NMR spectrum of Reaction A using 1 mol% PPh_3AuCl as catalyst. Run 2.

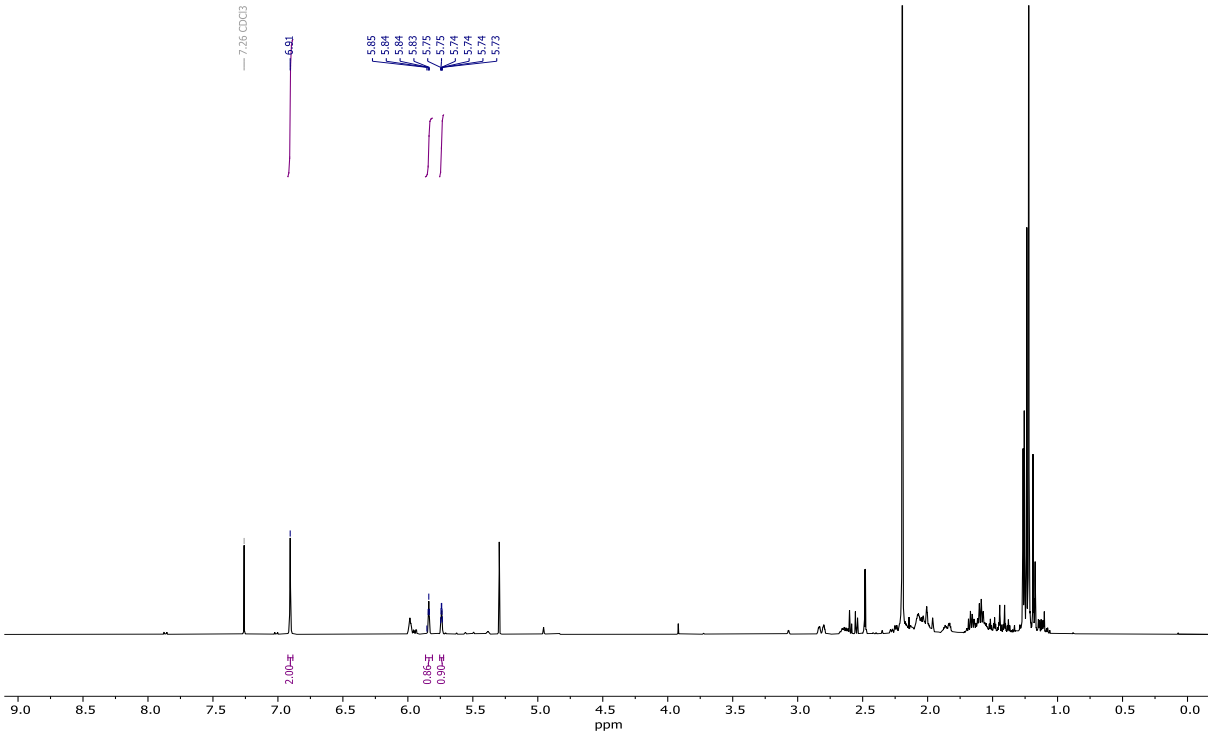

Figure A199. ^{1}H NMR spectrum of Reaction A using 1 mol% **29** as catalyst. Run 1.

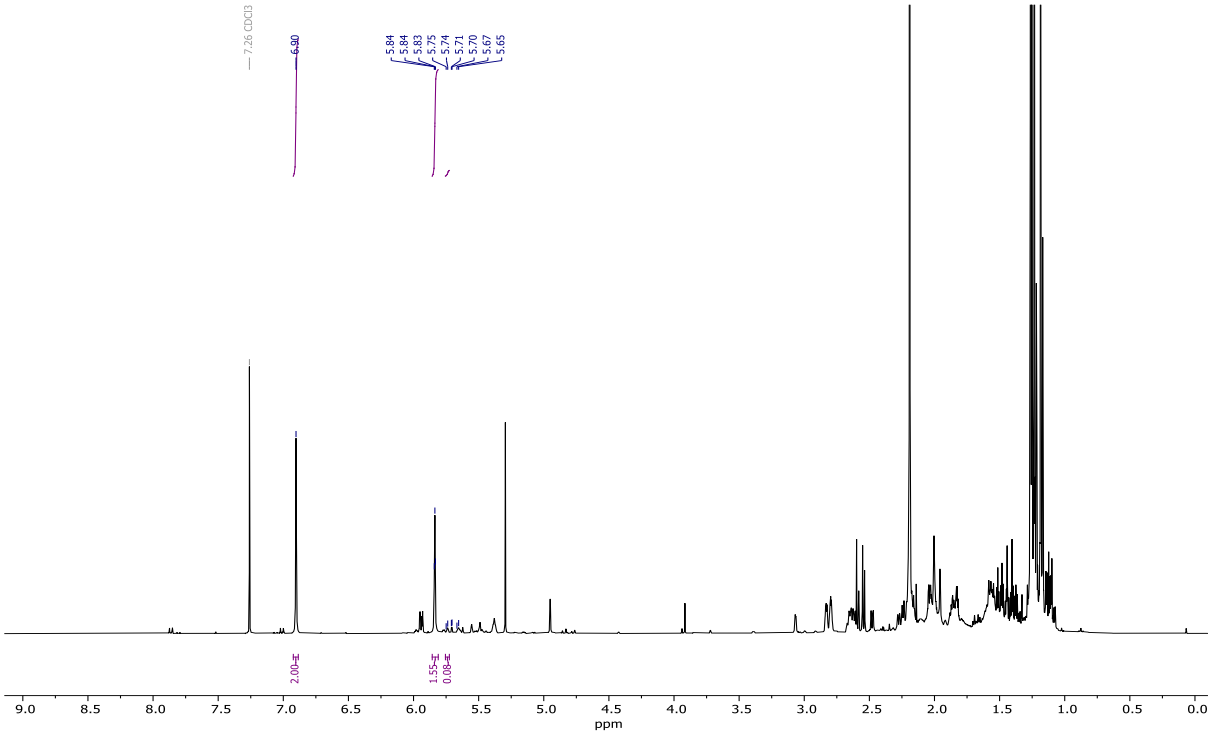

Figure A200. ^{1}H NMR spectrum of Reaction A using 1 mol% **29** as catalyst. Run 2.

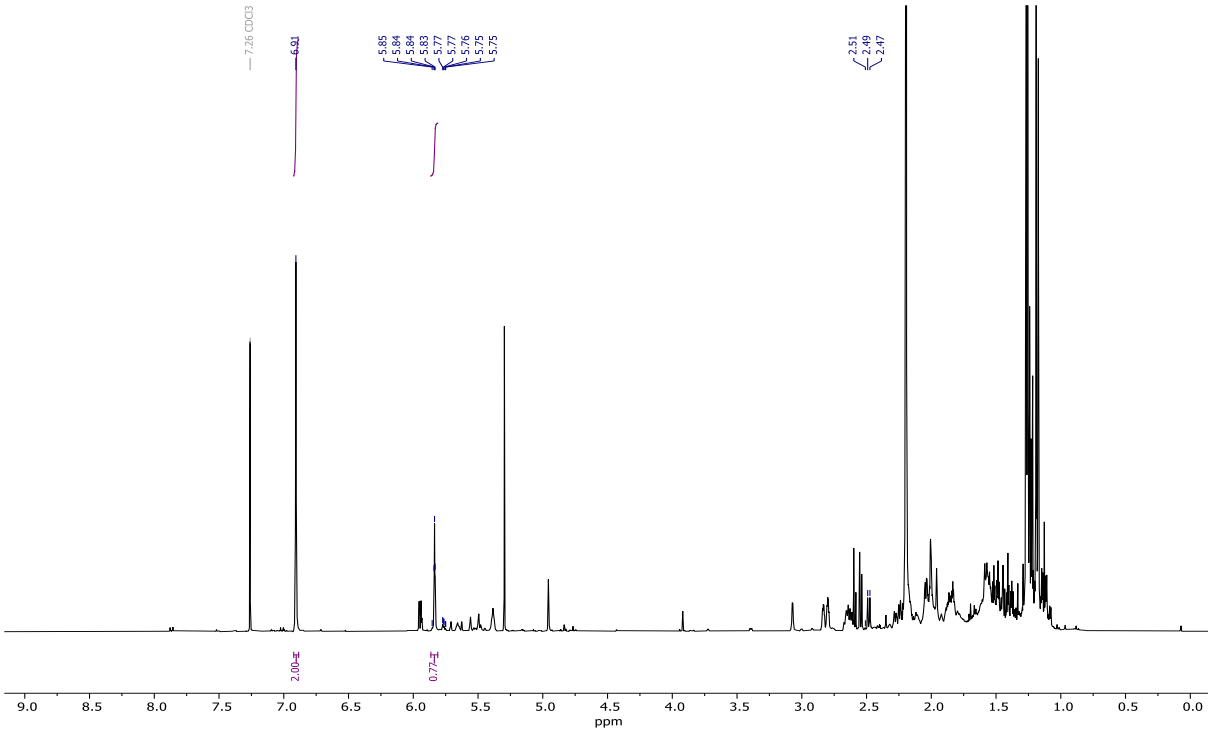

Figure A201. ^{1}H NMR spectrum of Reaction A using 1 mol% **30** as catalyst. Run 1.

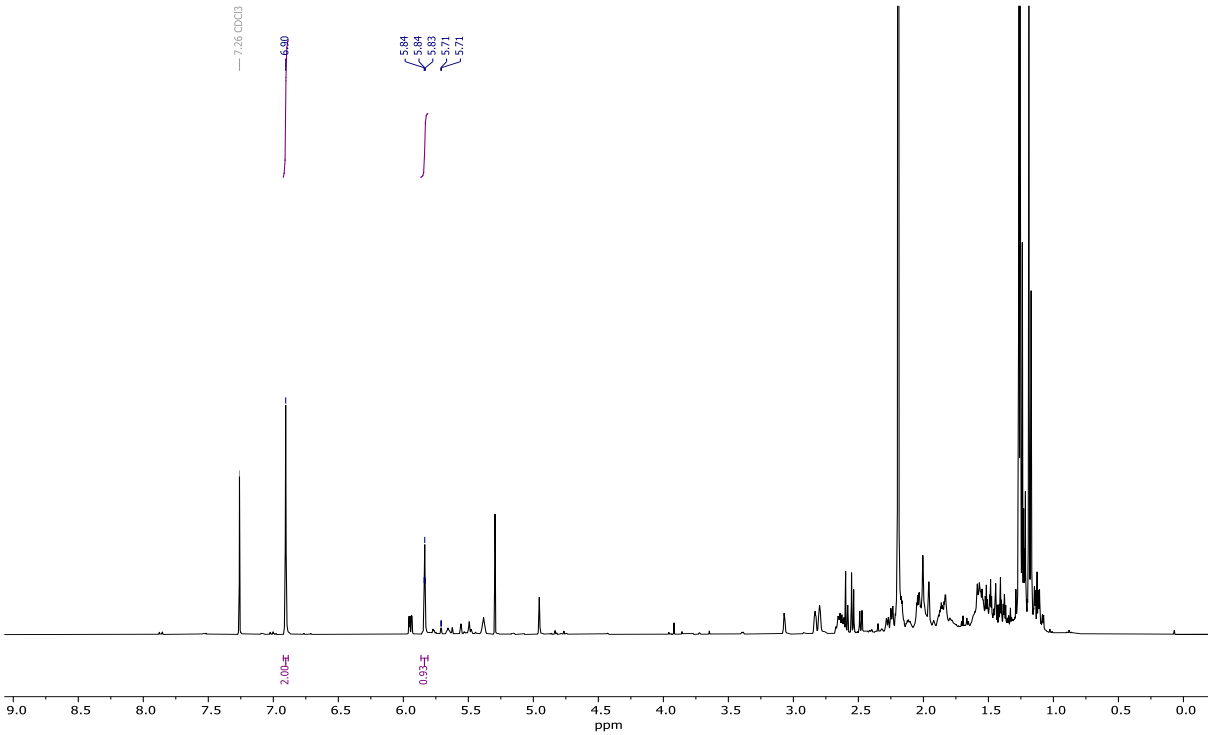

Figure A202. ^{1}H NMR spectrum of Reaction A using 1 mol% **30** as catalyst. Run 2.

4.2.2 Reaction B

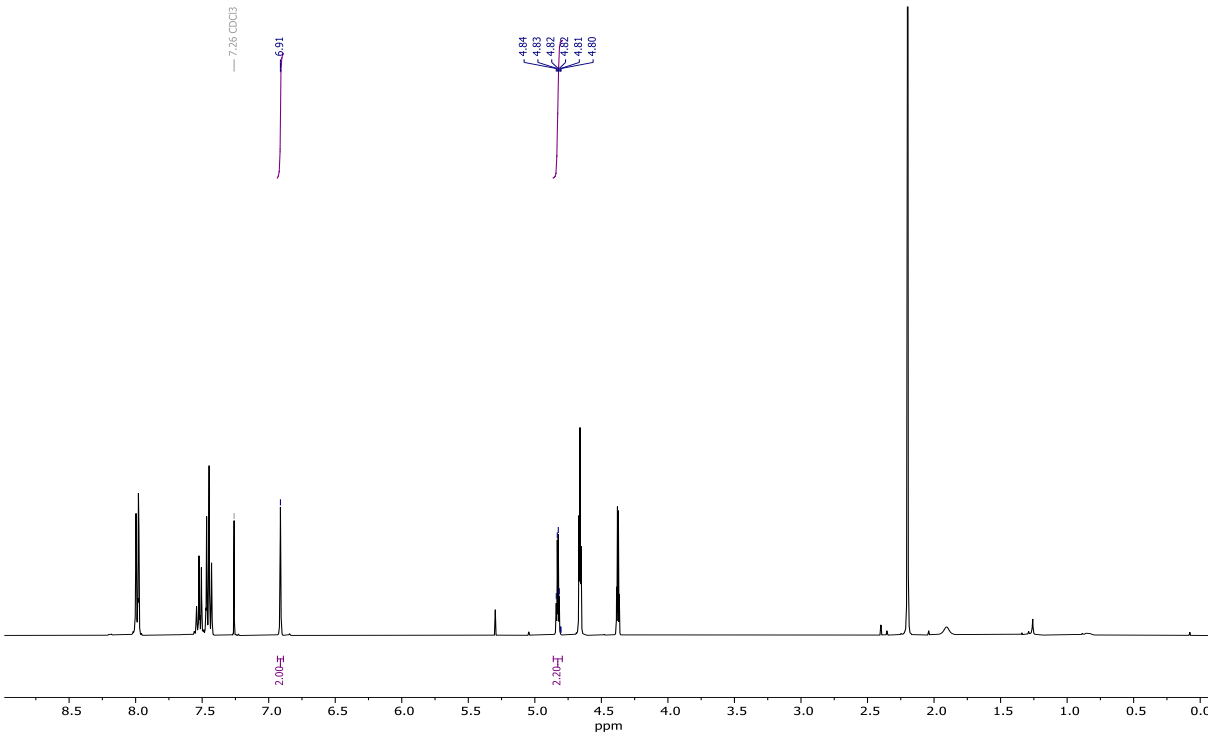

Figure A203. ^{1}H NMR spectrum of Reaction B using 1 mol% PPh_3AuCl as catalyst. Run 1.

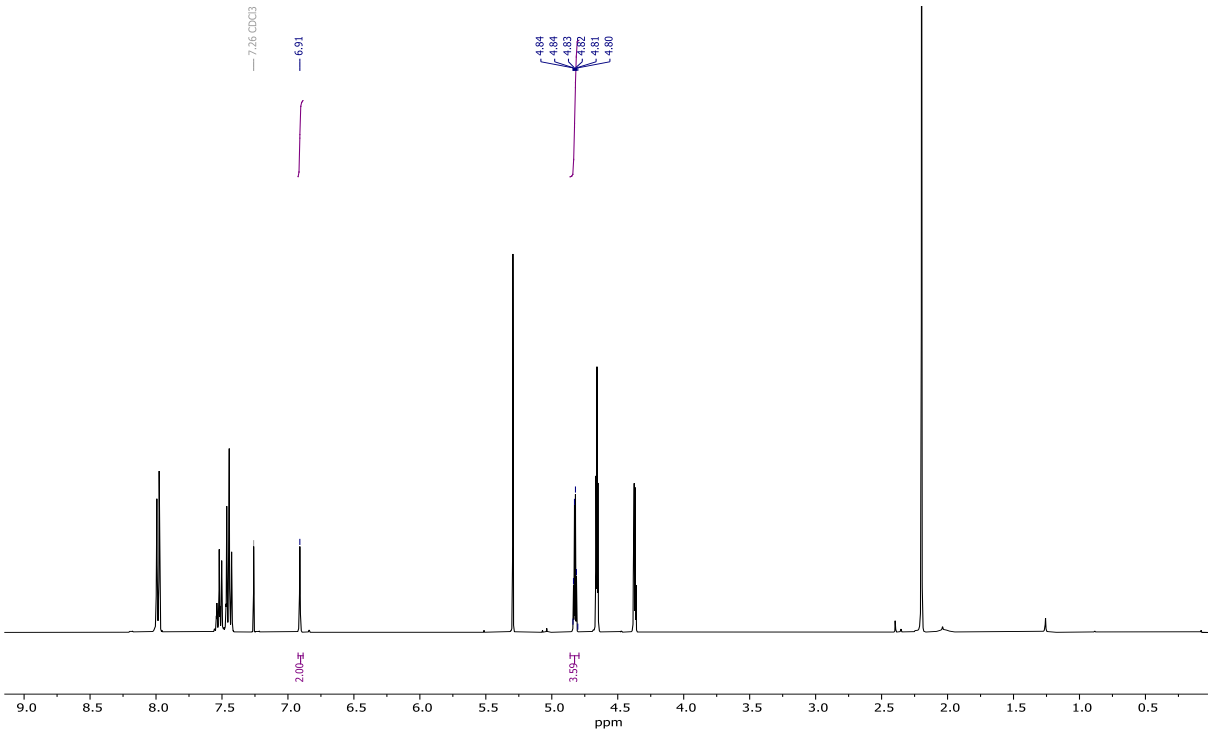

Figure A204. ^{1}H NMR spectrum of Reaction B using 1 mol% PPh_3AuCl as catalyst. Run 2.

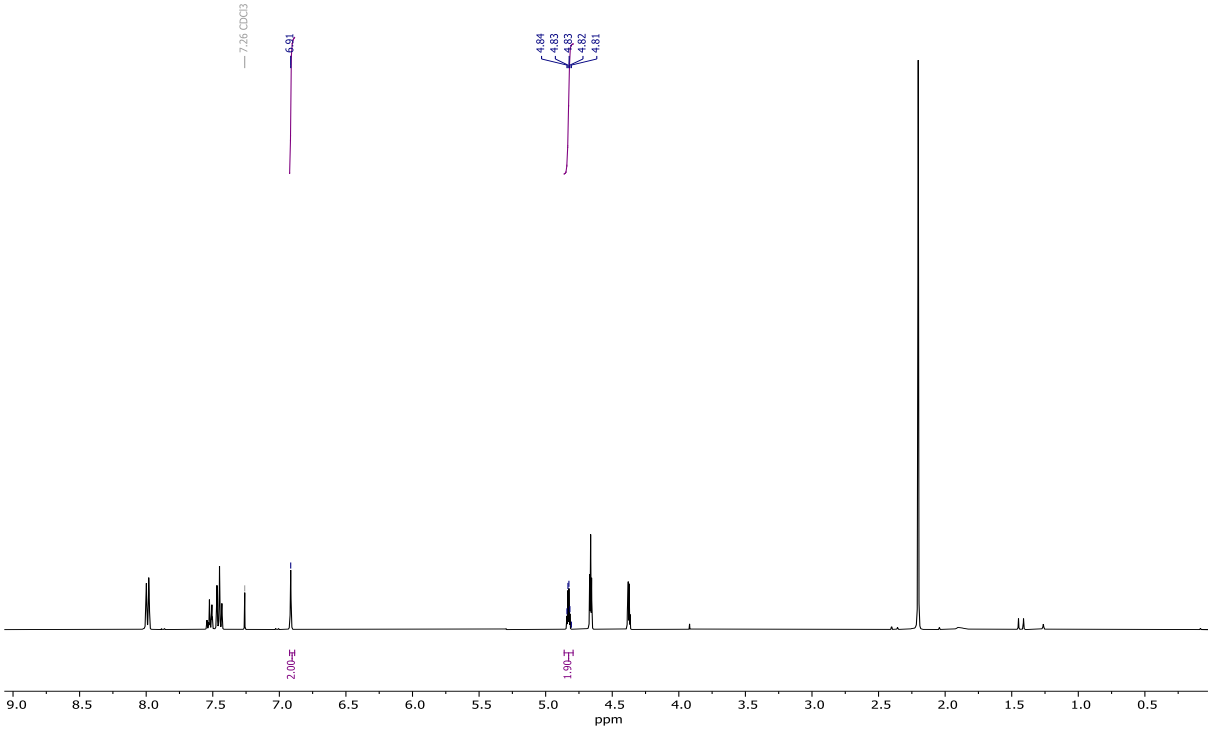

Figure A205. ^{1}H NMR spectrum of Reaction B using 1 mol% **29** as catalyst. Run 1.

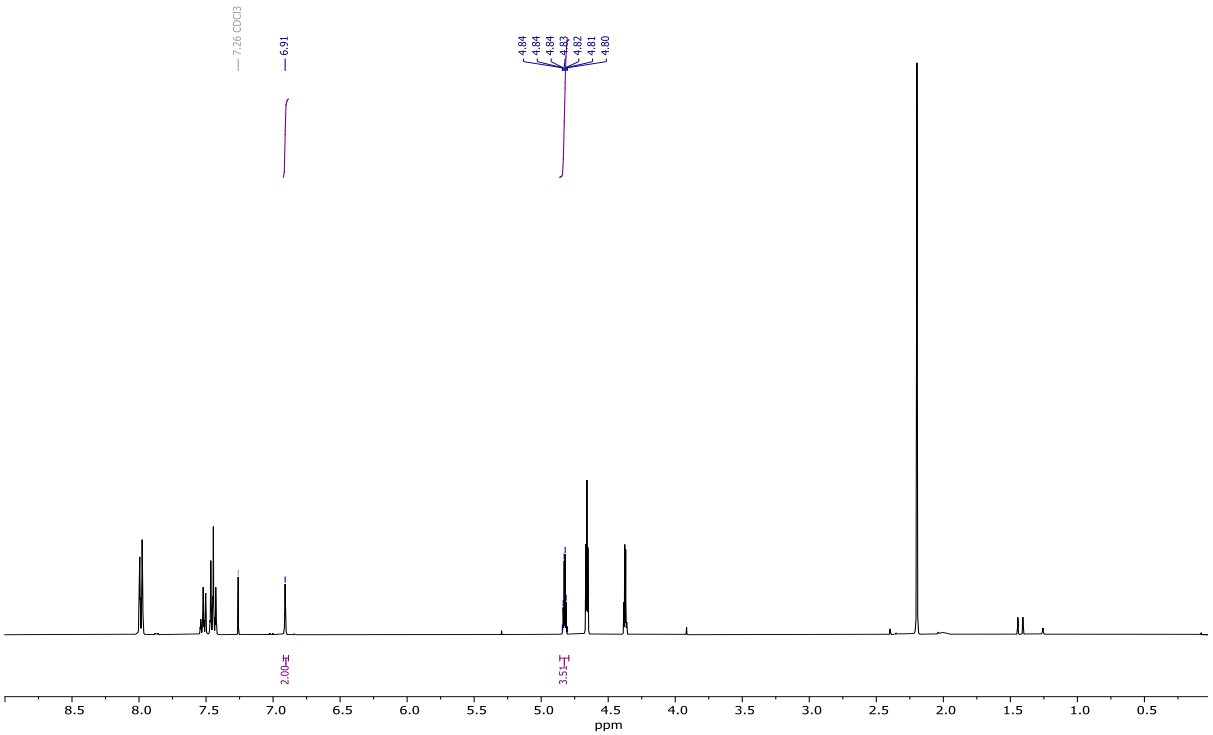

Figure A206. ^{1}H NMR spectrum of Reaction B using 1 mol% **29** as catalyst. Run 2.

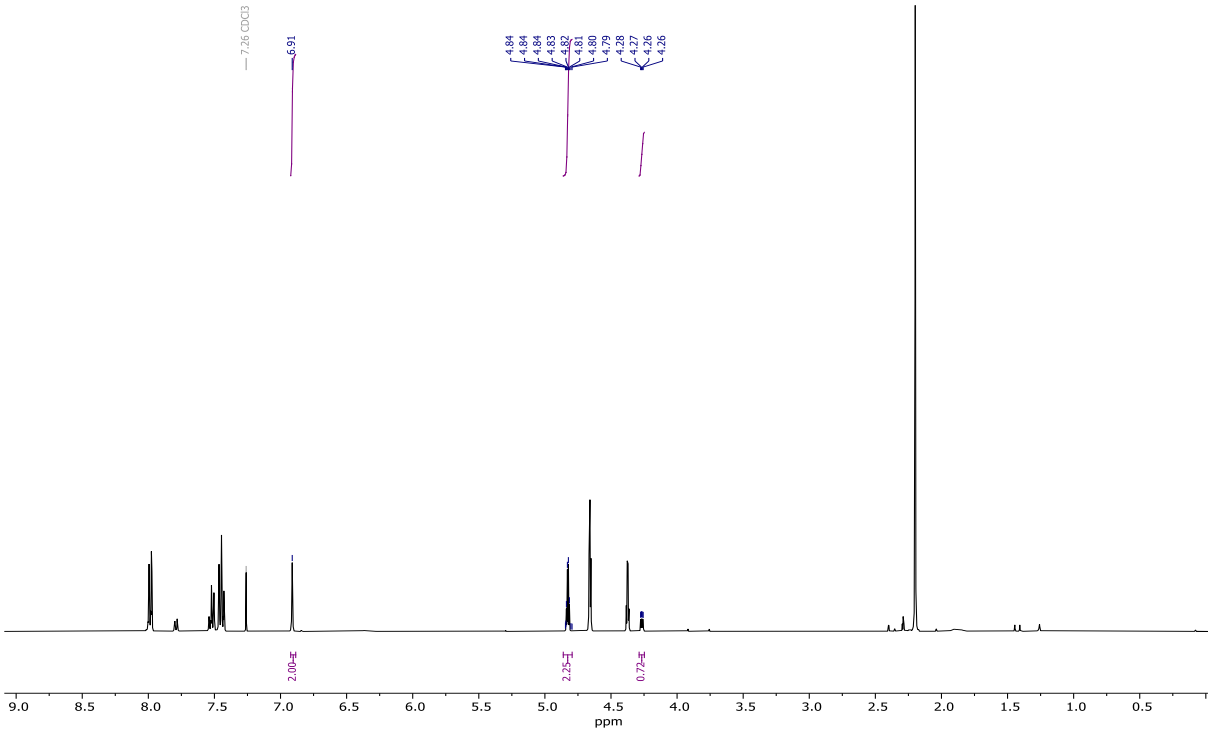

Figure A207. ^{1}H NMR spectrum of Reaction B using 1 mol% **30** as catalyst. Run 1.

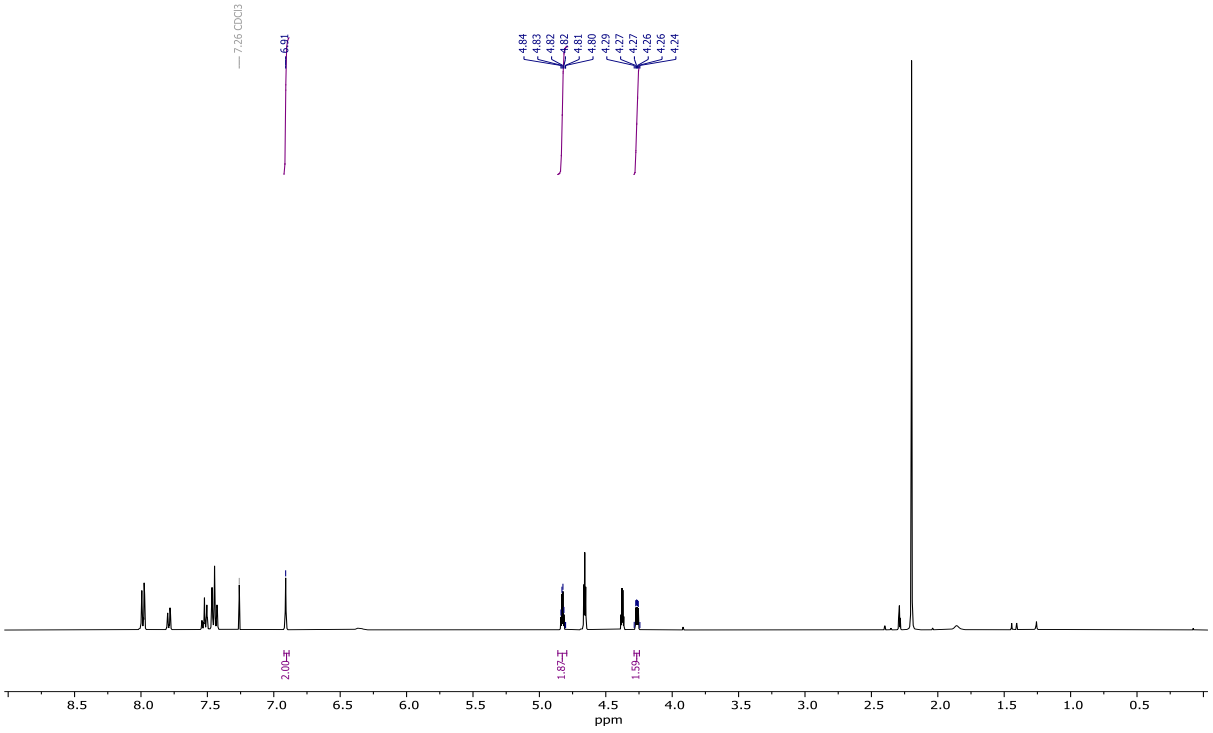

Figure A208. ^{1}H NMR spectrum of Reaction B using 1 mol% **30** as catalyst. Run 2.

4.2.3 Reaction C

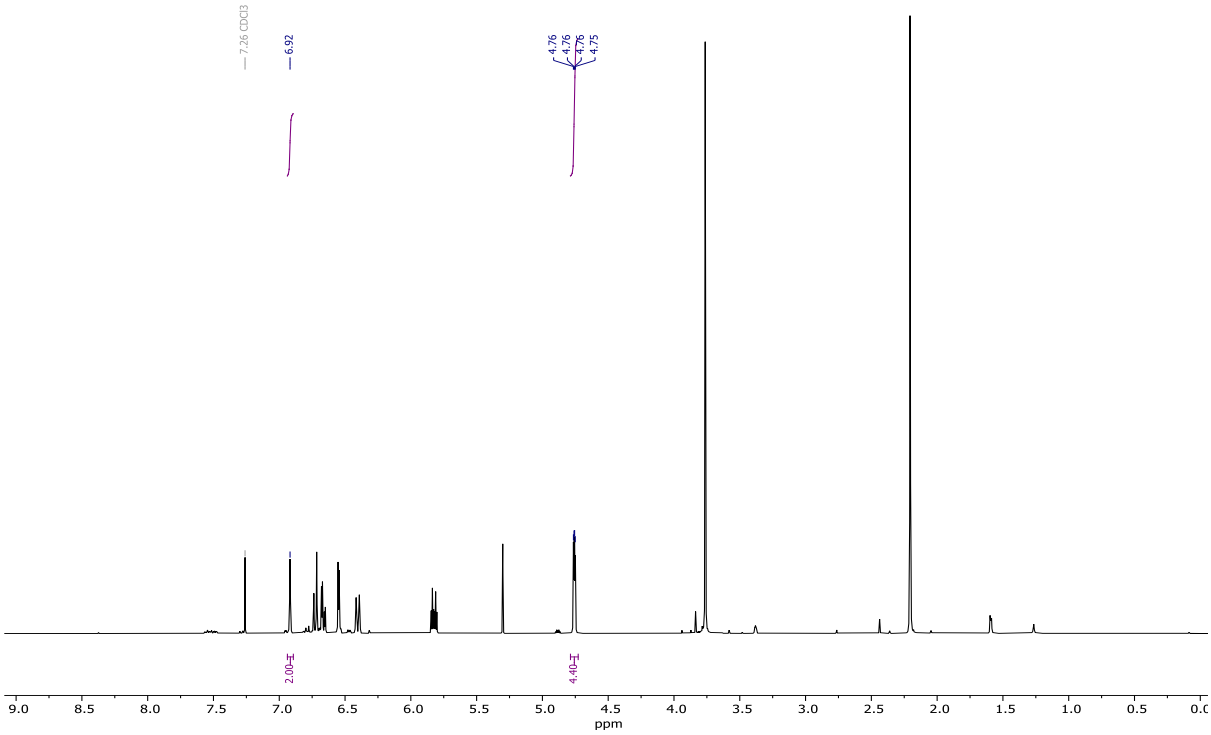

Figure A209. ^{1}H NMR spectrum of Reaction C using 1 mol% PPh_3AuCl as catalyst. Run 1.

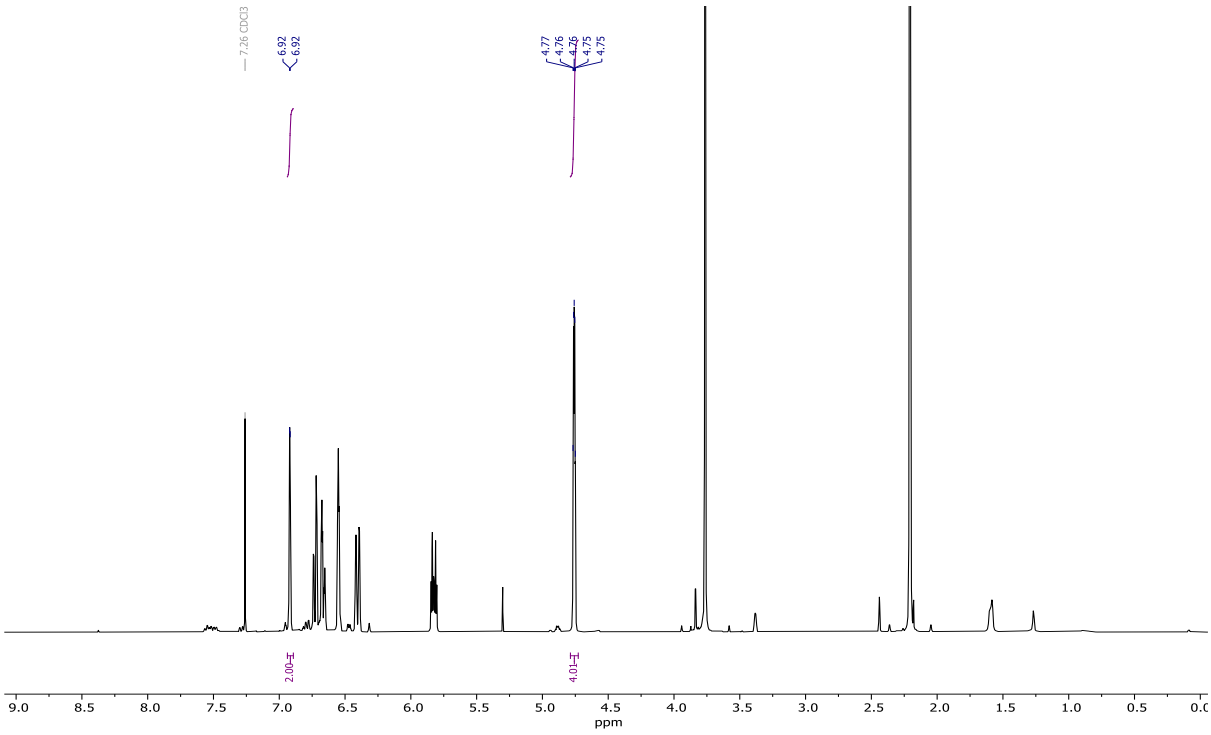

Figure A210. ^{1}H NMR spectrum of Reaction C using 1 mol% PPh_3AuCl as catalyst. Run 2.

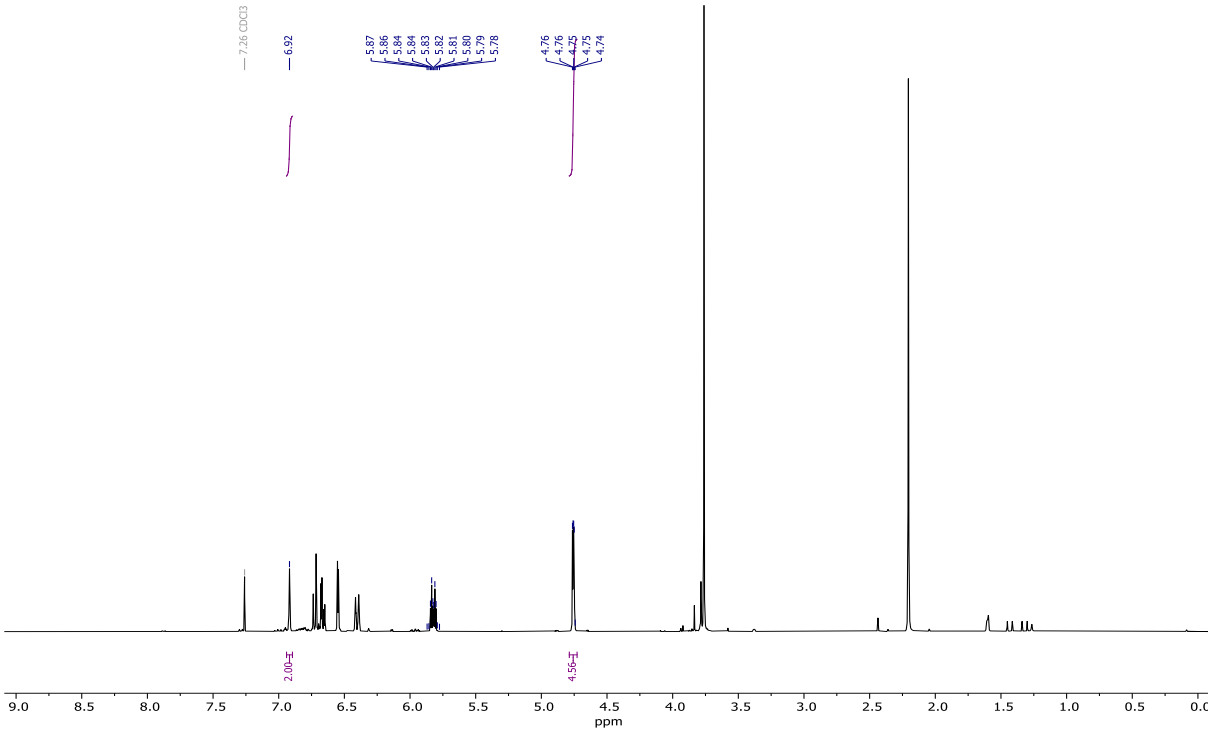

Figure A211. ^{1}H NMR spectrum of Reaction C using 1 mol% **29** as catalyst. Run 1.

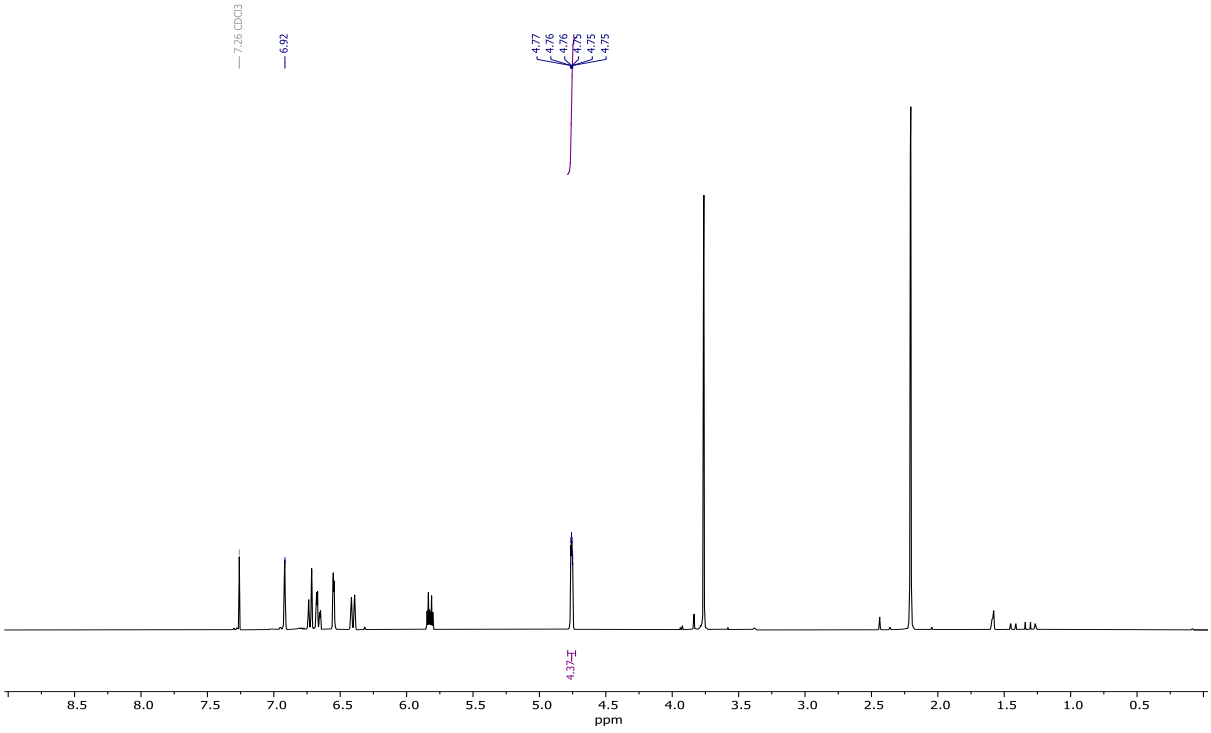

Figure A212. ^{1}H NMR spectrum of Reaction C using 1 mol% **29** as catalyst. Run 2.

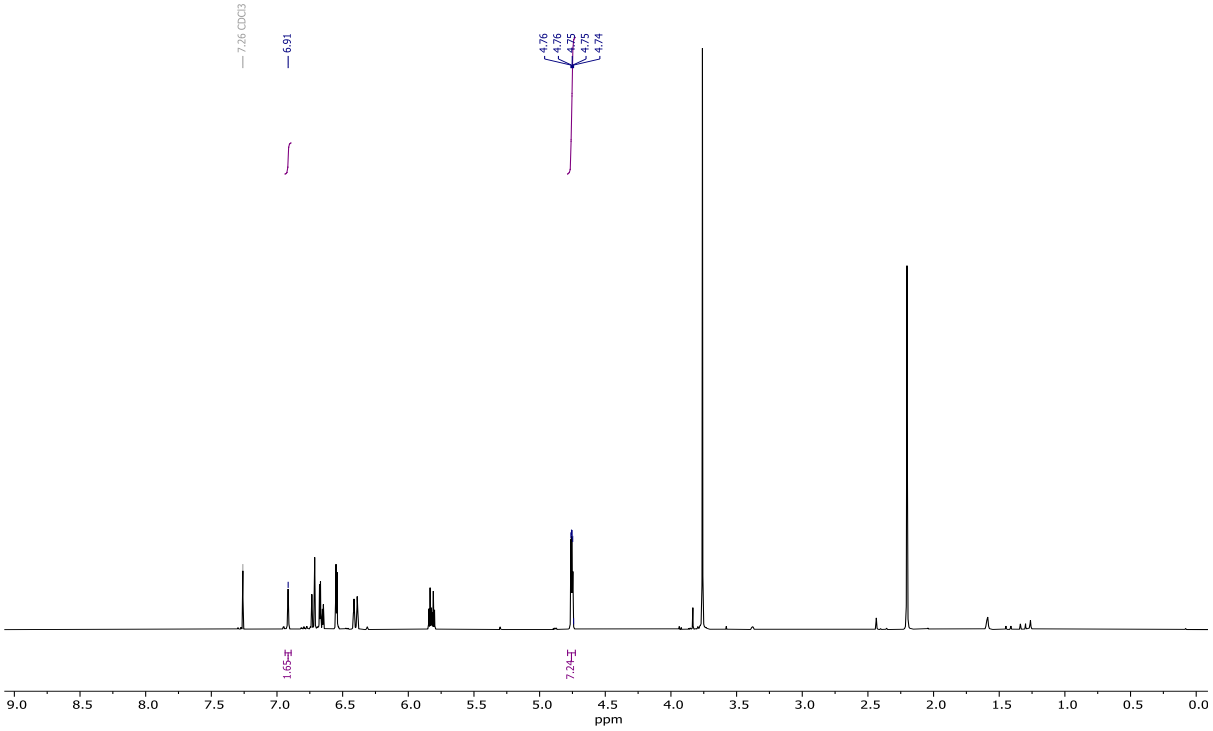

Figure A213. ^{1}H NMR spectrum of Reaction C using 1 mol% **30** as catalyst. Run 1.

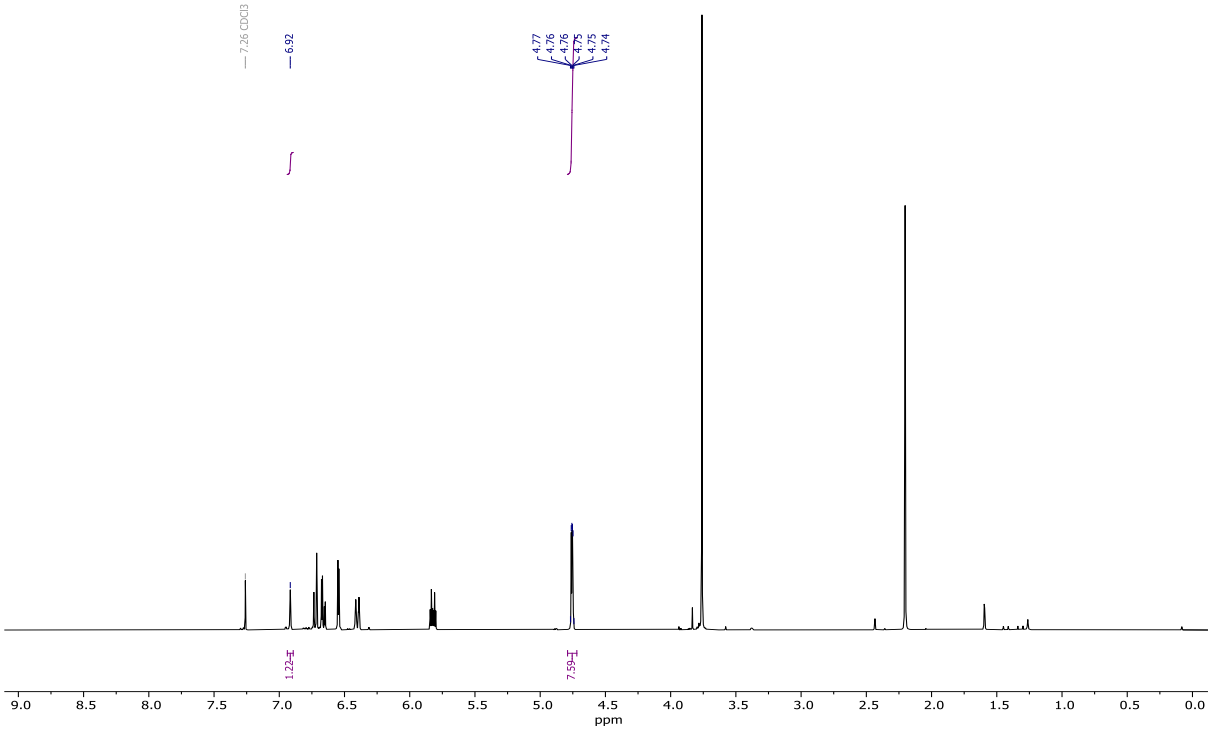

Figure A214. ^{1}H NMR spectrum of Reaction C using 1 mol% **30** as catalyst. Run 2.

4.2.4 Reaction D

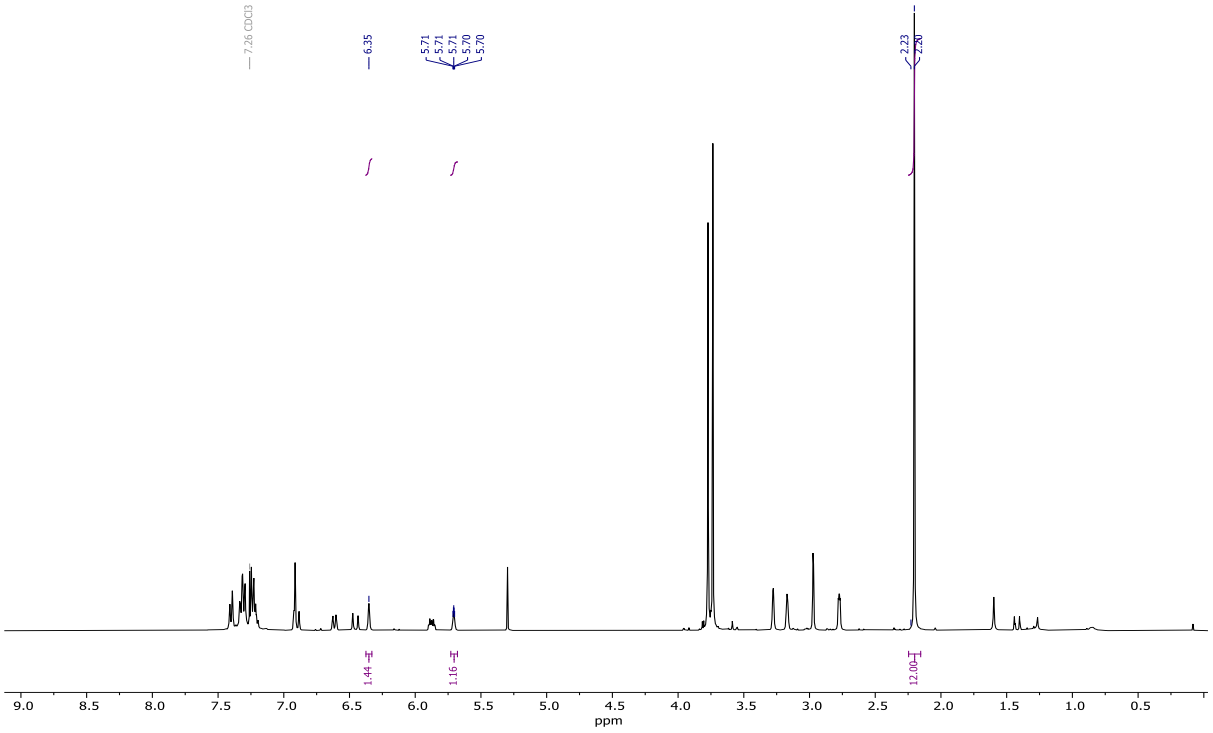

Figure A215. ^{1}H NMR spectrum of Reaction C using 1 mol% JohnPhosAuCl as catalyst. Run 1.

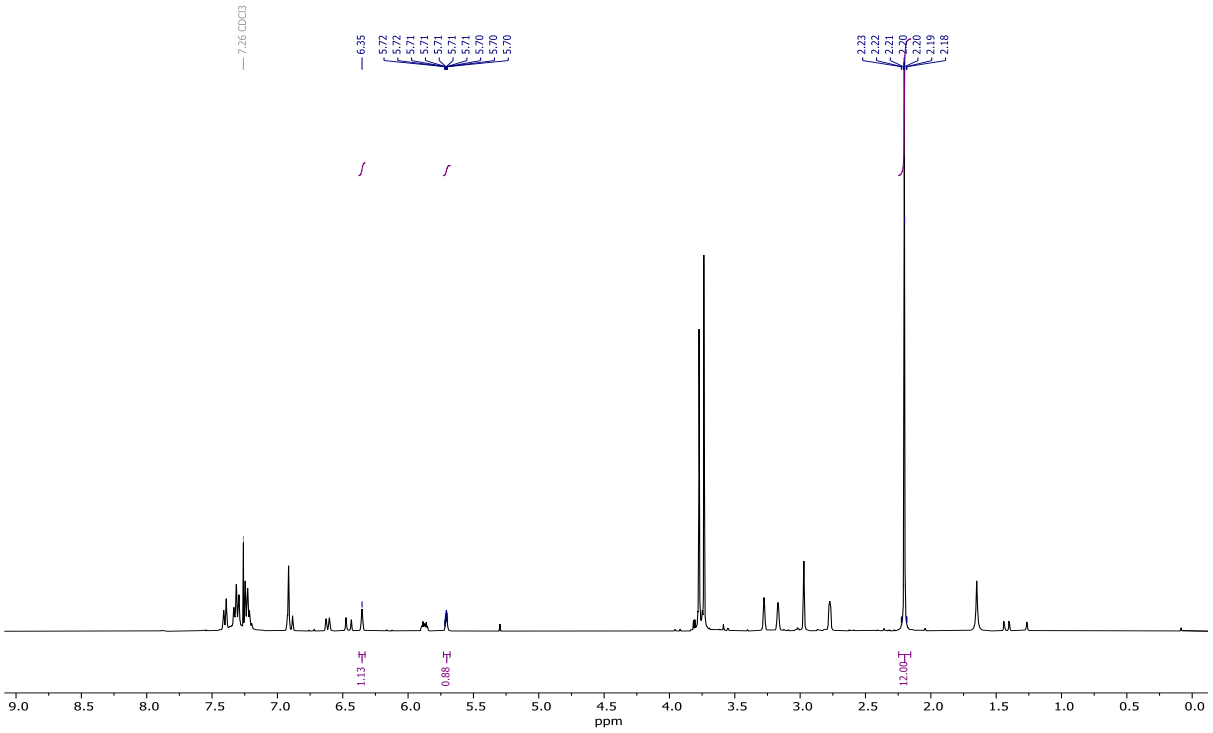

Figure A216. ^{1}H NMR spectrum of Reaction C using 1 mol% JohnPhosAuCl as catalyst. Run 2.

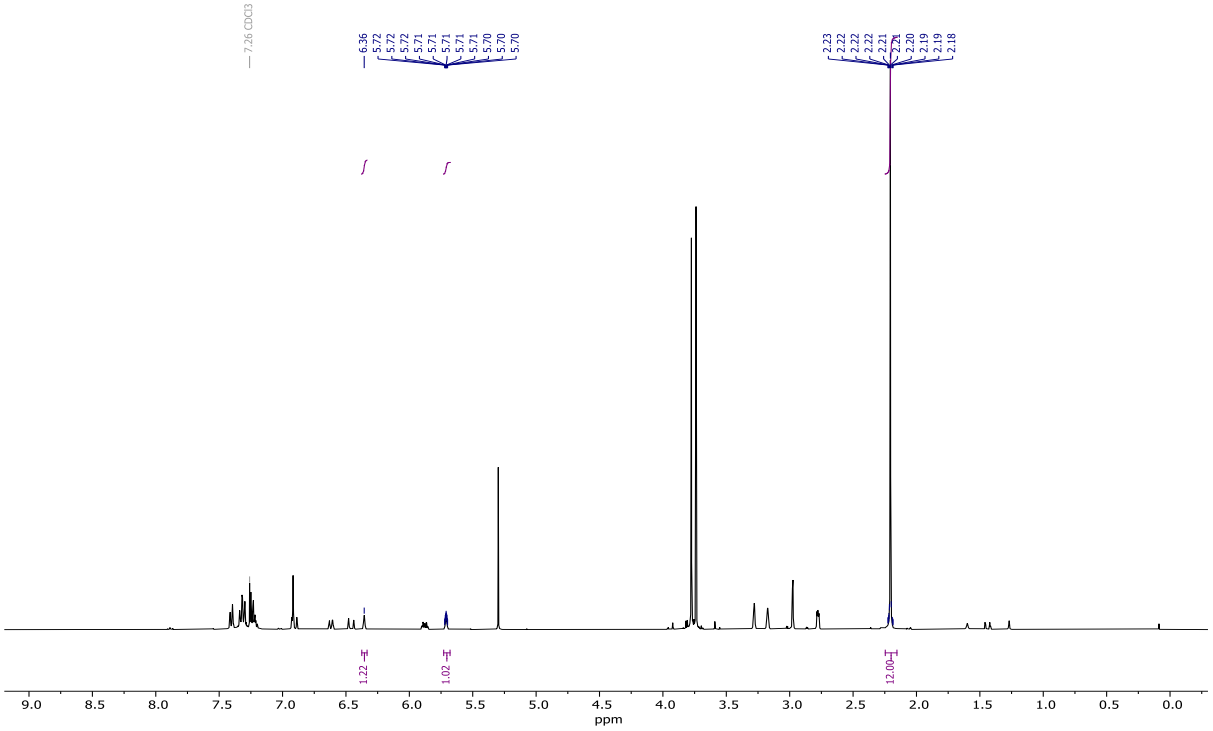

Figure A217. ^{1}H NMR spectrum of Reaction C using 1 mol% **29** as catalyst. Run 1.

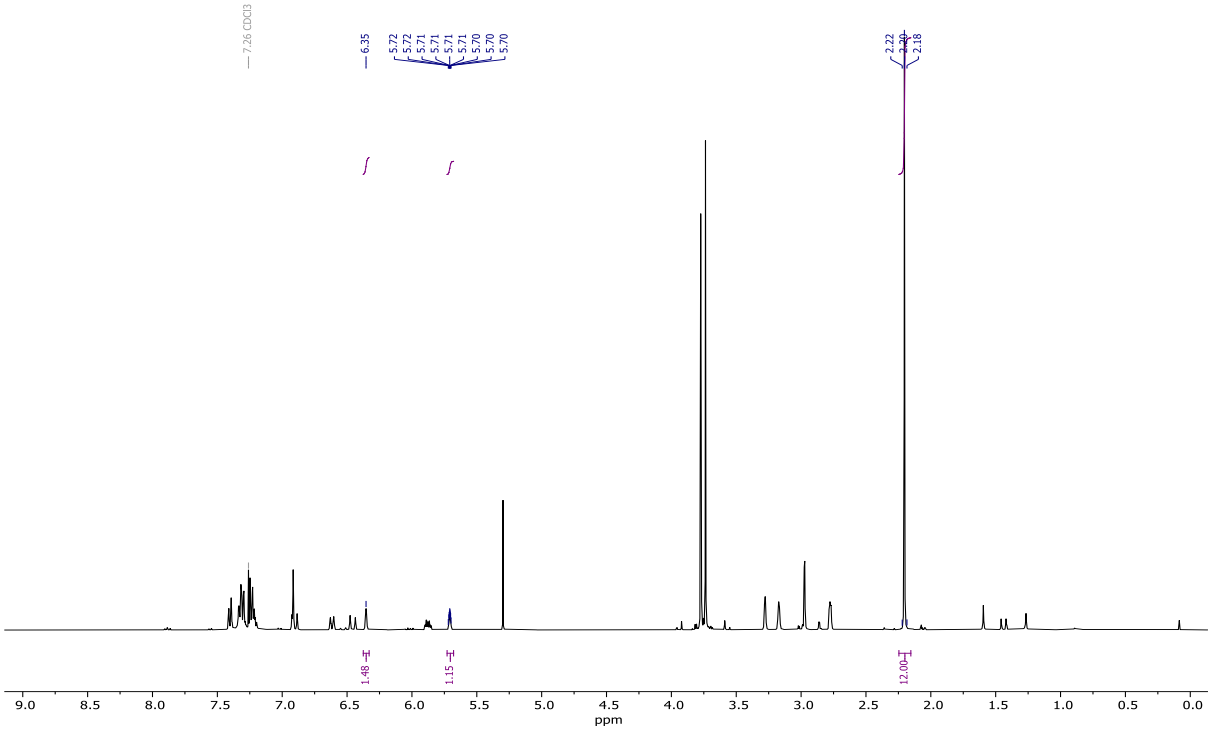

Figure A218. ^{1}H NMR spectrum of Reaction C using 1 mol% **29** as catalyst. Run 2.

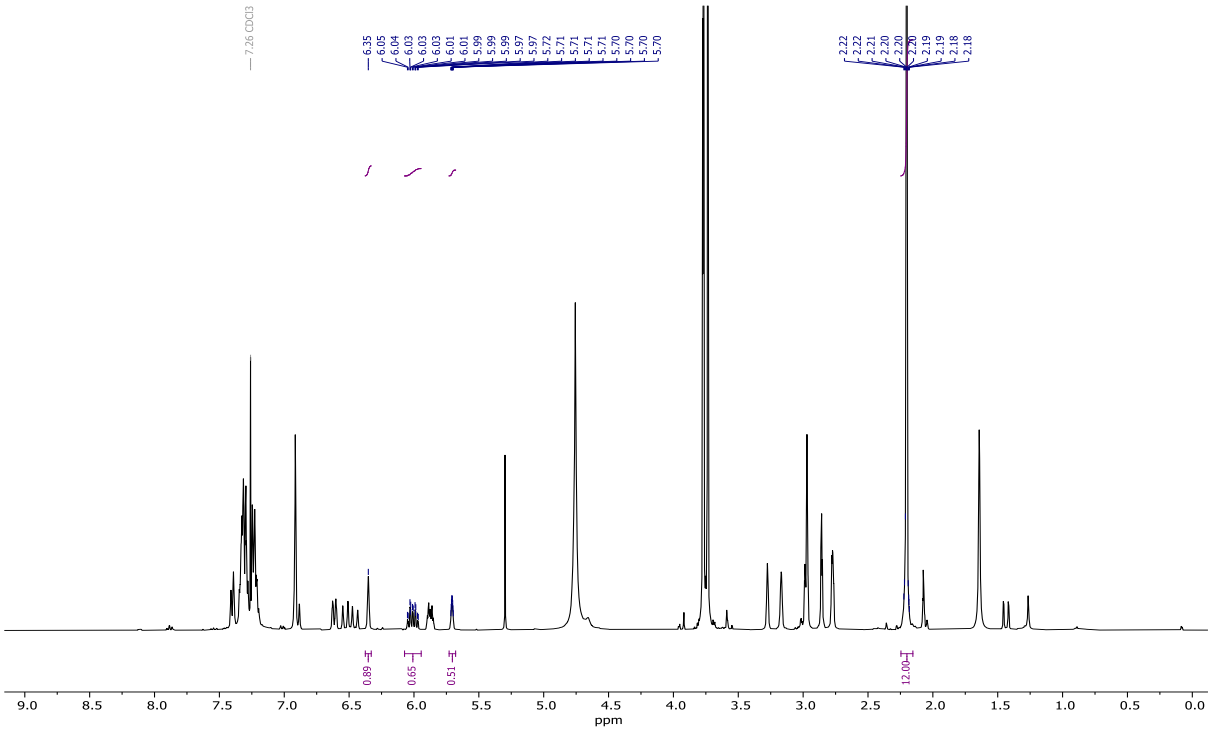

Figure A219. ^{1}H NMR spectrum of Reaction C using 1 mol% **30** as catalyst. Run 1.

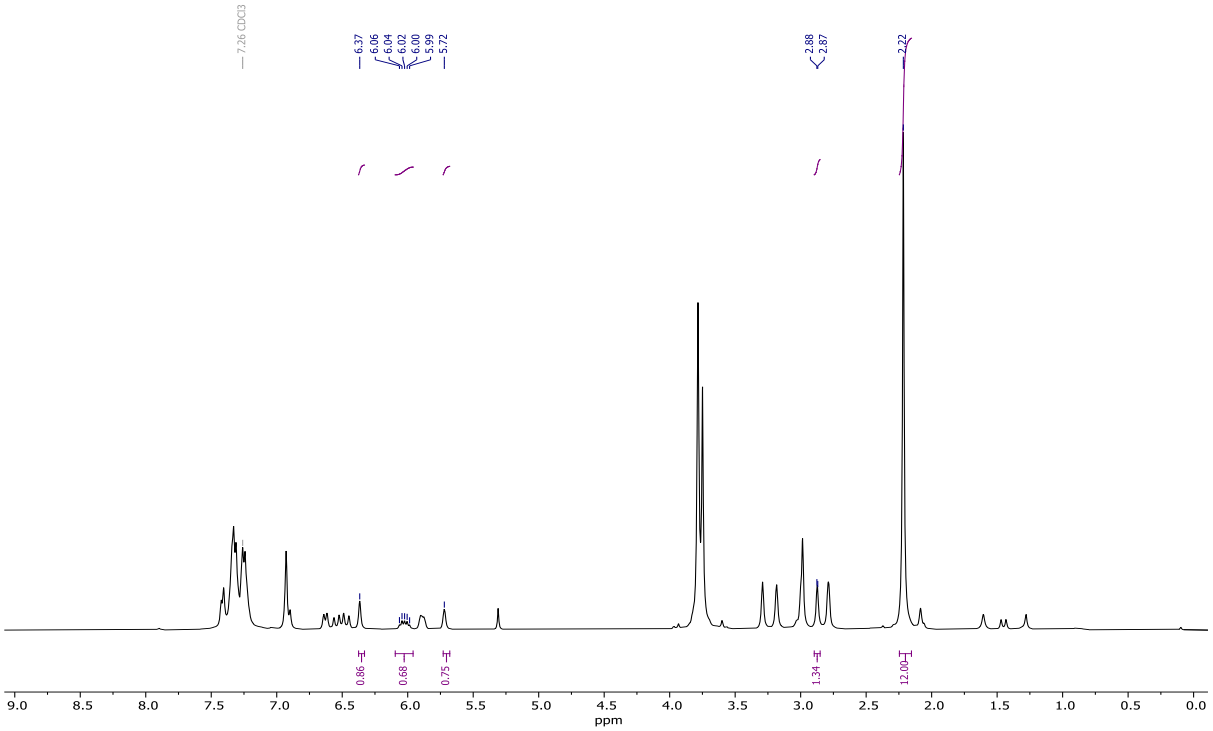

Figure A220. ^{1}H NMR spectrum of Reaction C using 1 mol% **30** as catalyst. Run 2.

5.0 Computational Details

The computational calculations discussed in Chapters 3 and 4, performed by Ethan Calder, have been published in *Chemistry - A European Journal*[1] and *Organometallics*[2] For details, the reader is referred to the supporting information of these publications.

1 E. J. Jordan, E. D. E. Calder, H. V. Adcock, L. Male, M. Nieger, J. C. Slootweg and A. R. Jupp, *Chem. – Eur. J.*, **30**, 35, e202401358.

2 E. J. Jordan, E. D. E. Calder, B. L. Greene, H. V. Adcock, L. Male, P. W. Davies and A. R. Jupp, *Organometallics*, 2024, **43**, 2674–2685.